Climate Change Impact Assessment and Uncertainty Analysis of the Hydrology of a Northern, Data-Sparse Catchment Using Multiple Hydrological Models

By

Steven Kurt Bohrn, B.Sc., EIT

A Thesis submitted to the Faculty of Graduate Studies of
The University of Manitoba
in partial fulfillment of the requirements of the degree of

MASTER OF SCIENCE

Department of Civil Engineering
University of Manitoba
Winnipeg, Manitoba

Declaration

I hereby declare that this thesis is solely the work of the author. This is a true copy of the thesis which has been accepted by the thesis committee and includes all required revisions.

Permission has been granted to the Library of the University of Manitoba to lend/sell copies of this thesis, to the National Library of Canada to microfilm this thesis and to lend or sell copies of the film, and to the University Microfilms Inc. to publish an abstract of this thesis.

This reproduction or copy of this thesis has been made available by authority of the copyright owner solely for the purpose of private study and research, and may only be reproduced and copied as permitted by copyright laws or with express written authorization from the copyright owner.

Abstract

The objective of this research was to determine the impact of climate change on the Churchill River basin and perform analysis on uncertainty related to this impact.

Three hydrological models were used to determine this impact and were calibrated to approximately equivalent levels of efficiency. These include WATFLOOD^{TM}, a semi-physically based, distributed model; HBV-EC, a semi-distributed, conceptual model; and HMETS, a lumped, conceptual model. These models achieved Nash-Sutcliffe calibration values ranging from 0.51 to 0.71.

Climate change simulations indicated that the average of simulations predict a small increase in flow for the 2050s and a slight decrease for the 2080s. Each hydrological model predicted earlier freshets and a shift in timing of low flow events.

Uncertainty analysis indicated that the chief contributor of uncertainty was the selection of GCM followed by hydrological model with less significant sources of uncertainty being parameterization of the hydrological model and selection of emissions scenario.

Acknowledgements

Table of Contents

List of Tables

List of Figures

List of Copyright Material for Which Permission was Obtained

List of Appendices

Glossary of Terms

Albedo – reflection coefficient for snow. This term is used as a parameter in hydrological models in order to compute the energy budget. Typical values for this parameter range from 50% reflection for ripe snow to as high as 90% reflection for freshly fallen snow.

Baseflow – the only portion of the hydrograph which contributes flow during the lowest flow periods of the year. This flow is contributed from the subsurface and defines the lowest level which the hydrograph can recede to.

Calibration – the process of adjusting parameters of a model in order to force the output to match some observed values. In this study, it also refers to the period which was used to calibrate the hydrological models (1986-1989).

Climate change – the process by which the earth's climate is changing. There are many theories which attempt to explain this change but the consensus is that carbon dioxide emissions is the main anthropogenic contributor to this process.

Conceptual – (hydrological model) refers to a model which uses concepts and empirical equations to estimate the streamflow in a basin rather than physics based equations. Conceptual hydrological models are generally referred to as the opposite of physically-based hydrological models in terms of the method used in the calculation of flow.

Distributed – (hydrological model) refers to a model which divides the watershed into small areas in order to calculate runoff rather than considering the entire

basin at once. Distributed hydrological models are the opposite of lumped hydrological models in terms of the method used to discretize the watershed.

Emissions scenario – estimations of the amount of carbon dioxide which will be emitted by future societies. These were developed by the Intergovernmental Panel on Climate Change (IPCC) in order to attempt to quantify climate change. These scenarios are used to force the global climate models and determine the state of the climate in the future.

Evapotranspiration – hydrological process in which the sun and plants take up surface moisture. Because neither evaporation or transpiration is quantifiable individually, they are often grouped together in hydrological models and used as an "error" term to close the hydrologic budget.

GCM – (global climate model) these models use emissions scenarios in order to develop an estimation of the conditions which will make up the future climate. This type of model has a very coarse resolution and covers the entire surface of the earth.

Hydrological model – mathematical model which estimates the flow which will be generated by a given watershed. These models are useful tools and can have varying complexities. They are used for many reasons ranging from flood and drought forecasting to hydroelectric generating station operations.

Infiltration – hydrological process which involves the downward movement of water through the soil. This process relies on gravity and capillary action. In

hydrological models, water which undergoes infiltration is often placed in a lower zone reservoir where it is not subject to evaporation for later computations.

Interception – hydrological process which prevents precipitation from reaching the surface. This is usually caused by vegetation and is often a parameter of the land cover types in hydrological models.

Interflow – the portion of flow which enters the stream channel directly from below the surface in the vadose (unsaturated) zone. This process is faster than groundwater flow but slower than surface runoff and is incorporated in some hydrological models.

Lumped – (hydrological model) refers to a model which considers the entire basin in one computation. This is often used to speed computation time in small models and is the opposite of distributed hydrological models in terms of how the watershed is discretized.

Physically-based – (hydrological model) refers to a model which bases its runoff calculations on physics and physical processes rather than empirical equations. Some models use physics-based equations for many processes but a truly physically-based model is impossible as the complexities of the hydrological cycle are such that computation time would become extremely cumbersome and there are many aspects of the processes which are unknown.

RCM – (regional climate model) these models are dynamically-downscaled versions of the global climate models. They estimate the future climate of the earth on a smaller scale and finer resolution than these larger models.

Uncertainty – refers to the amount of information which is not known for certain. In this study, uncertainty is used to describe the amount of difference between different hydrological output for the same future scenario.

Validation – the process of checking a models calibration by testing it using another time period or area to provide a measure of confidence in the chosen parameter. In this study it may also refer to the time periods which were used to validate the hydrological models (1982-1985 and 1990-1995).

Watershed – the area which is drained by a river at a given outlet point. Other terms which are also used in this study include drainage basin, catchment, and drainage area. Each of these terms is used synonymously within this thesis to avoid extreme repetition.

Preface

Climate change is anticipated to have a sweeping impact on the entire population of the world. It is believed that these relatively small changes in the global climate have the potential to affect nearly every natural cycle which human civilization relies on to function.

As a result, a great deal of resources has been invested in understanding what the extent of this impact may be and developing plans to not only deal with it but thrive upon it. It is believed that with proper planning it is possible to optimize many of our engineered systems to make significant gains from climate change.

However, because future climate changes have not yet occurred, there is a great deal of uncertainty related to understanding its impact on these systems. The future climate of the earth may take on an infinite number of possibilities. The best that we can do is to estimate and try to define a best and worst case scenario.

This study has been commissioned by a major hydroelectric utility to not only estimate the impacts of climate change on a large northern basin, but also to identify the sources which contribute uncertainty to the process and perform thorough analysis to determine which of these are the most prevalent and require further understanding.

Chapter 1: Introduction

The following sections outline the motivation behind this project, as well as the scope and objectives. The chapter concludes with a brief overview of the contents of each of the chapters of this document.

1.1 Project Motivation

Climate change is a process which is believed to have a significant impact on the climate throughout the world. These changes have been shown to be especially prevalent in northern locations (Bring & Destouni, 2011). Further to this, it is expected that these changes in the climate will lead to significant changes in the hydrological regime of the watersheds located in these regions. It is this impact which will be examined in some detail in this study.

The Churchill River basin (CRB) is a large watershed in the northern portion of the Canadian provinces of Alberta, Saskatchewan and Manitoba. Relative to many drainage basins located further south, the Churchill River basin contains very little in the way of human developments and as a result the flows in some of its streams are relatively untouched by human interference. This fact makes the basin ideal for studying and quantifying the impact that climate change will have on the individual processes which occur within the natural hydrological cycle.

The CRB is of particular interest to Manitoba Hydro which is a large utility company which operates several large hydroelectric generating stations. The Nelson/Burntwood river system is connected to the downstream end of Churchill

River via the Churchill River Diversion as shown in the schematic below (Figure 1). Currently there are four hydroelectric generating stations on the Nelson/Burntwood river system, with one currently under construction and several more in various stages of planning and development.
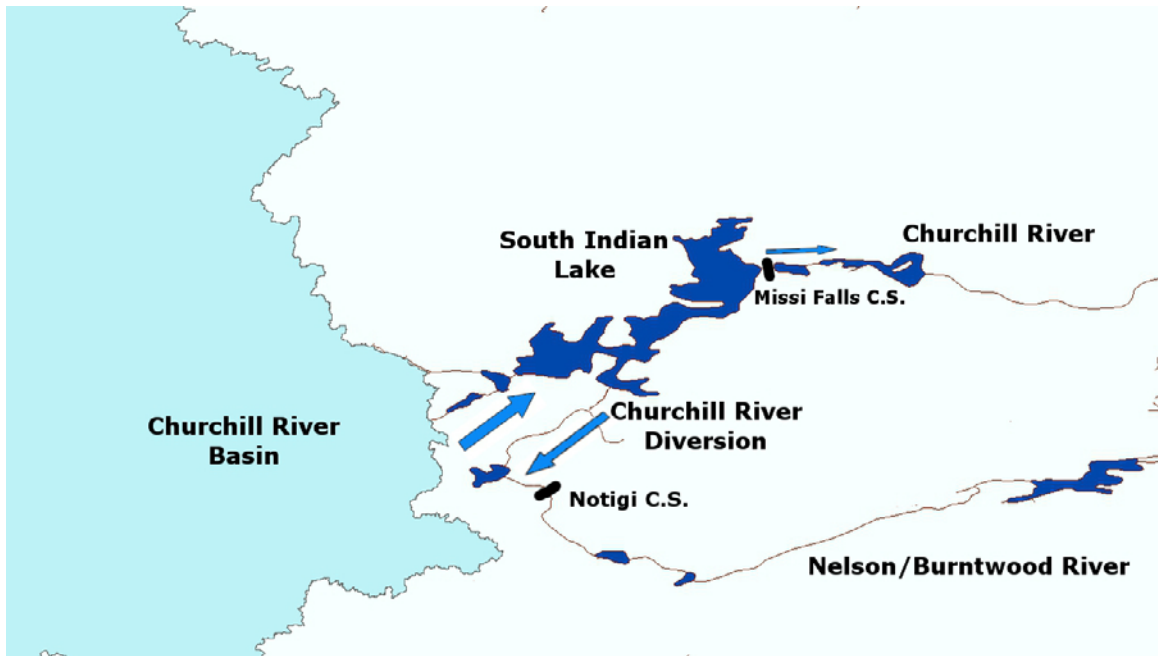
Figure 1: Schematic view of Churchill River Diversion (adapted from (Manitoba Hydro, 2009))

Understanding the impacts of climate change as well as the uncertainties related with them will give Manitoba Hydro a useful watershed management tool. This tool will prove useful for not only managing the assets which they currently operate, but also in the development and planning of those which will enter their network of generating facilities in the future.

1.2 Scope

This project may be broken down into three distinct portions. The first stage involves choosing, developing and calibrating hydrological models to simulate the

conditions within the Churchill River watershed. Models were chosen based on robustness of their calculations, their proven ability in previous climate change studies, and their ability to simulate watersheds the size of the Churchill River basin in a feasible manner. This portion entails collecting the required physiographic, meteorological, and hydrometric data required to set up and calibrate each model. Once this data is collected, each of the models may be implemented, calibrated and validated to a sufficient standard.

The secondary portion of this project examines the impacts of climate change on the hydrological response of the Churchill River basin. This task will be accomplished through using the hydrological models which were previously set up. These models will be used to simulate the full range of global circulation models made available for this project. The model results from these runs will be used to represent the projected impact of climate change on the hydrological response of the basin.

Upon completion of the climate change modelling portion of the project, the final stage of the project involves performing uncertainty analysis on the results which were obtained previously. This includes examining several what-if scenarios, performing sensitivity analysis on several groups of parameters, and identifying all areas of the modelling process which introduce uncertainty to the results and analyzing these with the goal of limiting the impact of this uncertainty.

1.3 Objectives/Long Term Goals

This project has three main objectives. The first is to prove that modelling large, data sparse watersheds with a reasonable amount of certainty is possible with current hydrological modelling technology. Further to that, the objective is to set up multiple hydrological models to simulate the hydrological conditions within the Churchill River Basin. This portion of the project will serve to expand the usage of hydrological models and promote their usage in areas where they were previously dismissed as impractical or unusable due to unreasonable amounts of uncertainty.

The second objective of the project is to quantify the projected impact that climate change will effect on the hydrological response of the basin. Each of the global circulation models made available for this project will be used and an envelope curve of hydrographs will represent the best, worst and median scenarios of what may be expected as the climate continues to change in the region. This analysis will contain results obtained from all available climate models (approximately 140 GCM simulations for each future time period) for three of the most commonly used emissions scenarios. Achieving this objective will supply the project sponsors with enough information to be able to better support their resource management decisions.

The final objective of the project deals with both identifying and understanding the uncertainty which is related with the calculations made in the previous sections. By understanding these uncertainties, areas which require more focus

can be determined and explored in detail. This extra study will allow for an increased understanding of the changes in the hydrological regime as they begin to be realized in the physical watershed.

Overall, the long-term goal of the project is to develop a framework to understand the potential effects of climate change in this large, data-sparse basin. This will provide the scientific community with the tools which are prerequisite to creating an asset management strategy for their generating stations located within the basin. This will allow for the most efficient usage of the water resources which have been made available to them.

1.4 Document Organization

The following section outlines the organizational structure of this thesis. Included below are the titles of each chapter which are followed by a brief summary. This is intended to guide reading and assist the reader in locating pertinent information. Any aspects of the document which have been published are noted as well.

Chapter 2: Background Information

This chapter details some of the most important information required to fully understand this thesis. The concepts of hydrological modelling and the current state of climate change research are discussed.

Chapter 3: Description of Study Area

In this chapter, the layout of the study region is discussed. The current climate, as well as geography and hydrology of the basin will be discussed and analyzed. How the basin's water resources are currently utilised is also addressed, including any diversions as well as any plans for future development in the region.

Chapter 4: Model Calibration over the Churchill River Basin

An introduction to each of the three hydrological models used in this project as well as details on their implementation and calibration are discussed in this chapter. The hydrological model selection process as well as choice of calibration metrics used during the modelling and calibration portion of the project is also discussed here. Results from this section were presented to the 64th annual CWRA National Conference in St. John's, NL, Canada in June 2011.

Chapter 5: Climate Change Quantification

In this chapter, the current methods for predicting and quantifying the potential effects that climate change may have on the earth's climate are explored. As well, the selection process and which models were selected for the study for climate models are detailed. This chapter also discusses the methodology which is used to implement the predicted climate change results in each of the hydrological models in this study.

Chapter 6: Climate Change Impact Assessment using Hydrological Models

This chapter is where the climate change simulations performed in this project are discussed. Changes to the flow regime resulting from each of the climate change simulations are examined and general trends are identified. The differences in results between each hydrologic model are examined and the groundwork is laid for the uncertainty analysis which follows.

Chapter 7: Uncertainty Analysis and Discussion

In this chapter, the uncertainty related to the climate change impact assessment on the hydrological response of the basin is examined. The major sources of uncertainty are identified and quantified in order to define the portions of the project which convey the most uncertainty to the final result. To conclude the chapter, the uncertainty results obtained in this chapter as well as the climate change results from the previous chapter are also discussed and the main points emphasized.

Chapter 8: Conclusions

The conclusions of the project are summarized in this chapter. The results of each the previous chapters are consolidated here and overall conclusions are drawn. Finally, the significance of the findings is discussed, and possible research initiatives for future projects are laid out.

Chapter 2: Background Information

The following sections give the background information required to fully comprehend the study. Information presented includes background on hydrological modelling, climate change and climate change modelling, and the ClimHydro project which this study is a part of.

2.1 Background on Hydrological Modelling

Watersheds are essentially just complex systems where water progresses through a water cycle and completes several complex processes. This characteristic lends itself well to the development of numerical models which are able to mathematically represent these processes to varying degrees. Hydrological models vary in their degree of complexity and while each is able to estimate the amount of water which passes through the system, each model arrives at this result in a slightly different way. Computer-based hydrological models range in complexity from simplistic spreadsheet-based models capable of estimating flow in small basins, to large-scale distributed models that simulate the hydrology of basins covering one million square kilometres or more. The following section provides a brief introduction to the types of hydrological models used in this study and the reasons they were chosen for this study, but should not be considered a complete reference on the science of hydrological modelling.

The most basic form of hydrological model is the Rational Method (Mulvany, 1850; Thompson, 2007). The use of this method is recommended only for very

small watersheds and uses the following equation to estimate discharge given a certain rainfall event:

$$Q = C_u CiA \qquad\qquad (2.1)$$

where: Q = computed discharge (cms, cfs),

C_u = units conversion coefficient (unitless),

C = runoff coefficient (unitless),

i = rainfall intensity (mm/hr, in/hr), and

A = watershed drainage area (km^2, sq. mi.).

Examining this equation, only the total volume of runoff resulting from a rainfall event can be calculated, while the timing of the peak flow is neglected. In this method, each of the processes which occur in the basin to affect the volume of runoff are lumped into the dimensionless runoff coefficient, and as a result, they cannot be examined individually. Because the Rational Method is not recommended for large watersheds ($>13km^2$) (Thompson, 2007) it is not applicable in the case study of the Churchill River basin, and therefore warrants no further discussion, however, this equation does form the basis for how simple lumped models calculate runoff within watersheds.

In order to properly calculate the flow produced by an area as large as the Churchill River basin, a more complex type of model which takes into consideration some of the different characteristics of the catchment is necessary. There are two main characteristics which define how each hydrological model calculates the runoff in a catchment: (1) model structure, and (2) distribution

9

method. Models can either be conceptual or physically-based in structure, and either lumped or spatially distributed. The following explains how each of these characteristics affects the hydrological model and the strengths and weaknesses associated with each method.

Conceptual models are a relatively simple way to calculate runoff for a given basin and hydro-meteorological conditions. These models represent the processes which take place within the basin using a series of empirical equations using a variety of coefficients and parameters. There are many different conceptual models available, and each uses a slightly different set of empirical equations and coefficients/parameters to calculate the discharge in generated by certain conditions. The basic concept in each of them is that the model takes the existing conditions (temperature, precipitation, soil moisture, snowpack, etc.) that are supplied to the model, and applies a series of conceptual equations at each time step in order to determine the amount of runoff generated. These conceptual equations use coefficients and parameters which have no basis in reality and cannot be physically measured in any way. Many of the conceptual models portray the basin as a series of reservoirs which each have inputs and outlets. An example of a typical conceptual model schematic is shown below (Figure 2).
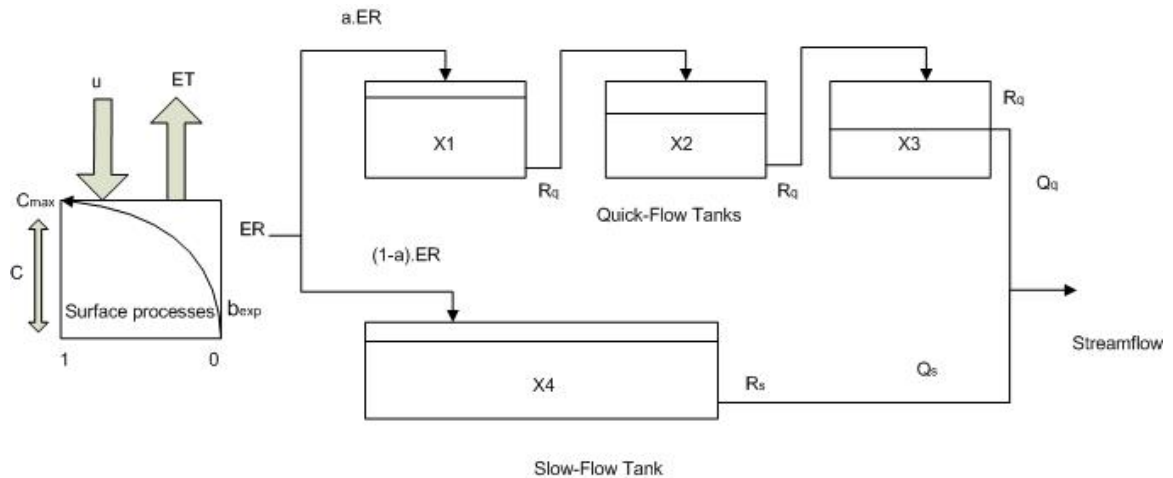
Figure 2: Schematic of a typical conceptual hydrological model (adapted from (Moradkhani, Hsu, Gupta, & Sorooshian, 2005))

By using a series of reservoirs in this way, it is possible to maintain the hydrologic budget (i.e. no water is lost or gained, just transported) while being able to differentiate between runoff which is generated relatively quickly and water which is not immediately translated into river discharge. Each of the models will differ in how many tanks are used in order to model the basin and what equations are used to distribute the water between these tanks, but in general they all follow the same concept. Because of their relative simplicity, these models are generally regarded as useful tools which are able to capture the dominant catchment dynamics while remaining computationally efficient (Kavetski, Kuczera, & Franks, 2006).

Perhaps a defining characteristic of conceptual models is that their parameters have no physical basis in reality. As a result they cannot be measured and must instead be inferred or calibrated using other data. This is most commonly done using a measured discharge from the catchment. There is much debate

11

surrounding the `best` method for calibrating these models, but in general each model has a known parameter range which is considered feasible based on results gathered in previous test cases. While a simple search algorithm may not return the optimal solution to the problem, it often will deliver a set of parameters which is able to simulate the hydrology of the basin well enough for the purposes of the particular study. In this study two of the models which are used (HMETS and HBV-EC) are considered to be conceptual hydrological models, and one (WATFLOOD^{TM}) is considered to be partially conceptual because while the routing equations are based on physics, processes like baseflow and interflow are calculated empirically.

Physically-based hydrological models are a more elaborate method for predicting the hydrology of a watershed. These models attempt to capture what is truly occurring in the catchment by expressing each hydrological process in terms of an equation rooted in pure physics. While all models have parameters, these equations often have parameters which are directly measurable from point field observations. Because they can show the modeller how much water is being used up by each of the processes, these models are able to provide the user with a much more detailed picture of what is actually happening within the basin, both in terms of water and energy transfer. The total discharge of the basin is the generally expressed as the sum of the water which enters (either via precipitation or runoff from upstream contributing area) less the amount of water used up by processes which do not contribute to discharge such as infiltration or evaporation. While calculating each of these small processes potentially

provides an additional output variable to calibrate to, it also adds considerable additional complexity to the process of calibration. An example schematic of a physically based hydrological model is shown below (Figure 3).
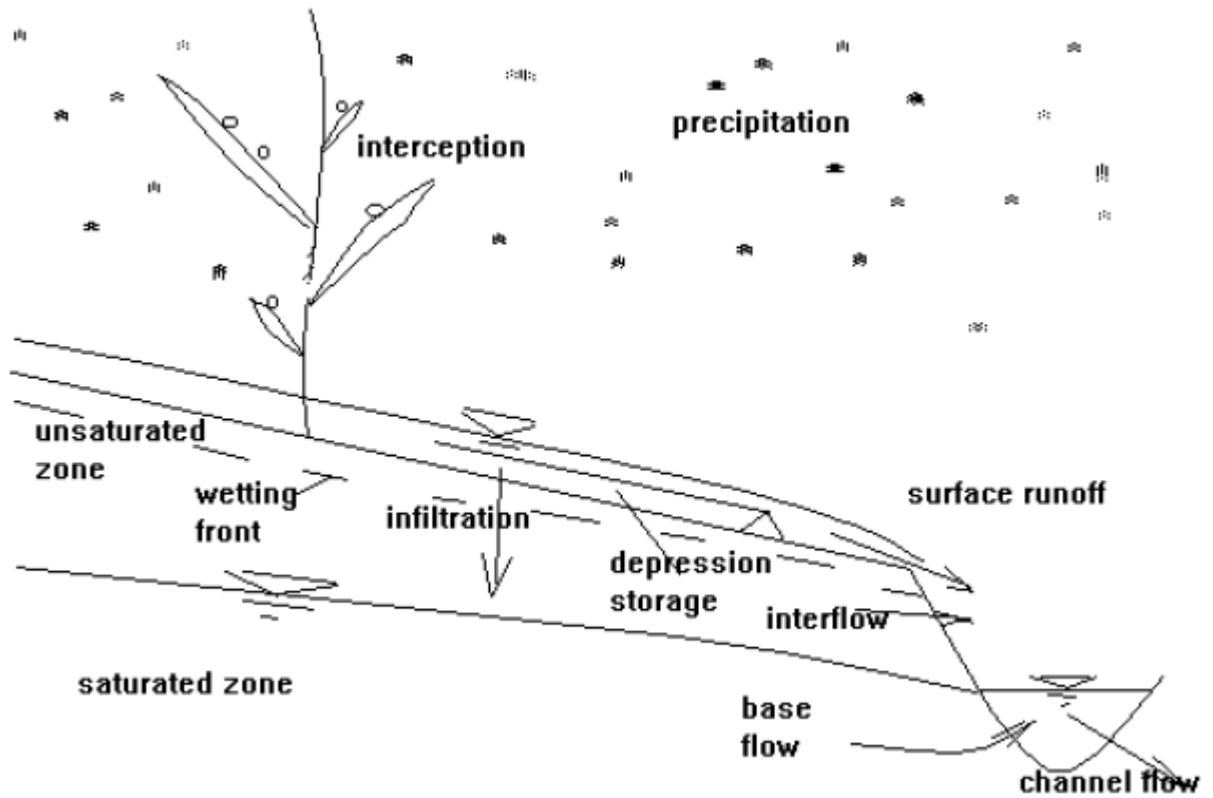
Figure 3: Schematic of a physically-based hydrological model (WATFLOOD[TM]) (Kouwen N. , 2011)

The processes which occur within the hydrological regime of a meso-scale catchment (>1000 km^2) are extremely complicated and practically impossible to model in totality. Even if they could, such a model would exceed the limits of practicality in computational power and runtime, even with today's technology. This means that any physically-based model does not respond exactly as a watershed would, but can operate as a reasonable simile for the purposes of most studies of the overall hydrological behaviour of the region. Often it is not

practical or even possible to measure the all of the characteristics which are required for the calculation of the basin response, particularly since parameterizations are based on field observations which are observed at individual points in space. As a result, they will require some measure of calibration. WATFLOOD^{TM} is the most physically-based model (classified as a partially physically-based model, with some processes rooted in physics and others that are conceptualized for computational efficiency and practicality) which was practical for use in this study.

In addition to the methodology which is used to calculate the basin response, hydrological models can either be lumped or distributed. Lumped hydrological models, as their name suggests, lump large areas together and perform the runoff calculations using these large areas. This method of runoff calculation is much simpler than the distributed alternative. While lumping large areas together reduces the expected accuracy of the results, it helps to keep computation times manageable. The HMETS model is considered to be a fully lumped hydrological model.

Conversely, distributed hydrological models break the basin down into several smaller areas which are chained together to determine the overall basin response. Often the models will discretize the basin into a rectangular grid, but some models allow the user to define their own regions in whichever shape they choose. Essentially, these grids are each independent watersheds on which the hydrological calculations are performed and a discharge is calculated. These grids are then linked together using some sort of routing scheme and the

response of the basin as a whole can be calculated. Another advantage of this type of system is that the same model can calculate the discharge at a wide variety of locations throughout the basin instead of only at the outlet. A lack of available data can cause the performance of distributed models to suffer because assumptions have to be made to replace measured data. The HBV-EC model is a partially distributed model while the WATFLOOD^{TM} model is considered to be fully distributed.

Each of the models which are being utilised in this study will be more fully described in their respective sections. Details will be provided on the structure each model utilises as well as the key differences and similarities between those models used as analytical tools in this project.

Each of the above described characteristics of types of hydrological models has their own set of advantages and disadvantages. The purpose of this study is not to determine which type of model is the best model for the Churchill River basin but rather to develop a system which facilitates an understanding of the uncertainties related to the modelling of the hydrological processes and climate change within the region. As a result, a modelling suite which provides a wide range of model types (i.e. lumped conceptual, semi-physically based distributed, etc.) will be used in order to assess the differences in results which are caused by the selection of hydrological model type.

2.2 Background on Climate Change

It has been widely reported that the climate of the earth is changing at a rate which far exceeds any other that is currently on record (IPCC, 2001; Bloschl & Montanari, 2010). Many reasons have been offered as to why this is occurring, ranging from entirely anthropogenic reasons to completely natural global warming. The fact remains that the climate of the earth is changing. According to reports issued by the IPCC, the average temperatures in the northern hemisphere during the previous 50 year period were "very likely" (>90% probability) the highest of any 50 year period seen in the past 500 years and "likely" (>66% probability) the highest period during at least the past 1300 years (IPCC, 2007). It has also been noted that the atmospheric concentration of CO_2 has increased significantly during the previous 250 years. Based on air samples taken from ice cores, it is estimated that the atmospheric CO_2 levels remained constant at 280±20 ppm. Since the advent of the industrial revolution, atmospheric levels have increased approximately exponentially to their current levels of ~380 ppm (IPCC, 2007).

As a result of this increased climatic variability and our increasing dependence on the climate to sustain quality of life, a concerted worldwide effort among scientists has invested a significant amount of resources into studying this phenomenon and attempting to develop an understanding of how to adapt to or mitigate the potential negative effects which it may cause (Axworthy, et al., 2001; van Vuuren, et al., 2011).

The Earth's climate is a complex system of interactions between many different components. Several earth systems play a role in the process of climate change. Changes can occur in the amount of solar radiation which is absorbed by the earth, the composition or circulation patter of the atmosphere and the evaporation/precipitation cycles of the earth's hydrology. The cryosphere (ice and snow), land surface usage and ocean systems can also experience changes which can cause a departure from climate equilibrium (Le Treut, et al., 2007). The changes to these systems can be caused by human interference or by the natural processes which occur without any artificial interference. Each of the aforementioned systems consists of a delicate balance of interactions which play an integral part in maintaining the earth climate as we know it. Small changes can cause significant disruptions to this system.

While the process of climate change is undoubtedly complex, so much so that complete human understanding is nearly impossible, it is widely believed that the increase in temperature is at least partially the result of an increased level of greenhouse gases (GHG) in the atmosphere. These gases (CO_2, NO_x, fluorocarbons, water vapour, etc.) have been shown to substantially increase the amount of heat which is reflected back to the earth in the form of long-wave radiation (Le Treut, et al., 2007). This in turn has lead to a surplus in the heat budget for the surface of the earth and a general gradual warming trend over the past several decades (IPCC, 2001)

These worldwide changes in temperature have had, and are expected to continue to have an impact on many aspects of the Earth system (ocean levels,

desert areas, etc.) (Rosenzweig, et al., 2007). Hydrologically speaking, higher temperatures lead to longer summers and higher evaporation rates (given sufficient sources of moisture) across large areas of the world. This translates to a reduction in the amount of streamflow generated in many catchments. Also of note is the change in the amount and timing of precipitation. In the northern hemisphere, wetter winters and drier summers, coupled with earlier spring flooding events are likely to be the result of the anticipated changes in climate (Rosenzweig, et al., 2007).

2.3 Background on global climate models

Where there exists a system with complex interactions that deeply affect the way that the human society functions, undoubtedly someone will try to develop an understanding of this system by modelling it. The global climate is no different, and several groups around the world have developed models to understand how the climate works and which of these complex interactions play a major role in determining the state of the world's climate.

These models are referred to as global climate models, or GCMs, and are generally very complex. The most recent versions of the models couple atmospheric, general circulation, and ocean and sea-ice aspects into one unit (Flato, et al., 2000). There may be as many as 40 output variables from each model, including temperature, precipitation, air pressure, and many others. These outputs can be used by those who require knowledge of trends in any of these variables in the past, present and future timeframes.

GCMs are evaluated at a series of discrete grid cells distributed throughout the surface of the globe. These grid cells are evenly distributed at the specified resolution of the model. The resolution of the GCMs range from as much as 5 degrees (~550 km in the study region) to as little as 1.125 degrees (~135 km in the study region). A brief description of each of the models used in this study is found below (Table 1).

Table 1: Description of climate models utilised for climate change impact assessment

Developer	Model Name	Country of Origin	Resolution (degrees LongxLat)
Bjerknes Centre for Climate Research	BCCR BCM2	Norway	1.875x1.875
Canadian Centre for Climate Modelling and Analysis	CCCMA CGCM3 T63	Canada	2.8x2.8
	CCCMA CGCM3	Canada	3.75x3.75
Centre National de Recherches Météorologiques	CNRM CM3	France	2.8x2.8
Commonwealth Scientific and Industrial Research Organization	CSIRO MK3_0	Australia	1.875x1.875
	CSIRO MK3_5	Australia	1.875x1.875
NOAA/Geophysical Fluid Dynamics Laboratory	GFDL CM2_0	United States	2.5x2.5
	GFDL CM2_0	United States	2.5x2.5
NASA/Goddard Institute for Space Studies	GISS AOM	United States	4x3
	GISS MODEL E H	United States	5x4
	GISS MODEL E R	United States	5x4
Institute of Atmospheric Studies	IAP FGOALS	China	2.8x2.8
Istituto Nazionale di Geofisica e Vulcanologia	INGV ECHAM4	Italy	1.125x1.125
Institute for Numerical Mathematics	INMCM3	Russia	5x4
Institut Pierre Simon Laplace	IPSL CM4	France	3.75x2.5
Centre for Climate System Research	MIROC3_2 HIRES	Japan	1.125x1.125
	MIROC3_2 MEDRES	Japan	2.8x2.8
Meteorologisches Institut der Universität Bonn	MIUB ECHO G	Germany	3.75x3.75
Max Planck Institute fur Meteorologie	MPI ECHAM 5	Germany	1.875x1.875
Meteorological Research Institute	MRI CGCM2_3_2a	Japan	2.8x2.8

National Centre for Atmospheric Research	NCAR CCSM3	United States	1.4x1.4
	NCAR PCM1	United States	2.8x2.8
Hadley Centre for Climate Prediction and Research	UKMO HADCM3	United Kingdom	3.75x2.5
	UKMO HADGEM1	United Kingdom	1.875x1.25

Many climate models are available that provide predictions of the future climate in the Churchill River basin and surrounding area. The raw temperature and precipitation data from these climate models was made available for this project through collaboration with the Ouranos Consortium on Regional Climatology and Adaptation to Climate Change and the ClimHydro Project. Data from each available GCM was used in order to give the widest range of possible results. Of the GCMs provide a different piece of information that is important to the analysis.

These GCMs are calibrated over the period of climate data which has been observed. Many of the models are spun up as far back as 1800. Observed data for the climate and any driving variables are used as input for as long as it is available to calibrate the model response. This calibration is undertaken in order to have these models predict the correct global climate response for the right reasons by simulating the climatic processes correctly to the fullest extent possible. Once this process has been completed to a given standard throughout the largest possible region of the globe, the model is forced using anticipated values for all of the same variables. These anticipated values are devised based on the scenarios and storylines which have been provided by the assessment

reports of the International Panel on Climate Change (IPCC, 1990; IPCC, 1996; IPCC, 2001; IPCC, 2007). A description of the scenarios and storylines may be found below in section 5.3, focusing on the models selected for this study. Results from these models provide policymakers and researchers with an estimate of the possible climate of the future. The models are run for varying lengths into the future providing estimates as far ahead as 2200 of the varying elements of the global climate under several sets of future conditions.

2.4 Regional climate models and downscaling methods

Regional climate models (RCMs) are very similar to GCMs. They generally can be used to predict the same set of variables, but on a finer scale. Whereas GCM resolution is usually on the order of hundreds of kilometres, RCM resolution may be as fine as tens of kilometres (Wilby, *et al.*, 2004; Xu, Widen, & Halldin, 2005; Kling, Fuchs, & Paulin, 2012). RCMs are dynamically downscaled and are dependent on the larger GCMs for their boundary conditions and utilise a finer grid to take into account local phenomena such as topography which may have an effect on the climate. Statistical downscaling is also based on the larger GCMs but fits trends between GCM outputs and smaller scale weather patterns which may be of consequence in smaller modelling studies. Each of these methods may be used to identify trends which may be present within smaller portions of a large area. According to Wilby *et al.* (2004), these smaller scale trends are well suited to providing input for small scale studies, as well as studies which involve regions where there is complex topography, highly heterogeneous land-cover, or for coastal or island regions.

The Churchill River basin is generally defined as a large basin, with a total drainage area into Southern Indian Lake of over 250,000 km^2. This makes the basin large enough that multiple grid points of even the GCMs with the coarsest resolution fall within the boundaries of the watershed. The topography of the area is not complex; the region exists mainly over a flat prairie with very small slopes throughout the majority of the basin. Finally, while the basin does contain several large lakes, the climate of the area is not referred to as a coastal or island region. For these reasons, and for the sake of simplicity and time restraints, RCMs were not used in this study. However, for future studies on this region, a comparison of GCM- and RCM-based climate predictions should be made.

2.5 Background on the ClimHydro Project

The ClimHydro project is a collaborative effort between Manitoba Hydro, Hydro-Quebec, University of Manitoba, Ecole-Technologie Superieure, and Ouranos. These entities are combining their resources in order to estimate the impact of climate change on meso-scale hydrological basins in Quebec and Manitoba that are of particular interest to the electrical utilities involved. The Churchill River basin is the primary interest for Manitoba Hydro and the University of Manitoba.

The project consists of several phases which chronicle the efforts which each of the involved entities are taking to limit the impacts that climate change will have on their operations, and to optimize resources for future power developments (Leconte, 2007).

The first phase of the project deals with the estimation of climatic projections. Some of the topics examined in this phase of the project include acquiring data from the GCM simulations, analyzing that data using statistical techniques, downscaling, and utilising RCM projections. The first phase of the project provides the data which is required to complete the second phase.

In the second phase of the project, the projections from the climate models are used to determine the potential impact which may be felt on the hydrological regimes of both Quebec and Manitoba. This phase also includes a detailed uncertainty assessment of the results which were caused by the changing climate. Several different hydrological models have been used extensively by researchers in Manitoba and Quebec in order to complete this portion of the project.

The final phase of the project deals with developing adaptation strategies. This phase utilises the impact assessment data from the previous phases in order to determine the optimal strategy for the major utilities in both provinces to employ in order to maximize their benefits or minimize the potential losses which may be caused by climate change. This strategy is the final deliverable for the project and gives the project sponsors solutions to deal with climate change effectively.

The climate change impact assessment and subsequent uncertainty assessment on the Churchill River basin falls into the hydrological modelling assessment phase of the project (phase two). Using climate projection data obtained during the previous phases of the project, this project will provide an estimate of the

impact of the anticipated changes on the availability of water resources in northern Manitoba and specifically from the Churchill River basin.

Results from this phase will be utilised both directly by the hydroelectric utilities (i.e., specifically Manitoba Hydro), but will also be used to develop mitigation and adaptation measures during the later phases of the project. These results will provide valuable information to water resource scientists and managers in Canada, including at Manitoba Hydro, which will assist them in developing strategies for the development of future generating stations and management plans.

Chapter 3: Description of Study Area

The following chapter describes the hydrological, geographical and physiographic conditions which exist within the Churchill River basin. Knowledge of the watershed will prove useful when examining the modelling results, which use, and attempt to simulate some of the observed conditions outlined here. Also discussed in this chapter will be the Churchill River diversion, which allows the flow from the Churchill River to be used in the Manitoba Hydro generating stations on the Nelson and Burntwood river systems to the south, and details on the generating stations located on these rivers.

3.1 Churchill River Basin

For the purposes of this study, the Churchill River basin (CRB) is the area that is drained by the Churchill River in the north-western portion of Canada. In the modelling portion of the project it was not feasible to simulate the entire basin. As a result, the upstream portion of the basin was used as a surrogate, and as a general simplification this modelled portion of the basin is referred to as the CRB. The map below (Figure 4) shows the location of the basin with respect to the other major drainage basins in the North American continent with the modelled portion upstream of Otter Rapids outlined in red.
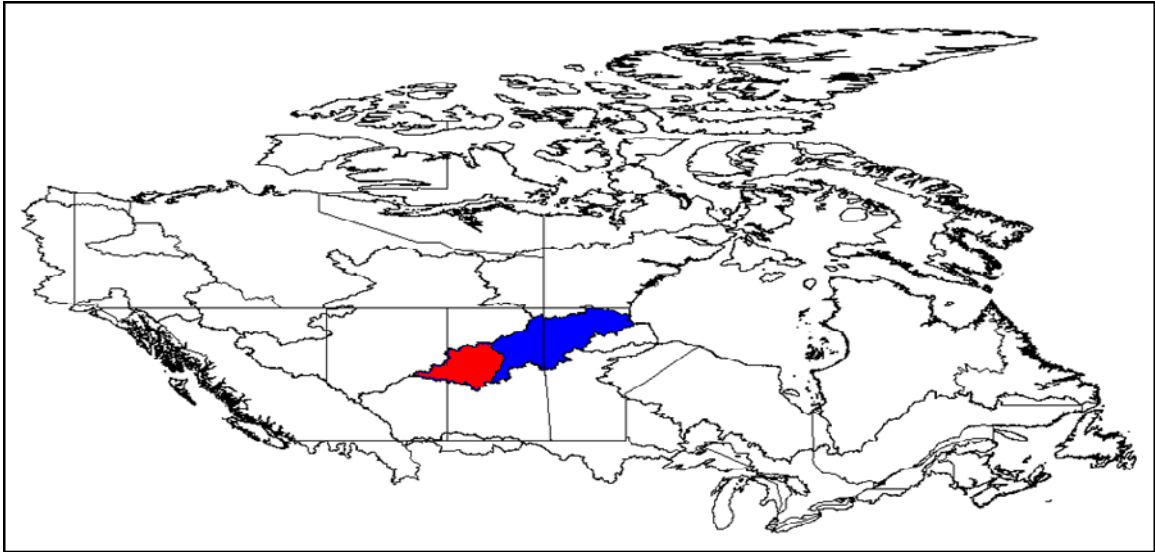
Figure 4: Major drainage basins of Canada, with the CRB highlighted in blue (Atlas of Canada, 1985)

In the sections that follow, many important aspects of the basin will be discussed, including the geography, hydrology and level of development within the CRB. An appropriate level of understanding of these conditions is vital to an in depth hydrological assessment of the Churchill drainage basin.

3.2 Geography and Climate

Of the approximately 2.8 million square kilometres which drain into Hudson's Bay, roughly 280,000 are from the Churchill River basin (Atlas of Canada, 1985). The headwaters of the basin extend nearly to Fort McMurray and Edmonton, Alberta while the outlet is located at the town of Churchill, Manitoba into Hudson's Bay. The drainage area of the Churchill River lies in parts of three Canadian provinces: Alberta, Saskatchewan and Manitoba. Population within the basin is sparse and settlements are separated by great distances. Notable communities include Cold Lake, AB, La Ronge, SK and Lynn Lake, MB. Larger

towns lying near the basin to the south include the Prince Albert, SK, and Thompson, MB and the aforementioned Edmonton, AB. The basin extends from approximately 113 degrees west longitude at the headwaters to roughly 94 degrees west where it empties into Hudson's Bay. The furthest southern portion of the watershed reaches 53 degrees north and at its northernmost point the basin reaches 59.5 degrees north latitude.

In terms of landcover and ecology, the watershed can be considered very diverse. Low-lying shrubs and pastureland are plentiful in the south-western portion of the basin (Figure 5), while wetlands and coniferous forest dominate the landscape of the north-eastern outlet portion of the basin.

Figure 5: Examples of the landscape in south-western, headwaters portion of CRB (Hryciuk, 2010)

Figure 6: Examples of the landscape in north-eastern, outlet portion of CRB

(Images above reproduced with the permission of Natural Resources Canada 2011, courtesy of the Geological Survey of Canada (Photo 2001-116 and 2001-136 by Lynda Dredge)(Dredge, 2001)**).**

The above images are intended to illustrate just how vastly contrasting the landscapes are on opposite ends of the basin. Grassland and deciduous trees are typical in the Boreal plains where the headwaters are found while bogs, rock outcroppings and coniferous trees dominate the Canadian Shield area where the downstream end of the CRB is located. A map showing the distribution of the land classes within the basin is provided below (Figure 7).
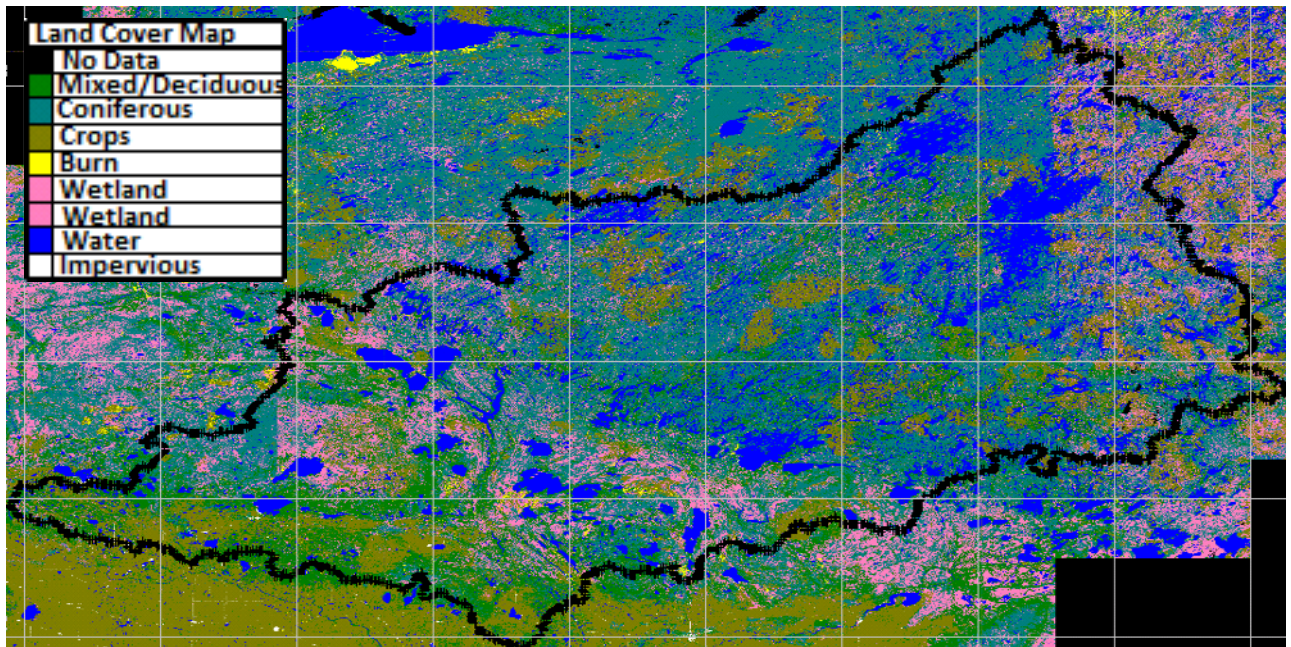
Figure 7: Land cover map of the Churchill River basin

The basin is classified as mostly cropland in the south western portion and transitions to wetlands towards the north and west. The mixed and deciduous forest from the western portion of the basin slowly becomes coniferous towards the east. Most of the areas classified as water are the lakes which cover a significant portion of the basin as well.

In addition to the land cover classification, the soil types also play an important role in the hydrology of the basin. The Churchill River basin exists within the boreal shield and boreal plains ecozones (Ecological Stratification Working Group, 1995). The boreal shield, which dominates the western portion of the basin, has very rocky soils and peat bogs. Glacial moraines and lacustrine deposits with fairly deep deposits of fertile soils on the surface are typical of the Boreal plains ecozone. Infiltration, the hydrological process most related to soil type, is generally higher in the boreal plains region than in the boreal shield.

The topography of the CRB is typical of most basins in the prairie region of North America in that the slopes are very gradual and the rivers tend to meander considerably, especially in the headwaters region. This causes delineation of the basins to be extremely difficult. Additionally, this characteristic causes the area's hydrograph to exhibit a slightly delayed response compared to basins with more substantial slopes, such as those founds in the mountainous regions.

The climate of the CRB may be classified as subarctic. The region is dominated by cold, long winters with a short, cool summer. Precipitation is relatively small, with the majority falling in rain form during the summer months. The long-term (1971-2000) climate normals observed at several Environment Canada weather stations located in or near the basin are shown below (Figure 8, Figure 9, Figure 10, Figure 11). The red bars represent the average monthly precipitation while the blue curve depicts the monthly averaged temperatures.
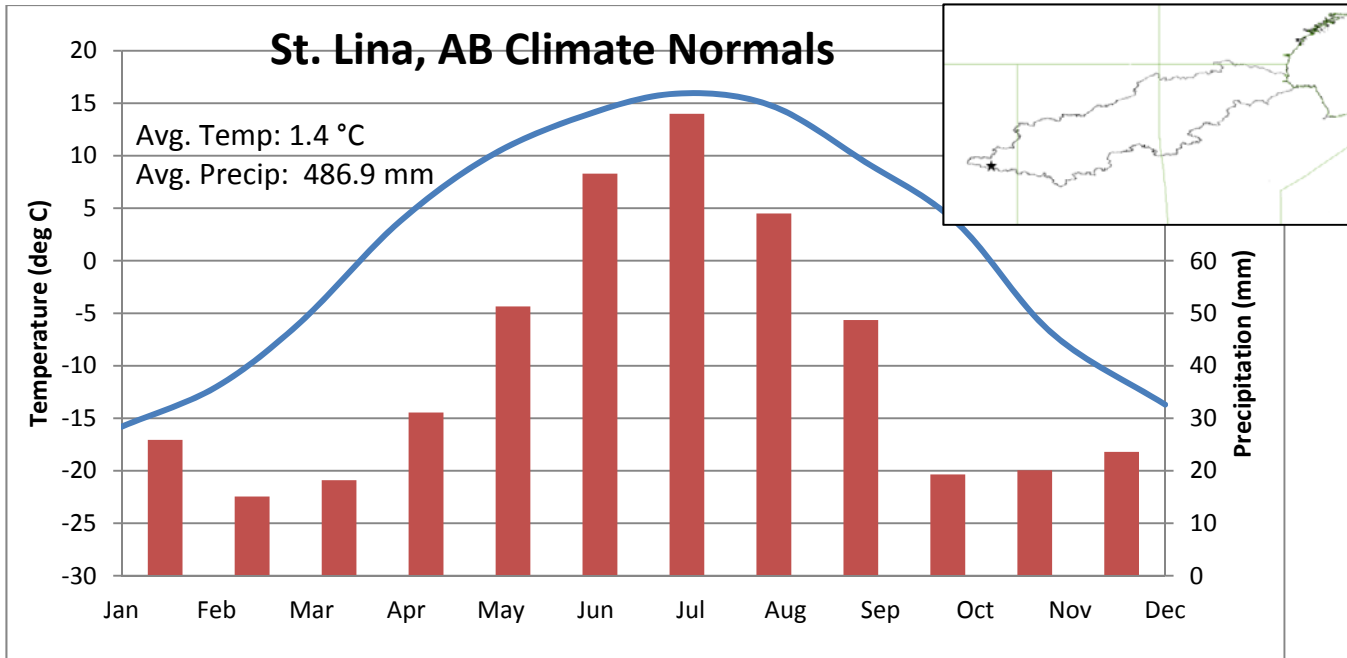
Figure 8: Climate normals for Environment Canada station at St. Lina, AB
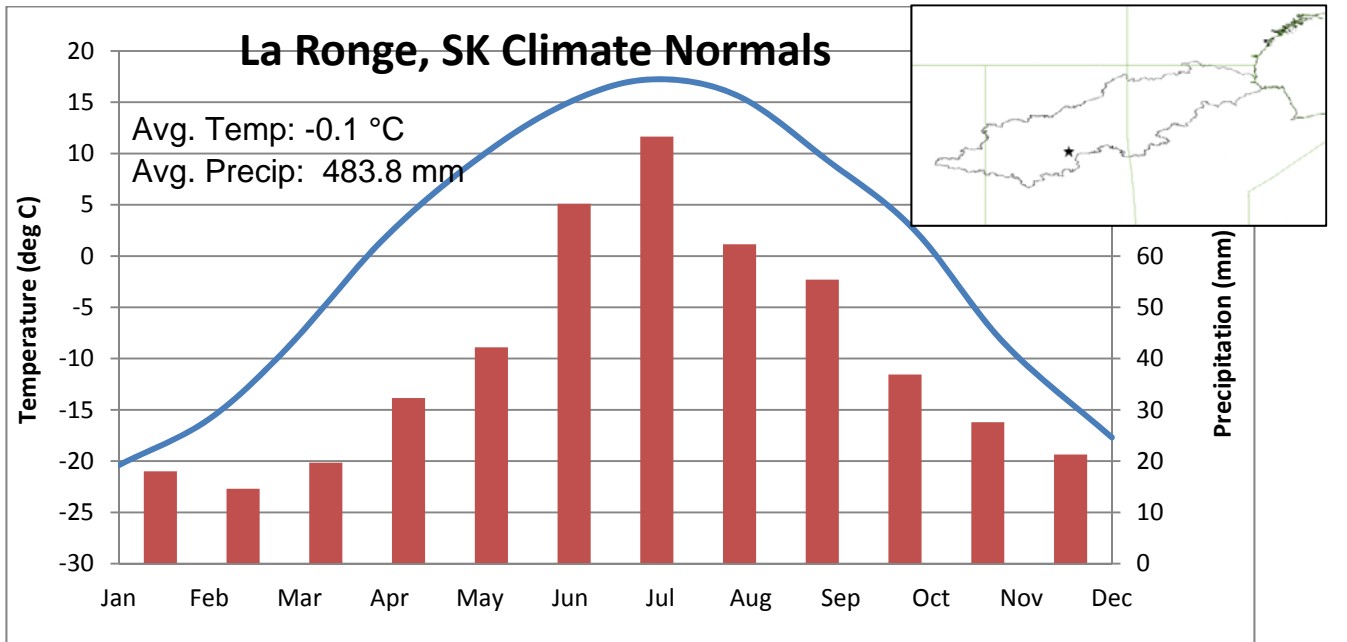
Figure 9: Climate normals for Environment Canada station at La Ronge, SK
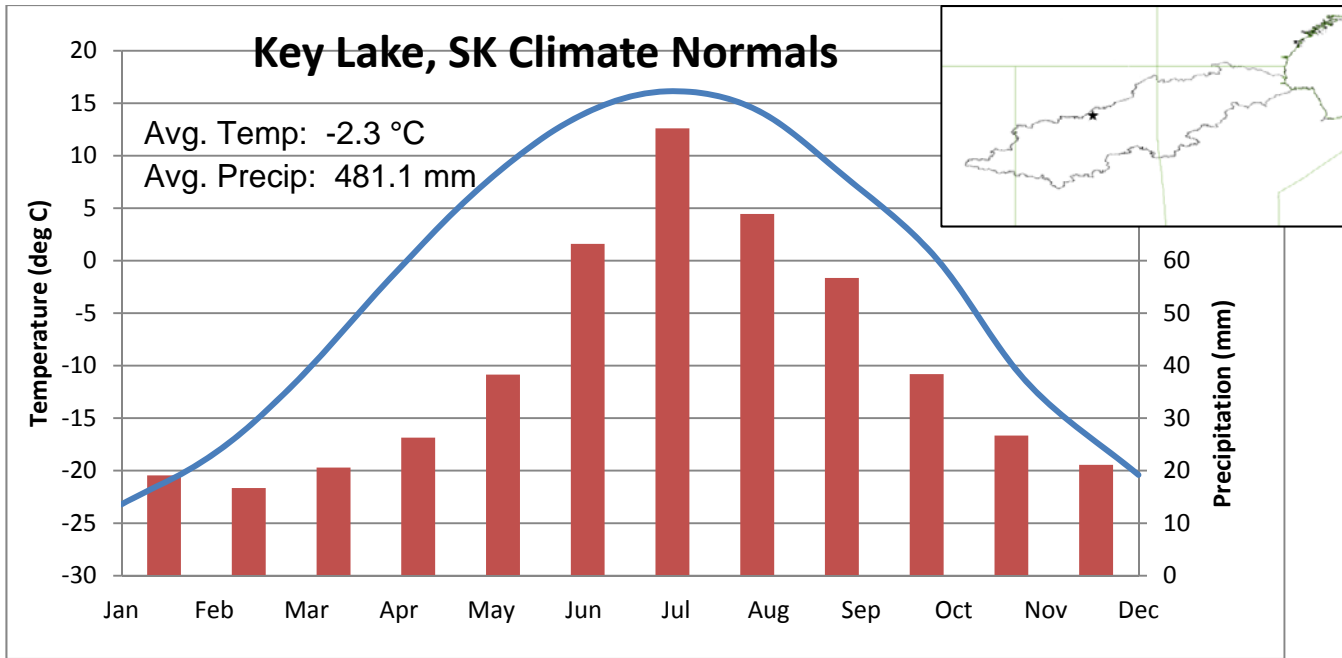
Figure 10: Climate normals for Environment Canada station at Key Lake, SK
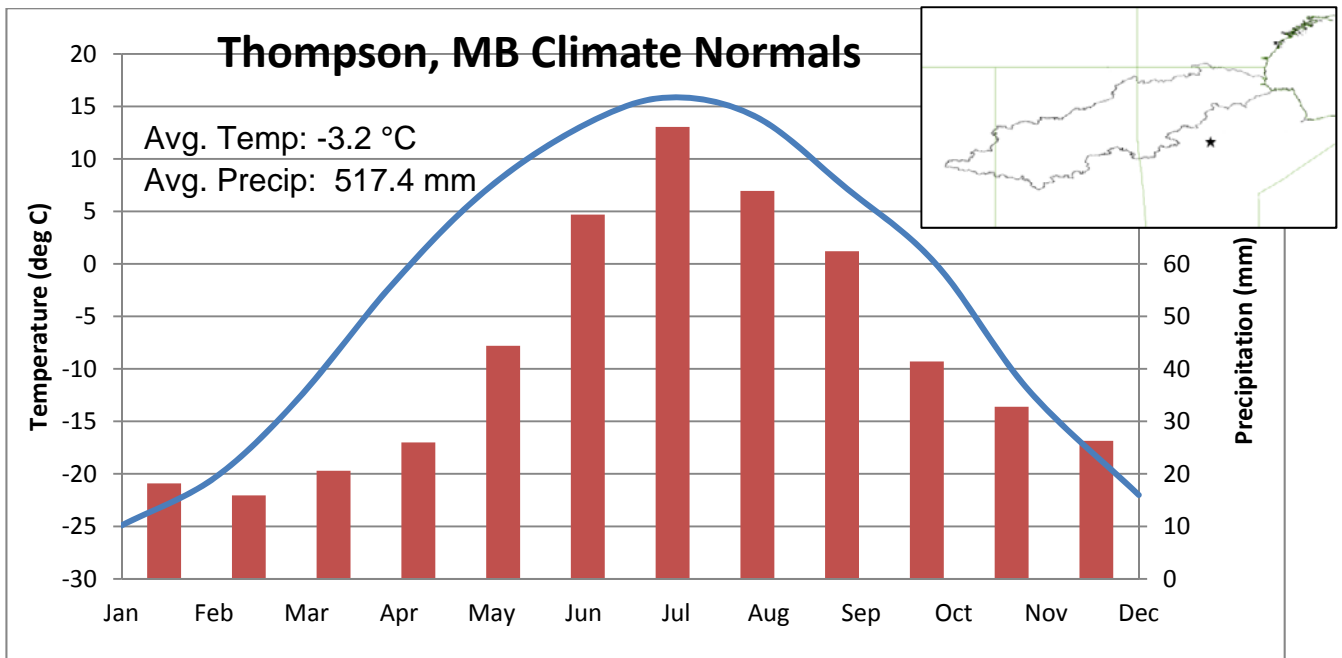
Figure 11: Climate normals for Environment Canada station at Thompson, MB

The CRB is located in the geographical centre of the North American continent.

This means that the climate of the watershed has little to no direct influence from

the ocean currents which may serve to moderate the climate. The summers in the area are considerably warmer than the winters while the climate is actually quite dry, especially in the winter months. The above climate normal plots indicate that while there is a general increasing trend in the temperature and a decreasing trend for precipitation moving from north to the south, there is not an extreme change from one end of the basin to the other given the massive distances involved. During the summer months, the climate in the basin is dominated by cyclonic systems which produce thundershower activity which is not spatially uniform. This can result in large differences observed in the amount of precipitation observed over relatively short distances. These large scale weather systems can often cover massive areas and are the result of large amounts of rapid evaporation and the mixing of hot and cold air masses. Moisture sources for these systems include surface and soil moisture and by the nature of these processes, the moisture is often recycled several times through re-evaporation and precipitation.

Approximately 200 meteorological stations provided some data for the area within the Churchill River basin. This equates to an average of approximately one station per 1400 km^2 although most of the stations are located in the southern portion of the basin and there is a much more sparse distribution in the northern section of the basin. The distribution of these stations is shown in the map below (Figure 12).
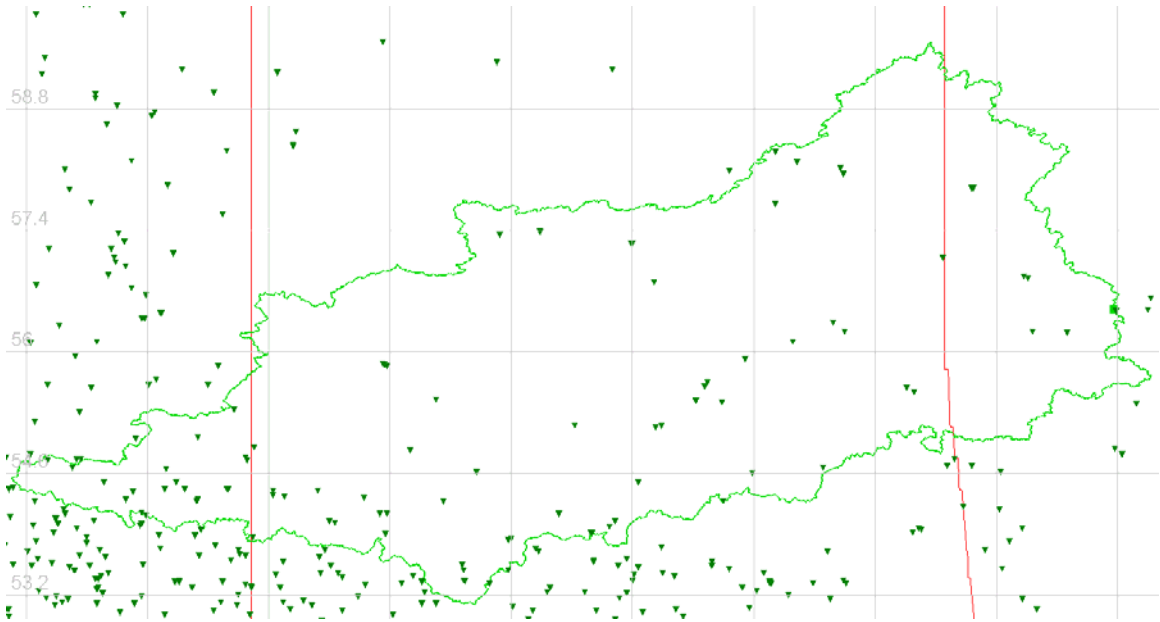
Figure 12: Distribution of meteorological stations in and around the Churchill River basin

The problem with these stations is that many do not have complete or continuous records. Many of the stations stopped recording temperature and precipitation during the 1990s. As a result there are times when less than the full set of 200 stations are used to determine the temperature and precipitation distribution of the basin. Further to that, the period which was considered for the modelling (1979-1995) reflected the availability of the most reliable meteorological records.

3.3 Hydrology

The hydrological process that has the largest visible impact on the hydrograph in this region is snowmelt at the conclusion of the winter season. This process results in a significant freshet event which is followed by lesser flows during the remainder of the summer and into the winter, when the rivers and lakes become covered in ice.

Another important process present in the region is evaporation. A large quantity of water is evaporated from the basin during the summer months due to higher temperatures and low relative humidity. The mild slopes and numerous lakes also lead to an increase of open water surface area which also leads to an increase in evaporation.

In the southwest portion of the basin (western Saskatchewan and eastern Alberta) the landscape is largely dominated by croplands and deciduous trees. This type of landscape is conducive to high levels of channel erosion as well as a great deal of infiltration and evapo-transpiration.

There are several large lakes within the portion of the basin which lies in northern Saskatchewan. These lakes act as reservoirs in the basin and "flatten out" the hydrograph. That is to say that the peaks flows are reduced and generally delayed. This effect is highly dependent on the size and level of the lake, among other factors.

The significant tributaries which contribute flow to the Churchill River include the Reindeer River, the Cochrane River and the Beaver River. The Beaver River is located in the southwestern portion of the basin. This river has a drainage area of approximately 50,000 km^2 and empties into the Churchill River in eastern Saskatchewan. The Reindeer and Cochrane Rivers are both located north of the main stem of the Churchill and have drainage areas of 65000 and 30000 km^2, respectively. The Reindeer empties into the Churchill near Reindeer Lake in

northeastern Saskatchewan while the Cochrane River empties into Reindeer Lake near the northern Manitoba community of Brochet.

In the northern portion of the basin, located in north-western Manitoba, there are large areas of wetlands and coniferous trees. These contribute to an area which has a very unique hydrological response. The coniferous trees provide a very limited amount of canopy storage while the wetlands serve to delay the flow. This combination of processes can lead to a delayed streamflow response from the region and higher levels of evaporation.

As was the case with the meteorological data, reliable hydrometric data was difficult to come by in this region as well. During the study period, a total of 11 Water Survey of Canada streamflow gauges provided data for the project. Their locations and delineated drainage areas are shown below (Figure 13), along with the elevation map of the basin.
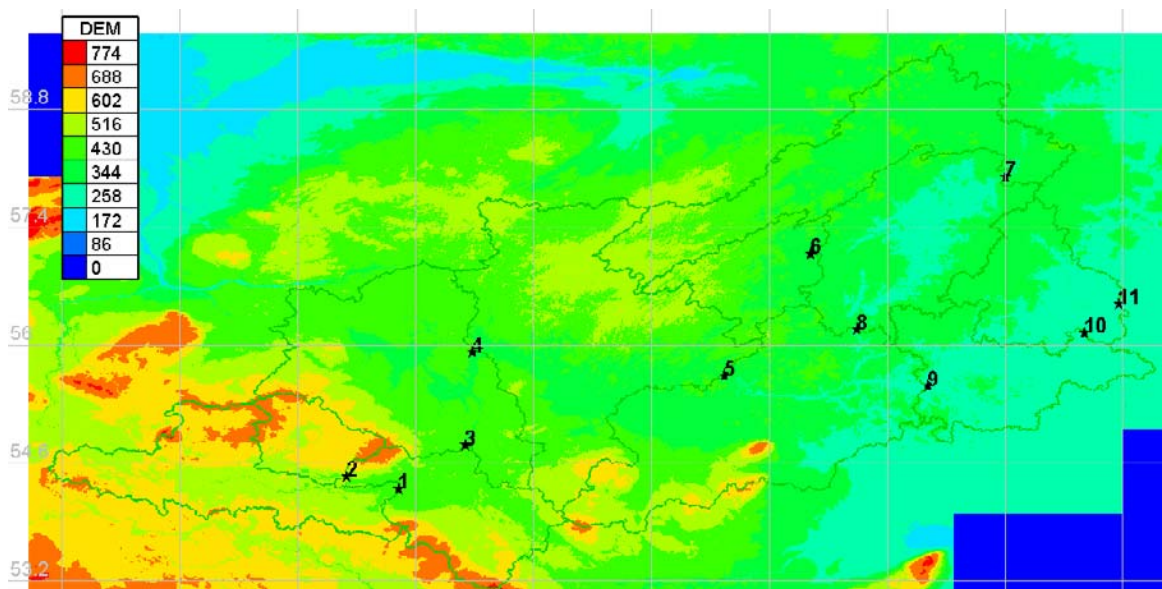
Figure 13: Location of hydrometric gauges in Churchill River basin

The gauges within the basin are fairly well spread out across the basin as well as on the main stem of the Churchill River as well as some of the significant tributaries (Cochrane River, Beaver River, and Reindeer River). The elevation map of the basin shows that there is a distinct difference between the headwaters region and the outlet region. The headwaters area has a generally higher slope while the basin flattens out approaching the outlet. This means that the watershed is more responsive to rainfall events and less flow is lost to infiltration in the southern portion while the time of concentration is higher in the northern region. The table below (Table 2) shows some information about each of the gauges, including their Water Survey gauge number, drainage area, average annual flow and the river which the gauge is located on.

Table 2: Hydrometric gauge information (courtesy Water Survey of Canada)

Station No.	WSC No.	Drainage Area (km^2)	Avg. Flow (cms)	River Location
1	06AD001	20909	14.34	Beaver R.
2	06AF005	7776	12.98	Waterhen R.
3	06AG001	47771	36.54	Beaver R.
4	06BB003	78951	106.06	Churchill R.
5	06CD002	124464	233.60	Churchill R.
6	06DC001	10220	51.57	Wathaman R.
7	06DA002	29448	178.98	Cochrane R.
8	06DD002	64442	386.88	Reindeer R.
9	06EA002	218453	681.55	Churchill R.
10	06EA006	235808	721.72	Churchill R.
11	06EB004	250823	817.18	Churchill R.

Of the 11 gauges, five are located directly on the main stem of the Churchill River while six are located on the major tributaries. Each of the gauges drains a relatively large area and in order to assist in gauge maintenance, they are generally located in or near the communities in the region. As with the

meteorological data, several of the hydrometric stations do not have a complete dataset and are not currently recording flows. The period chosen for the modelling exercise (1979-1995) was chosen due to this limited data availability.

3.4 Churchill River Diversion

The CRB is important to Manitoba for several reasons, but perhaps the most important is the flow which it contributes to the generating stations downstream on the Burntwood and Nelson River systems via the Churchill River diversion (Figure 14). Completed in 1977 by Manitoba Hydro, the diversion allows the utility to be able to utilise the hydroelectric potential of the CRB flows without incurring the substantial additional expense related to constructing generating stations on the much more remote Churchill River. It was also believed that construction on the lower Churchill River would also entail more social and environmental costs.
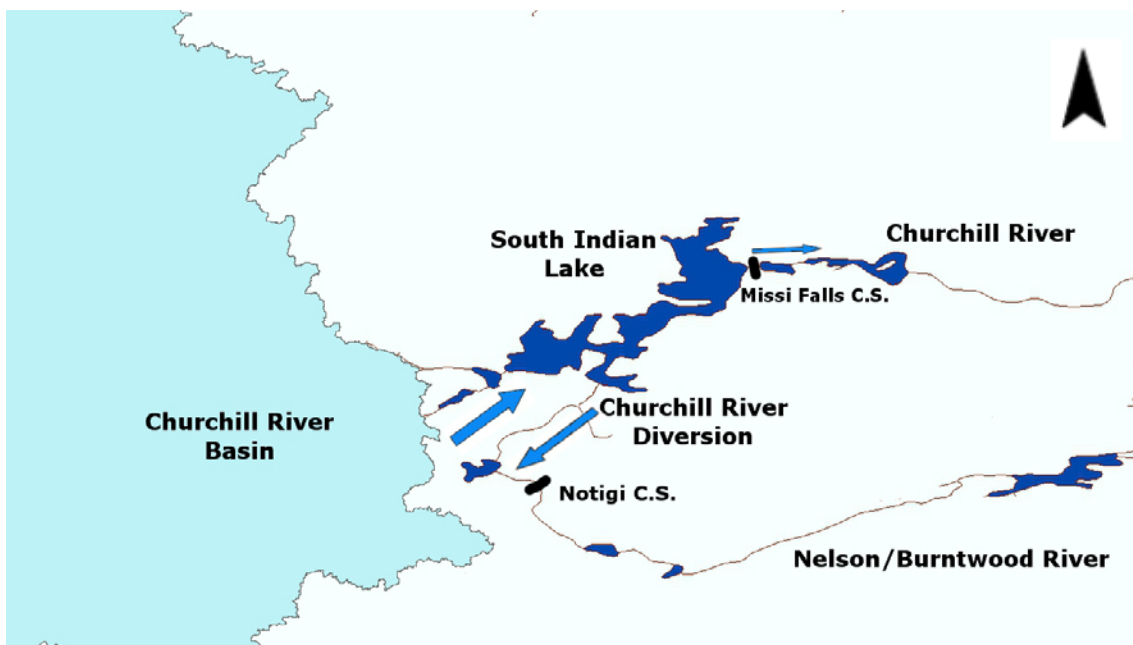
Figure 14: Schematic of the Churchill River Diversion (adapted from (Manitoba Hydro, 2009))

The Churchill River flows into Southern Indian Lake near the town of Leaf Rapids, Manitoba. The Churchill River diversion consists of three major components which allow the water to be removed and utilised to the south. The first is a control structure at Missi Falls. This is the location of the natural outlet of the river from Southern Indian Lake. The control dam regulates the outflow and facilitates a rise in the lake levels of three metres over its natural level. The license for the diversion stipulates that a minimum of 14 and 43 m^3/s must pass through Missi Falls during the open water and ice on periods, respectively.

The second is an excavated channel from the south basin of Southern Indian lake to Issett Lake, which is a part of the Burntwood River system. This is the portion of the diversion which truly facilitated the transport of water from one basin to the next. The approximately 50 km excavated channel is able to convey the as much as 850 m^3/s southward towards the large generating stations located in the Nelson River system.

The final component of the diversion is the Notigi control structure. This structure consists of a dam and spillway which allows the operators to control the amount of release from Southern Indian Lake into the Burntwood River system. This area also has potential for being the site of a generating station sometime in the future.

The Churchill River Diversion project also contains several other mitigation structures. These include ice booms and rock weirs which are meant to limit the

risk of ice jam related flooding and maintain habitat for the local fish populations. These structures do not greatly affect the flow of the river or the diversion.

Overall, the impact that the control structures had on the project was significant. The modelling portion of the study was confined to the unregulated headwaters portion of the river rather than modelling the flow into South Indian Lake directly. This allowed for the elimination of the effects of flow regulation on flows in the future and to concentrate completely on determining the direct impact of climate change.

3.5 Downstream Hydroelectric Generation

As alluded to above, there is a significant amount of hydroelectric generating potential located downstream of the Churchill River diversion in the Nelson River system. This includes six sites which are currently developed and operational along with two additional sites which have been proposed and are in the various stages of planning. A map detailing the locations of these stations is shown below (Figure 15).
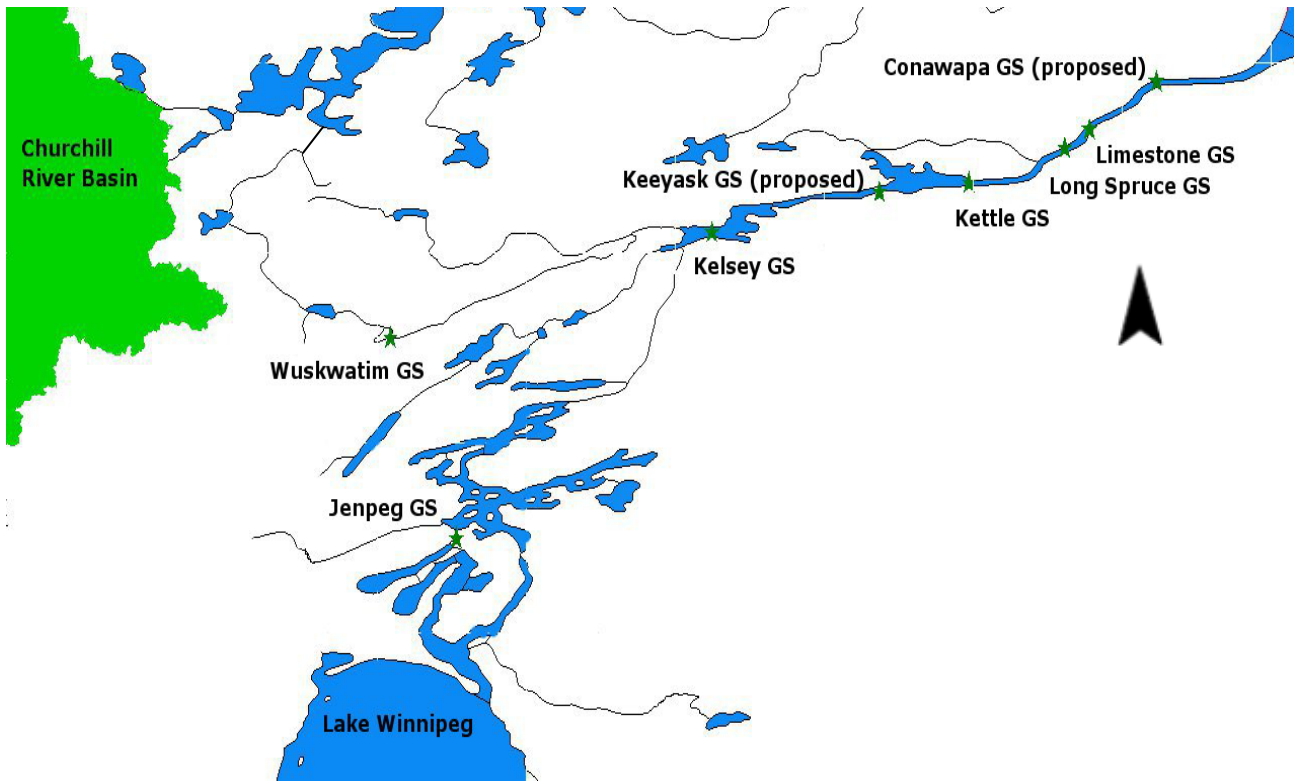
Figure 15: Existing and proposed hydroelectric generating stations in northern Manitoba (adapted from (Manitoba Wildlands, 2005))

The largest of the existing stations is Limestone generating station (GS). It is located on the Nelson and has a capacity of 1340 MW. It became operational in 1990, and as such is the newest generating station currently in operation on the Nelson. This is the furthest downstream generating station which is currently being operated by Manitoba Hydro.

Only 23 km upstream of Limestone is Long Spruce GS. This plant has a capacity of slightly in excess of 1000 MW, making it the third largest currently in operation in the province of Manitoba. Construction on the generating station was completed in 1979.

41

A further 18 km upstream on the Lower Nelson sits Kettle GS. This station has the ability to produce 1220 MW of electricity. The plant was completed in 1974, making it the second oldest of the generating stations built on the Lower Nelson.

Located at the junction of the Burntwood and Nelson Rivers is Kelsey GS. The oldest and smallest of the GS located on the Nelson, Kelsey was completed in 1961. It has a capacity of 250 MW (with the potential for 464 MW total after a potential expansion).

The Wuskwatim GS has just been completed and put into service and is also the only station located on the Burntwood River. It will have a capacity of 200 MW and is expected to be operational by the end of 2012. Potential construction of generating stations will be considered at each of the locations indicated on the map above (Figure 15). These projects will be developed according to market demands and as they fit into the corporate development plan. The projects which are the closest to being constructed are Keeyask GS (to be built at the Gull site) and Conawapa GS.

In total, there is approximately 3000 MW of downstream hydroelectric generation potential which rely on flows from the Churchill River basin (Manitoba Hydro). This represents the majority of the electricity which is generated by Manitoba Hydro. As a result, the state of the Churchill River basin is of vital importance to the long-term operations of Manitoba Hydro. Impacts to the flow regime caused by climate change will affect the day-to-day operations and short-term inflow forecasting at the existing hydroelectric generating stations as well as having an

impact on the development of future plants to further capitalize on this resource. Understanding the process of climate change will allow for the maximum benefit to be gained from the rivers under any possible future flow changes.

Chapter 4: Model Creation and Calibration over Churchill River Basin

As previously noted, the state of hydrological modelling technology is such that it is possible to create several different types of models to estimate the streamflow response of a watershed. For the purposes of this project, three hydrologic models were set up and calibrated for the CRB. The sections which follow give details on how each of these models was selected, set up, and finally calibrated.

4.1 Models Selected for Implementation

Before beginning the hydrological modelling phase of this project, it was first necessary to decide which modelling programs would be utilised. Models were chosen based on their technical merit as well as the availability of support services and familiarity with the model and data requirements within the working group. Differing levels of complexity and model structure were also chosen in order to determine the effect of these factors on climate change predictions.

4.1.1 WATFLOOD™

The WATFLOOD™ hydrological model is a semi-physically based, distributed model which was developed by Professor Nicolas Kouwen from University of Waterloo. It is an integrated set of programs which are used to forecast flood flows and complete simulations on watersheds with response times ranging from as little as one hour up to several weeks (Kouwen N. , 2011).

Before beginning to set up the model, the user is required to collect a digital elevation model. This is a file which identifies the elevation profile of the basin on a point-by-point basis. This file is used to define the general drainage scheme of the basin. The data required for this file is readily available online and can be downloaded at no cost (Government of Canada, Natural Resources Canada, Earth Sciences Sector, Centre for Topographic Information, 2000). This data was downloaded and resampled at a resolution of approximately 0.01 degrees (approximately 125 metres, from the source resolution of 0.0001 degrees) using ArcGIS in order to limit the file size and speed the computation time required when working with this data.

The user is also required to gather information about the land cover which is present in the basin. This data identifies which regions of the study area are covered by the different specified types of vegetation. This data is also available online and is free to download (Government of Canada, Natural Resources Canada, 1995). For the purposes of this model, the data was again resampled at the same resolution as the DEM (0.01 degrees from source resolution of 0.0001 degrees). The raw data contained many more land classes than were required by the modelling exercise. As a result, similar land cover types were grouped together and the land cover map was reclassified into eight land classes for which WATFLOOD^{TM} parameter sets were available from previous models. The fact that this is possible is a testament to the transferable nature of the WATFLOOD^{TM} land classes for similar land classes in different models. These classes are mixed/deciduous forest, coniferous forest, cropland, burn (refers to

areas which have a combination of shrubland and forest, similar to what would be found after a forest/brush fire), fens (connected wetlands), bogs (disconnected wetlands), water and impervious.

The WATFLOOD™ model uses grouped response units (GRUs) and a physically-based routing routine to simulate the response of the watershed to the given meteorological inputs. Each GRU is assigned an elevation and a percentage is given for each land cover type present within the cell based on the input files described above. The figure below (Figure 16) illustrates this concept.
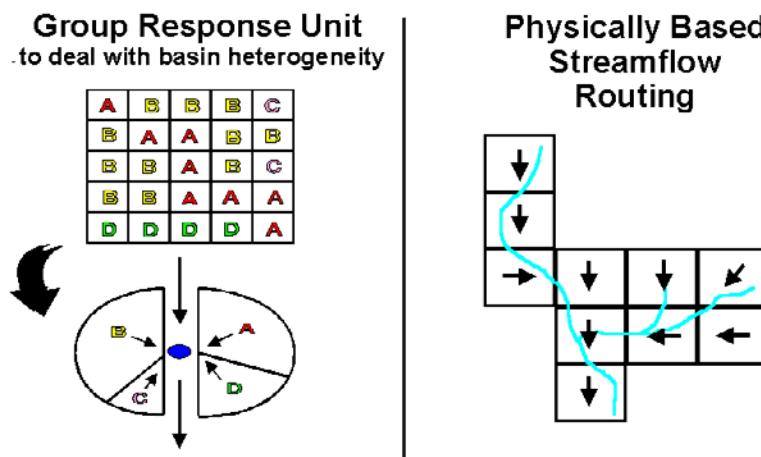
Figure 16: Illustration of the GRU concept and streamflow routing routine (Kouwen N. , 2011)

The GRU concept breaks the watershed down into a series of equally sized grids based on the user's specifications. Every GRU is given an elevation based on the digital elevation model (DEM) which is input the model. Each of these GRUs is also programmed with a gridded land cover map containing as many or as few land classes as the user specifies. Instead of having each of the land cover areas respond independently, the GRU assigns a percentage to each land cover

class in each cell and uses these values to calculate the runoff response characteristics of the cell. Due to the size of the basin and computation time constraints, it is impossible to construct a model that is entirely physically based. WATFLOOD[TM] is the closest approximation to a fully physically based model which is being used in this study. The model calculates runoff in each GRU using conceptual relations and uses a physically based routing method to calculate streamflow. The following illustration shows the processes which are simulated by separate subroutines within the modelling package (Figure 17).
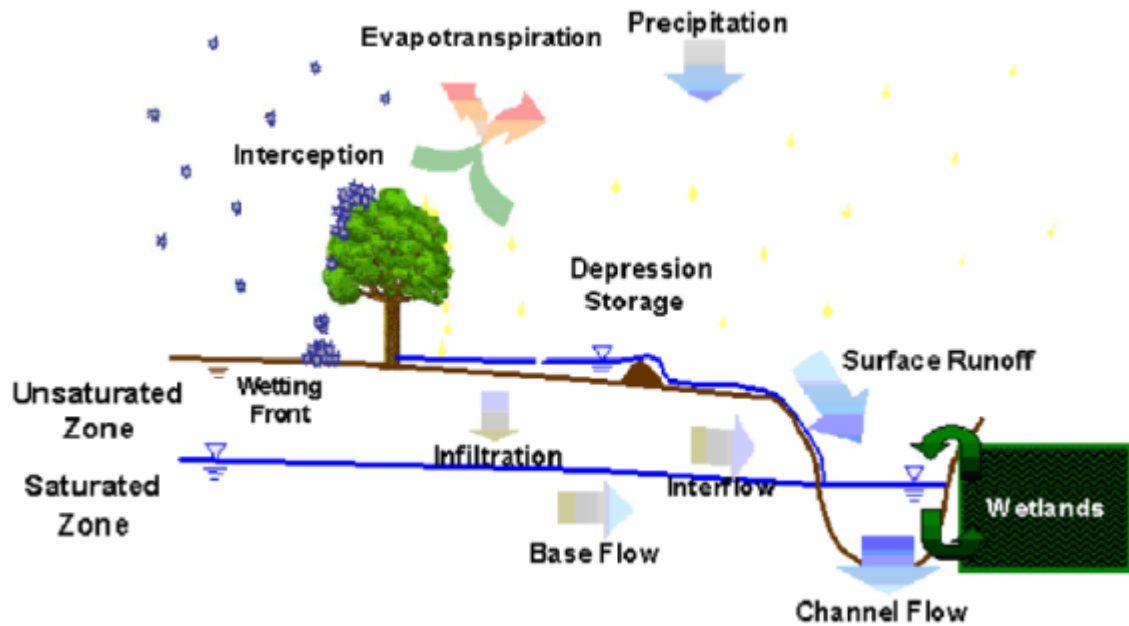
Figure 17: Illustration of the processes simulated by the WATFLOOD[TM] hydrological model, from (Stadnyk-Falcone, 2008)

Each of the processes illustrated above (Figure 17) are activated based on the amount of data that is loaded to the model. Due to the distributed nature of the model, each of these processes happens individually within each grid cell. For

example, the evaporation subroutine uses several different calculations which each require different combinations of temperature, humidity and wind data.

The precipitation input is triggered by a meteorological input file which has been created based on an inverse distance weighting technique using Environment Canada weather station data. Some of this precipitation is intercepted by the canopy. This ratio is changed based on the land cover type (i.e. deciduous trees would have a much higher interception ratio than a barren type land cover, etc.). The remaining precipitation falls to the ground where it enters the hydrologic cycle as either snow or liquid water. This is distributed amongst surface depressions, infiltration, and evapo-transpiration using a series of different coefficients and equations.

After these calculations are completed, the runoff is finally calculated. This is the amount of water which is available to be transferred from that cell to the next cell in drainage order. Cells are each assigned a uniform elevation value based on the average elevation obtained from a DEM. By draining water from the high cells into the low, water is routed from the headwaters to the outlet of the basin.

4.1.1.1 Input data required for WATFLOOD™

Before gathering data and going about creating a WATFLOOD™ watershed model, the first thing which must be done is to choose a basin name (this is shortened to bsnm when discussing the file structure and naming conventions). For the Churchill River basin, the name which was chosen was churll. This is an abbreviation for Churchill River and latitude/longitude to represent the fact that the data which makes up the basin is projected in a Geographical Coordinate

System (GCS). All files and directories were given appropriate names using this basin nickname and the convention described in the WATFLOOD^{TM} user manual (Kouwen N. , 2011).

The WATFLOOD^{TM} hydrological model is considered to be a data intensive model. In order to run the model, several types of files are needed. The high-level data process flow diagram may be found below (Figure 18). These files and a brief description of how they were gathered and properly formatted are included in the paragraphs below.
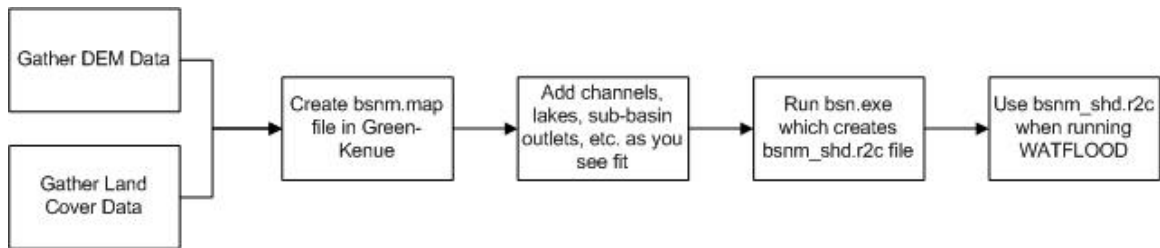
Figure 18: File process diagram required to create a WATFLOOD^{TM} model

The basis of any WATFLOOD^{TM} model is the watershed file. This file is most easily created using the pre-processing software package Green-Kenue (Canadian Hydraulics Centre, 2010) and contains data from the DEM, land cover, as well as other user specifications for options such as designating lakes and sub-basin outlet locations (maps illustrating how each of these was handled for the Churchill River basin model are shown below in Figure 19 through Figure 22). Green-Kenue creates a bsnm.map file which combines each of these data sources and allows the user to make any changes that they see fit before utilising it within the model. The WATFLOOD^{TM} model requires that the bsnm.map file be converted to an r2c (two dimensional rectangular cell grid file) format which is

49

distributed into the size of grids which are specified by the modeller. This distribution is accomplished using the bsn.exe utility which may be downloaded from www.WATFLOOD.ca and is a part of the WATFLOOD™ model suite. This r2c file is commonly referred to as the shed file by modellers because it is named with the bsnm_shd.r2c convention (an example view of the shd.r2c file used for the Churchill River basin is presented below in Figure 23).
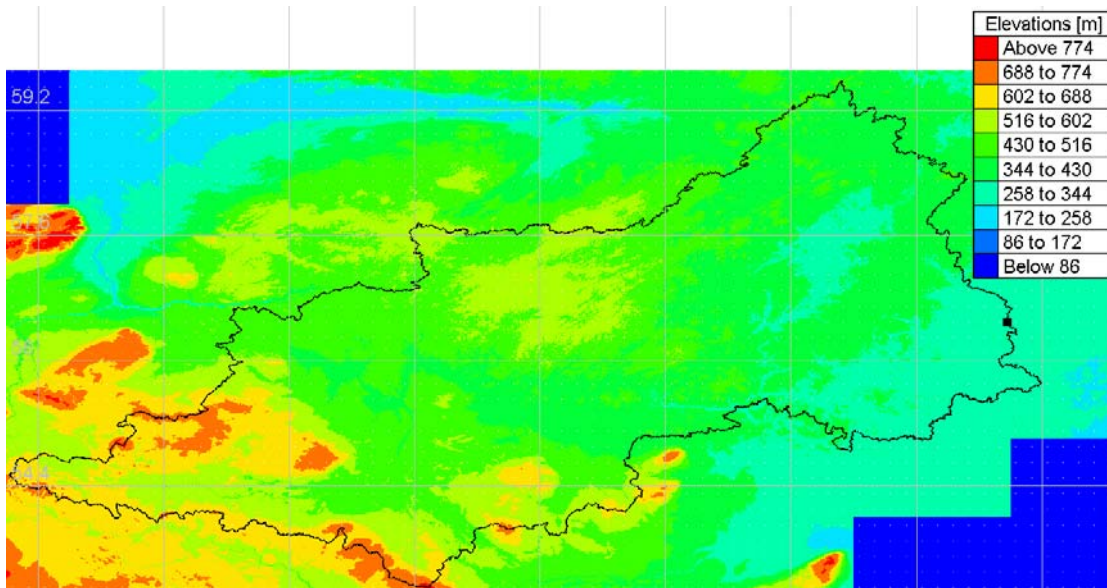
Figure 19: DEM showing elevations of the Churchill River Basin
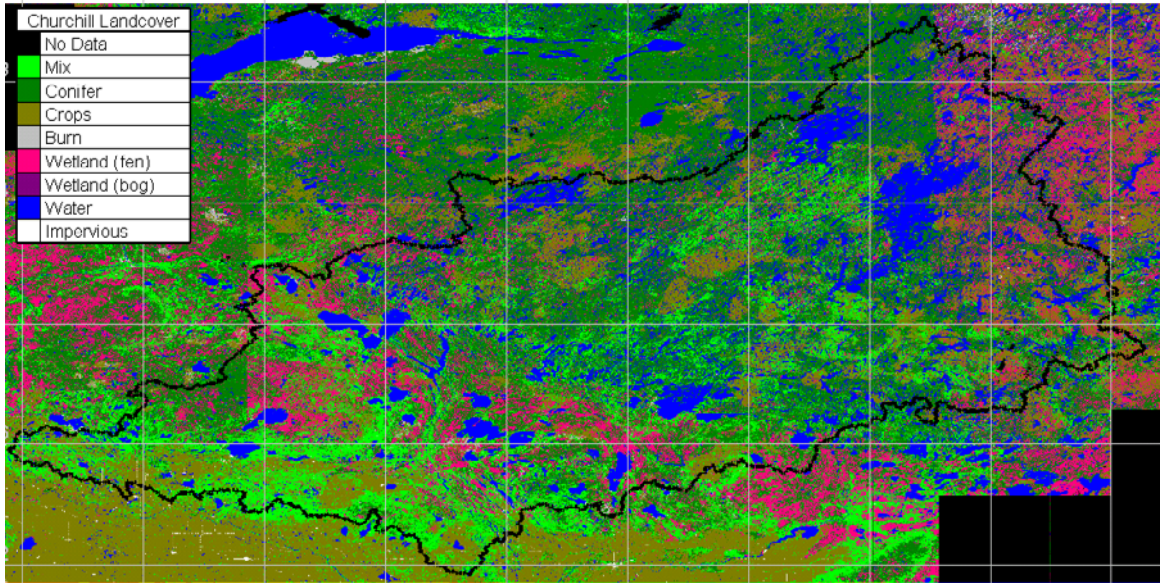
Figure 20: Land classification map for the Churchill River basin used in the WATFLOOD^{TM} model
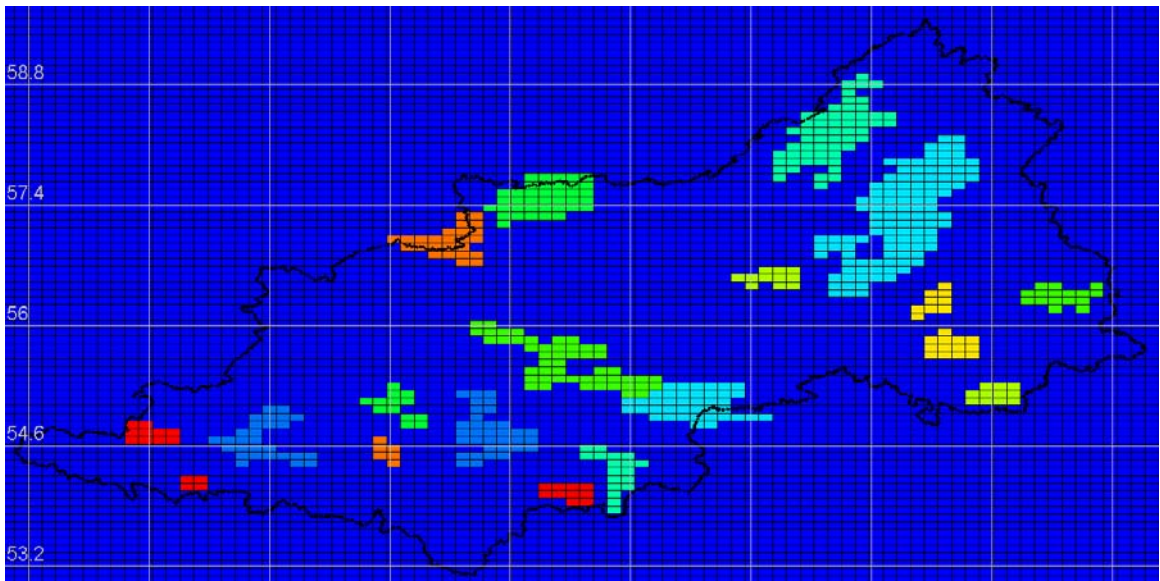
Figure 21: Illustration of lakes which were programmed into Churchill River using the bsnm.map file
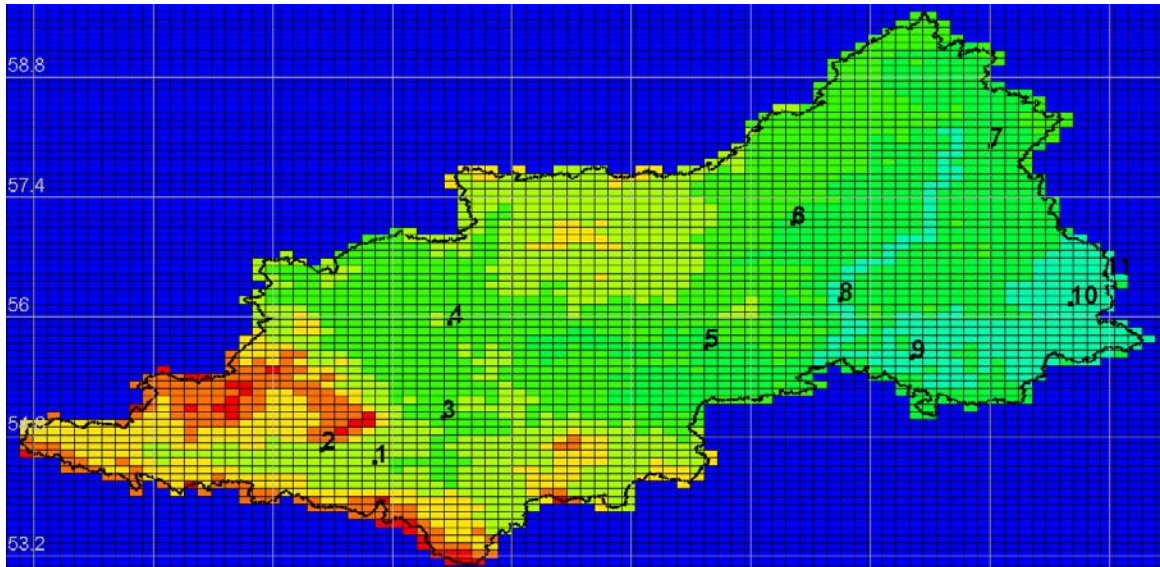
Figure 22: Churchill River map file with points designating sub-basin outlet locations
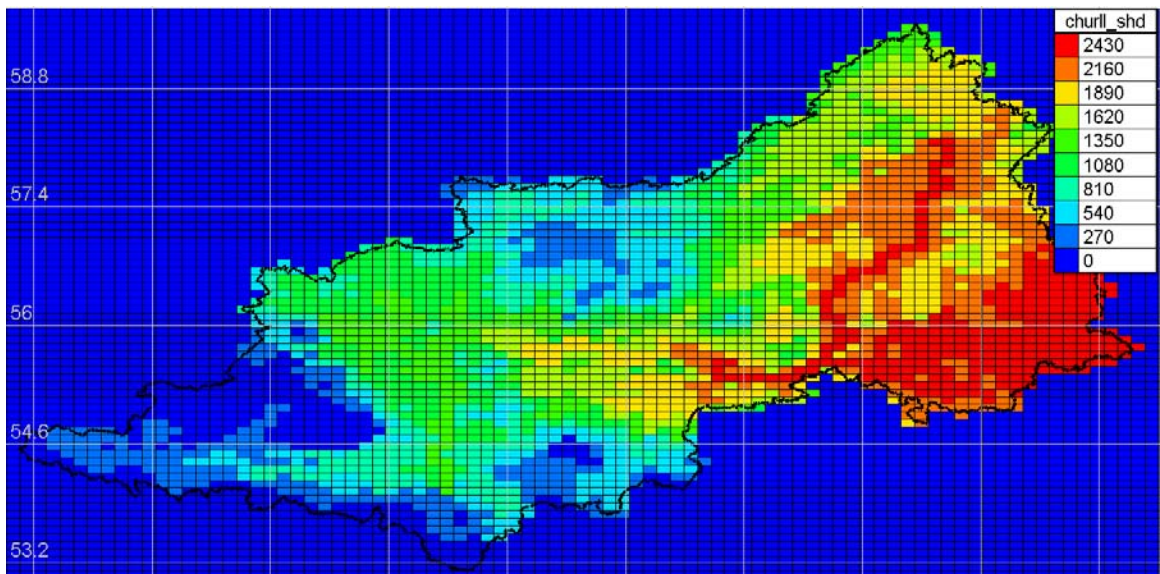
Figure 23: WATFLOOD^{TM} bsnm_shd.r2c file showing the rank of each of the 2705 model cells

WATFLOOD^{TM} was chosen for use in this study due to its distributed nature. Because the basin is very large, the concept of breaking the basin into smaller grids facilitates more accurate modelling of the individual processes within the system. The choice of grid size is a very important decision in the creation of any distributed hydrological model, and the WATFLOOD^{TM} model is no different. Grids which are too large will result in poor basin definition and important basin

features can be missed. Conversely, grids which are two small will create a model which is overly complex. This leads to simulation times which are excessively long and makes analysis of the results quite tedious. As a result, it is very important that an appropriate grid size be chosen when setting up any gridded hydrological model.

For the Churchill River basin, the grid size was chosen to be 0.16 degrees longitude by 0.90 degrees latitude (very close to 10 km by 10 km). This resulted in 2705 cells being within the basin boundary and contributing to the modelled hydrograph. This size was chosen as a result of the limitations of the model on number of cells. Additionally, any smaller grids would not have added value to the model due to the sparse nature of the input data in the region.

4.1.2 HBV-EC Hydrological Model
The second model used in the ensemble for this study is the HBV-EC hydrological model. This model is a semi-distributed conceptual model which was originally developed by Lindstrom, *et al.* (1997) at the Swedish Meteorological and Hydrological Institute. It has been adapted by Environment Canada (hence the EC designation) and the University of British Columbia to simulate hydrological response of many types of watersheds and is run through the same Green-Kenue (Canadian Hydraulics Centre, 2010) interface which handles much of the WATFLOOD^{TM} preprocessing.

The model was originally developed for smaller, mountainous watersheds. The Churchill River basin is not mountainous and could be classified as flat. As a result, the model uses elevation banding which may not be the most effective

way to model this basin due to the different mechanisms of runoff (quicker runoff with minimal losses in the mountains and more deliberate runoff with infiltration and losses in flatter areas). Elevation banding is an effective technique to accomplish semi-distributed hydrological modelling and warranted the use of HBV-EC in this case.

Unlike WATFLOOD^{TM}, the HBV-EC model does not break the watershed into a series of equally sized grids. Instead the user has the option to enter as many or as few climate zones to the model as they require. These zones form the basis for the semi distributed nature of the model. A schematic of this is shown below (Figure 24) and the chosen delineation of the climate zones may be found in a later section (Figure 34).
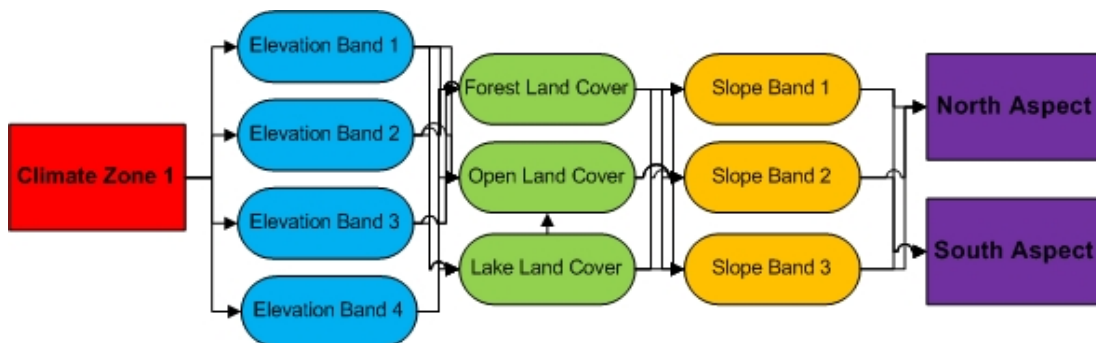
Figure 24: Schematic view of semi-distributed nature of the HBV-EC hydrological model

Within each of the climate zones which the user specifies, the model identifies a series of elevation bands which are based on the elevation values which are given to it by a DEM. Each of these elevation bands are broken down further into one of four possible land cover classes (Forest, Open and Lake were the land cover types utilised in this application as there are no areas within the CRB

covered by glaciers) which are based on a GeoTIFF image supplied by the user. The image used for the Churchill River basin may be found below (Figure 25). The same concept applies with slope and aspect bands which are each derived from the same DEM file as the elevation bands (the DEM used for the Churchill River basin HBV-EC model was the same as the file which was used to create the WATFLOOD^{TM} model). In the above example (Figure 24), runoff would be calculated for 1x4x3x3x2 = 72 separate contributing areas at each time step for this one climate zone.

The model uses these contributing areas to distribute precipitation into fast and slow reservoirs. Water here contributes to streamflow according to depletion curves defined by coefficients input by the user.
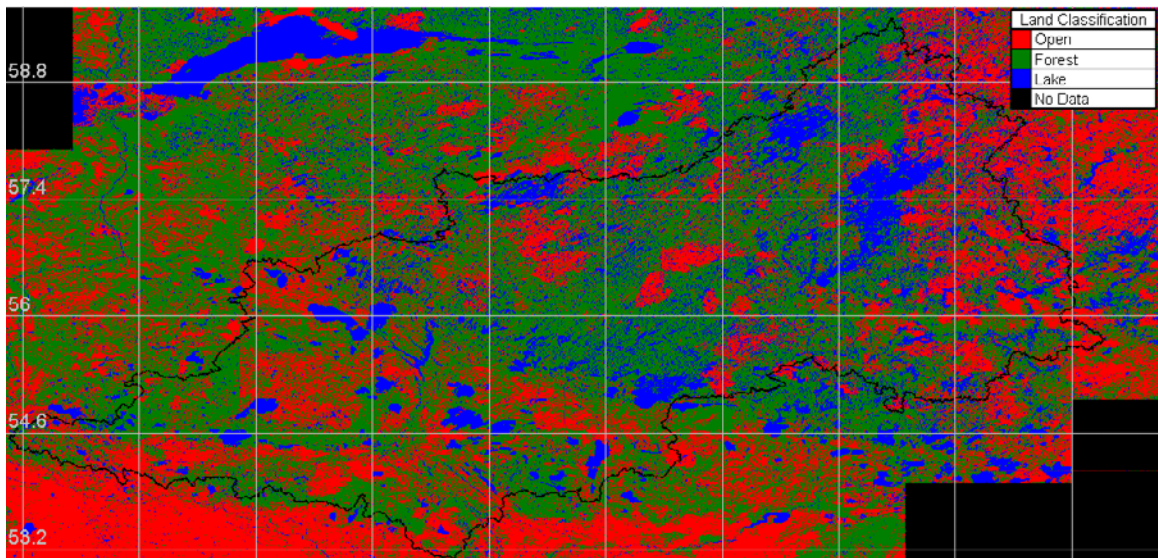
Figure 25: Land classification map for the Churchill River basin used in the HBV-EC model

The HBV-EC model was chosen for addition to the ensemble for this project for several reasons. The conceptual framework of the model provides good contrast to the semi-physically based nature of WATFLOOD^{TM} The model also requires a

similar dataset to be input which drastically reduced model set up time. Finally, the model has been proven in several previous climate change studies in northern regions of the world which shared some characteristics with the CRB (Andersson, Samuelsson, & Kjellstrom, 2011).

4.1.3 HMETS Hydrological Model

HMETS is a fully lumped, conceptual hydrological model which was developed by Dr. Francois Brissette, a professor at École de technologie supérieure in Montreal, Quebec (Brissette, 2010). HMETS, which is an abbreviation for Hydrological Model – École de technologie supérieure, is a Matlab based model which has a very simple parameter set in comparison to those required for both WATFLOOD^{TM} and HBV-EC. The model works using a modified version of the unit hydrograph concept and the reservoir concept described in Section 2.1: Background on hydrological modelling. As a result, the model is able to compute several different components of the hydrograph, including baseflow and surface flow.

Unlike the WATFLOOD^{TM} and HBV-EC models that are at least partially distributed, the HMETS model does not require any information about the shape of the basin or the landcover which exists within its boundaries. These properties are taken into account using one of the several adjustable parameters. All that the model requires is the area of the watershed and the latitude and longitude of the centroid of the basin area. The user must also input a file which contains the minimum and maximum temperatures as well as precipitation (with snow and rain differentiated).

With such a minimal amount of data required and seemingly such a small amount of computations, this model is the least complex model which was included for use in this project. The reasoning for including it was to provide a broader range of model types as well as to attempt to observe the difference between a more complex semi-physically based model and a simpler lumped model which combines the uncertainty within the basin into a series of coefficients and parameters.

4.1.4 Multi-model ensemble technique for uncertainty assessment

While each of these models has a unique set of characteristics which make them valuable to this exercise, it is perhaps the combination of all three which makes the most important contribution to this study. Utilising multiple hydrological models for an impact assessment is a technique which is widely used in studies within the area of climate change impact assessment (e.g. Miller, Butler, Piechota, *et al.*, 2012; Maurer, Brekke, & Pruitt, 2010).

The use of multiple models using completely different hydrological modelling techniques to estimate the anticipated future runoff using the same input data serves to make the results of the study more robust and allows the modeller to isolate and analyze the amount of uncertainty which is related to the choice of hydrological model.

4.2 Model Calibration Techniques and Results

Each of the models used in the ensemble were calibrated until they each predicted the discharge on the Churchill River to a roughly equivalent level of

precision. While the end goal was always the same, each of the models required a slightly different approach to achieve the desired result.

Because it is very difficult to calibrate two (or more for that matter) models to perform identically well, each of the models were calibrated until they reached a similar combination of the performance metrics in an acceptable range for each statistic. Each model used the same 4 year calibration period (1986-1989) and was validated using the four year period prior (1982-1985) and the six year period directly after (1990-1995). For each model, the same performance statistics were calculated for each of these periods. Each of the models was calibrated according to instructions in their respective user manuals and to the best level possible within the time frame available and the constraints provided within this project. Each of the methods and models used is described in detail in the sections which follow.

4.2.1 Calibration of WATFLOOD™ hydrological model

The most current version of the Churchill River basin WATFLOOD^{TM} model was derived from one which had been set up previously for a different project. Because the model is a distributed one, a projection system had to be chosen. In the previous model, all of the basin data was projected using the Universal Transverse Mercator (UTM) projection system. The CRB exists mainly within UTM zone 13 (WGS 1984), but significant portions of the basin are also in located within zones 12 and 14. Because the DEM and land cover maps can only be projected into one zone, the result is a skewed projection of the basin, as seen below (Figure 26 and Figure 27).
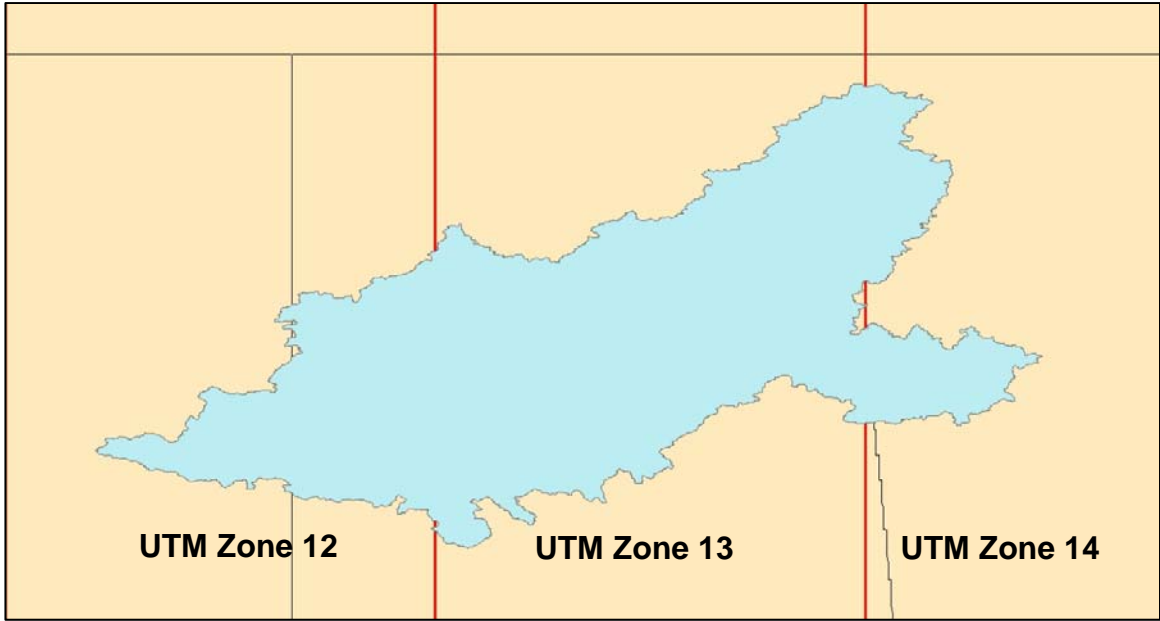
Figure 26: Visualization of WATFLOOD^{TM} model basin created using UTM projection
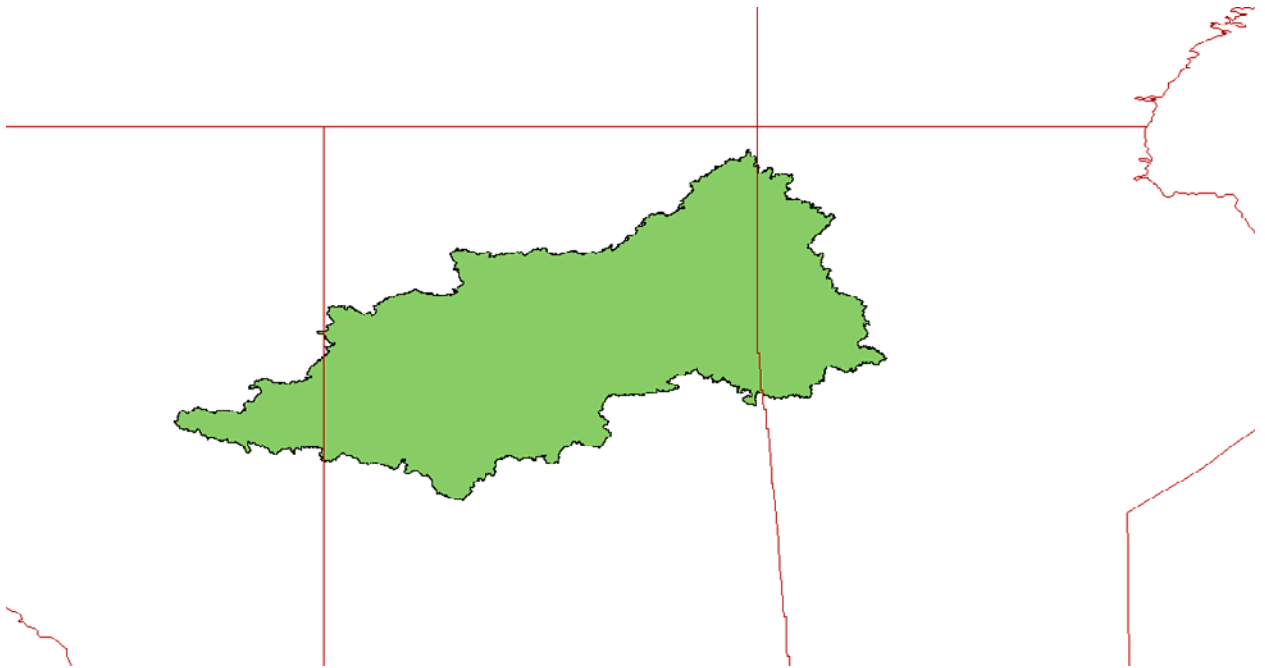
Figure 27: Visualization of WATFLOOD^{TM} model basin created using GCS projection

Based on these perceived inaccuracies, it was decided that the use of a geographical coordinate system (GCS, namely the North American Datum 1983)

was warranted and a new model was created. It may be noted that while the data that was input was essentially the same, the projections make the maps appear quite different. The WATFLOOD™ model constructs the grid it uses to perform calculations on the basin using the inputted maps. The GCS NAD83 projection is already in a similar form to this type of grid, and it was determined that this would be the most appropriate projection to use in going forward with in the model.

As a result of using this new basin projection, the effective area of grids on the extreme eastern and western portions of the basin was changed considerably. The GCS projection gave an equal weight to all areas of the basin, regardless of their location, while the UTM projection represented areas in the southern portion of the basin as considerably larger than an equivalent area located at higher latitude. These deficiencies in the UTM projected model generated results which were believed to be erroneous. As a result, the first step in calibrating the WATFLOOD™ model was to convert all files into the GCS projection.

The total area of the basin, which drains into Southern Indian Lake at Water Survey of Canada (WSC) gauge 06EC002, is greater than 260,000 km^2. However, it is not practical to model the hydrological regime of a large portion of this area due to regulations which are located on the river (dams, weirs, etc.). As a result there are two areas of the basin which the calibration was initially focused on. These areas each drain into WSC gauges and are highlighted below (Figure 28).
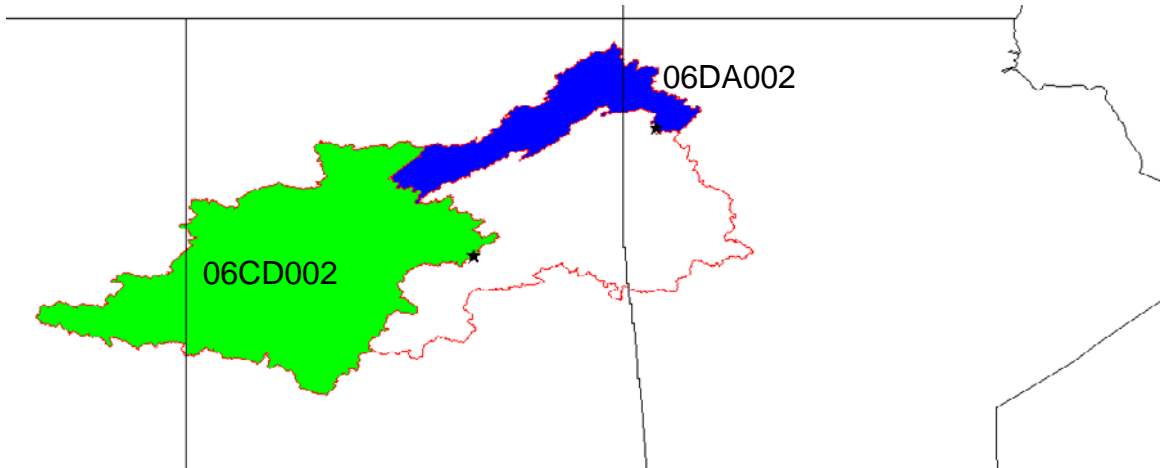
Figure 28: Feasible calibration gauges and their drainage areas

The region in green (outlet at WSC gauge 06CD002 on the Churchill River above Otter Rapids, SK) has an area of 119,000 km^2 while the smaller blue region (outlet at WSC gauge 06DA002 on the Cochrane River near Brochet, MB) has an area of 28,400 km^2. The larger region was chosen for more in-depth calibration for several reasons, including that it was on the main stem of the Churchill River, it contained several additional gauges to aid in calibration, and the density of meteorological gauging within this region was higher than the more northern blue region. For these reasons, the area draining into 06CD002 was chosen to be the main focus of the calibration of the WATFLOOD^{TM} model, and later on for each of the other models used in this project. This is not to say that the smaller area was neglected totally. Acceptable performance statistics were achieved after an initial calibration of the model in this area. The parameters corresponding to this region were not adjusted further in order to concentrate efforts on calibrating the model to simulate the proper hydrograph at Otter Rapids.

After choosing which gauge to calibrate the hydrological models to, the next step was to adjust the parameter files in order to match the timing and volume of runoff to a statistically acceptable level using performance metrics. WATFLOOD^{TM} parameter files (naming convention: bsnm_par.csv) contain the coefficients which are used in calculations of the different hydrological processes. The parameters are organized into three main categories. The first are known as the routing parameters and are related to the river type areas which are specified by the user in the map and shed files. These parameters define the baseflow regime as well as the flow characteristics within the channel of the river itself. The second set of parameters is linked to the land cover classes which are specified within the shed file. These parameters are known as the hydrological parameters and define the interflow regime, the overland flow characteristics as well as several other processes such as interception and soil porosity. The third and final set of parameters deal with the snow melt routine and are also linked to the land classes. These snow parameters define the important parameters within the snow melt regime such as melt rate, albedo, and snow density, among others.

In order to get an initial estimate of the parameters, several methods were attempted. The first was to use the parameters which had been utilised within the previous version of the model. These parameters were adjusted manually to some degree but an acceptable set could not be found. As a result, a new initial parameter set was chosen as a starting point.

Manitoba Hydro, in conjunction with WATFLOOD^{TM} model developer Dr. Nicholas Kouwen have set up several models on basin which share some similarities with the Churchill River basin. These parameter sets were analyzed and similar land cover types and river class parameters were selected and inserted into the parameter Churchill River parameter file which is a major advantage of the transferrable nature of WATFLOOD^{TM}. These parameters were again manipulated manually until an acceptable hydrograph fit was accomplished.

After manual calibration achieved an acceptable starting point for the model, the Dynamically Dimensioned Search (DDS) automatic calibration algorithm was utilised in order to find a better set of parameters (Tolson & Shoemaker, 2007). The DDS algorithm searches for a parameter set which produces a hydrograph most similar to the one observed using its unique search algorithm. The algorithm begins as a global search in which each of the variables selected for calibration are randomly sampled around the initial guess using a user specified standard deviation. These new values are evaluated until a better solution than the current one is found. Once this happens, the search begins using the new set of parameters as a starting point. This algorithm is no necessarily designed to find the global optimum value of the objective function, but rather to converge to an area near the global optimum value in the best case and converge to a good local maximum in the worst case (Tolson & Shoemaker, 2007). The pseudo-code for the DDS algorithm is shown below (Figure 29).

Step 1: Define DDS inputs – neighborhood size parameter, max # of function evals (m), vectors for lower and upper bounds for all decision variables, and initial solution
Step 2: Set counter to 1, evaluate objective function at intial solution
Step 3: Randomly select some of the decision variables, using probability based on current iteration count
Step 4: Perturb selected decision variables based on bounds using a standard normal distribution factor.
Step 5: Evaluate new objective function and compare to best solution, updating if necessary.
Step 6: Update iteration count and stop if required, otherwise return to start.

Figure 29: Dynamically Dimensioned Search (DDS) algorithm pseudo-code, adapted from (Tolson & Shoemaker, 2007)

The DDS algorithm was implemented multiple times in different ways to arrive at the solution which was used for the later portions of the project. These separate implementations optimized separate variables individually at first then in larger groups in order to arrive at the current "good" solution. In order to define a "good" solution, some calibration metric had to be developed. In this case several were used, including most importantly the Nash-Sutcliffe efficiency (NSE) (Nash & Sutcliffe, 1970) which is calculated as follows:

$$NSE = 1 - \frac{\Sigma(Q_{meas} - Q_{sim})^2}{\Sigma(Q_{sim} - \overline{Q_{meas}})^2} \qquad (4.1)$$

Where: Q_{meas} is the measured or observed streamflow at each time step

Q_{sim} is the simulated streamflow at each time step, and

$\overline{Q_{meas}}$ is the average of all measured streamflows at every time step.

This statistic compares the model's performance to the alternative of using the average flow as an estimator. In other words, a positive NSE value indicates that

the model is better than using the mean flow, while a negative signifies that the average flow is (statistically speaking) a better predictor of the flow than the model being used and zero means that the model is exactly as useful as the mean measured flow to estimate flow on any given day. One weakness of the NSE is that it places high weight on very high flow events and tends to disregard lower flow events. This can be mitigated by using the log value of the flows. The formula for the coefficient of determination (r^2) value, which is another useful statistic, is given below:

$$r^2 = 1 - \frac{\sum(Q_{meas} - Q_{sim})^2}{\sum(Q_{meas} - \overline{Q_{meas}})^2}$$ *(4.2)*

This statistic has a very similar formulation to the NSE and as a result the values are very similar in most cases. The final statistic that was used to ensure that the model was performing well was the percent deviation in flow (%Dv). Its formulation is given below:

$$\%Dv = \frac{\sum(Q_{sim} - Q_{meas})}{\sum Q_{meas}}$$ *(4.3)*

This statistic expresses the models ability to estimate the total amount of flow being generated. The statistic will be negative if the model is not producing enough flow and positive if there is an abundance of runoff being generated. These three calibration statistics (NSE, r^2, and %Dv) were used in combination to calibrate each of the three models in the ensemble. Each of the metrics were assigned equal weight in the analysis so as not to favour one over the other.

When calibrating a hydrological model, it is beneficial to use the longest runs possible to ensure that the model is performing properly over all time periods in which sufficient data is available. Because the modelled region is remote there is a limited amount of data available for running the model. As a result the calibration period was limited to 4 years (1986-1989) while the model was validated over the periods from 1982-1985 and 1990-1995. This split sample calibration/validation combination was found to give the best results for all periods after attempting to use each of these periods in some combination. A final "validation" run was completed over the entire period from 1979-1995 for which adequate flow and meteorological data was most available.

During the calibration process, individual parameters were calibrated first in order to correct the most visibly obvious issues with the hydrograph (timing of snowmelt, volume of baseflow, etc.). After resolving these issues, several variables were grouped together for further optimization in order to produce a better value of the NSE objective function, while still considering each of the other statistics.

The parameters which were found to have the greatest impact on the results (and therefore were the most useful for calibration) were the infiltration coefficients (WATFLOOD^{TM} parameter codes ak and akfs (snow covered)), interflow coefficient (rec), overland flow roughness coefficient (r3), lower zone coefficient and exponent (flz and pwr) and channel roughness (r2n). By setting limits for these parameters in the DDS run, a suitable combination of these parameters was found which optimized the chosen performance statistic (NSE) at the gauge

of interest (Churchill River at Otter Rapids, 06CD002). The hydrographs from the model used to conduct climate change simulations are shown below along with their corresponding performance statistics (Table 3, Figure 30, Figure 31, Figure 32, and Figure 33).

Table 3: Performance statistics for WATFLOOD^{TM} model at WSC station 06CD002

Period	Time Series Nash-Sutcliffe	Correlation Coefficient (r^2)	% Dv	Annual Average Nash-Sutcliffe	Average flow [cms]
1982-1985 (validation 1)	0.43	0.69	11.84	0.68	206.41
1986-1989 (calibration)	0.71	0.74	-5.03	0.72	233.60
1990-1995 (validation 2)	0.45	0.66	17.88	0.34	166.97
1979-1995	0.45	0.54	0.42	0.63	209.29
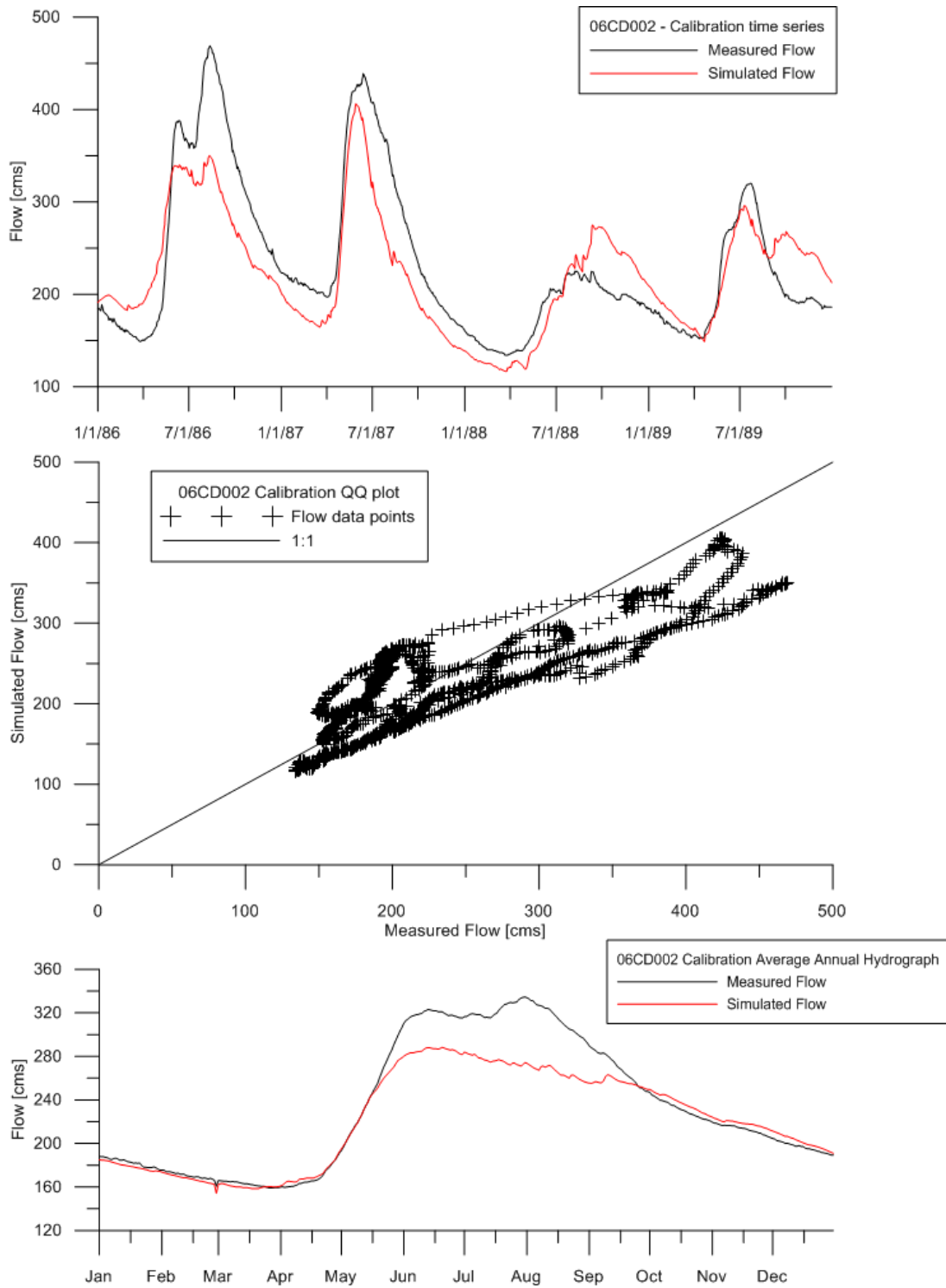
Figure 30: Flow time series, QQ plot and average annual hydrograph for calibration period (1986-1989) WATFLOOD^{TM}
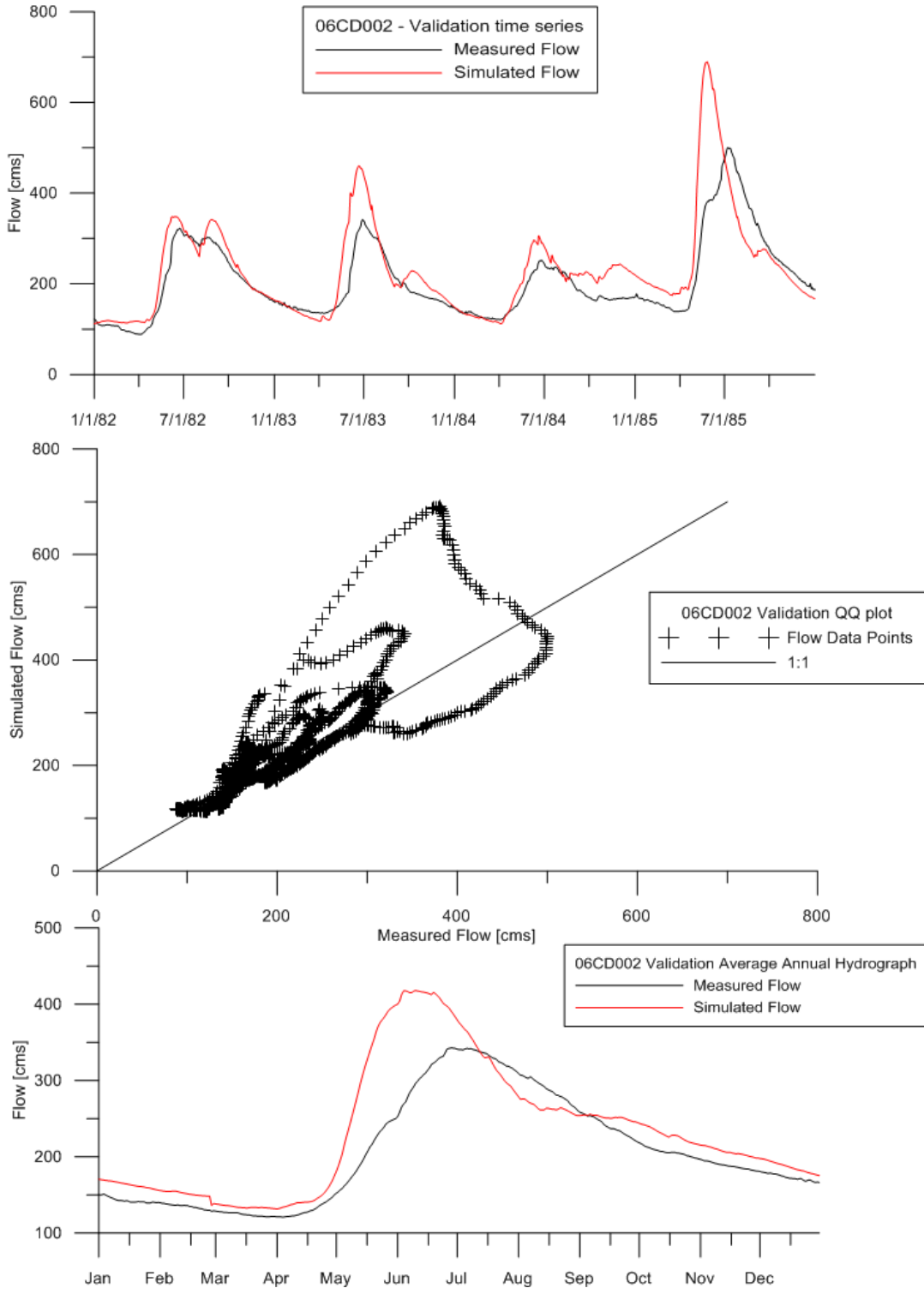
Figure 31: Flow time series, QQ plot and average annual hydrograph for validation period (1982-1985) WATFLOOD^{TM}
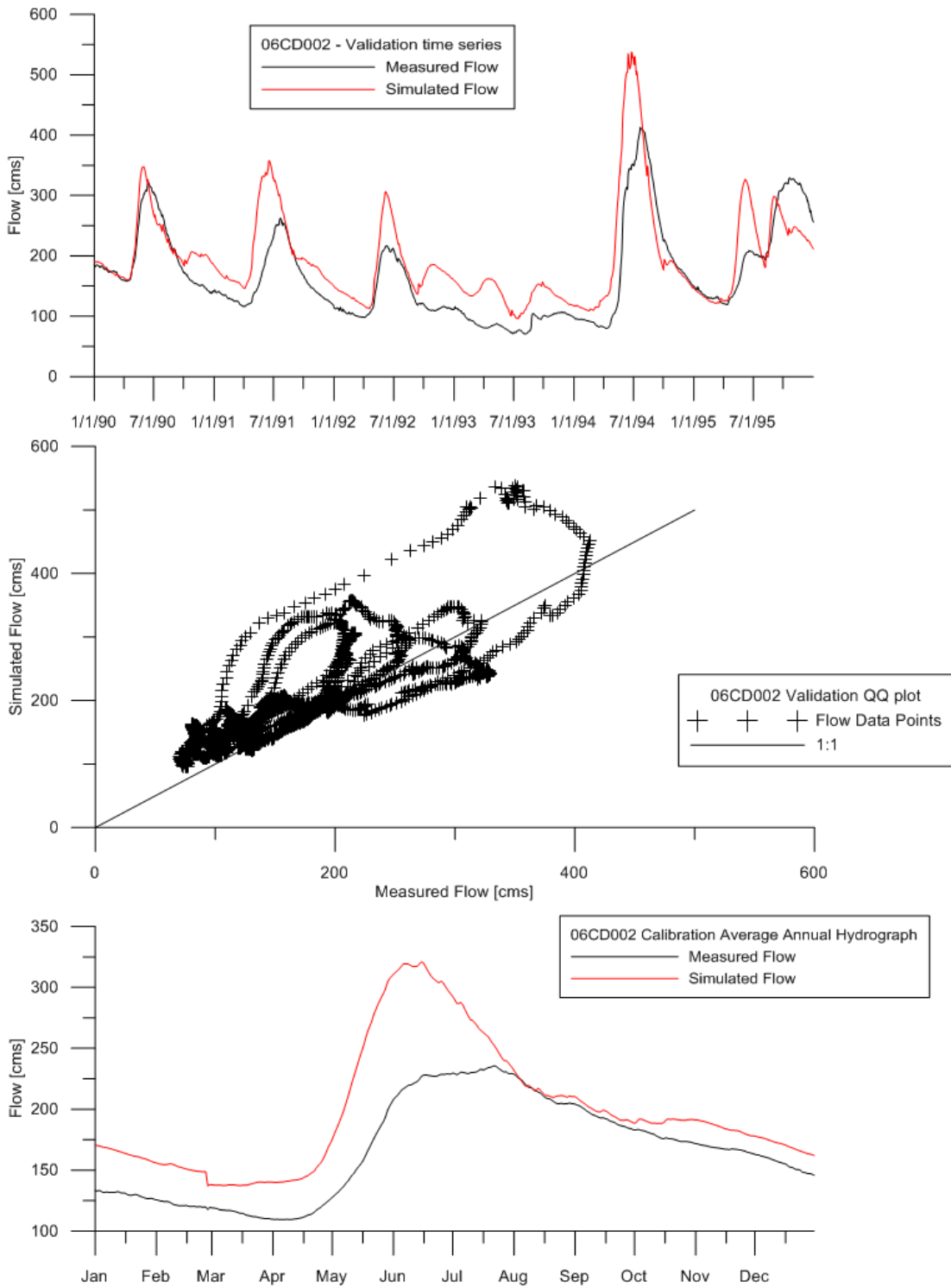
Figure 32: Flow time series, QQ plot and average annual hydrograph for validation period (1990-1995) WATFLOOD™
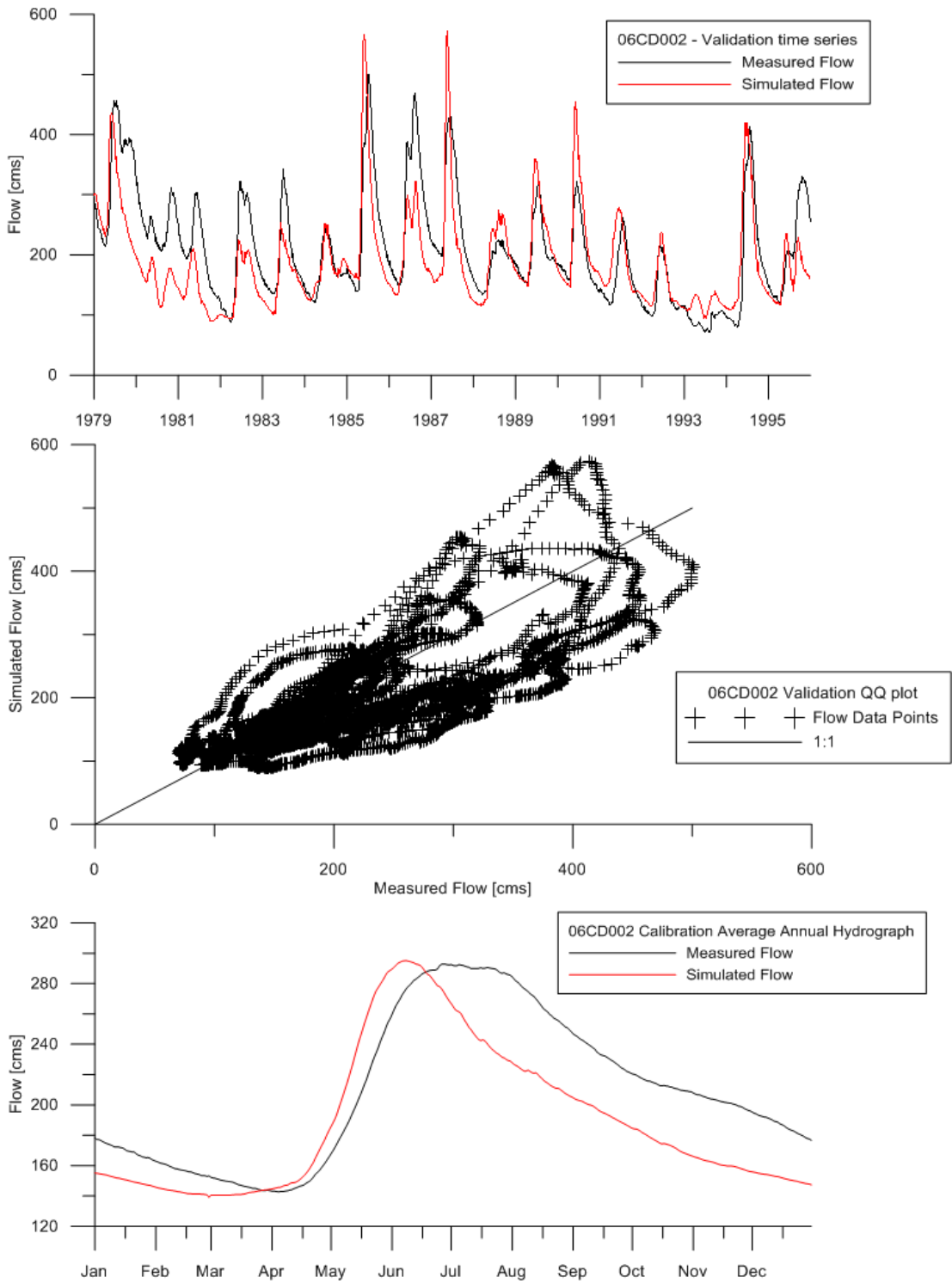
Figure 33: Flow time series, QQ plot and average annual hydrograph for entire model period (1979-1995) WATFLOOD™

Each of the above sets of plots shows the behaviour of the model within each time period. The first plot is of the time series data. The second plot shows the

71

same data in a different manner: each point represents one point in the time series, with the measured value on the horizontal axis and the model's simulated value for the same time on the vertical axis. Each point on this plot that lies above the 1:1 line indicates that the model is overestimating the flow while the opposite is true for a point below this line. The final plot shows the average annual hydrograph over each period. This plot makes it easier to see specific trends at different parts of the year than the full time-series plot and is a great aid in correcting specific issues with the model setup.

The above plots show that the model is able to predict the flow in the Churchill River basin well during the periods of the year where the flow is relatively low. During the calibration period (1986-1989, Figure 30) when the spring flows were quite high, the model slightly underestimated the flow. When points on a QQ plot appear to follow a path away from the 1:1 line it indicates that the model is off on the timing of a flow event.

During the first validation period (1982-1985, Figure 31), the model is simulating the peak flow to be slightly higher and earlier than was observed. The model overestimates the peak flow in the basin for each spring freshet while also predicting that the peak flow will happen approximately one week earlier than measured. The model also overestimates the flow during the winter period for the majority of the time period.

The model generally overestimates the flow during the second validation period (1990-1995, Figure 32). It is worth noting that 1991, 1992 and especially 1993

72

are lower flow years, especially during the freshet period. The model performance suffers during this time which suggests that the model is not as well suited to predicting the flow during these drier years as during the more average-to high flow conditions which were more prevalent during the calibration period and the earlier validation period.

The hydrograph generated for the complete time period (1979-1995, Figure 33) confirms the concepts and trends which were observed during the shorter model runs. Overall, the model over- and under-estimations of the peak flow during the spring average out, but the model generally predicts that this peak will occur slightly earlier than was observed at the flow station.

In general, it was found that the WATFLOOD^{TM} model for the Churchill River basin was useful to predict the flow at Otter Rapids. The physical basis behind parameters lent a measure of confidence to the process of model calibration. It was found that the parameter ranges were comparable to those used in other calibrated WATFLOOD^{TM} models which are set up in similar regions. The complete set of parameters used in the climate change impact assessment portion of the project may be found in the Appendix A.

4.2.2 Calibration of HBV-EC hydrological model

The HBV-EC model requires a calibration approach which is quite different from the one which was used for the WATFLOOD^{TM} model. Because no automated calibration routine was available, the calibration had to be done manually. The process and results are outlined in the paragraphs that follow.

In order to set up the HBV-EC model, the user must first delineate a series of climate zones which are used to provide the model with the meteorological data which it requires to run. Several climate zone delineation methods were attempted before the final gridded alignment was arrived at (Figure 34). These fifteen zones each have their own time series of temperature and precipitation (rain and snow separated) that are used to drive the hydrological processes within the model. This resolution of climate data is not ideal (having smaller zones would allow for small meteorological abnormalities, such as localized thunderstorms, to be more fully represented within the model) but the addition of further climate zones would have made the model simulation times considerably longer. In the current incarnation of the model, loading and launching the simulation takes approximately 20 minutes, which compares unfavorably with the simulation times of WATFLOOD^{TM} (~10 minutes) and HMETS (less than 30 seconds).
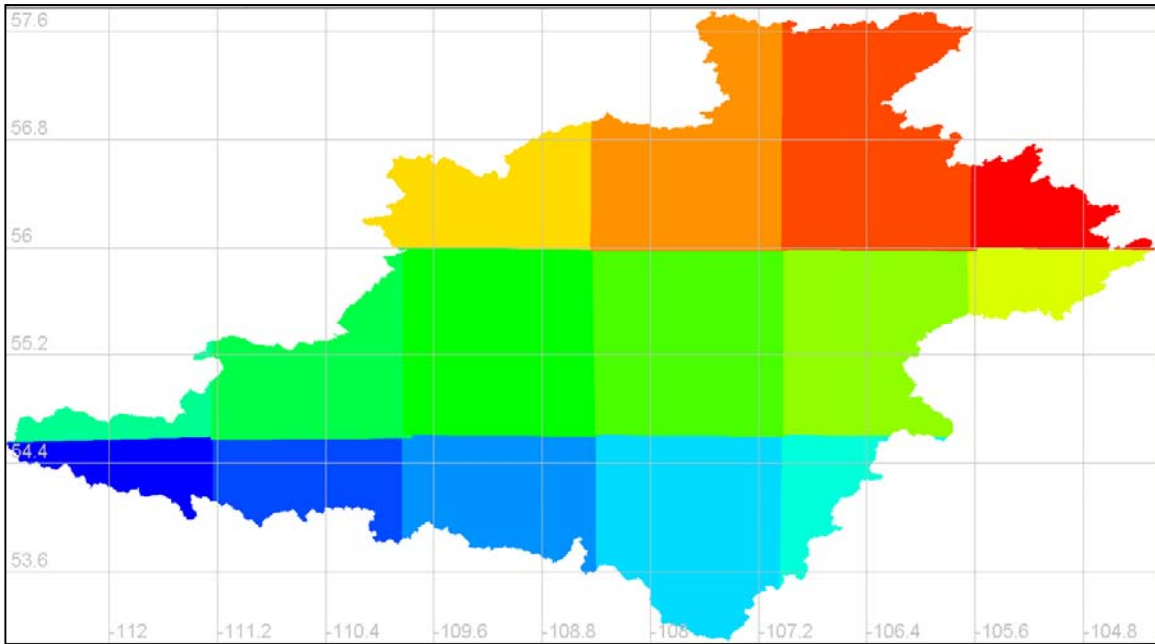
Figure 34: Gridded climate zones used within the HBV-EC model of the CRB

The addition of the meteorological data was another important element of the calibration process for the HBV-EC model. While the WATFLOOD™ model utilised its own gridding system to distribute the station data to the grids within the model, there is no such option available for the HBV-EC model. As a result, the NLWIS gridded temperature and precipitation datasets were used to force the model (Hutchinson, et al., 2009). This dataset is a gridded product which uses the same station data that drives the WATFLOOD™ model's gridded data generating software. While the data is not identical, the NLWIS product and the results of the WATFLOOD™ precipitation and temperature gridding procedure were found to have strong correlation (correlation coefficients of 0.98 and 0.99 for daily temperature and from 0.8 to 0.98 for monthly precipitation totals with precipitation differences at any of the test points being less than 10%). This warranted the use of the NLWIS product within the scope of this project although

the slight differences in the input data may lead to uncertainty in subsequent portions of the study.

The HBV-EC model, being conceptual in nature, does not have as many parameters to calibrate as the previously discussed WATFLOOD[TM] model. Due to the fact that an automated calibration scheme was not made available for the HBV-EC model, a manual calibration method was utilised. As with the WATFLOOD[TM] model, initial efforts concentrated on solving major visible issues with the hydrograph such as peak timing and magnitude as well as low-flow conditions. After resolving these to an acceptable level, more minute adjustment of some parameters began on a trial and error basis. A spreadsheet was used to calculate the performance statistics and determine the relative quality of one set of model parameters compared to the previous set. In order to keep model calibration as even as possible between the different models, the same performance statistics were used as in the WATFLOOD[TM] model calibration. A summary of the final parameter set used for subsequent simulations may be found in Appendix B.

The following table and plots show the hydrographs which were produced by the calibrated HBV-EC model (Table 4, Figure 35, Figure 36, Figure 37, and Figure 38).

Table 4: Performance statistics for HBV-EC model at WSC station 06CD002

Period	Time Series Nash-Sutcliffe	Correlation Coefficient (r^2)	% Dv	Annual Average Nash-Sutcliffe	Average flow [cms]
1982-1985 (validation 1)	0.73	0.74	1.25	0.84	206.41
1986-1989 (calibration)	0.63	0.62	5.31	0.84	233.60
1990-1995 (validation 2)	-0.05	-0.48	38.57	0.05	166.97
1979-1995	0.21	0.28	5.99	0.64	209.29
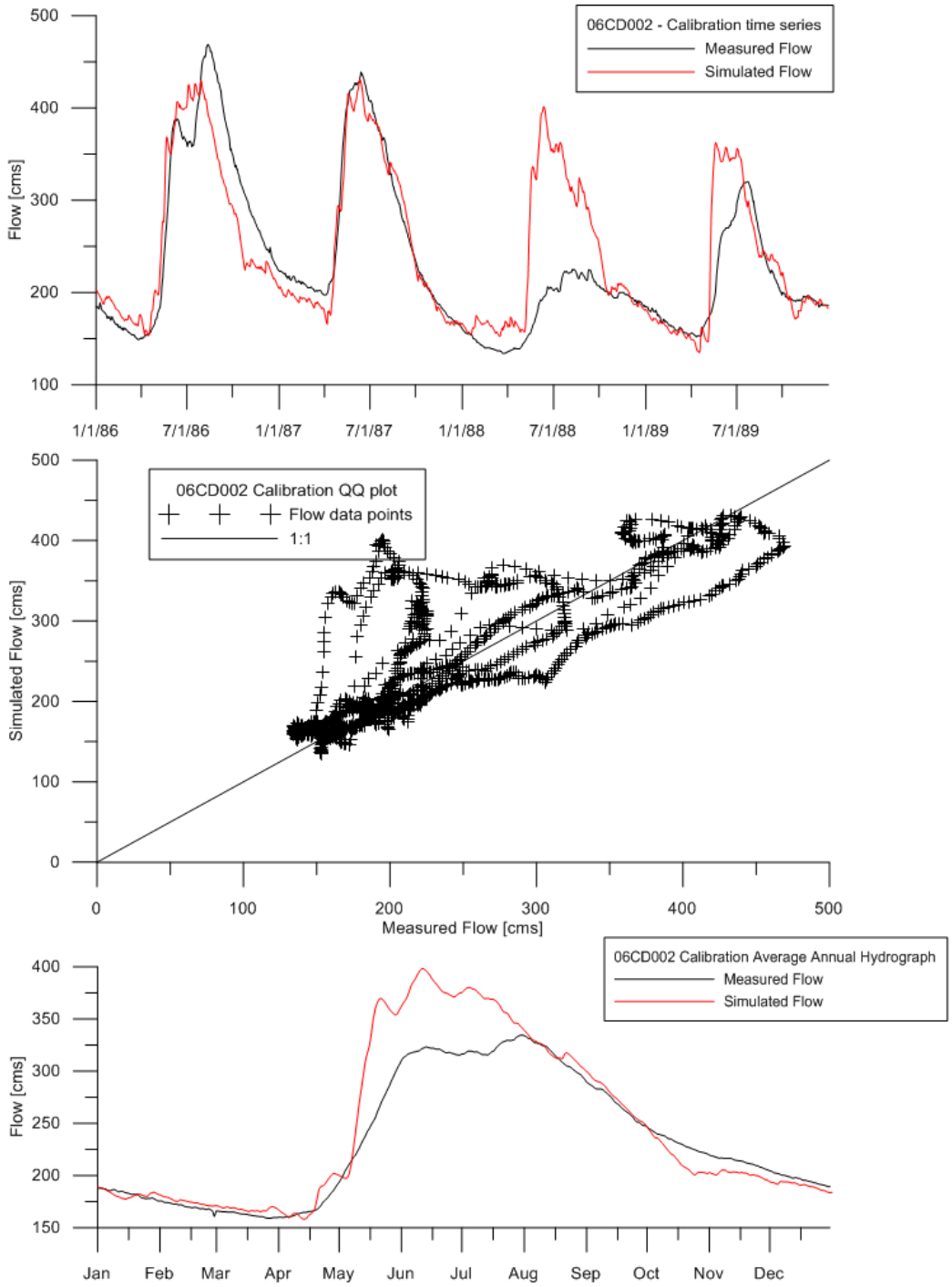
Figure 35: Flow time series, QQ plot and average annual hydrograph for calibration period (1986-1989) HBV-EC
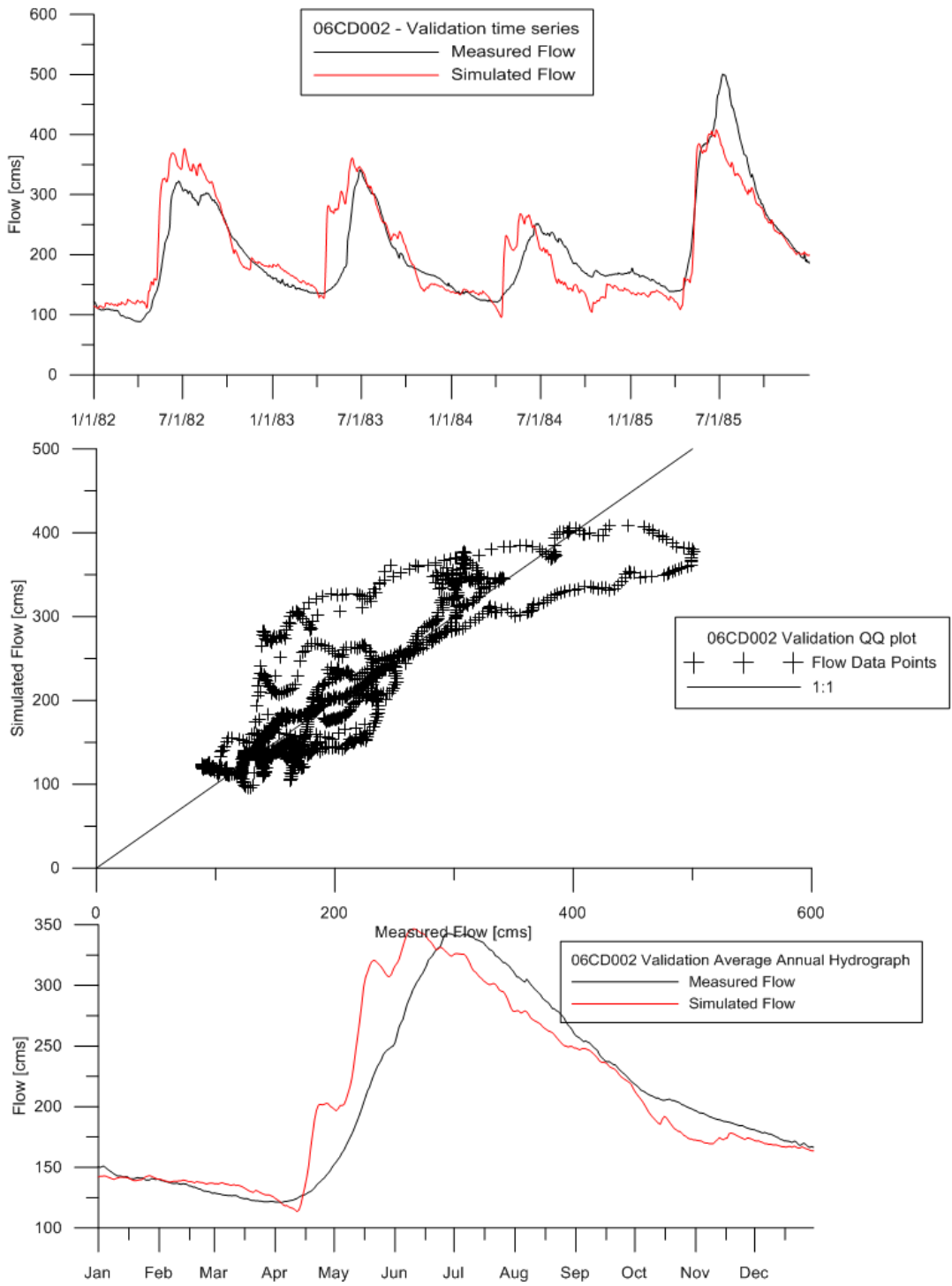
Figure 36: Flow time series, QQ plot and average annual hydrograph for validation period (1982-1985) HBV-EC
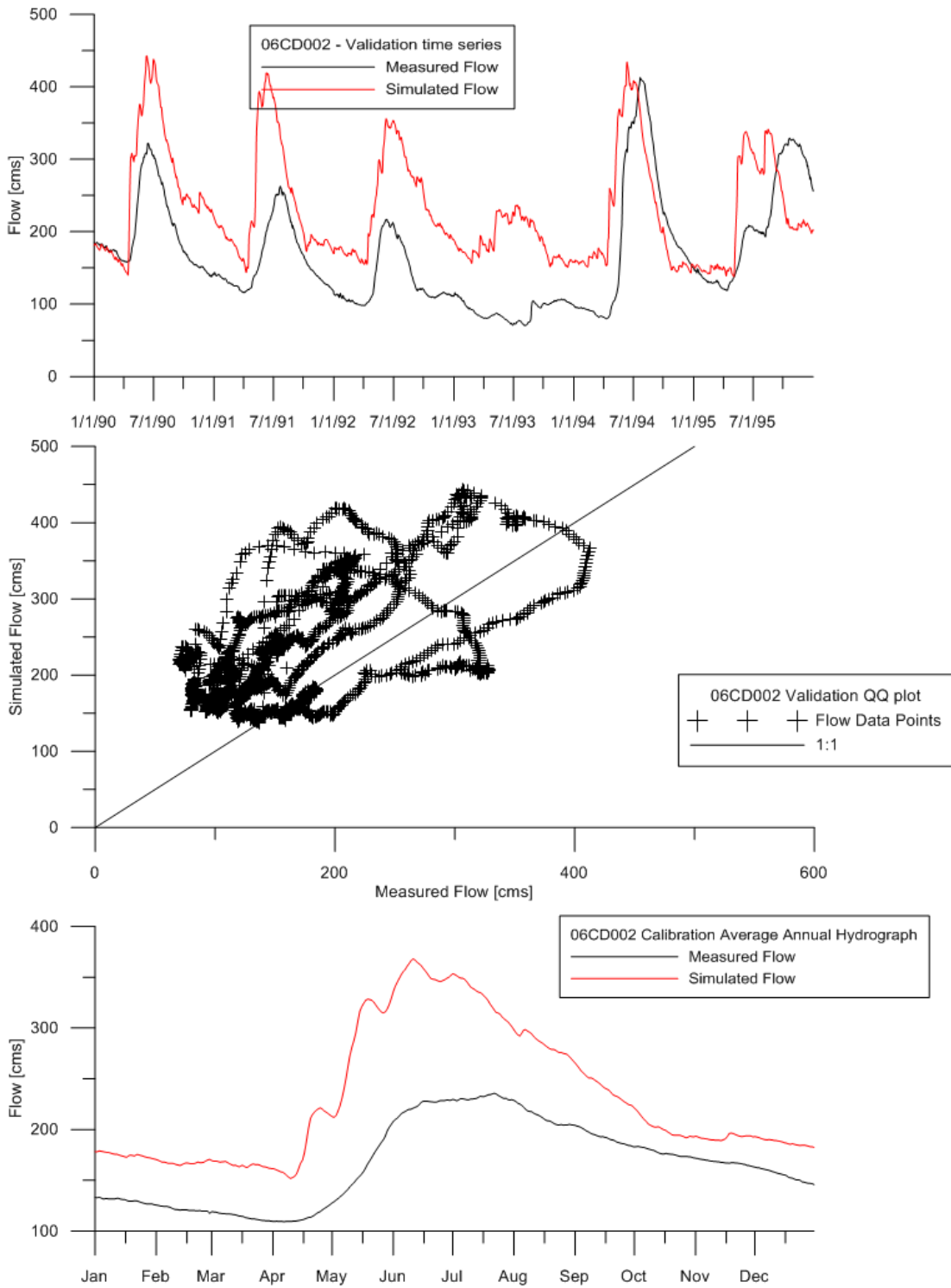
Figure 37: Flow time series, QQ plot and average annual hydrograph for validation period (1990-1995) HBV-EC
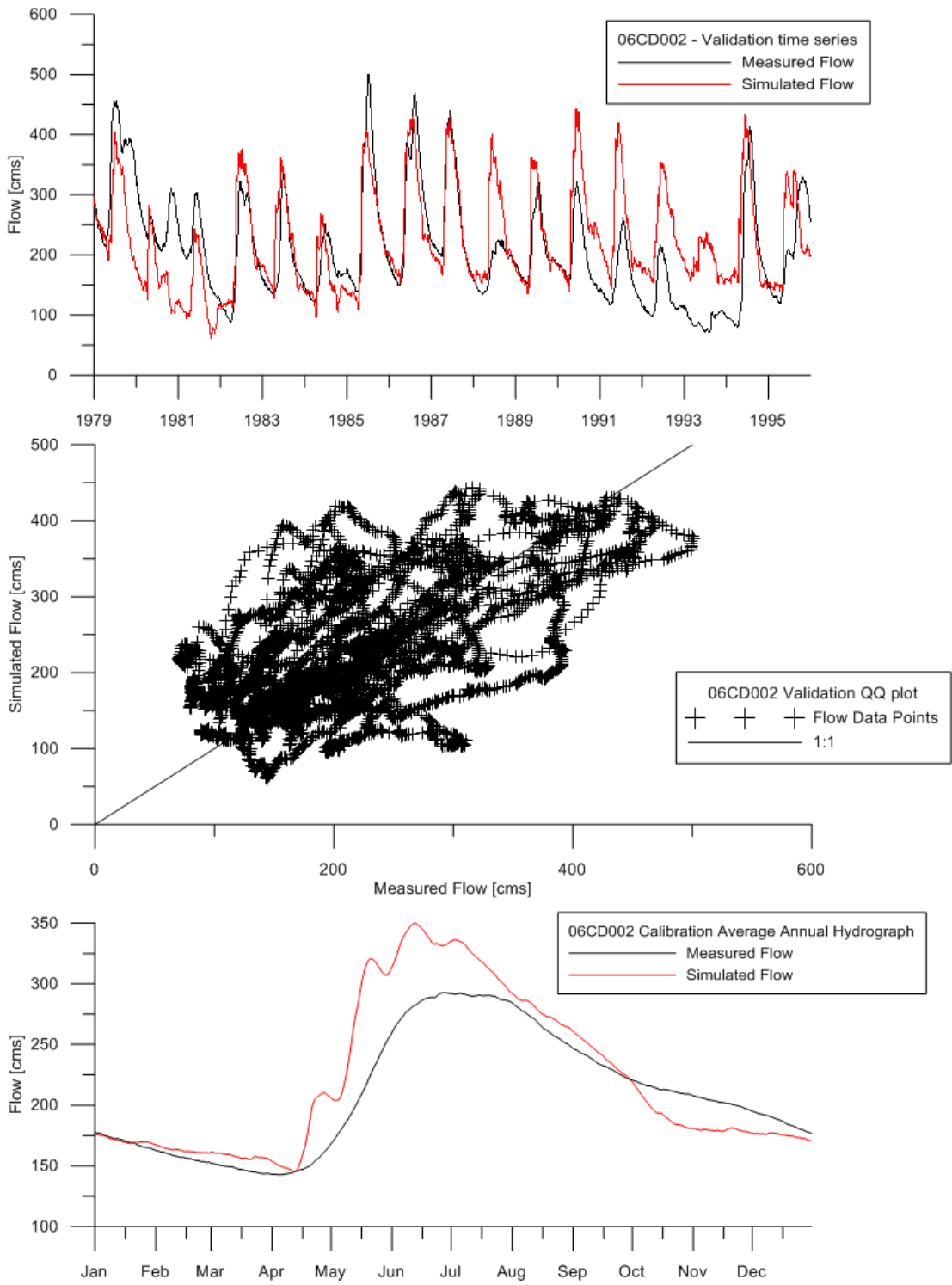
Figure 38: Flow time series, QQ plot and average annual hydrograph for entire model period (1979-1995) HBV-EC

The shape of the hydrographs generated by the HBV-EC model appears quite different than the ones created by the WATFLOOD^{TM} model. The fact that there are several small peaks in the hydrographs may be attributed to the fact that the model uses more, larger areas (due to the elevation banding approach) for calculating runoff, and those areas may not contribute their peak flow to the outflow hydrograph on the same day. Despite this, the model was able to simulate a hydrograph with acceptable calibration statistics for each of the time periods examined.

During the calibration period (Figure 35), the HBV-EC model is able to simulate the hydrograph for three of the four years quite well. The lowest peak flow was recorded in the 1988 freshet period. During this year, the model overestimates the flow by a significant margin. The reason for this anomaly is difficult to determine, but it may be due to a combination of errors in the input data (meteorological and streamflow), model structure and calculation methods, and hydrological processes which are not able to be modelled by the HBV-EC conceptual framework. It is interesting to note that the HMETS model also was unable to simulate the freshet properly during this year. Also of note is that the lower flow portions of the year were simulated quite accurately throughout the calibration period.

During the first validation period (Figure 36) the model is able to accurately simulate each of the freshet peaks. As a result, the performance statistics are actually higher for this time period than for the period which the model was calibrated for. One area where the model performance does seem to suffer is in

predicting the timing of the peak flow. The modeled peak is consistently earlier than was observed at the gauging station. The second validation period (Figure 37) is another story entirely. The flow is overestimated during this period for nearly every day within the period. This fact is reflected in the poor performance statistics that are yielded during this period. Errors may be due to a number of reasons such as over-estimation of evaporation and other losses during low flow periods, but because the model was able to simulate flow so well for the other time periods, this was deemed to be sufficient.

The hydrograph generated for the entire modelled period (Figure 38) shows this fact quite well. During the early portion of the period, the model is underestimating the flow and during the later portion the flow is overestimated. These errors balance out quite well, as witnessed by the low deviation of volume (5.99%, Table 4). Overall, the HBV-EC model is able to do a reasonable job of simulating the hydrology of the Churchill River basin.

4.2.3 Calibration of HMETS hydrological model
The HMETS hydrological model is by far the simplest of the models chosen for this study. The parameter set for the model consists of a series of coefficients which are not able to be measured directly.

The model does not require a DEM or land cover map, as the previous two models did. The user needs only to input the size of the basin and the approximate location of the centre point of the drainage area. The latter is so that the program can determine the amount of solar radiation present in the

basin, which the model uses to calculate the potential evapotranspiration using a simple energy balance method.

As with the other models, HMETS requires that the user supply a time-series of data for the meteorological inputs as well as the measured discharge for comparison in calibrating the model. The model can only accept one set of meteorological data for the entire drainage basin. The average from three spatially distributed CDCD stations with good data quality was determined to represent the approximate average of the data within the modelled region. The model is only capable of estimating at one outflow location, so once again the WSC gauge at Otter Rapids was chosen as the outlet location of the model in order to maintain consistency throughout each of the models used.

Calibration of the model parameters was a relatively simple process as the model runs were quite short (approximately 10 seconds per model run), making a simple trial and error approach possible. The parameters which the user can change within the model form four distinct groups: hydrograph parameters (four parameters including time to peak and shape factors), snow model parameters (10 parameters including degree-day factor and water retention coefficients), one evapotranspiration parameter, and three parameters defining the subsurface flow regime. Each of these parameters has a range which has been shown to provide reliable results in previous studies. As the CRB is considerably larger than any other catchment for which this model has been implemented, the hydrograph parameters, and especially the time to peak, was predictably out of the range of those values used for any other basin. A complete list of the final parameters

which were chosen for this model is given in Appendix C. The following table and plots show the hydrographs created using the "good" set of parameters which were used when conducting climate change simulations in the following chapters (Table 5, Figure 39, Figure 40, Figure 41, and Figure 42).

Table 5: Performance statistics for HMETS model at WSC station 06CD002

| Period	Time Series Nash-Sutcliffe	Correlation Coefficient (r^2)	% Dv	Annual Average Nash-Sutcliffe	Average flow [cms]
1982-1985 (validation 1)	0.69	0.70	-10.32	0.88	206.41
1986-1989 (calibration)	0.51	0.44	7.65	0.84	233.60
1990-1995 (validation 2)	-0.25	-1.08	26.22	0.22	166.97
1979-1995	0.34	0.12	6.06	0.82	209.29
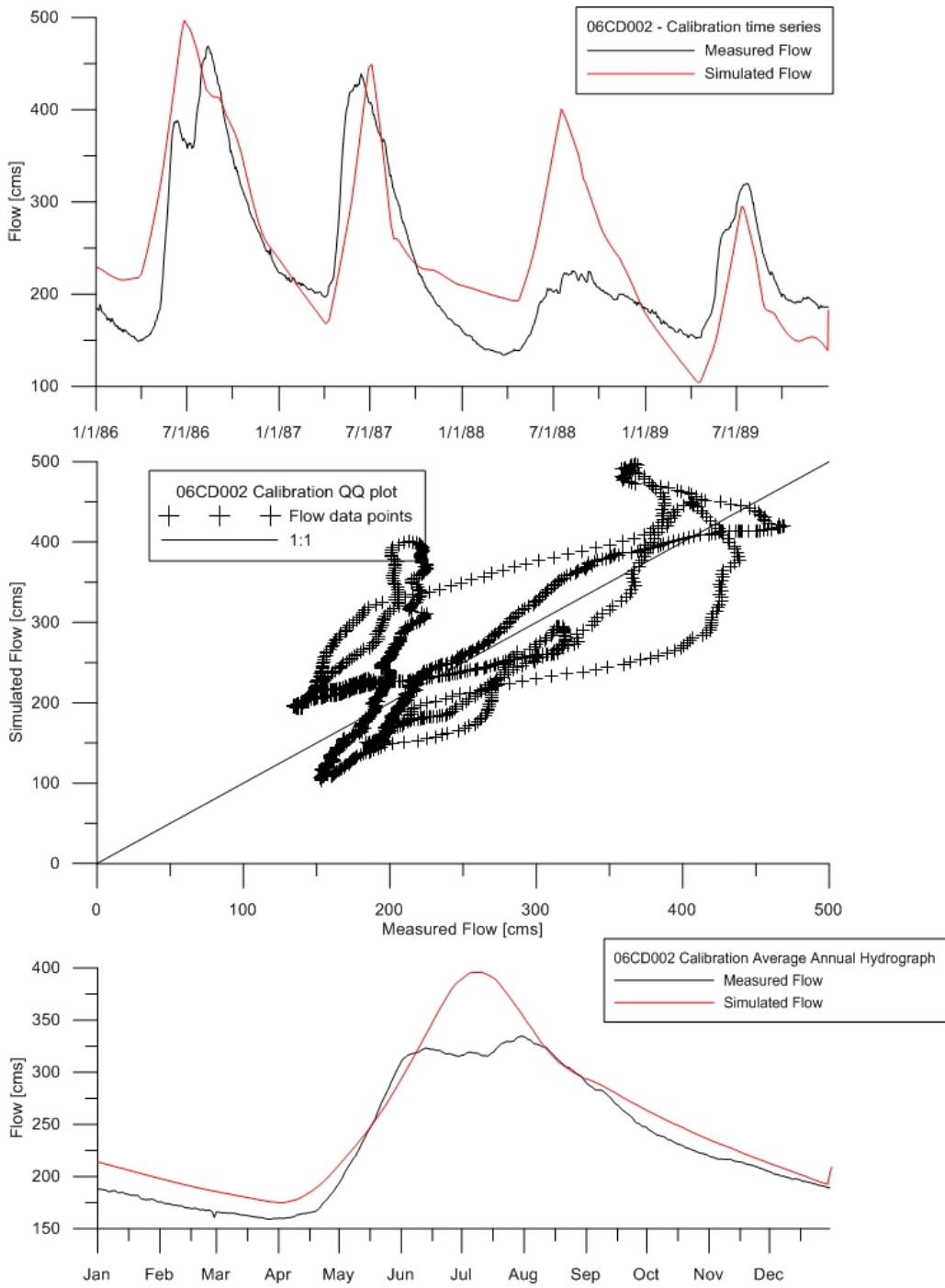
Figure 39: Flow time series, QQ plot and average annual hydrograph for calibration period (1986-1989) HMETS
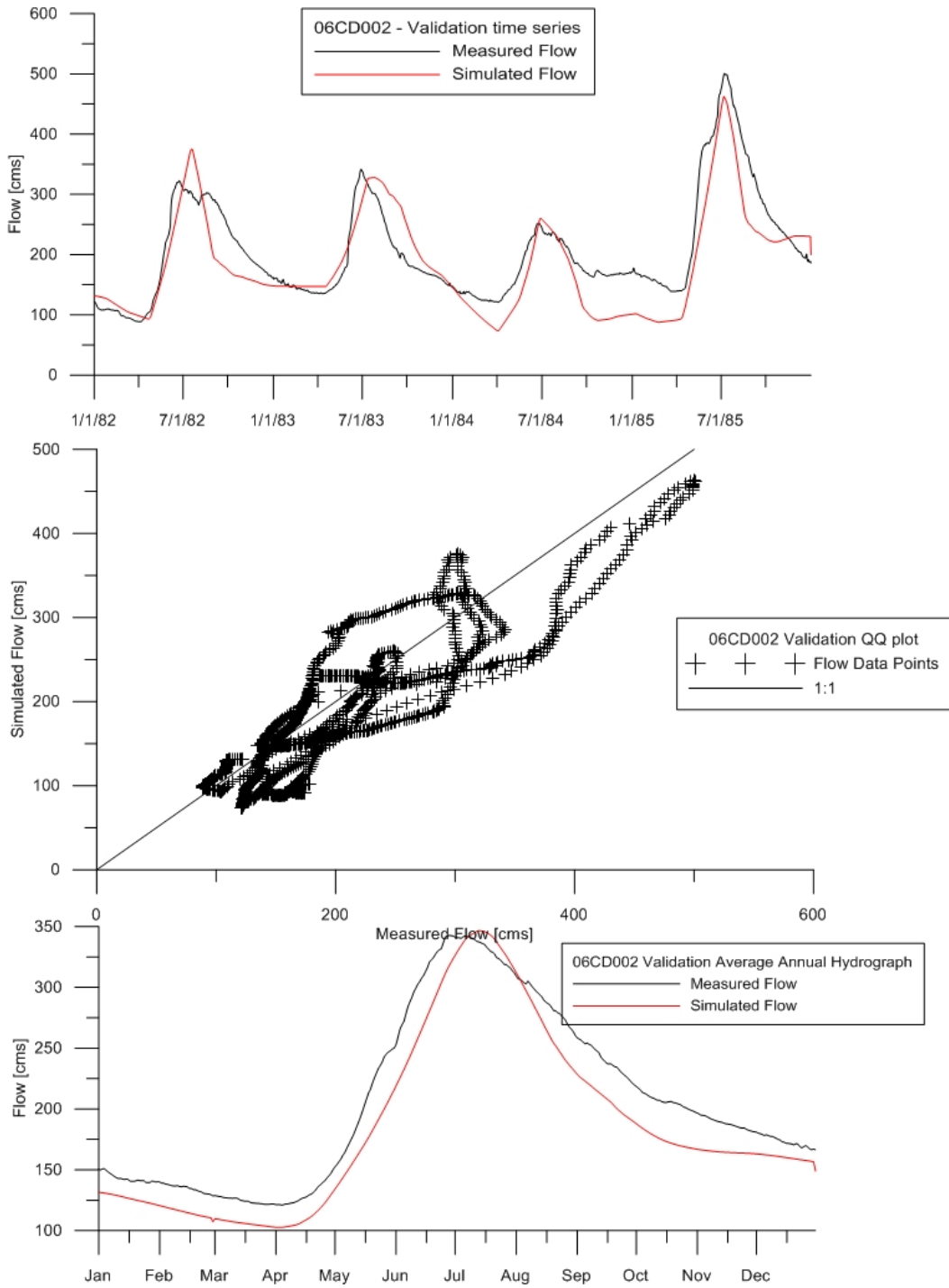
**Figure 40: Flow time series, QQ plot and average annual hydrograph for validation period (1982-1985) HMETS**
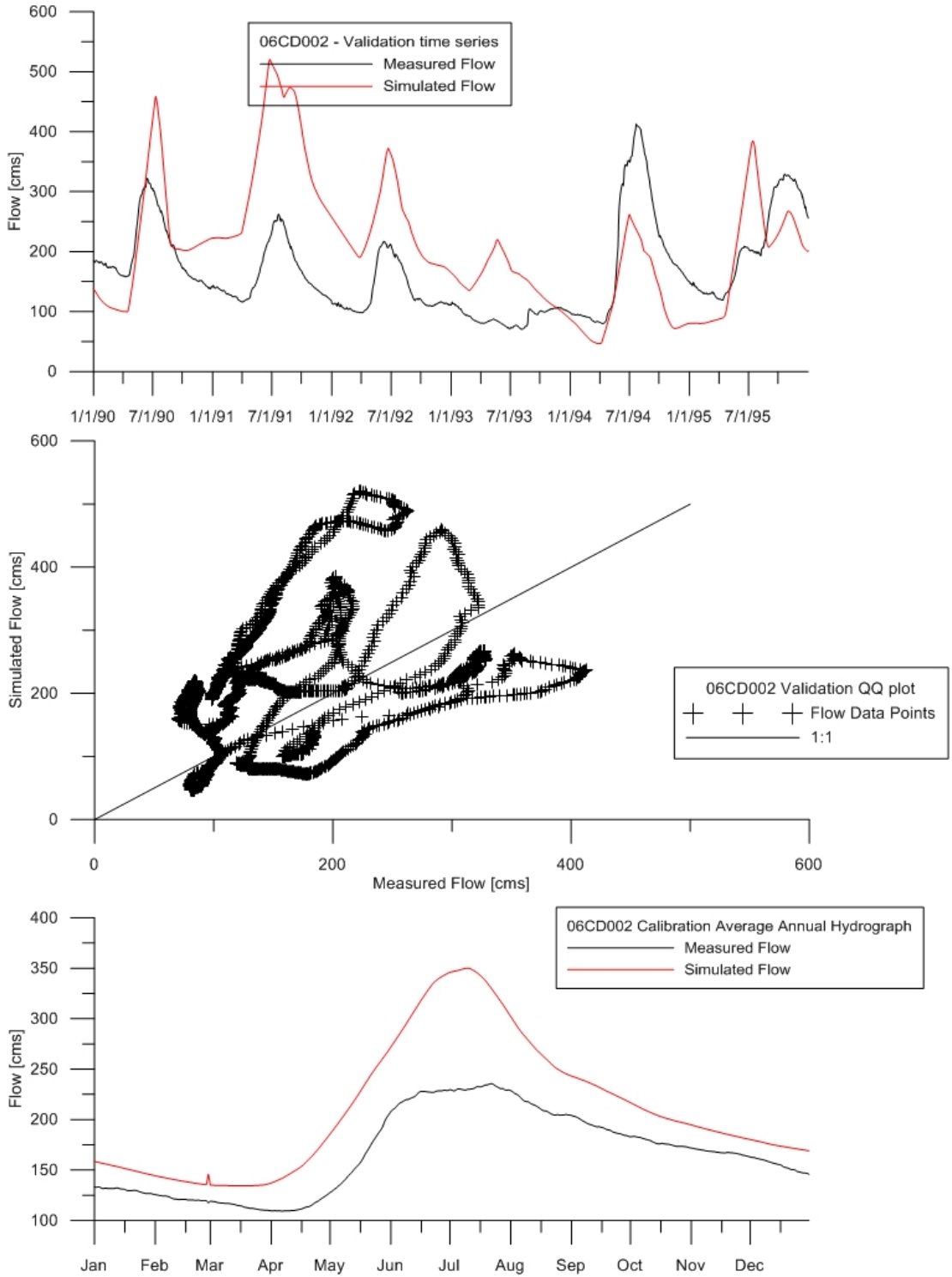
Figure 41: Flow time series, QQ plot and average annual hydrograph for validation period (1990-1995) HMETS
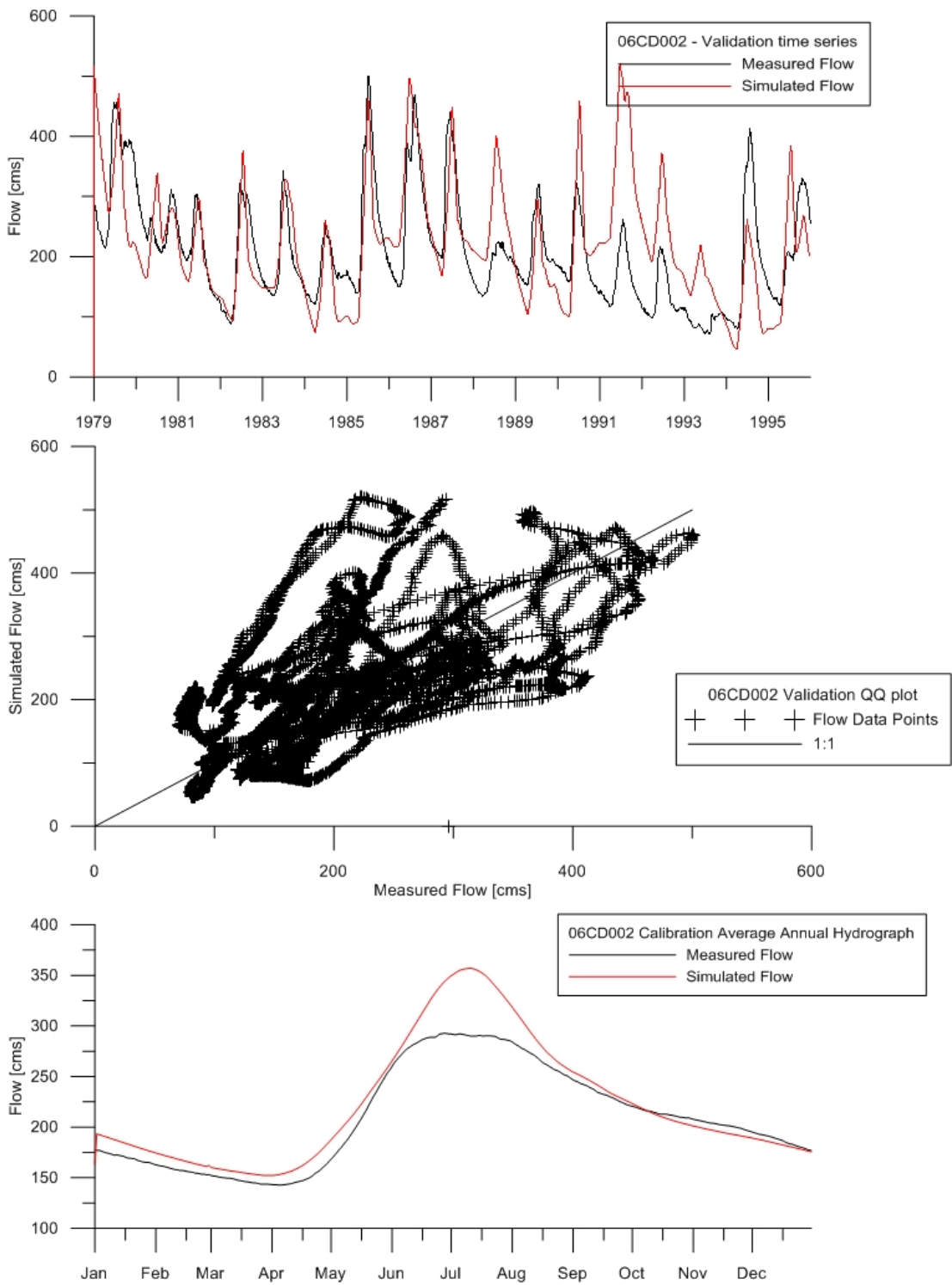
Figure 42: Flow time series, QQ plot and average annual hydrograph for entire model period (1979-1995) HMETS

89

The results obtained using the HMETS model appears to be quite different from those achieved by the other models in the suite. The result of the simplicity of the lumped-conceptual model is that the hydrograph is considerably simplified (i.e. one rising and falling portion of the hydrograph with less small fluctuations, which is the expected result of using a single meteorological time series for the entire basin). Despite this, the model was able to predict the volume of the freshet peak relatively well for 3 of the 4 years used for calibration (Figure 39). The year that was overestimated (1988) had a considerably lower peak and was similarly overestimated by the semi-distributed HBV-EC model as well. It is possible that baseflow or snowmelt have errors which are only apparent during low flow years causing this anomaly as the WATFLOOD^{TM} model is able to simulate this peak properly.

During the validation period (Figure 40), the HMETS model once again performs admirably, with statistics that exceed those achieved during the calibration period. This is a result of the model not overestimating a freshet peak as it did during the calibration period. During this period, the model estimates the peak flows quite well, but tends to slightly underestimate the flow during the lower flow periods of the year.

During the second validation period (Figure 41), the HMETS model consistently overestimates the flow for all periods of the year. The exception is during the 1994 freshet, where the peak flow is actually under-predicted. This may be a result of the input data that was chosen not being 100% representative of the conditions which were observed throughout the basin. This is a limitation of the

lumped model type which cannot be avoided or overcome without changing the model composition significantly and eliminating the model's principal advantage of short run times and low data requirements.

The simulation for the entire model period (Figure 42) once again reinforces the concepts and trends which were observed throughout the shorter simulations. In general the peak freshet flow was overestimated while the flow during the lower flow periods of the year was simulated very close to that which was observed. The fact that the model was able to simulate the flow to within 6% for the total period was deemed to be acceptable.

4.3 Inter-comparison of hydrological model performance

The easiest way to fully understand how the model results compare to each other and to identify similarities and differences between the resulting hydrographs is to compare them directly to each other. The following plot (Figure 43) shows the annual average hydrograph from 1979-1995 for each of the models along with the annual average measured flow for comparison.
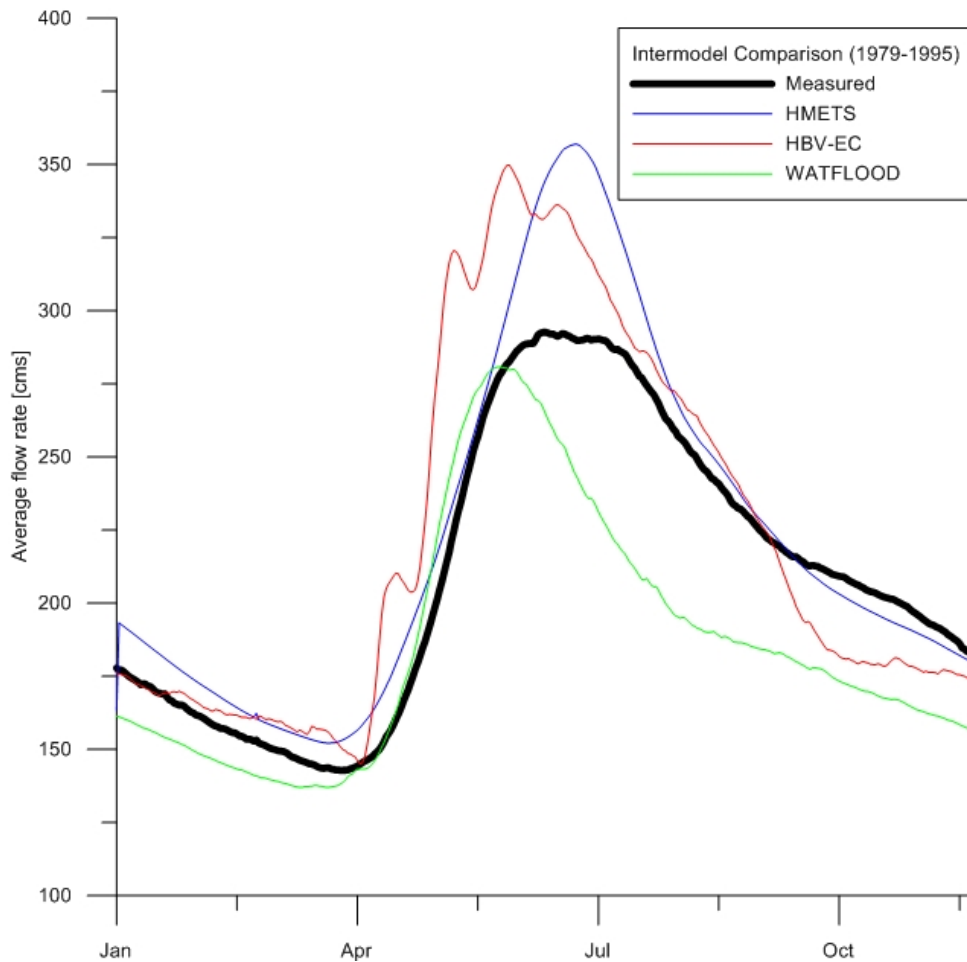
Figure 43: Comparison of annual average hydrograph for all hydrological models

The above plot shows that HBV-EC predicts an earlier spring freshet than the other two models. It is followed by WATFLOOD™, which predicts the freshet slightly earlier than the measured event, and finally by HMETS which actually predicts the freshet later than the measured data. The highest annual peak belongs to the HMETS model, followed closely by the HBV-EC model and then WATFLOOD™. During low-flow portions of the year (late summer, fall and winter) the WATFLOOD™ model predicts the lowest flow levels with HBV-EC being slightly higher and HMETS being just higher still. This plot also shows that the WATFLOOD model has the lowest average yearly flow (189.1 cms)

compared to the HBV-EC and HMETS models (221.86 and 222.01 cms, respectively). Each of these values compare well to the observed average flow of 209.3 cms.

These results show that while the models each achieve similar calibration statistics, their performance during the year is actually quite different. It appears that the HBV-EC model melts the snowpack fastest (as indicated by the slope of the leading edge of the hydrograph) while WATFLOOD^{TM} recedes to baseflow faster than the other two models (seen in the slope of the trailing edge of the hydrograph). These differences are the results of the different model types and distributions as well as the different methods used to calculate each of the hydrological processes.

It is important to note that the performance of a hydrological model is dependent on the study which is being undertaken as well as the characteristics of the basin. Because the Churchill is a large basin with a long time to peak and prolonged high flow period, timing errors on the order of one week are acceptable where they would not be in a smaller basin.

Chapter 5: Climate Change Quantification

It is generally accepted that the earth's climate is going through dramatic changes. Fluctuations in the amount of precipitation and the average temperature have been recorded at many different locations (IPCC, 2007). These changes have a significant impact on many of the various earth systems which human civilizations have come to rely heavily on for their survival and success, including, but not limited to, potable water supply, flood prediction and prevention, and hydroelectric generation potential (Barnett, Adam, & Lettenmaier, 2005).

Realizing that the climate is changing is fairly obvious when one considers that less than 1000 years ago the majority of North America was covered in ice. Temperatures and precipitation are recorded at meteorological stations, or extracted from proxy records such as ice cores (Edwards, et. al, 2008) or tree ring studies (Beriault & Sauchyn, 2006) for the period before weather records exist. Trends can be extracted from this data to determine whether the current climate changes are significant compared to the past. Understanding the reasons behind these changes and trying to estimate the future changes that may occur is much more difficult. This involves understanding the processes which drive the climatic system, and estimating how the inputs to these processes will change throughout the course of time. This task has been taken up by several groups worldwide who have created GCMs which utilise climate change scenarios developed by the IPCC in order to project what the global

climate of the future will look like. These models and why and how they were used in this project are explained in the paragraphs which follow.

5.1 Assigning value to climate change

In order to use the data from the climate models to estimate the impact of climate change on the environment, some method for analyzing the data must be implemented. There are several methods which have been utilised in previous studies predicting the impact of climate change on various regions of the globe. These methods are outlined in the reference work on the state of the science of climate change (Xu, Widen, & Halldin, 2005).

The first, and most simple method, is to use the output of the GCM directly. Many GCMs provide predictions of the regional hydrological response directly. These predictions have inherent uncertainties related to them and their coarse resolution and inability to predict precipitation without large errors (IPCC, 2001). While these predictions provide some estimate of the hydrological response to climate change, they are not useful for accurate estimation at the sub-basin scale. One study concluded that the simulations of 23 major river basins by the third generation GCM of the Canadian Centre for Climate Modelling and Analysis were inaccurate and only 4 river basins were predicted to within 20% of annual estimates of the mean annual runoff (Arora, 2001).

The second method is quite similar to the first except that it involves using an RCM. The basis of the RCM is that it uses the GCM as a boundary condition. Some of the shortcomings of using this type of model are that they are still

dependent on the coarse scale GCM and all of the errors which are inherent from this type of model, that the simulations are computationally intensive, and that the model results still need to be downscaled to determine the impacts at a meaningful scale for hydrological basin analysis (Xu, Widen, & Halldin, 2005).

A third method for determining the hydrological impact of the GCM predicted climate change is evaluating a global water balance model. These models are generally evaluated on a coarse hydrological grid (0.5 x 0.5 degrees) to determine the impact of climate change on the global hydrological cycle. These models use the output from the GCM directly in order to determine the magnitude of the change. They are limited by the fact that they require some calibration of conceptual parameters and that they are dependent on the quality of the input data which is at a coarser resolution than the water balance model.

Another method for estimating the impact of climate change is to use a macroscale (continental) hydrological model simulated with forcing data from GCMs or RCMs. These models are generally evaluated on a smaller scale than the global water balance models mentioned above and focus on particularly large catchment areas. These models use physically-based parameters and are transferrable from basin to basin. These models are useful for determining the impact on this continental scale but are limited by the fact that some remote areas may not have the required information to run this model properly (Xu, Widen, & Halldin, 2005).

A fifth method uses statistical downscaling to prepare the inputs from a GCM or RCM for use in basin scale hydrological models. This is the prescribed method from the IPCC Second Assessment Report (IPCC, 1996) and has been used in various hydrological impact studies (Graham, Andreasson, & Carlsson, 2007; Vivoni, et al., 2011). The benefits of this type of modelling are that it is less computationally intense than dynamical downscaling, and does not require the same amount of information about basin topography and other characteristics that RCMs require. However, these methods do require that a long series of reliable observed data and are affected by any biases present in the GCM (Xu, Widen, & Halldin, 2005).

The final method, and the one chosen for use in this project was to set up a catchment scale hydrological model and drive it into the future using hypothesized climate scenarios. This method can use a prescribed change factor, which adjusts observed input temperature records by a certain amount, chosen at random (Barnett, Adam, & Lettenmaier, 2005); or via a prescribed delta value (i.e., change in temperature and precipitation) obtained directly from RCM or GCM output. In the delta method, the difference between the GCM present and GCM future values is applied to the observed time series in order to represent the future climate of the region. This method has been utilised extensively in research (Poulin, *et al.*, 2011; Ruelland, *et al.*, 2012), and is useful in determining the expected trends in annual streamflow (i.e. timing of peak flow, overall volume, etc.). A major shortcoming of the method is that it cannot predict the occurrence of future drought or flood events, as the observed climate record

is not able to account for anticipated changes in these factors. This results in a future synthetic climate that is not entirely indicative of the anticipated future climate but allows for a very simple comparison of the magnitude of future flows to those simulated for the present time period. In reality the frequency of extreme events may change and the delta method as utilised in this study is not able to capture this effect.

5.1.1 Description of delta method
As outlined above, the delta method for quantifying the climatic changes occurring in the future will be utilised for this project. This method allows the user to compare a hydrograph generated by the model for the present time period to one that *may* occur in the future, given the predicted climatic shifts (i.e., increase/decreases in temperature and precipitation). For this method, only one time series of observed climate data is required. In order to simulate the effects of climate change, the differences between the future and present values predicted by the GCM model (for different scenarios) are applied to the observed precipitation and temperature time series.   The formulae used in the transformations are given below (*5.1* and *5.2*).

$$T_{future} = T_{observed} + \left(T_{GCM,future} - T_{GCM,present}\right) \qquad (5.1)$$

$$P_{future} = P_{observed} X \left(\frac{P_{GCM,future}}{P_{GCM,present}}\right) \qquad (5.2)$$

For both temperature and precipitation, the values are adjusted on a monthly basis (i.e. there is one change factor applied for all temperature and precipitation values in January, and a different one for all values in February, etc.). Using this

method allows the modeller to see trends in the overall hydrological regime which may be expected in the future under the assumed climate change conditions. This process is repeated for each of the GCM runs used and for each of the future time periods being considered.

The delta method is implemented in the WATFLOOD^{TM} model using a special climate change subroutine. If the subroutine is activated, the model reads in the temperature and precipitation delta values from a text file and adjusts the gridded temperature and precipitation values for each grid at each time step. This method was first developed by researchers at the University of Manitoba (Slota, 2009) and was then refined and implemented into the commercial model. Both HBV-EC and HMETS require the modeller to manually implement the delta method by adjusting the precipitation and temperature input files by the prescribed change amounts.

5.2 Selection of climate models

In order for a GCM to be selected for use in this study, it had to meet several criteria. The first was that it needed to have data available for both the "present" time period (1970-1999) and for both of the future time horizons which are being considered: 2050s (2040 – 2069) and the 2080's (2070 – 2099). The GCM also must have a sufficient number of data points within the spatial bounds of the Churchill River basin. Based on these criteria, 139 simulations were used throughout the climate change impact assessment. Since this study was focused on identifying uncertainty in the estimation of the climate change impacts, as

many of the GCMs were used as possible. This methodology was used in order to give the broadest range of results possible for intercomparison.

The second portion of the modelling exercise was to determine the uncertainty related to the parameterisation of the WATFLOOD^{TM} hydrological model. For this portion of the study, several versions of the WATFLOOD^{TM} parameter file which were found to perform well were forced with the future climate scenarios. Because of the excessive number of model runs required to perform the parameter uncertainty analysis, output from only one GCM was used in this portion. The Canadian Centre for Climate Modelling and Analysis' CGCM 3.1 was chosen because it has five simulations for each of the three chosen emissions scenarios, contains several grid points within the Churchill River basin to base the delta values on, and was developed by a Canadian group. This GCM provides the combination of quality and quantity of data required for this portion of the study.

5.3 Selection of emissions scenarios

The IPCC has released several reports detailing how the estimation of future climate should be conducted for climate change impact assessment studies (IPCC, 1990; IPCC, 1996; IPCC, 2001; IPCC, 2007). Due to the fact that the state of the future climate is not a certainty, several different possible scenarios have been developed, encompassing several different ways in which future development of the globe may evolve. These scenarios have been created in order to cover the broad spectrum of what could be expected from the future

climate. A simplified schematic of the driving variables and governmental focuses which lie behind the development of each of the scenarios is shown below (Figure 44).
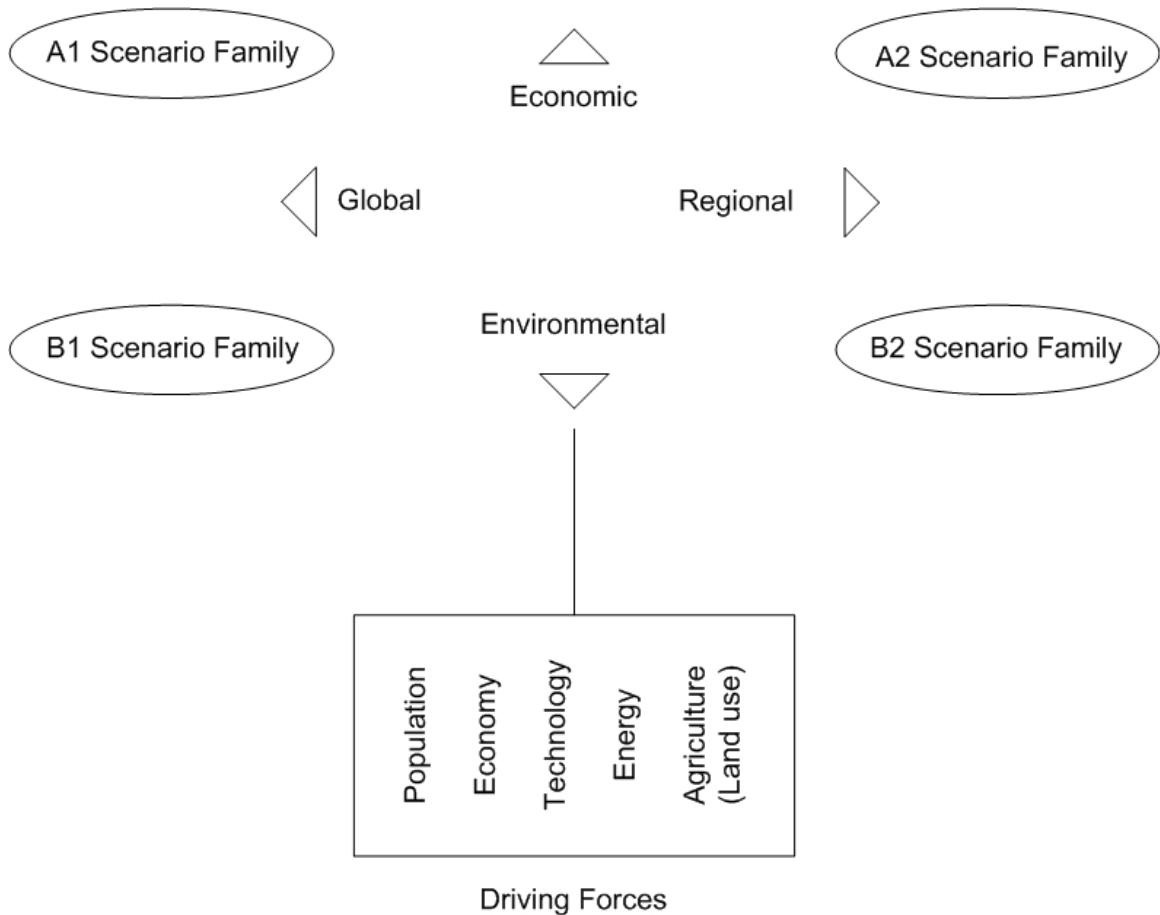
Figure 44: Driving forces behind the development of IPCC climate change scenarios (adapted from (IPCC, 2000))

The main storyline "families" of the IPCC Special Report on Emissions Scenarios (SRES) (IPCC, 2000) are A1, A2, B1, and B2. This two dimensional tree shows in very simplistic terms the orientation of global and regional policy making and development strategies associated with each of the families. Within each of these groups there are a series of scenarios which each detail a more specific direction which the future world policies and development may take. Important

factors in each of these scenarios are the global population trends and carbon emissions, among the many other drivers (IPCC, 2000).

The A1 storyline describes a world of rapid economic growth with a global population that peaks near the year 2050 and slightly declines thereafter. The regions of the world converge with the development of more efficient technologies and a reduction in the difference of per capita income between regions. There are three main groups of scenarios which correspond to the technological emphasis which dominates them: A1FI focuses intensively on fossil fuel related technologies, A1T is based heavily on non-fossil fuel energy sources and A1B is more balanced across all sources of energy (IPCC, 2000).

The A2 scenario family depicts a world in which the world is quite divided. Unlike the A1 storyline, the regions of the world do not converge very quickly, resulting in the preservation of a regional identity throughout the world. This is generally regarded as the worst case scenario in terms of changes to the global climate (IPCC, 2000).

The B1 storyline describes a world with the same population trends as the A1 family with a peak in the middle of the 21st century and a subsequent decline. This is accompanied by changes to the global economic structures and an emphasis on clean and resource-efficient technologies and global solutions to economic, social, and environmental sustainability. This family is used as the best case in most impact assessment studies (IPCC, 2000).

Finally, the B2 scenario family is one in which the world emphasizes local solutions while dealing with a continuously increasing global population. Governments focus on solving environmental and social issues, but do so at a regional scale (IPCC, 2000).

In order to provide this study with as broad a range of potential future climate scenarios as possible, several of the above storylines were selected for assessment in this study. The A2 and B1 scenarios were chosen to represent the best and worst possible situations. As a median, the A1B scenario was used to provide even more breadth to the modelling suite. It should be noted that A1B and this combination of model scenarios are commonly used throughout the climate change impact studies around the world (Chiew, et al., 2009; Bae, Jung, & Lettenmaier, 2011; Kling, Fuchs, & Paulin, 2012).

Several models were made available for this project providing data about the future climate for each of the above listed scenarios. The models used in this project account for 46 simulations from the B1 scenario, 54 from the A1B scenario, and 39 corresponding to the A2 future climate scenario. The differences are a result of each model simulating each of the scenarios in different combinations.

5.3.1 GCM delta values for Churchill River basin
The following scatter plots (Figure 45 through Figure 48) show the range of the delta values for the study area for each month during each of the future time horizons. Temperature deltas are given in degrees Celsius of change while the precipitation deltas are a percentage increase or decrease of the original

precipitation. Each point represents the data from one simulation of one GCM, with the x coordinate being the temperature delta and the y coordinate being the precipitation coordinate. These plots are helpful for identifying monthly and seasonal trends as well as the range of future results predicted by the ensemble of climate models. These trends will be discussed in detail below.
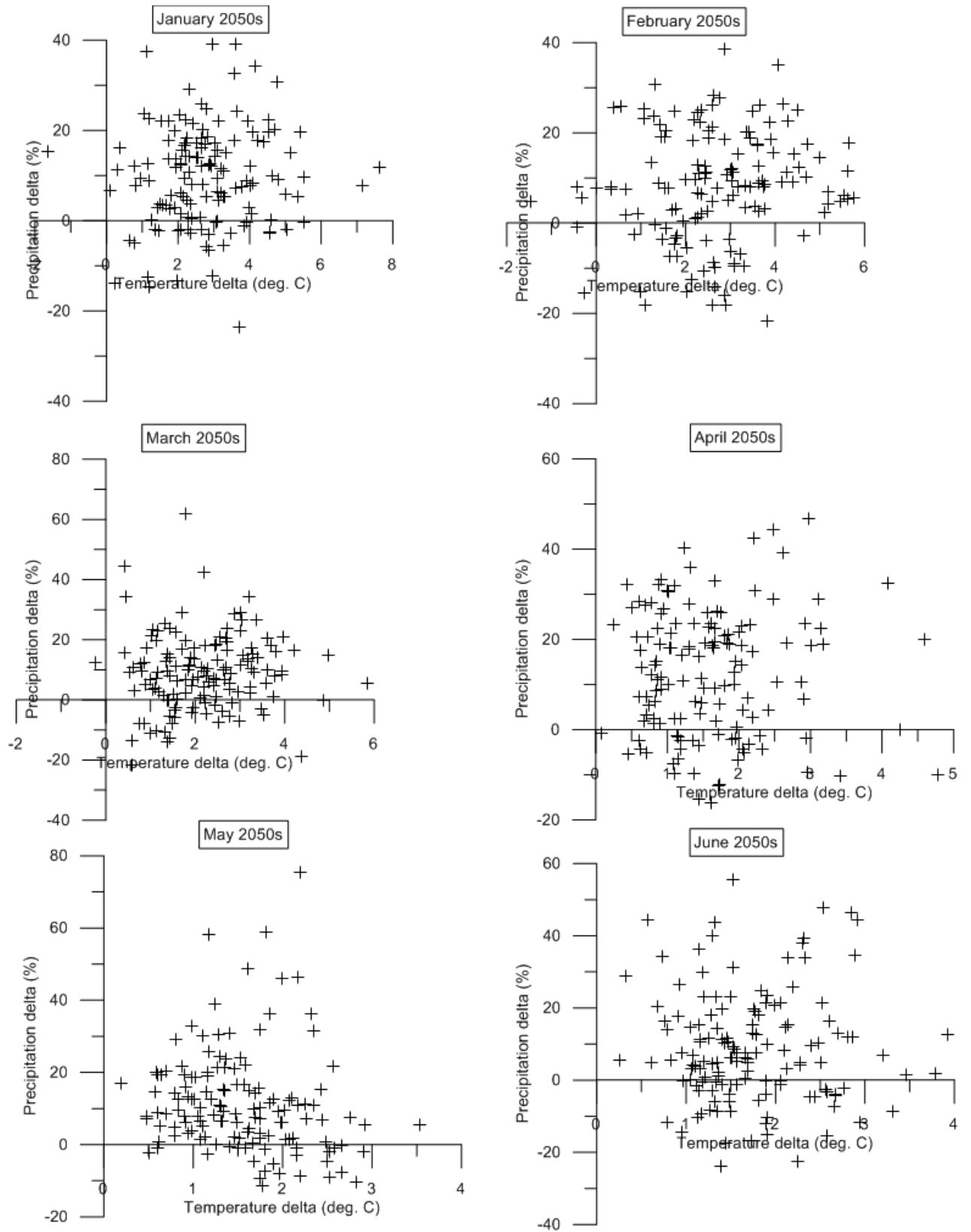
Figure 45: 2050s January – June temperature and precipitation delta values

105
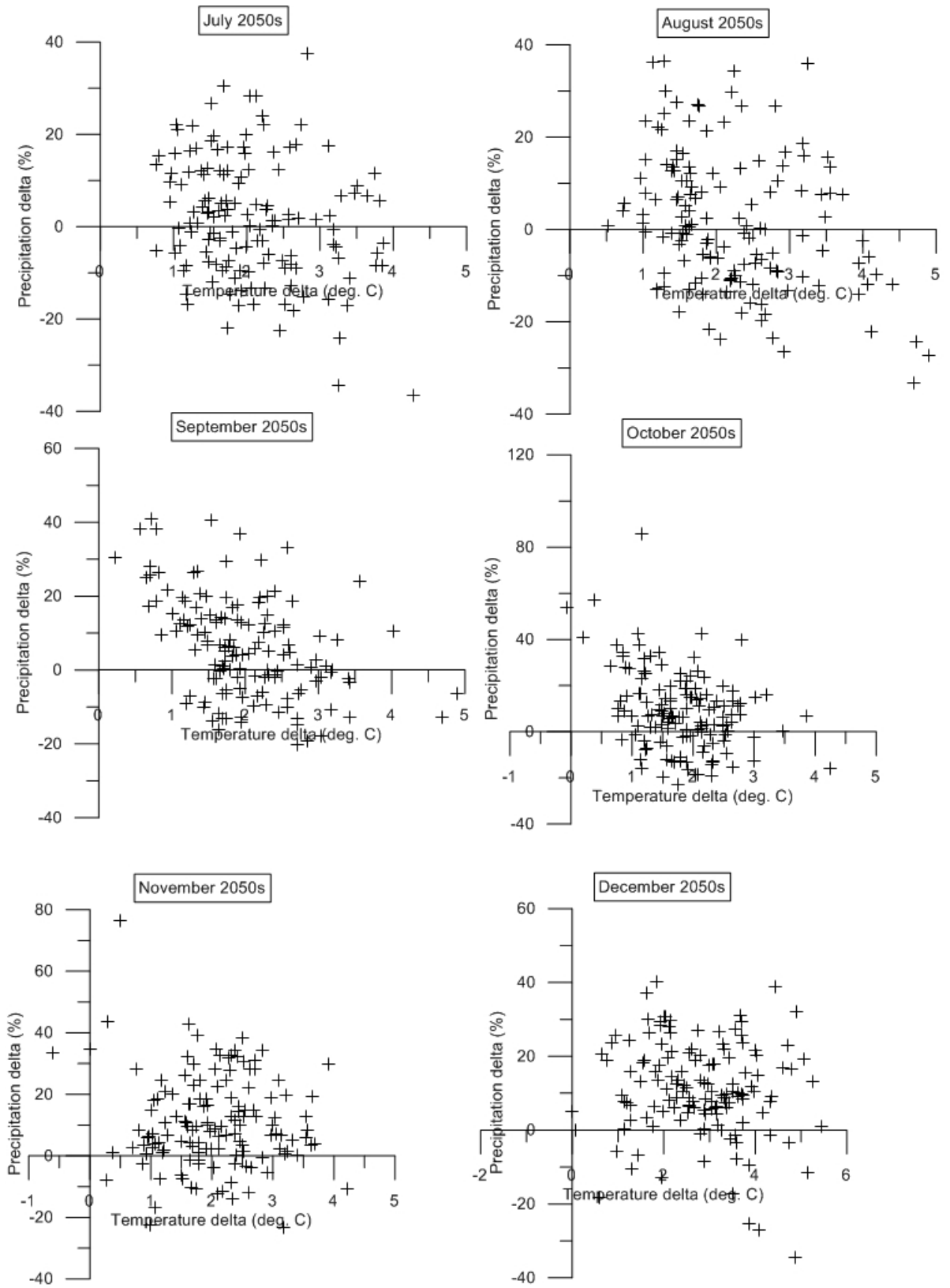
Figure 46: 2050s July – December temperature and precipitation delta values

106
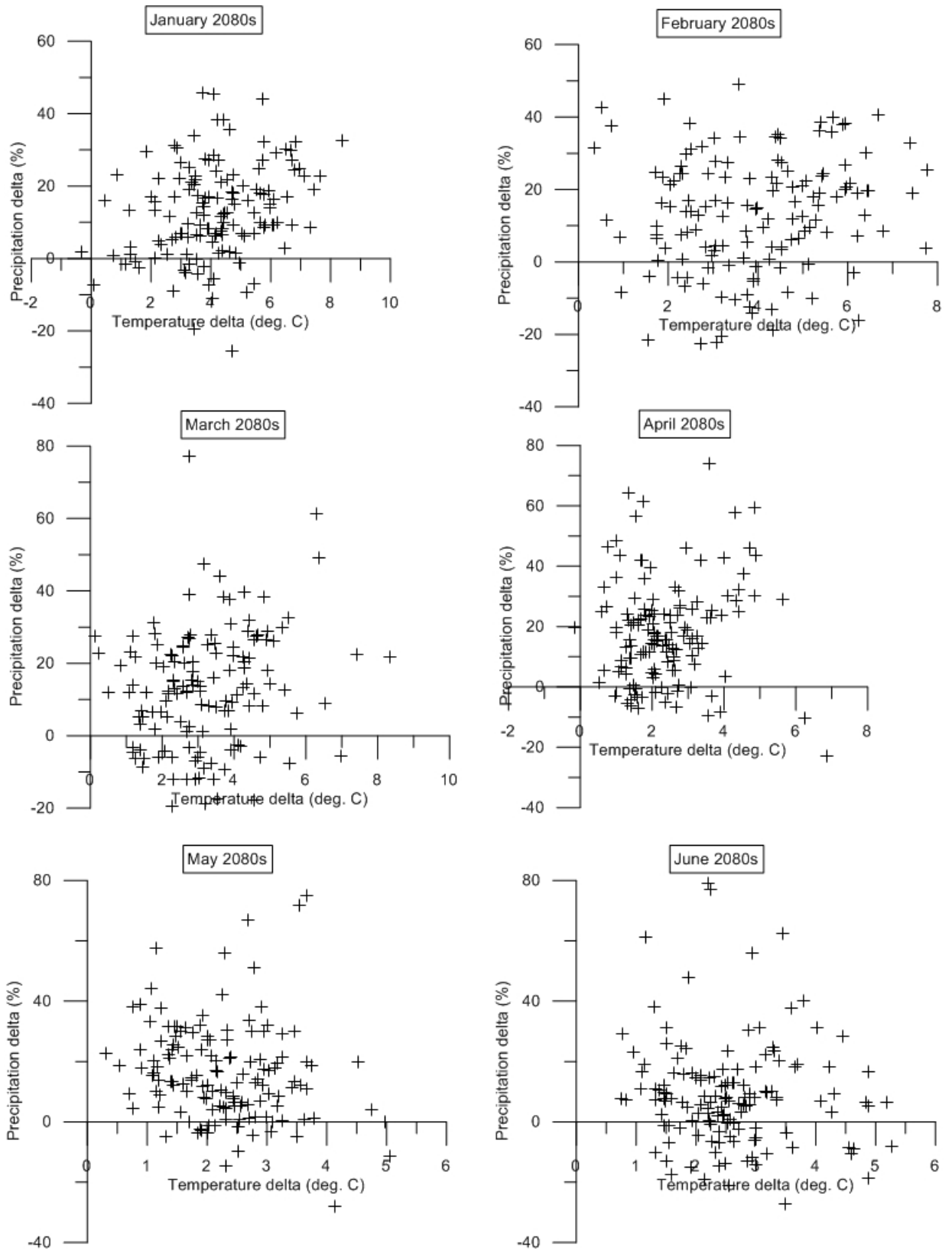
Figure 47: 2080s January – June temperature and precipitation delta values

107
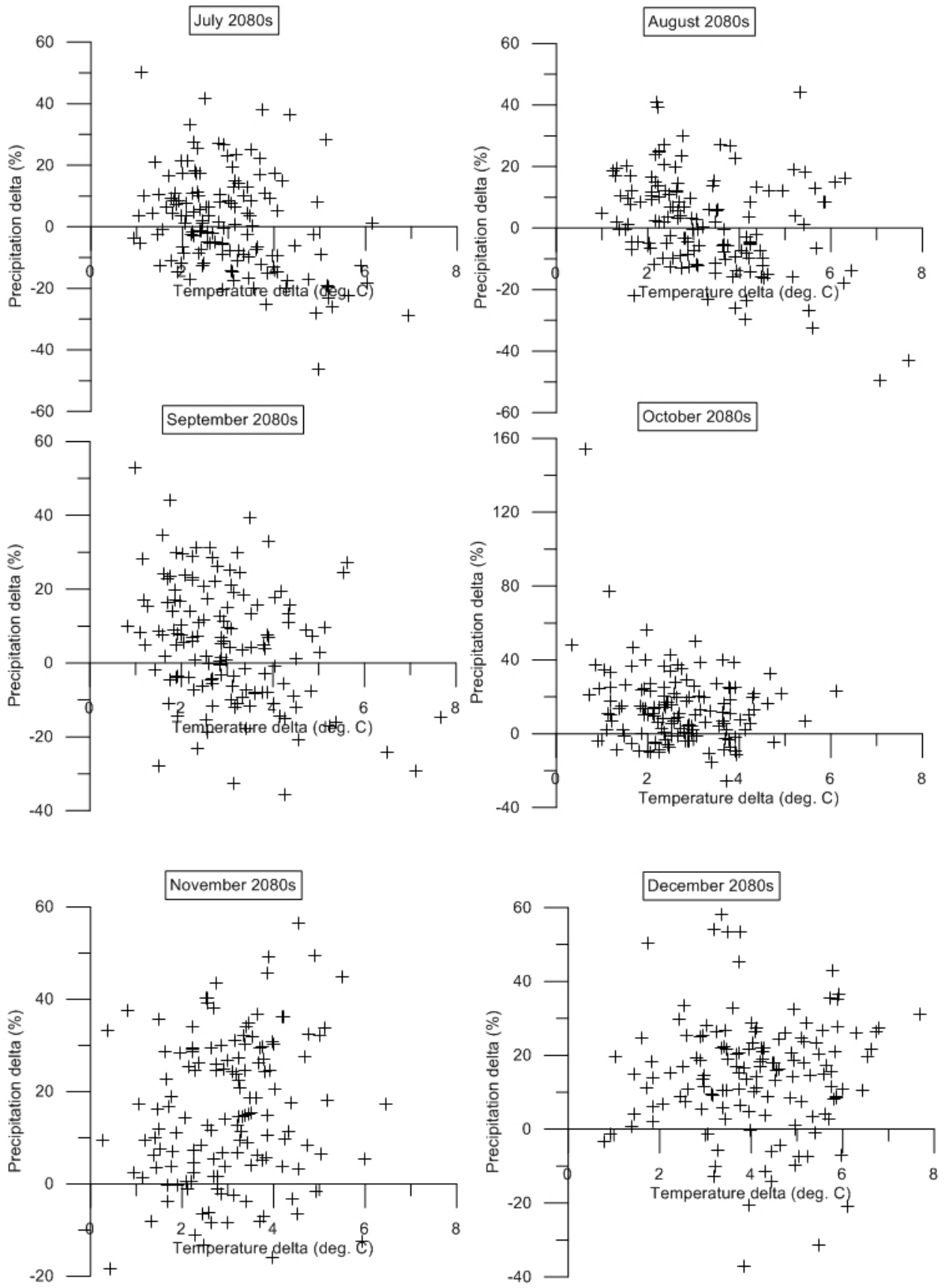
Figure 48: 2080s July – December temperature and precipitation delta values

108

Precipitation trends for the 2050s (Figure 45, Figure 46) show that most of the GCMs are projecting an increase in precipitation for the winter and spring/early summer months (October – June) and most models predict a decrease during the summer months. The majority of predictions indicate a change of around 15% or less, increasing or decreasing for the 2050s future time horizon.

Precipitation trends in the 2080s (Figure 47, Figure 48) indicate the same tendency towards an increase throughout the majority of the year. The exception to this rule being a large number of the models predicting that precipitation will decrease slightly in the summer months of July and August. In general, the trends observed in the 2050s are more evident and pronounced in the 2080s horizon, with average monthly precipitation increasing by approximately 11.3% compared to 8.4% in the 2050s.

Temperature delta values predicted from the GCMs indicate that temperatures in the CRB almost unanimously increase in all months over both future time horizons and all emissions scenarios (Figure 45 through Figure 48). In general, temperatures are expected to increase more in the winter months (November – February) than during the summer months for the both the 2050s and 2080s. The increases in temperature are expected to become more pronounced throughout the 21st century. According to the overall ensemble average, the temperature in the Churchill River basin is expected to increase 2.1°C in the 2050s and 3.1°C in the 2080s.

The hydrological modelling portion of this study will use these projected changes to both temperature and precipitation to anticipate future trends in the hydrological regime, including to the volume of flow anticipated. Knowledge of the hydrological response will indicate what impacts may be felt throughout the basin, and on hydroelectric generating stations in the Nelson and Burntwood River systems as the climate continues to change over the coming century.

Chapter 6: Climate change impact assessment with hydrological models

As mentioned previously, this study will make use of multiple hydrological models to assess the impacts of the projected climate change from a selection of the scenarios developed for the IPCC Special Report on Emissions Scenarios. The use of multiple hydrological and GCM models helps to alleviate uncertainty and provides the study with more reliable information than simply relying on the results provided by one model(Knutti, *et al.*, 2010; Chiew, *et al.*, 2009; Kling, Fuchs, & Paulin, 2012; Ruelland, *et al.*, 2012; Woo, Long, & Thome, 2009). These scenarios were used to create synthetic climate forcing for the future in order to drive the hydrological models using the delta method approach described in Section 5.1.1 Description of delta method.

The following sections present the modelled results using each future scenario and time horizon. All hydrographs are shown for Water Survey of Canada gauge 06CD002, located at Otter Rapids. The WATFLOOD^{TM} model found that similar trends were realized at the gauge locations further downstream for each of the climate scenarios.

6.1 Predicted changes in streamflow

The hydrographs presented in the following section are obtained using meteorological forcing data generated from the output of the CCCMA CGCM 3.1 climate model. This GCM was chosen for display because it had multiple runs

worth of data available for each of the selected emissions scenarios and although all GCMs were developed for use throughout the globe, CGCM 3.1 was developed by a Canadian group (CCCMa). Choosing this model for use does not indicate any sort of superiority and the hydrographs created from the other GCM models are available in Appendix D. Additionally, tables presented in this section include data from all 139 GCM model simulations which were run for each of the time periods. All flows are presented as daily average flow in cubic meters per second (cms) over the modeled period (1979-1995). At the conclusion of the analysis, the hydrographs from each of the model runs are compared in the form of an envelope curve to show how the results from all models compare to each other.

After completing the model simulations, an enormous amount of data was generated. Several methods are available to display the range of flows generated from the GCM predictions.

The method used in this study to simplify the results is outlined in Knutti *et al.* (2010). At first glance, it appears that there are 139 different projections of the future climate which were made (from the GCM output) and were available for hydrological analysis. But closer examination shows that many of the GCM runs are merely different realizations of the same model using different initial conditions. As a result, these separate runs of the same model provide very little additional information to the study and tend to sway the overall results towards one model or the other. This is accounted for by using one average of all available initializations for each GCM, so that each model gets an equal weight

regardless of how many runs were used in the analysis. This is known as the "one model, one vote" approach and is especially useful in this case as there is not a dependable way of defining the quality of one model simulation over another, as there is no observed truth when it comes to future climate(Knutti, *et al.*, 2010). This method was implemented by computing the hydrological change simulated by each of the sets of climate delta values for a particular GCM, and then computing the average of these simulations for that GCM. Lastly, the average from each of the emissions scenarios was calculated to determine the most likely hydrological impact from each scenario during each future time horizon, or an ensemble average.

6.1.1 2050s, B1

As a part of the climate change modelling portion of this exercise, 46 different sets of B1 climate delta values from 21 GCMs for the 2050s time frame were used to force the three hydrological models in the suite. The following graphs (Figure 49) depict the results from the CCCMA CGCM3.1 climate model. These results are representative of the results from all simulations. The remainder of the hydrographs are shown in Appendix D for the sake of brevity within the report.
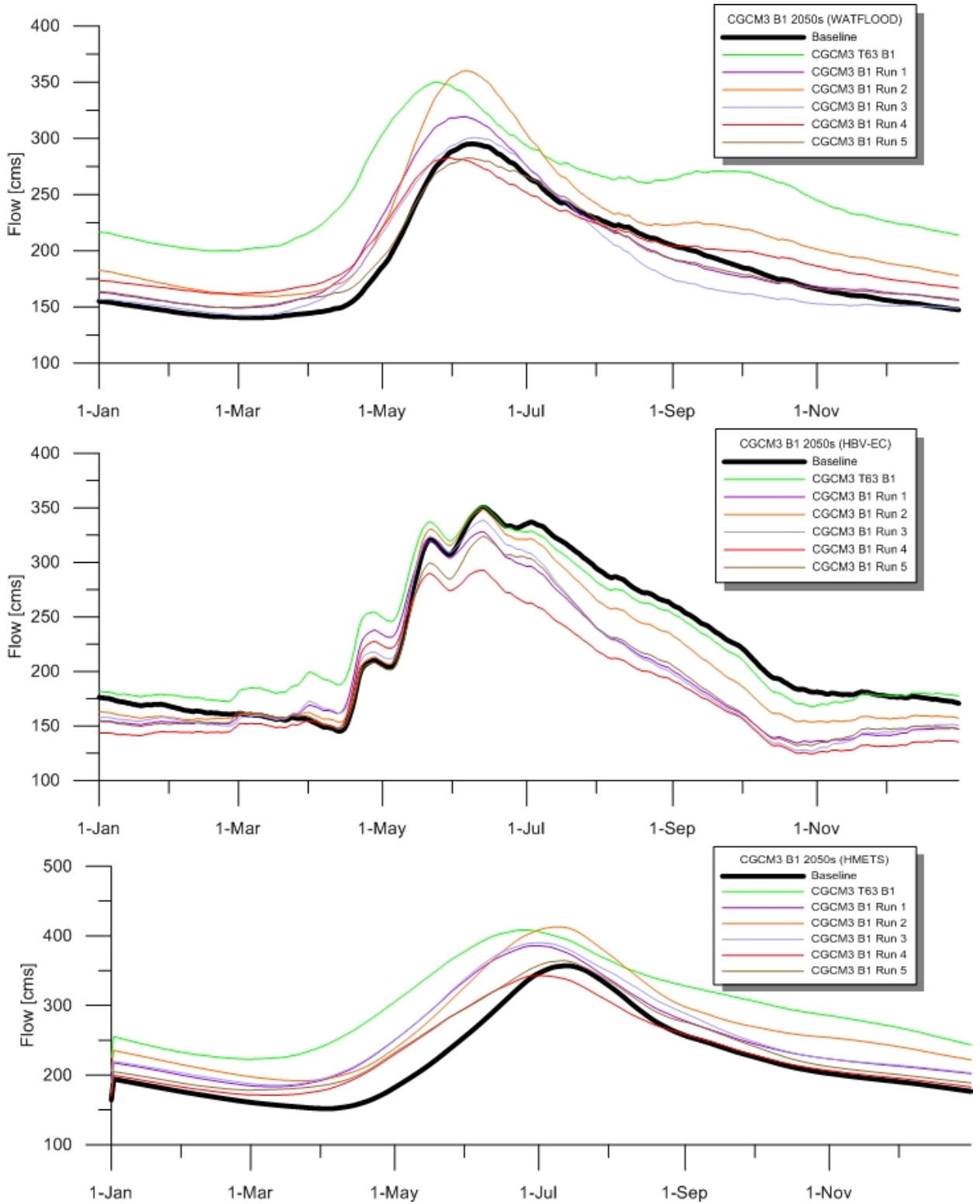
Figure 49: Annual average hydrographs, 2050s time horizon, B1 emissions scenario

The most optimistic climatic scenario (i.e., B1) for the 2050s time horizon shows several interesting trends with respect to the annual average hydrographs (Figure 49). Each of the CGCM3.1 model runs seems to predict that the freshet will occur at least slightly earlier, and while WATFLOOD^{TM} and HMETS predict that the peak flow will be higher, HBV-EC predicts a very small change either positive or negative. Many of the other simulations agreed with the CGCM3.1 results but the following tables show the numeric analysis of the results of using each of the GCM delta values within each of the hydrological models (Table 6, Table 7, and Table 8; all flow values in [cms], GCMs with more than one run have been averaged, minimum values have been bolded, and maximum values italicized).

Table 6: Average, maximum and minimum values (cms) for WATFLOOD^{TM}, 2050s B1

GCM Name	Avg. Q	Max Q	Date of Max Q	Min Q	Date of Min Q
Baseline	189.10	295.06	08-Jun	140.44	06-Mar
BCCR BCM2	265.92	422.66	29-May	180.44	18-Mar
CCCMA CGCM3	238.94	431.12	31-May	151.78	26-Feb
CNRM CM3	206.89	**313.27**	29-May	149.53	*23-Mar*
CSIRO MK3_0	213.81	357.69	*04-Jun*	151.02	07-Mar
CSIRO MK3_5	273.75	428.19	29-May	195.92	16-Mar
GFDL CM2_0	203.84	332.51	29-May	145.68	**18-Feb**
GFDL CM2_1	232.78	370.18	29-May	164.08	02-Mar
GISS AOM	231.00	377.23	04-Jun	153.01	12-Mar
GISS MODEL E R	264.84	419.62	30-May	175.62	15-Mar
IAP FGOALS	229.40	389.94	31-May	153.63	24-Feb
INMCM3	*306.53*	485.48	04-Jun	**201.87**	20-Feb
IPSL CM4	238.88	329.94	20-May	178.62	21-Feb
MIROC3_2 HIRES	221.74	375.19	**15-May**	171.19	20-Feb
MIROC3_2 MEDRES	222.14	414.65	25-May	148.58	02-Mar
MIUB ECHO G	**195.59**	333.01	29-May	130.11	03-Mar
MPI ECHAM 5	249.99	521.65	29-May	125.38	01-Mar
MRI CGCM2_3_2a	212.93	380.33	04-Jun	**124.32**	13-Mar
NCAR CCSM3	240.10	448.66	31-May	153.91	28-Feb
NCAR PCM1	276.61	*522.49*	29-May	189.56	02-Mar
UKMO HADCM3	202.81	352.08	04-Jun	138.58	16-Mar
Overall Avg.	**236.42**	**400.29**	**29-May**	**159.14**	**04-Mar**

Table 7: Average, maximum, and minimum flow values (cms) for HBV-EC, 2050s B1

GCM Name	Avg. Q	Max Q	Date of Max Q	Min Q	Date of Min Q
Baseline	221.86	350.54	13-Jun	145.23	13-Apr
BCCR BCM2	228.67	355.56	*13-Jun*	149.73	12-Apr
CCCMA CGCM3	200.52	351.54	12-Jun	124.37	29-Oct
CNRM CM3	**155.84**	**263.02**	12-Jun	106.81	24-Oct
CSIRO MK3_0	190.76	321.00	13-Jun	132.65	30-Oct
CSIRO MK3_5	207.33	340.89	12-Jun	152.43	12-Apr
GFDL CM2_0	183.64	316.58	12-Jun	111.76	30-Oct
GFDL CM2_1	191.04	317.14	12-Jun	128.74	30-Oct
GISS AOM	192.49	334.17	12-Jun	120.92	21-Jul
GISS MODEL E R	201.31	328.00	13-Jun	146.45	**22-Feb**
IAP FGOALS	187.92	326.61	12-Jun	111.44	*31-Oct*
INMCM3	227.18	364.65	13-Jun	166.10	30-Oct
IPSL CM4	158.23	266.70	12-Jun	97.30	24-Oct
MIROC3_2 HIRES	159.51	293.27	**20-May**	82.67	23-Oct
MIROC3_2 MEDRES	170.89	320.82	04-Jun	91.59	25-Oct
MIUB ECHO G	165.20	291.53	12-Jun	91.56	29-Oct
MPI ECHAM 5	204.76	392.73	12-Jun	**80.32**	02-Jun
MRI CGCM2_3_2a	179.78	332.57	12-Jun	111.02	19-Sep
NCAR CCSM3	190.06	376.07	12-Jun	112.70	25-Sep
NCAR PCM1	*239.22*	*403.39*	13-Jun	*166.74*	12-Apr
UKMO HADCM3	160.63	295.83	12-Jun	88.98	30-Oct
Overall Avg.	**189.75**	**329.60**	**10-Jun**	**118.71**	**30-Aug**

116

Table 8: Average, maximum, and minimum flow values (cms) for HMETS, 2050s B1

GCM Name	Avg. Q	Max Q	Date of Max Q	Min Q	Date of Min Q
Baseline	222.01	357.14	13-Jul	151.73	02-Apr
BCCR BCM2	280.64	430.61	08-Jul	194.30	*30-Mar*
CCCMA CGCM3	259.60	412.89	03-Jul	171.14	09-Mar
CNRM CM3	*203.40*	*315.12*	05-Jul	145.25	16-Mar
CSIRO MK3_0	241.06	373.60	07-Jul	171.53	21-Mar
CSIRO MK3_5	297.51	442.08	06-Jul	213.04	21-Mar
GFDL CM2_0	230.33	349.14	01-Jul	167.56	**04-Mar**
GFDL CM2_1	256.43	379.50	27-Jun	184.94	12-Mar
GISS AOM	235.71	395.24	04-Jul	145.93	17-Mar
GISS MODEL E R	263.73	396.56	*09-Jul*	184.39	16-Mar
IAP FGOALS	242.21	408.47	03-Jul	157.09	14-Mar
INMCM3	*304.88*	431.42	04-Jul	*216.82*	11-Mar
IPSL CM4	233.30	341.51	25-Jun	169.61	04-Mar
MIROC3_2 HIRES	256.62	379.01	**21-Jun**	189.49	05-Mar
MIROC3_2 MEDRES	251.83	407.89	30-Jun	171.39	12-Mar
MIUB ECHO G	204.82	337.00	30-Jun	139.12	13-Mar
MPI ECHAM 5	270.26	*490.76*	05-Jul	130.70	11-Mar
MRI CGCM2_3_2a	223.09	399.64	08-Jul	**130.30**	22-Mar
NCAR CCSM3	250.33	422.06	05-Jul	169.68	14-Mar
NCAR PCM1	303.86	489.53	07-Jul	208.76	14-Mar
UKMO HADCM3	222.01	362.21	08-Jul	154.38	30-Mar
Overall Avg.	**251.58**	**398.21**	**03-Jul**	**170.77**	**14-Mar**

These tables (Table 6, Table 7, and Table 8) show the general trends simulated during the modelling portion of this study. The average, maximum, and minimum flows increased for both the WATFLOOD[TM] and HMETS simulations, while the HBV-EC simulations show decreases in each of the same categories. WATFLOOD[TM] saw an increase in the average flow of 47 cms, while HMETS showed an increase of 29 cms and HBV-EC predicts a decrease of 33 cms. The HBV-EC model results are different than the results from the other two models for a number of reasons. Principal among these are the model structure and evaporation formulations. HBV-EC predicted a large increase in the amount of evaporation which leads to a decrease in the amount of streamflow at the outlet.

Because HBV-EC models evaporation based on a table that was entered during the model calibration phase and the difference in temperature to some reference evaporation temperature, the small to moderate increases in temperature prescribed in the climate change scenarios cause increases in evaporation that balance out any increases in precipitation.

The volume of the peak flow displayed similar patterns, with WATFLOOD^{TM} and HMETS showing increases of 105 and 42 cms, respectively; while HBV-EC expects that the peak yearly flow will decrease by 21 cms. Finally, WATFLOOD^{TM} and HMETS simulations show an increase in the yearly low flow volume by 19 cms and HBV-EC showed a decrease by 27 cms.

Each of the models saw an advance in the timing of the annual peak flow. WATFLOOD^{TM} and HMETS each saw the peak occur 10 days earlier, while HBV-EC estimated a more modest 3 day advance in timing of the peak flow. WATFLOOD^{TM} and HMETS both predicted the annual low flow would occur earlier (2 days for WATFLOOD^{TM}, 19 for HMETS). The differences in the timing of the peak flow can be tied back to the snowmelt method used in each of the hydrological models. HBV-EC and HMETS each use a degree day of melting method, but the slope of the hydrograph generated by the HBV-EC model is much steeper, meaning that snowmelt happens faster within the model, possibly due to the fact that the HBV-EC model was developed for mountainous terrain. As a result, the increase in temperature only serves to move the melt event forward by a few days. In the case of the other two models, the melt events happens sooner as well, but the slope of the hydrograph increases slightly as

well, resulting in a more advanced peak flow. Many of the climate change runs which were completed with HBV-EC showed an annual low flow shifted from the end of the winter period to the late summer. As a result, the average was shifted towards the end of the summer (approximately 4.5 months) when in fact some of the simulations actually saw the low flow occur at the end of the ice-on winter period.

The following table (Table 9) shows the general trends which were observed over three month periods (DJF – December, January, February, MAM – March, April, May, JJA – June, July, August, and SON – September, October, November) throughout the year. This illustrates the seasonality of the trends which are expected to occur for each period and each hydrological model, allowing for a more in-depth analysis of the increases and decreases in streamflow that may occur in the future.

Table 9: Seasonal changes in flow, 2050s B1

	WATFLOOD^{TM}	HBV-EC	HMETS
DJF			
Avg % change	25.35	-14.08	13.32
Max % change	53.61	8.64	39.83
Min % change	1.07	-28.42	-10.55
Std. dev. (%)	15.82	11.00	14.43
MAM			
Avg % change	32.54	-0.13	24.43
Max % change	63.79	14.19	49.27
Min % change	9.77	-17.06	-0.31
Std. dev. (%)	15.37	7.83	14.47
JJA			
Avg % change	17.21	-16.84	8.45
Max % change	65.85	5.57	29.08
Min % change	-5.76	-35.78	-10.35
Std. dev. (%)	16.99	11.37	11.42
SON			
Avg % change	28.18	-25.44	11.19
Max % change	65.81	4.37	42.03
Min % change	2.44	-50.26	-12.76
Std. dev. (%)	17.75	15.47	15.37

Several trends become evident in examining the above table (Table 9). WATFLOOD^{TM} and HMETS both predict increases during all four of the three month periods, while HBV-EC predicts a reduction during all portions of the year. Each of the models shows the largest increase (or smallest decrease) during the spring freshet (i.e., MAM portion of the year). This is a result of the increased precipitation during the winter and the fact that the increased temperatures during the winter do not lead to a corresponding increase in evaporation to negate these effects. Conversely, the smallest increases (or largest decreases) occur during the ice-off period (i.e., JJA), which is the late summer (and open-water evaporation) portion of the year. This is a result of higher evaporation caused by increased summer temperatures. WATFLOOD^{TM} simulations show

that the results were very similar for both the fall and ice-on periods (i.e., SON and DJF, respectively), while the same was true for HMETS. However, HBV-EC shows a much smaller reduction in streamflow during the ice-on season (i.e., DJF). It is also interesting to note that the model with the highest standard deviation for each season was WATFLOOD^{TM}, suggesting that model may be more sensitive to the variations in changes that each of the GCM simulations presents.

6.1.2 2050s, A1B

During the modelling phase of this project, 54 simulations corresponding to the 2050s A1B scenario were completed. Included in this section are the hydrographs generated using the CCCMA CGCM3.1 climate model data (Figure 50), as well as full statistical analysis of the results from all 54 simulations (Table 10 through Table 13). A complete set of hydrographs from each of the GCM/hydrological model simulations may be found in Appendix D.
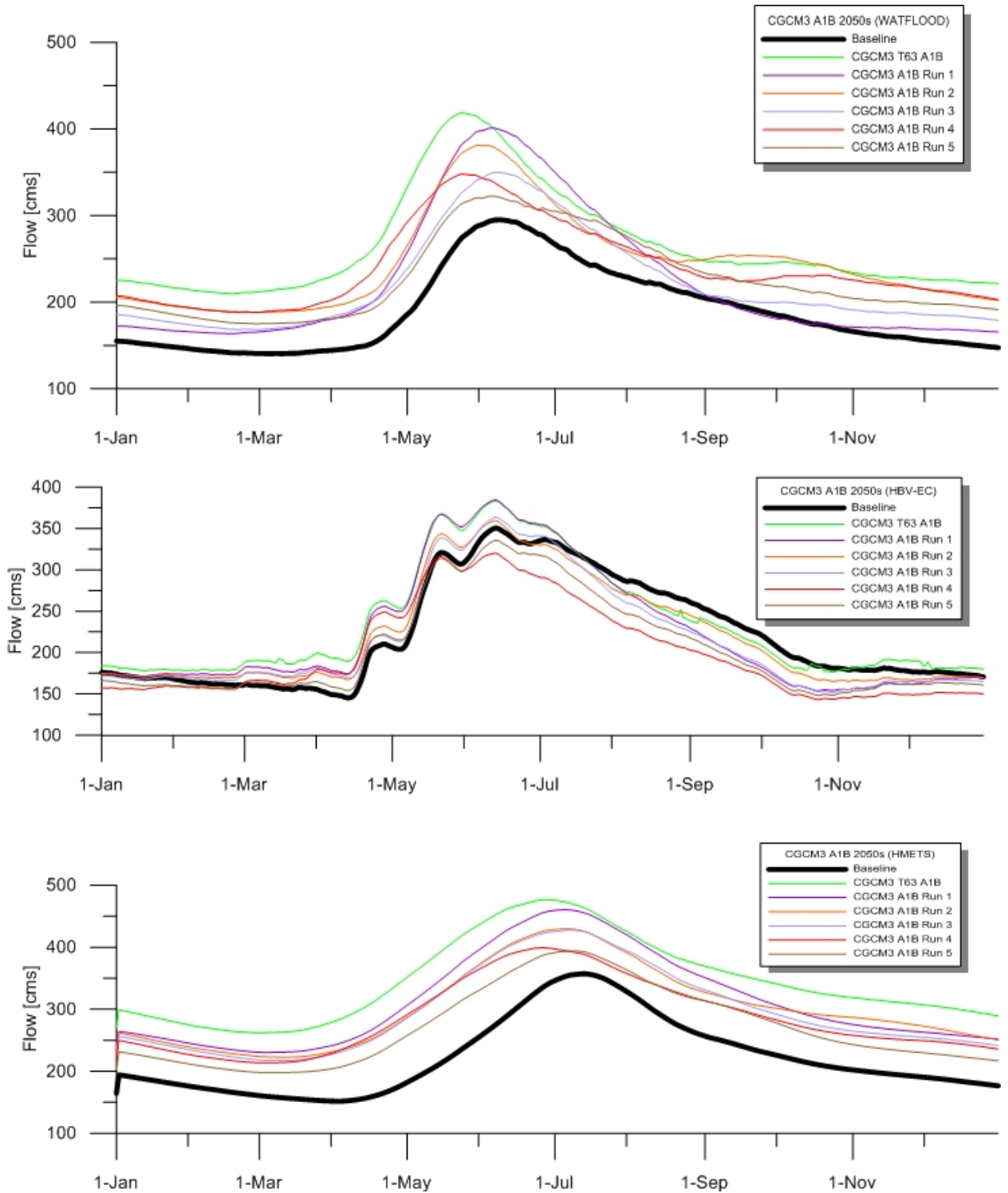
Figure 50: Annual average hydrographs, 2050s time horizon, A1B emissions scenario

The A1B climate scenario for the 2050s timeframe displays many of the same

trends that were evident in the results from the B1 scenario. In the annual

average hydrographs produced using the CCCMA CGCM3.1 climate data (Figure 50), the timing of the freshet peak flow occurs earlier in the year and has a higher volume than the baseline values for nearly every case and each of the hydrological models. HMETS and WATFLOOD^{TM} each predict increases in the volume of flow during the winter, while HBV-EC predicts a decrease during these times. The most likely explanation for this phenomenon is that the flow at the end of the summer, open water period are reduced by the evaporation in the HBV-EC model, leading to a lower level of flow during the winter ice-on period because winter precipitation is not translated into runoff until the spring melt begins. The following tables (Table 10 through Table 13) show a summary of the results using each of the 54 climate models which were considered for this scenario.

Table 10: Average, maximum, and minimum flow values (cms) for WATFLOOD^{TM}, 2050s A1B

GCM Name	Avg Q	Max Q	Date of Max Q	Min Q	Date of Min Q
Baseline	189.10	295.06	08-Jun	140.44	06-Mar
BCCR BCM2	260.93	423.81	29-May	188.80	16-Mar
CCCMA CGCM3	271.17	490.56	29-May	178.59	19-Feb
CNRM CM3	**164.88**	**236.90**	***04-Jun***	127.47	16-Mar
CSIRO MK3_0	275.72	457.15	30-May	182.71	08-Mar
CSIRO MK3_5	252.93	445.89	23-May	178.14	20-Feb
GFDL CM2_0	206.28	329.10	23-May	150.28	18-Feb
GFDL CM2_1	205.86	363.56	23-May	155.75	18-Feb
GISS AOM	234.28	394.27	02-Jun	161.65	04-Mar
GISS MODEL E H	215.11	***511.44***	31-May	**126.10**	10-Mar
GISS MODEL E R	223.15	447.84	29-May	151.39	11-Mar
IAP FGOALS	212.54	323.06	22-May	155.68	07-Jun
INGV ECHAM4	233.83	380.85	24-May	164.69	02-Mar
INMCM3	***301.93***	502.88	23-May	***200.21***	24-Feb
IPSL CM4	257.70	353.34	15-May	191.83	25-Feb
MIROC3_2 HIRES	187.91	314.74	**13-May**	126.50	***30-Aug***
MIROC3_2 MEDRES	229.97	421.14	20-May	158.30	**14-Feb**
MIUB ECHO G	198.65	330.97	29-May	140.69	02-Mar
MPI ECHAM 5	210.29	415.20	28-May	135.58	23-Feb
MRI CGCM2_3_2a	211.16	363.39	02-Jun	142.75	05-Mar
NCAR CCSM3	237.13	430.95	29-May	148.80	22-Feb
NCAR PCM1	246.68	424.71	26-May	159.40	18-Feb
UKMO HADCM3	228.89	446.25	03-Jun	157.36	02-Mar
UKMO HADGEM1	177.88	310.34	22-May	133.01	18-Feb
Overall Avg	**228.04**	**396.45**	**26-May**	**157.20**	**11-Mar**

Table 11: Average, maximum, and minimum flow values (cms) for HBV-EC, 2050s A1B

GCM Name	Avg Q	Max Q	Date of Max Q	Min Q	Date of Min Q
Baseline	221.86	350.54	13-Jun	145.23	13-Apr
BCCR BCM2	203.28	336.52	12-Jun	149.06	**12-Apr**
CCCMA CGCM3	217.08	***384.39***	12-Jun	142.98	27-Oct
CNRM CM3	**119.39**	**221.79**	21-May	64.62	23-Oct
CSIRO MK3_0	***226.44***	362.94	***13-Jun***	***164.46***	12-Apr
CSIRO MK3_5	204.58	350.67	12-Jun	134.83	23-Oct
GFDL CM2_0	161.20	277.44	21-May	92.09	24-Oct
GFDL CM2_1	171.26	305.85	12-Jun	93.71	24-Oct
GISS AOM	185.32	320.03	13-Jun	117.52	***15-Nov***
GISS MODEL E H	181.11	378.78	12-Jun	79.26	27-Oct
GISS MODEL E R	188.30	345.18	12-Jun	115.49	23-Oct
IAP FGOALS	161.80	284.37	28-May	81.86	27-Oct
INGV ECHAM4	193.01	322.15	13-Jun	127.18	30-Oct
INMCM3	223.29	361.00	12-Jun	156.12	29-Oct
IPSL CM4	162.11	275.99	**20-May**	94.21	24-Oct
MIROC3_2 HIRES	129.43	255.33	20-May	**49.14**	13-Oct
MIROC3_2 MEDRES	169.06	325.21	21-May	80.23	25-Oct
MIUB ECHO G	170.62	303.38	12-Jun	99.03	29-Oct
MPI ECHAM 5	170.95	320.56	01-Jun	80.81	27-Oct
MRI CGCM2_3_2a	169.34	318.22	12-Jun	88.89	27-Oct
NCAR CCSM3	169.01	326.65	05-Jun	64.81	24-Oct
NCAR PCM1	193.11	339.50	06-Jun	100.39	29-Oct
UKMO HADCM3	183.82	348.67	12-Jun	100.01	30-Oct
UKMO HADGEM1	130.18	254.69	20-May	54.53	13-Oct
Overall Avg	**177.55**	**318.23**	**04-Jun**	**101.36**	**08-Oct**

Table 12: Average, maximum, and minimum flow values (cms) for HMETS, 2050s A1B

GCM Name	Avg Q	Max Q	Date of Max Q	Min Q	Date of Min Q
Baseline	222.01	357.14	13-Jul	151.73	02-Apr
BCCR BCM2	279.80	423.59	05-Jul	199.31	22-Mar
CCCMA CGCM3	302.11	476.40	03-Jul	197.83	06-Mar
CNRM CM3	**155.64**	**256.75**	08-Jul	**111.22**	21-Mar
CSIRO MK3_0	289.55	429.95	08-Jul	203.75	16-Mar
CSIRO MK3_5	289.58	436.80	01-Jul	210.17	12-Mar
GFDL CM2_0	222.24	328.62	25-Jun	163.27	01-Mar
GFDL CM2_1	259.67	390.50	23-Jun	191.99	04-Mar
GISS AOM	234.81	396.23	05-Jul	152.04	15-Mar
GISS MODEL E H	265.11	*496.96*	08-Jul	145.03	*27-Mar*
GISS MODEL E R	270.79	441.61	08-Jul	189.05	27-Mar
IAP FGOALS	217.13	343.14	26-Jun	155.50	13-Jun
INGV ECHAM4	253.63	382.22	30-Jun	181.24	14-Mar
INMCM3	*309.49*	451.75	26-Jun	*219.34*	12-Mar
IPSL CM4	240.04	351.66	25-Jun	174.60	09-Mar
MIROC3_2 HIRES	234.57	343.22	**11-Jun**	181.14	**27-Feb**
MIROC3_2 MEDRES	258.86	410.53	25-Jun	181.51	03-Mar
MIUB ECHO G	222.37	358.77	02-Jul	156.99	15-Mar
MPI ECHAM 5	232.04	383.98	29-Jun	145.83	06-Mar
MRI CGCM2_3_2a	220.19	371.19	05-Jul	122.54	14-Mar
NCAR CCSM3	258.11	410.54	01-Jul	162.07	09-Mar
NCAR PCM1	250.00	410.23	02-Jul	141.87	02-Mar
UKMO HADCM3	289.80	441.64	*09-Jul*	212.85	18-Mar
UKMO HADGEM1	204.17	315.33	26-Jun	153.52	08-Mar
Overall Avg	**250.42**	**393.55**	**30-Jun**	**171.85**	**16-Mar**

The results from the A1B climate change scenario show similar trends to those observed for the B1 scenario. Both WATFLOOD^{TM} and HMETS simulated modest increases in average, yearly maximum and yearly minimum flow (39, 101, and 17 cms, respectively for WATFLOOD^{TM} and 28, 36, and 20 cms for HMETS), while HBV-EC once again predicts decreases for each (44, 32, and 44 cms, respectively).

As with volume of flow, trends in the timing of maximum and minimum flow were similar to those from the 2050s B1 scenario. WATFLOOD^{TM} and HMETS both

project that the freshet will be advanced by approximately two weeks (on average while HBV-EC predicts that the peak will occur one week earlier. In the timing of the minimum flow, HMETS simulates that the lowest flow will happen approximately two weeks earlier at the end of the winter period. HBV-EC and WATFLOOD™ both observe the same trend as seen in the HBV-EC results for the 2050s B1 scenario: some of the simulations saw a decrease in flow at the end of the summer period and beginning of the winter period, which was enough to affect the average date of the minimum flow for both models. While the results for nearly every climate model have a minimum flow in late fall for HBV-EC, only one simulation using WATFLOOD™ displays the same trend. The single WATFLOOD™ simulation which saw the shift of minimum flow timing to late August (MIROC3_2 HIRES) has the highest temperature increase of any climate model run coupled with significant decreases in precipitation during the summer months. As a result, the average date for the HBV-EC simulations is much later than for the WATFLOOD™ simulations. A more in depth look at the seasonality of the flow changes may be seen below (Table 13).

Table 13: Seasonal changes in flow, 2050s A1B

	WATFLOOD™	HBV-EC	HMETS
DJF			
Avg % change	19.39	-20.32	11.33
Max % change	48.70	1.77	37.10
Min % change	-8.28	-44.63	-31.54
Std. Dev. (%)	15.05	11.69	16.39
MAM			
Avg % change	33.64	-1.22	26.55
Max % change	79.12	20.19	56.01
Min % change	-11.49	-30.13	-23.54
Std. Dev. (%)	17.66	9.50	15.58
JJA			
Avg % change	10.96	-23.42	6.49
Max % change	53.71	1.38	30.98
Min % change	-25.43	-51.54	-28.10
Std. Dev. (%)	19.10	13.49	14.61
SON			
Avg % change	17.42	-36.57	7.41
Max % change	57.27	-3.63	39.78
Min % change	-17.33	-67.83	-36.49
Std. Dev. (%)	20.86	16.14	17.41

As with the simulations for the B1 climate scenario before, WATFLOOD™ and HMETS both predict increases in the average flows for every three month period of the year, while HBV-EC predicts a decrease in the average flow throughout the entire year. Once again, the highest increases (smallest decreases) for each of the hydrological models are during the freshet period (MAM). The smallest increases for HMETS and WATFLOOD™ occur during the late summer months (JJA), which is similar to the results from 2050s B1. However, the HBV-EC results show a larger decrease during the late fall/early winter months (SON) than during any other portion of the year. These results indicate that the future will likely see increases in the amount of evaporation during the summer months. The hydrological models predict that these increases in evaporation will lead to

the smallest increases or largest decreases in flow despite the increases in precipitation during the summer. As with the B1 scenario, WATFLOOD^{TM} shows the highest standard deviation for each of the seasons.

Relative to the 2050s B1 simulations, the A1B scenario shows lower flows throughout the entire year for the HBV-EC simulations, while WATFLOOD^{TM} and HMETS predicts smaller increases for each of the three month periods except the spring period (MAM) where they both predict larger increases. These changes are a result of the increases in temperature and decreases in precipitation relative to the B1 scenario which serve to decrease the amount of flow throughout the year.

6.1.3 2050s, A2

The final group of simulations which will be examined for the 2050s time period correspond to the A2 emissions scenario. In total there were 39 different sets of delta values for this time period/scenario combination for a total of 139 sets of data overall for the period. As with the previous two sections, the annual average hydrographs for the CCCMA CGCM3.1 forced simulations are shown below (Figure 51) and the accompanying tables (Table 14 through Table 17) show summaries of the results for all simulations completed for the most pessimistic A2 emission scenario. As with the previous sections, the remainder of the hydrographs for all of the GCM simulations may be found in Appendix D.
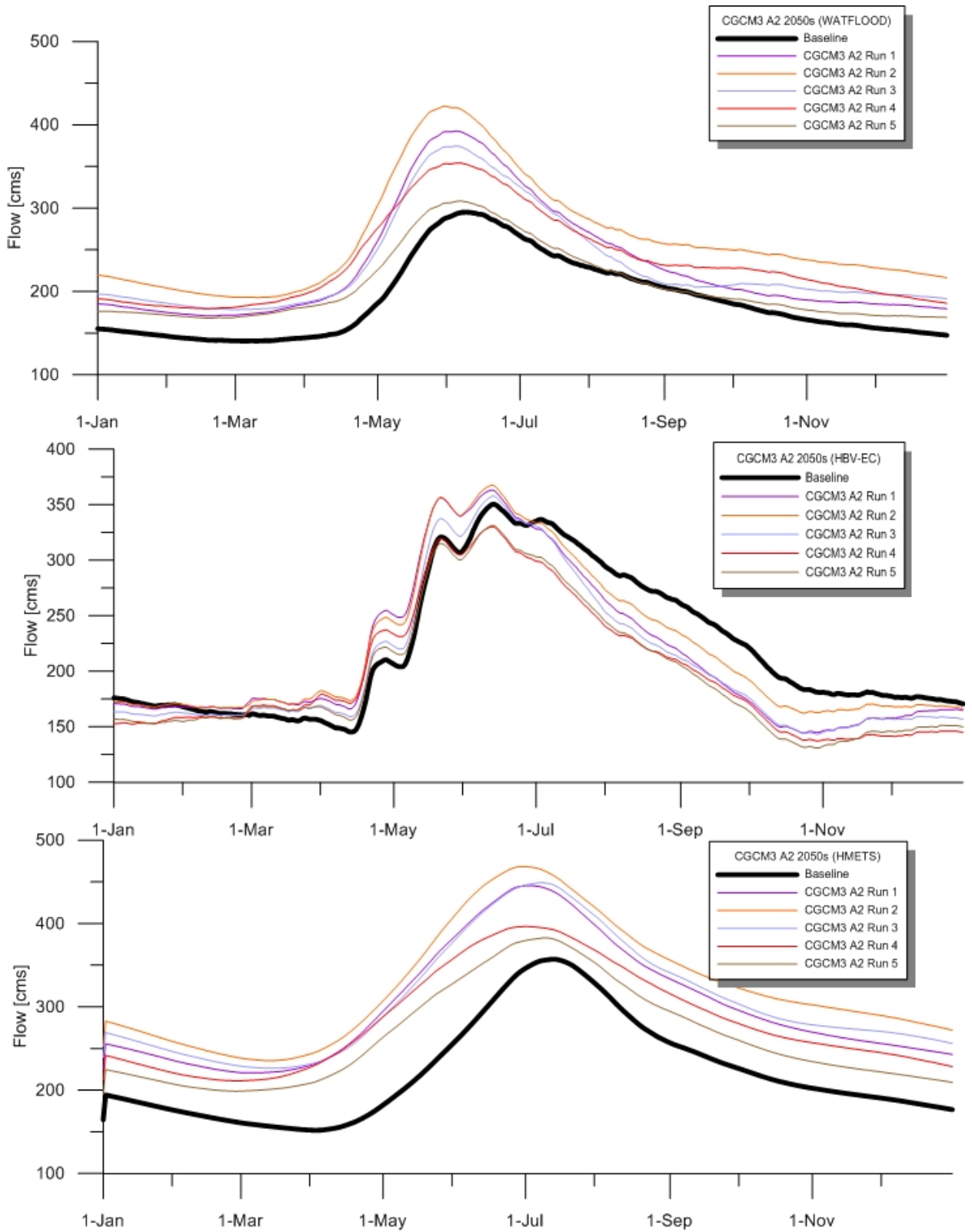
Figure 51: Annual average hydrographs, 2050s time horizon, A2 emissions scenario

The hydrographs from the 2050s A2 simulations (Figure 51) show many similar trends to those realized for the two more optimistic emissions scenarios. Again, each of the models predicts that the freshet peak will increase using the data from the CCCMA CGCM3.1, while the WATFLOOD™ and HMETS simulations predict increases in flow during the low-flow periods versus HBV-EC predicting a decrease during these times. The following tables (Table 14 through Table 17) summarize the results for each of the models considered for the A2 emissions scenario.

Table 14: Average, maximum, and minimum flow values (cms) for WATFLOOD™, 2050s A2

GCM Name	Avg Q	Max Q	Date of Max Q	Min Q	Date of Min Q
Baseline	189.10	295.06	08-Jun	140.44	06-Mar
BCCR BCM2	244.96	407.54	30-May	170.31	17-Mar
CCCMA CGCM3	266.55	500.28	29-May	178.82	23-Feb
CNRM CM3	**160.84**	**240.71**	***04-Jun***	120.38	***23-Mar***
CSIRO MK3_0	240.52	398.36	30-May	167.81	02-Mar
CSIRO MK3_5	245.00	411.81	29-May	167.61	02-Mar
GFDL CM2_0	177.88	305.65	29-May	128.19	**17-Feb**
GFDL CM2_1	227.35	348.71	30-May	168.43	02-Mar
GISS MODEL E R	237.14	405.38	29-May	164.41	15-Mar
INGV ECHAM4	188.04	334.61	24-May	137.54	20-Feb
INMCM3	***338.03***	***520.36***	04-Jun	***207.51***	20-Feb
IPSL CM4	235.61	334.86	**18-May**	182.59	18-Feb
MIROC3_2 MEDRES	222.40	411.49	24-May	161.17	22-Feb
MIUB ECHO G	199.45	342.48	27-May	138.09	03-Mar
MPI ECHAM 5	207.34	437.80	29-May	**119.73**	22-Feb
MRI CGCM2_3_2a	208.00	338.80	03-Jun	142.39	09-Mar
NCAR CCSM3	241.59	460.31	26-May	141.77	25-Feb
NCAR PCM1	268.98	484.94	30-May	169.69	02-Mar
UKMO HADCM3	210.98	405.29	04-Jun	142.10	06-Mar
UKMO HADGEM1	177.20	318.12	23-May	126.48	18-Feb
Overall Avg	**226.20**	**389.87**	**28-May**	**154.48**	**28-Feb**

Table 15: Average, maximum, and minimum flow values (cms) for HBV-EC 2050s A2

GCM Name	Avg Q	Max Q	Date of Max Q	Min Q	Date of Min Q
Baseline	221.86	350.54	13-Jun	145.23	13-Apr
BCCR BCM2	197.01	329.05	12-Jun	138.77	12-Apr
CCCMA CGCM3	208.20	367.57	12-Jun	130.90	27-Oct
CNRM CM3	**111.38**	**214.62**	21-May	57.39	23-Oct
CSIRO MK3_0	200.23	334.07	12-Jun	135.01	***30-Oct***
CSIRO MK3_5	187.70	323.85	12-Jun	122.42	24-Oct
GFDL CM2_0	166.23	294.30	12-Jun	138.38	**17-Feb**
GFDL CM2_1	180.37	306.17	12-Jun	119.10	29-Oct
GISS MODEL E R	192.17	332.92	12-Jun	133.15	13-Oct
INGV ECHAM4	165.59	296.55	12-Jun	93.58	29-Oct
INMCM3	***221.10***	354.29	***13-Jun***	***155.88***	30-Oct
IPSL CM4	157.05	273.68	**20-May**	89.85	23-Oct
MIROC3_2 MEDRES	175.40	314.27	28-May	94.56	27-Oct
MIUB ECHO G	171.41	298.38	12-Jun	102.68	29-Oct
MPI ECHAM 5	178.81	357.77	04-Jun	64.37	28-Oct
MRI CGCM2_3_2a	173.66	307.27	12-Jun	108.87	17-Sep
NCAR CCSM3	168.91	349.38	06-Jun	64.36	24-Oct
NCAR PCM1	215.19	***389.15***	12-Jun	137.46	20-Jul
UKMO HADCM3	185.85	342.66	12-Jun	104.99	30-Oct
UKMO HADGEM1	139.71	271.84	21-May	**55.71**	24-Oct
Overall Avg	**178.73**	**318.83**	**07-Jun**	**107.76**	**25-Sep**

Table 16: Average, maximum, and minimum flow values (cms) for HMETS, 2050s A2

GCM Name	Avg Q	Max Q	Date of Max Q	Min Q	Date of Min Q
Baseline	222.01	357.14	13-Jul	151.73	02-Apr
BCCR BCM2	264.16	413.89	*08-Jul*	184.05	29-Mar
CCCMA CGCM3	296.14	468.41	04-Jul	198.65	05-Mar
CNRM CM3	**149.48**	**249.65**	08-Jul	**106.39**	18-Mar
CSIRO MK3_0	261.65	391.03	06-Jul	188.61	13-Mar
CSIRO MK3_5	257.05	391.77	06-Jul	182.94	14-Mar
GFDL CM2_0	218.06	324.62	28-Jun	162.88	**17-Feb**
GFDL CM2_1	253.75	375.16	28-Jun	183.37	13-Mar
GISS MODEL E R	273.94	423.48	05-Jul	194.17	21-Mar
INGV ECHAM4	227.07	358.22	01-Jul	166.13	13-Mar
INMCM3	*315.16*	442.78	04-Jul	*218.98*	13-Mar
IPSL CM4	239.61	351.51	**25-Jun**	176.80	01-Mar
MIROC3_2 MEDRES	258.01	409.43	28-Jun	180.59	12-Mar
MIUB ECHO G	224.56	362.38	01-Jul	159.08	15-Mar
MPI ECHAM 5	229.54	438.50	29-Jun	113.51	06-Mar
MRI CGCM2_3_2a	221.32	358.45	06-Jul	141.04	16-Mar
NCAR CCSM3	249.67	434.95	01-Jul	155.26	12-Mar
NCAR PCM1	283.64	*474.08*	05-Jul	175.68	10-Mar
UKMO HADCM3	263.14	424.70	08-Jul	186.12	*30-Mar*
UKMO HADGEM1	213.94	329.52	25-Jun	158.50	04-Mar
Overall Avg	**247.36**	**390.66**	**02-Jul**	**170.15**	**12-Mar**

As with the hydrographs, the tabulated results for the A2 emissions scenario are similar to the more optimistic scenarios that were previously considered. WATFLOOD™ and HMETS both predict increases in the average, maximum, and minimum flows (37, 94, and 14, respectively for WATFLOOD™; and 25, 33 and 19 cms, respectively for HMETS). HBV-EC predicts a decrease for each flow (43, 32, and 38 cms, respectively). Compared to the other climate scenarios for the 2050s time period, these flow results are very similar. The A2 scenario has the smallest gains in each category for WATFLOOD™ and HMETS, and the largest decreases for HBV-EC. This is not unexpected, as the A2 scenario has the highest atmospheric carbon levels and in turn higher temperatures and

therefore evaporation rates. However the average over each of the climate models was within a small range of each other (emissions scenario averages from the 2050s were within 4% of each other overall).

In terms of timing of the major flow events, WATFLOOD^{TM} and HMETS both predict that the yearly peak flow will occur 11 days earlier each year, while HBV-EC predicts a slightly smaller advance in the timing on the order of 6 days. Again, HBV-EC saw a shift in the timing of the yearly minimum flow to the fall period for most climate model simulations, while HMETS and WATFLOOD^{TM} predict advances of minimum flow timing of 21 and 6 days, respectively. The following table represents the changes in the timing of the flow events in more detail (Table 17).

Table 17: Seasonal changes in flow, 2050s A2

	WATFLOOD™	HBV-EC	HMETS
DJF			
Avg % change	18.29	-19.11	10.76
Max % change	57.03	-1.51	37.31
Min % change	-12.53	-48.36	-34.16
Std. Dev. (%)	19.69	11.75	16.82
MAM			
Avg % change	30.30	-2.02	24.26
Max % change	78.49	15.74	51.40
Min % change	-12.94	-31.92	-26.00
Std. Dev. (%)	19.59	9.40	16.76
JJA			
Avg % change	13.55	-21.19	6.97
Max % change	85.63	-2.63	33.08
Min % change	-23.15	-52.43	-30.62
Std. Dev. (%)	23.25	12.08	14.37
SON			
Avg % change	18.38	-34.35	7.75
Max % change	87.35	-10.07	50.88
Min % change	-18.93	-64.73	-40.00
Std. Dev. (%)	25.45	15.05	19.34

Many of the same trends present in the previous two emissions scenarios are again prevalent in the 2050s A2 figures above. Each of the three month periods shows an increase, on average, for the WATFLOOD™ and HMETS models while the HBV-EC simulations show a decrease for each of the three month periods. In general, the A2 flows were higher than the other scenarios in summer (JJA) and fall (SON) while they were slightly lower during winter (DJF) and spring (MAM). Each model again showed the greatest increase or smallest decrease during the freshet period (MAM), while HBV-EC saw the largest decrease during the fall (SON). WATFLOOD™ and HMETS saw the smallest increases in the summer months (JJA). As well, WATFLOOD™ simulations have the highest

standard deviation for each season. These trend results were the same as those which were seen for the A1B scenario.

6.1.4 2080s, B1

For the 2080s future time period, 46 simulations were conducted to simulate the conditions that may be present within the Churchill River basin under the most optimistic B1 emissions scenario. The following hydrographs (Figure 52) show the results for the six runs of the CCCMA CGCM3.1. A more complete set of results for each of the runs is included in the tables which follow (Table 18 through Table 21). Once again, the remainder of the hydrographs for each of the GCMs not shown in this section are displayed in Appendix D.
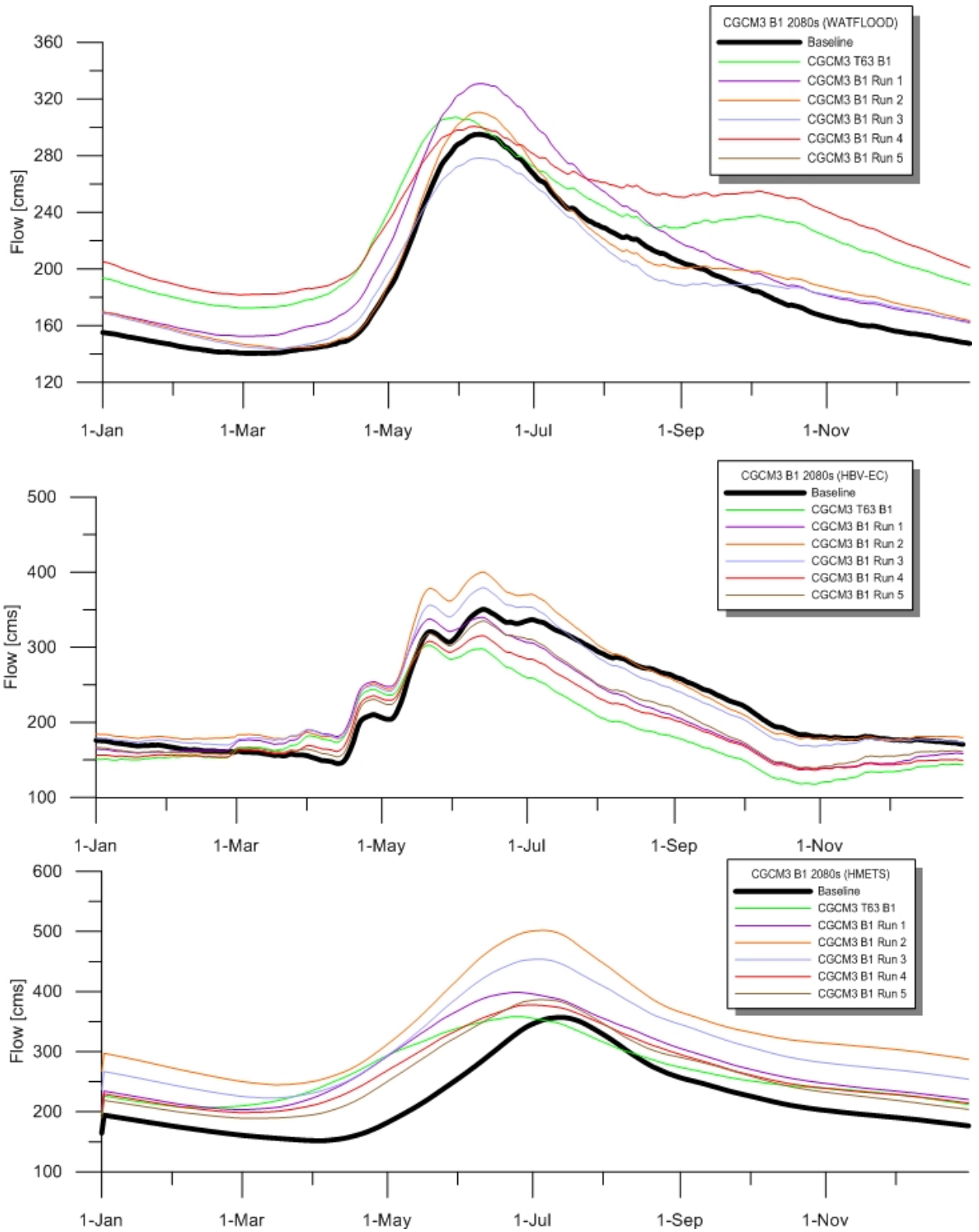
Figure 52: Annual average hydrographs, 2080s time horizon, B1 emissions scenario

The annual average hydrographs for the CCCMA CGCM3.1 once again show that the HMETS and WATFLOOD™ models generally predict an increase in flow by the 2080s, while the HBV-EC model predicts a decrease during much of the year. A further numeric analysis of the results is given in the tables below (Table 18 through Table 21).

Table 18: Average, maximum and minimum flow values (cms) for WATFLOOD™, 2080s B1

GCM Name	Avg. Q	Max Q	Date of Max Q	Min Q	Date of Min Q
Baseline	189.10	295.06	08-Jun	140.44	06-Mar
BCCR BCM2	236.62	412.29	04-Jun	160.19	*01-Apr*
CCCMA CGCM3	215.79	382.25	03-Jun	143.55	05-Mar
CNRM CM3	**168.32**	269.84	06-Jun	123.32	16-Mar
CSIRO MK3_0	191.10	300.62	*12-Jun*	135.69	19-Mar
CSIRO MK3_5	206.65	319.83	06-Jun	149.63	16-Mar
GFDL CM2_0	184.40	290.23	06-Jun	137.72	01-Mar
GFDL CM2_1	215.46	303.02	08-Jun	161.54	16-Mar
GISS AOM	188.10	303.31	06-Jun	121.69	16-Mar
GISS MODEL E R	196.23	317.59	04-Jun	142.39	15-Mar
IAP FGOALS	189.76	311.71	05-Jun	140.72	12-Mar
INMCM3	218.13	318.80	06-Jun	151.52	17-Mar
IPSL CM4	198.15	300.28	30-May	147.27	16-Mar
MIROC3_2 HIRES	170.33	**263.92**	**23-May**	139.75	02-Mar
MIROC3_2 MEDRES	193.63	312.02	03-Jun	136.07	15-Mar
MIUB ECHO G	178.54	295.91	08-Jun	**120.60**	15-Mar
MPI ECHAM 5	197.04	354.62	05-Jun	129.09	15-Mar
MRI CGCM2_3_2a	182.66	308.73	10-Jun	120.78	20-Mar
NCAR CCSM3	206.74	410.48	02-Jun	131.38	05-Mar
NCAR PCM1	*271.79*	*479.99*	01-Jun	*188.56*	**17-Feb**
UKMO HADCM3	181.79	294.26	29-May	134.76	05-Mar
Overall Avg.	**199.56**	**327.48**	**04-Jun**	**140.81**	**12-Mar**

Table 19: Average, maximum and minimum flow values (cms) for HBV-EC, 2080s B1

GCM Name	Avg. Q	Max Q	Date of Max Q	Min Q	Date of Min Q
Baseline	221.86	350.54	13-Jun	145.23	13-Apr
BCCR BCM2	183.74	307.87	12-Jun	125.81	23-Oct
CCCMA CGCM3	209.61	*400.09*	08-Jun	117.86	*05-Nov*
CNRM CM3	**119.77**	**223.76**	21-May	63.42	23-Oct
CSIRO MK3_0	208.23	347.37	*13-Jun*	145.31	30-Oct
CSIRO MK3_5	191.05	328.50	12-Jun	123.95	23-Oct
GFDL CM2_0	188.71	318.58	12-Jun	112.74	30-Oct
GFDL CM2_1	167.93	309.80	12-Jun	95.28	24-Oct
GISS AOM	182.80	324.71	12-Jun	108.61	30-Oct
GISS MODEL E R	202.33	350.88	12-Jun	147.77	**19-Jan**
IAP FGOALS	178.90	322.80	28-May	107.59	27-Oct
INMCM3	227.18	364.65	13-Jun	*166.10*	30-Oct
IPSL CM4	136.16	250.05	**20-May**	64.65	23-Oct
MIROC3_2 HIRES	136.11	262.23	20-May	**52.07**	13-Oct
MIROC3_2 MEDRES	153.82	305.08	20-May	63.51	25-Oct
MIUB ECHO G	160.78	287.89	04-Jun	87.69	29-Oct
MPI ECHAM 5	157.33	304.25	28-May	66.55	27-Oct
MRI CGCM2_3_2a	163.36	294.73	12-Jun	94.31	27-Oct
NCAR CCSM3	184.38	352.39	06-Jun	87.15	25-Sep
NCAR PCM1	*228.01*	372.85	12-Jun	162.92	12-Apr
UKMO HADCM3	137.67	264.36	21-May	62.85	24-Oct
Overall Avg.	**175.89**	**314.64**	**04-Jun**	**102.81**	**30-Sep**

Table 20: Average, maximum and minimum flow values (cms) for HMETS, 2080s B1

GCM Name	Avg. Q	Max Q	Date of Max Q	Min Q	Date of Min Q
Baseline	222.01	357.14	13-Jul	151.73	02-Apr
BCCR BCM2	253.80	392.74	01-Jul	181.55	*21-Mar*
CCCMA CGCM3	286.30	*501.84*	02-Jul	189.16	03-Mar
CNRM CM3	**160.08**	**262.03**	07-Jul	**115.68**	15-Mar
CSIRO MK3_0	273.07	407.82	08-Jul	197.15	14-Mar
CSIRO MK3_5	268.26	400.13	05-Jul	194.53	09-Mar
GFDL CM2_0	249.83	370.30	25-Jun	182.95	03-Mar
GFDL CM2_1	242.60	375.93	04-Jul	178.78	15-Mar
GISS AOM	216.36	367.73	07-Jul	134.06	06-Feb
GISS MODEL E R	283.95	440.95	*09-Jul*	*203.91*	21-Mar
IAP FGOALS	238.06	384.88	01-Jul	158.38	06-Mar
INMCM3	258.12	367.43	26-Jun	187.35	09-Mar
IPSL CM4	198.81	300.41	26-Jun	146.27	**01-Jan**
MIROC3_2 HIRES	228.48	337.20	**12-Jun**	176.79	27-Feb
MIROC3_2 MEDRES	242.34	385.26	25-Jun	171.96	12-Feb
MIUB ECHO G	215.71	338.97	30-Jun	157.17	12-Mar
MPI ECHAM 5	224.47	377.86	23-Jun	137.45	20-Jan
MRI CGCM2_3_2a	221.44	368.85	03-Jul	143.02	13-Mar
NCAR CCSM3	257.61	437.26	05-Jul	168.96	01-Mar
NCAR PCM1	*294.27*	454.71	08-Jul	202.28	07-Mar
UKMO HADCM3	202.74	320.49	30-Jun	146.44	14-Mar
Overall Avg.	**240.82**	**379.64**	**01-Jul**	**168.69**	**01-Mar**

Results from the most optimistic scenario included in this modelling exercise display some interesting trends. WATFLOOD^{TM} results show increases in the average flow (10 cms) and maximum flow (32 cms), and essentially no change in average yearly minimum flow (+0.37 cms). HBV-EC again showed decreases in each of the three categories (46, 36 and 43 cms, respectively), while HMETS results showed increases (19, 22 and 17 cms, respectively). In all cases, the overall average of the climate models showed a lower flow than was seen during the 2050s under the B1 emissions scenario. This means that under the B1 emissions scenario, some of the increases which will be realized in the 2050s will

be lost in the 2080s. This decrease in streamflow is a result of increased temperatures which lead to an increase in potential evapotranspiration.

The timing of maximum and minimum flows also shows some interesting trends. WATFLOOD^{TM} predicts that the maximum flow will only occur 4 days earlier than the baseline period, while HBV-EC and HMETS predict slightly longer advances of 9 and 12 days, respectively. WATFLOOD^{TM}, on average, predicts that the minimum flow event will occur 6 days later; while HMETS predicted the minimum would occur one month sooner and HBV-EC again predicted that the minimum flow value would no longer occur shortly before the spring melt event, but rather at the end of the open water season in September or October for most cases. This shift is once again the result of the HBV-EC model configuration's sensitivity to increases in temperature leading to an increase in evaporation that contributes to the reduction of summer flows. The following table (Table 21) shows a further breakdown of the changes in timing predicted by each of the hydrological models.

Table 21: Seasonal changes in flow, 2080s B1

	WATFLOOD™	HBV-EC	HMETS
DJF			
Avg % change	8.71	-20.37	7.31
Max % change	39.74	3.07	33.02
Min % change	-9.48	-43.94	-29.40
Std. Dev. (%)	11.50	12.96	15.74
MAM			
Avg % change	7.38	-1.58	23.52
Max % change	52.43	14.19	48.14
Min % change	-10.11	-29.12	-19.66
Std. Dev. (%)	13.40	10.27	16.26
JJA			
Avg % change	0.92	-23.17	3.76
Max % change	36.00	0.74	24.76
Min % change	-25.39	-48.59	-26.62
Std. Dev. (%)	13.47	15.07	13.55
SON			
Avg % change	7.58	-36.29	3.76
Max % change	49.07	-3.75	33.66
Min % change	-12.99	-65.12	-35.39
Std. Dev. (%)	14.94	18.31	17.02

During the 2080s for the B1 emissions scenario, both WATFLOOD™ and HMETS predict that, on average, there will be increases during each of the three month periods during the year; while HBV-EC predicts a decrease during the same periods. WATFLOOD™ predicts that the largest increase will occur during the winter (DJF) period while the smallest increase is during the summer (JJA) period. Similar to the 2050s period, HMETS predicts that the largest increase will occur during the spring freshet (MAM) period, and the smallest decreases occur jointly during summer (JJA) and fall (SON). HBV-EC predicts that the largest flow decrease will occur in fall (SON), and the smallest decrease will happen during spring freshet (MAM). The consistent increases seen in the HMETS results are a result of the increased precipitation levels driving the unit

hydrograph outflow, while its evapotranspiration routine is less sensitive to changes in temperature than the routine used in the HBV-EC model. The changes from all three hydrological models in general are smaller than those seen in the 2050s, which were expected based on the climate model trends toward more atmospheric carbon and higher temperatures/evaporation levels, as well the discussions above from the results of each hydrological model individually.

6.1.5 2080s, A1B

A total of 54 simulations were utilised in order to examine the predicted impacts associated with the A1B emissions scenario for the 2080s future time horizon. The following annual average hydrographs (Figure 53) show the hydrological impacts associated with the climate projections from the CCCMA CGMC3.1 climate model. The subsequent tables (Table 22 through Table 25) display the results for each of the models used in the ensemble. The hydrographs generated from the remainder of the GCM models are displayed in Appendix D.
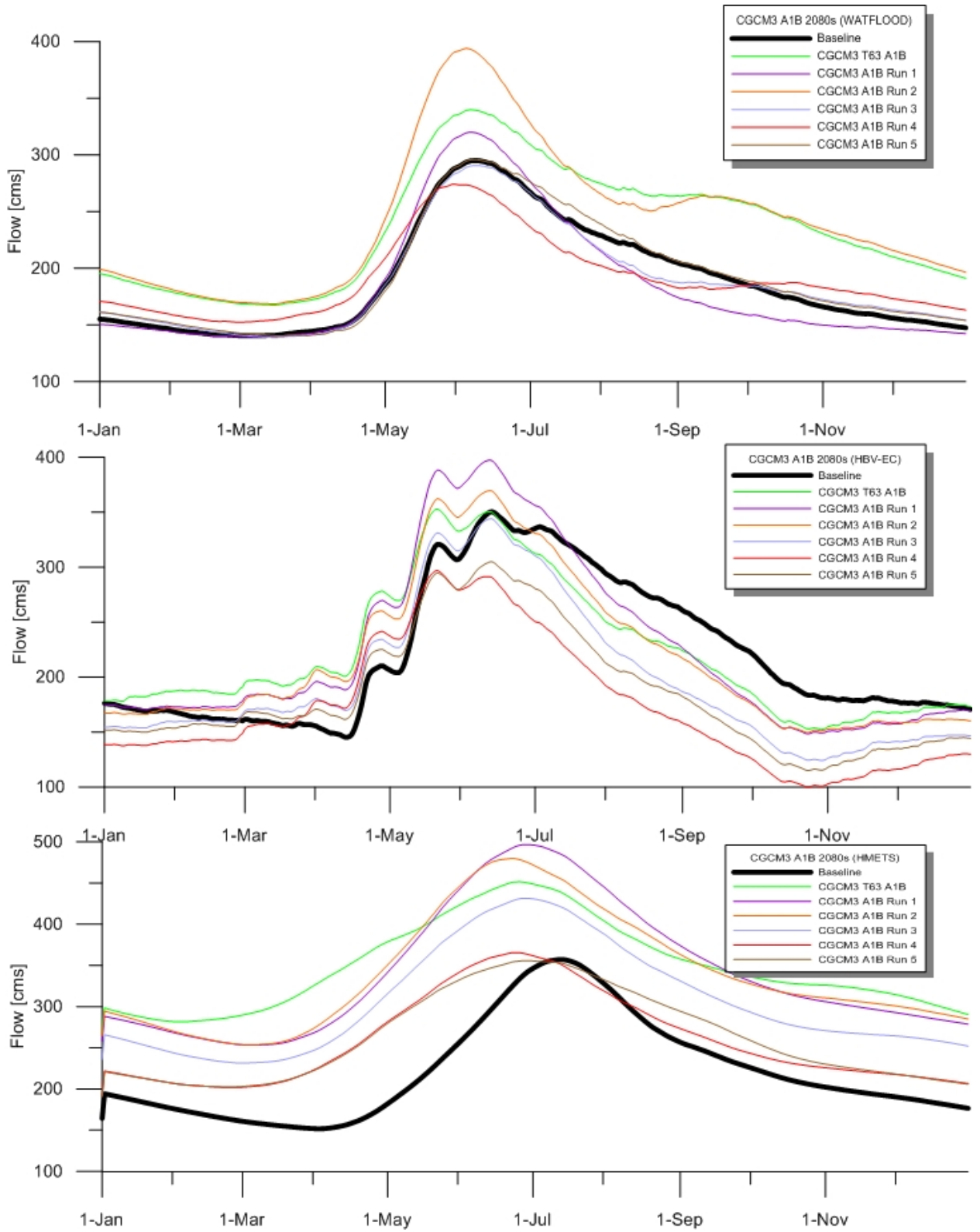
Figure 53: Annual average hydrographs, 2080s time horizon, A1B emissions scenario

The patterns prevalent in each of the other scenarios are once again displayed in the above hydrographs (Figure 53). In general all of the models seem to predict an increase in the peak volume of the spring melt freshet event. HMETS and WATFLOOD[TM] additionally predict increases in flow during the other portions of the year, while HBV-EC predicts that the flow during the summer and winter months will be less than those modelled by the baseline climate data. The following tables (Table 22 through Table 25) give a more in-depth numerical analysis of the results obtained using each of the hydrological models.

Table 22: Average, maximum and minimum flows (cms) for WATFLOOD[TM], 2080s A1B

GCM Name	Avg Q	Max Q	Date of Max Q	Min Q	Date of Min Q
Baseline	189.10	295.06	08-Jun	140.44	06-Mar
BCCR BCM2	182.51	280.24	06-Jun	137.54	31-Mar
CCCMA CGCM3	205.70	393.99	05-Jun	138.86	12-Mar
CNRM CM3	**146.31**	**195.76**	08-Jun	**114.78**	03-Apr
CSIRO MK3_0	205.44	337.98	06-Jun	143.94	30-Mar
CSIRO MK3_5	188.74	276.06	06-Jun	141.94	14-Mar
GFDL CM2_0	191.82	266.22	06-Jun	142.22	02-Mar
GFDL CM2_1	220.85	298.29	04-Jun	167.09	14-Mar
GISS AOM	189.53	309.19	07-Jun	136.56	22-Mar
GISS MODEL E H	225.71	429.96	06-Jun	125.92	22-Mar
GISS MODEL E R	176.55	306.59	07-Jun	121.16	24-Mar
IAP FGOALS	192.48	310.05	07-Jun	138.49	17-Mar
INGV ECHAM4	174.92	269.25	06-Jun	129.61	16-Mar
INMCM3	201.12	277.12	29-May	149.51	02-Mar
IPSL CM4	230.25	326.52	29-May	165.74	16-Mar
MIROC3_2 HIRES	208.33	331.26	29-May	155.69	14-Mar
MIROC3_2 MEDRES	188.90	328.07	03-Jun	125.72	13-Mar
MIUB ECHO G	173.92	263.34	08-Jun	123.98	16-Mar
MPI ECHAM 5	192.46	334.84	07-Jun	117.26	16-Mar
MRI CGCM2_3_2a	183.20	296.31	***09-Jun***	132.69	17-Mar
NCAR CCSM3	196.02	383.16	08-Jun	115.24	07-Apr
NCAR PCM1	***270.62***	***477.48***	23-May	***186.56***	**18-Feb**
UKMO HADCM3	208.49	388.16	23-May	150.28	21-Feb
UKMO HADGEM1	183.52	369.58	**15-May**	114.91	***15-Oct***
Overall Avg	**197.28**	**323.89**	**03-Jun**	**138.07**	**25-Mar**

Table 23: Average, maximum and minimum flows (cms) for HBV-EC, 2080s A1B

GCM Name	Avg Q	Max Q	Date of Max Q	Min Q	Date of Min Q
Baseline	221.86	350.54	13-Jun	145.23	13-Apr
BCCR BCM2	168.76	293.06	21-May	108.33	**13-Oct**
CCCMA CGCM3	203.74	*397.57*	04-Jun	100.07	25-Oct
CNRM CM3	**104.71**	**209.74**	21-May	42.47	13-Oct
CSIRO MK3_0	*214.07*	355.18	*13-Jun*	*148.39*	*30-Oct*
CSIRO MK3_5	201.67	338.03	12-Jun	129.16	23-Oct
GFDL CM2_0	142.59	261.62	20-May	59.31	29-Oct
GFDL CM2_1	160.66	285.93	21-May	79.51	24-Oct
GISS AOM	147.36	249.74	21-May	78.81	24-Oct
GISS MODEL E H	168.46	348.12	12-Jun	67.23	16-Oct
GISS MODEL E R	194.82	372.33	12-Jun	114.95	23-Oct
IAP FGOALS	149.71	280.70	20-May	74.22	25-Oct
INGV ECHAM4	176.75	315.55	21-May	97.84	24-Oct
INMCM3	195.43	304.29	12-Jun	129.10	29-Oct
IPSL CM4	118.34	235.52	**27-Apr**	**39.21**	13-Oct
MIROC3_2 HIRES	142.19	279.50	18-May	42.63	13-Oct
MIROC3_2 MEDRES	151.56	312.22	20-May	51.04	20-Oct
MIUB ECHO G	155.62	302.08	21-May	68.59	25-Oct
MPI ECHAM 5	171.34	309.76	21-May	73.22	26-Oct
MRI CGCM2_3_2a	147.40	279.69	25-May	80.24	24-Oct
NCAR CCSM3	176.07	369.48	27-May	65.73	25-Oct
NCAR PCM1	198.08	370.18	06-Jun	112.67	26-Oct
UKMO HADCM3	157.93	308.79	12-Jun	70.78	23-Oct
UKMO HADGEM1	141.88	290.15	20-May	43.29	13-Oct
Overall Avg	**164.75**	**307.36**	**27-May**	**81.60**	**22-Oct**

146

Table 24: Average, maximum and minimum flows (cms) for HMETS, 2080s A1B

GCM Name	Avg Q	Max Q	Date of Max Q	Min Q	Date of Min Q
Baseline	222.01	357.14	13-Jul	151.73	02-Apr
BCCR BCM2	269.43	391.32	30-Jun	204.82	14-Mar
CCCMA CGCM3	309.86	496.42	25-Jun	201.82	24-Feb
CNRM CM3	**156.22**	**249.80**	05-Jul	**113.36**	**01-Jan**
CSIRO MK3_0	296.30	426.66	05-Jul	219.29	04-Mar
CSIRO MK3_5	*314.97*	437.13	23-Jun	*234.79*	27-Feb
GFDL CM2_0	222.05	313.21	22-Jun	165.27	01-Jan
GFDL CM2_1	242.86	347.50	23-Jun	181.65	01-Jan
GISS AOM	188.71	282.46	28-Jun	137.67	01-Jan
GISS MODEL E H	288.11	485.25	05-Jul	175.01	17-Mar
GISS MODEL E R	297.19	*499.48*	07-Jul	201.04	*29-Mar*
IAP FGOALS	213.09	324.23	25-Jun	141.24	01-Jan
INGV ECHAM4	255.96	392.20	27-Jun	187.55	13-Mar
INMCM3	294.55	385.11	*08-Jul*	210.69	27-Feb
IPSL CM4	222.99	314.30	10-Jun	181.52	01-Jan
MIROC3_2 HIRES	262.42	370.23	**06-Jun**	209.57	01-Jan
MIROC3_2 MEDRES	270.55	399.55	22-Jun	193.22	01-Jan
MIUB ECHO G	238.31	372.97	25-Jun	170.68	07-Mar
MPI ECHAM 5	262.94	386.32	24-Jun	179.54	29-Jan
MRI CGCM2_3_2a	214.96	348.75	29-Jun	137.58	08-Mar
NCAR CCSM3	276.03	446.87	27-Jun	175.97	17-Feb
NCAR PCM1	289.27	459.65	28-Jun	185.58	11-Feb
UKMO HADCM3	267.60	406.83	30-Jun	199.15	13-Mar
UKMO HADGEM1	253.24	368.55	21-Jun	192.10	01-Jan
Overall Avg	**256.85**	**387.16**	**26-Jun**	**182.57**	**07-Feb**

The results obtained from the 2080s A1B simulations are similar to those from the 2080s B1 scenario (WATFLOOD[TM] and HBV-EC each predict small decreases in flow, while HMETS predicts that the flows will actually be higher), however generally the flows are forecasted to be slightly lower than was predicted for the 2050s A1B scenario. Once again, small increases were typical for the results from WATFLOOD[TM] (8, 29 and -2 cms for average, maximum, and minimum flows, respectively), while HMETS saw moderate increases (34, 30, and 31 cms, respectively), and HBV-EC saw moderate decreases (57, 43, and

64 cms, respectively).   Based on the results from each of the other climate change scenarios, these results are not unexpected.   The average changes in temperature and precipitation lead to less flow in the further future, usually a result of higher evaporation levels caused by slightly higher summer temperatures.

The timing of the major flow events showed similar trends to those seen in the 2080s B1 simulation results.   Each of the hydrological models showed that the freshet peak timing was advanced (5 days for WATFLOOD^{TM}, and 17 each for HBV-EC and HMETS), while WATFLOOD^{TM} and HBV-EC each predicted that the minimum flow would happen later the baseline simulated data (19 days for WATFLOOD^{TM}, and a similar shift from the late winter to the fall for HBV-EC as was seen in each of the previous emissions scenarios), and HMETS predicts an approximately 2 month advance of the minimum flow into early February from early April.   This shift in the timing of the minimum flow is a result of the increasing winter temperatures increasing late winter and early spring flows as a result of snowmelt.   A more in-depth numerical summary of these results may be found in the table below (Table 25).

Table 25: Seasonal changes in flow, 2080s A1B

	WATFLOOD™	HBV-EC	HMETS
DJF			
Avg % change	8.03	-25.18	15.04
Max % change	53.74	-2.45	41.77
Min % change	-12.91	-49.92	-31.08
Std. Dev. (%)	14.37	11.91	18.62
MAM			
Avg % change	8.21	0.57	37.24
Max % change	59.81	16.12	71.25
Min % change	-24.59	-31.35	-17.47
Std. Dev. (%)	18.79	10.69	20.31
JJA			
Avg % change	-1.97	-31.32	5.76
Max % change	21.05	-4.69	30.39
Min % change	-31.00	-58.75	-29.93
Std. Dev. (%)	11.25	13.97	16.08
SON			
Avg % change	5.36	-47.32	8.31
Max % change	48.46	-14.66	42.27
Min % change	-31.72	-73.17	-38.18
Std. Dev. (%)	17.46	16.75	19.79

These results (Table 25) confirm the trends noticed above. WATFLOOD™ shows a small increase or decrease, on average, for each of the time periods while HBV-EC predicts decreases throughout the year (except for a small increase during MAM). HMETS predicts increases throughout the year across all seasons. Each of the models predicts the largest increases during the spring freshet (MAM) period, while WATFLOOD™ predicts its only decrease and HMETS predicts the smallest increase during the summer months (JJA). This is a result of the higher temperatures causing an increase in evaporation during the open water season and a subsequent decrease in streamflow. HBV-EC predicts the largest percentage decrease in flow will occur slightly later, during the fall (SON) period.

6.1.6 2080s, A2

The final case examined in this study is the 2080s A2 emissions scenario. In order to simulate this scenario, 39 simulations from 19 different GCMs were used. As with each of the previous sections, the hydrographs which follow (Figure 54) represent the results from the CCCMA CGCM3.1 data and the subsequent tables. (Table 26 through Table 29) show the results from each of the climate models utilised in the suite. The remainder of the hydrographs generated from each of the other GCMs may be found in Appendix D.
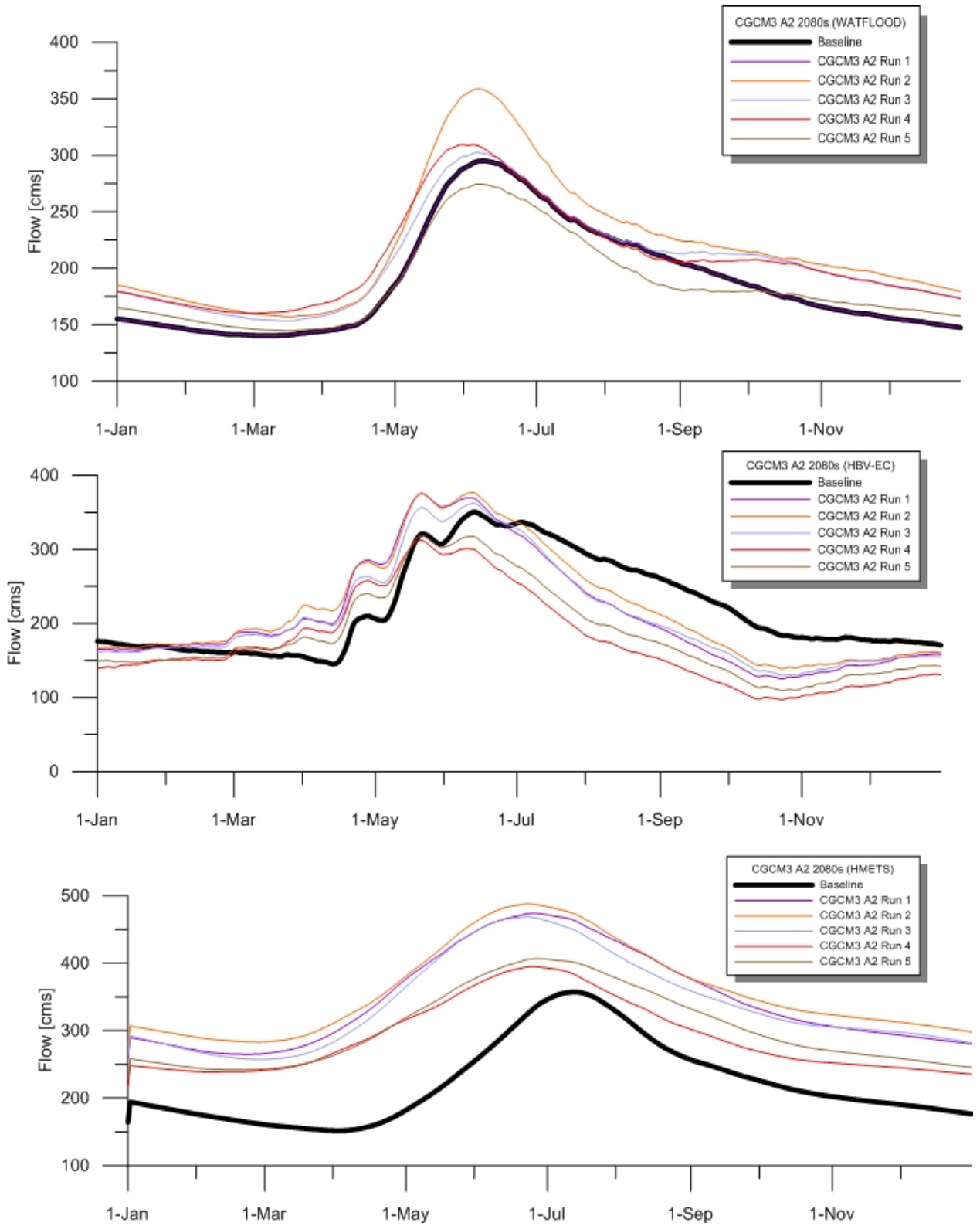
Figure 54: Annual average hydrographs, 2080s time horizon, A2 emissions scenario

The above hydrographs (Figure 54) indicate that for the 2080s A2 scenario there will once again be an advance the timing of the freshet peak, and increase in magnitude of peak flow (in most cases). The results from the remainder of the climate models are displayed in the following tables (Table 26 through Table 29) and a full analysis follows.

Table 26: Average, maximum, and minimum flow values (cms) for WATFLOOD[TM], 2080s, A2

GCM Name	Avg Q	Max Q	Date of Max Q	Min Q	Date of Min Q
Baseline	189.10	295.06	08-Jun	140.44	06-Mar
BCCR BCM2	201.76	299.48	05-Jun	148.39	03-Apr
CCCMA CGCM3	224.48	*509.95*	03-Jun	144.58	06-Mar
CNRM CM3	163.92	**237.17**	09-Jun	124.58	29-Mar
CSIRO MK3_0	214.65	336.31	06-Jun	151.40	16-Mar
CSIRO MK3_5	216.50	329.34	08-Jun	155.75	29-Mar
GFDL CM2_0	188.36	284.90	06-Jun	140.88	**17-Feb**
GFDL CM2_1	**163.79**	254.14	08-Jun	126.56	10-Mar
GISS MODEL E R	199.46	331.53	04-Jun	141.72	15-Mar
INGV ECHAM4	188.17	267.85	06-Jun	139.04	15-Mar
INMCM3	238.27	358.71	09-Jun	159.98	16-Mar
IPSL CM4	236.88	356.09	04-Jun	165.54	19-Mar
MIROC3_2 MEDRES	180.52	311.61	02-Jun	125.30	12-Mar
MIUB ECHO G	176.31	299.19	09-Jun	122.26	20-Mar
MPI ECHAM 5	203.40	397.59	10-Jun	**114.86**	14-Mar
MRI CGCM2_3_2a	189.76	314.94	*11-Jun*	134.03	20-Mar
NCAR CCSM3	217.39	371.05	02-Jun	137.44	06-Mar
NCAR PCM1	*279.00*	487.45	25-May	*203.76*	23-Feb
UKMO HADCM3	237.83	463.76	29-May	162.56	02-Mar
UKMO HADGEM1	195.23	387.78	**14-May**	116.91	*01-Oct*
Overall Avg	**206.09**	**347.31**	**04-Jun**	**142.92**	**24-Mar**

152

Table 27: Average, maximum, and minimum flow values (cms) for HBV-EC, 2080s, A2

GCM Name	Avg Q	Max Q	Date of Max Q	Min Q	Date of Min Q
Baseline	221.86	350.54	13-Jun	145.23	13-Apr
BCCR BCM2	181.62	313.46	21-May	112.43	24-Oct
CCCMA CGCM3	200.91	*376.62*	29-May	97.13	23-Oct
CNRM CM3	**107.28**	**216.34**	21-May	46.27	13-Oct
CSIRO MK3_0	209.14	365.47	*12-Jun*	126.48	*30-Oct*
CSIRO MK3_5	210.64	362.60	21-May	132.14	24-Oct
GFDL CM2_0	131.29	257.23	20-May	122.43	17-Feb
GFDL CM2_1	150.69	286.32	21-May	64.07	23-Oct
GISS MODEL E R	201.84	363.11	12-Jun	*140.95*	**13-Oct**
INGV ECHAM4	156.12	289.10	20-May	71.61	24-Oct
INMCM3	*214.10*	356.50	21-May	127.41	29-Oct
IPSL CM4	109.01	220.84	**25-Apr**	**30.99**	13-Oct
MIROC3_2 MEDRES	148.94	305.51	20-May	55.98	16-Oct
MIUB ECHO G	139.17	273.97	20-May	53.05	23-Oct
MPI ECHAM 5	151.25	332.04	20-May	45.32	22-Oct
MRI CGCM2_3_2a	140.45	262.44	25-May	64.53	24-Oct
NCAR CCSM3	171.10	340.61	26-May	67.47	25-Oct
NCAR PCM1	196.97	353.75	06-Jun	106.42	25-Oct
UKMO HADCM3	199.50	369.83	12-Jun	108.40	30-Oct
UKMO HADGEM1	147.51	303.63	20-May	43.97	13-Oct
Overall Avg	**166.71**	**313.12**	**24-May**	**85.11**	**09-Oct**

Table 28: Average, maximum, and minimum flow values (cms) for HMETS, 2080s, A2

GCM Name	Avg Q	Max Q	Date of Max Q	Min Q	Date of Min Q
Baseline	222.01	357.14	13-Jul	151.73	02-Apr
BCCR BCM2	285.09	419.63	28-Jun	212.59	14-Mar
CCCMA CGCM3	327.93	487.69	24-Jun	232.07	12-Feb
CNRM CM3	**177.91**	**268.76**	***08-Jul***	136.82	**01-Jan**
CSIRO MK3_0	322.13	459.80	27-Jun	242.02	04-Mar
CSIRO MK3_5	*353.12*	499.19	24-Jun	*264.17*	03-Mar
GFDL CM2_0	204.61	300.00	22-Jun	158.75	17-Feb
GFDL CM2_1	257.48	369.93	22-Jun	199.42	01-Jan
GISS MODEL E R	339.56	*516.52*	08-Jul	242.68	*24-Mar*
INGV ECHAM4	233.93	361.42	23-Jun	173.39	10-Mar
INMCM3	337.74	449.22	26-Jun	253.64	27-Feb
IPSL CM4	197.61	283.06	**03-Jun**	158.32	01-Jan
MIROC3_2 MEDRES	263.75	384.95	23-Jun	203.37	01-Jan
MIUB ECHO G	221.40	342.51	25-Jun	163.66	24-Jan
MPI ECHAM 5	234.65	411.80	18-Jun	135.63	01-Jan
MRI CGCM2_3_2a	206.26	325.33	26-Jun	**132.53**	20-Feb
NCAR CCSM3	287.26	427.76	22-Jun	196.56	27-Feb
NCAR PCM1	288.16	462.55	29-Jun	204.18	17-Feb
UKMO HADCM3	311.42	470.37	01-Jul	228.07	14-Mar
UKMO HADGEM1	277.36	393.51	21-Jun	217.10	01-Jan
Overall Avg	**269.86**	**401.79**	**24-Jun**	**197.63**	**08-Feb**

The A2 emissions scenario in the 2080s future time horizon is the most advanced and pessimistic case of global climate change examined in this study. These results from this scenario and future time horizon outline the impacts of a future where world development has led to the highest levels of atmospheric carbon and attempts to mitigate the effects on the climate have not been successful. The future flows predicted by the models in this study are the highest for the 2080s future time horizon under the A2 scenario for each of the hydrological models. HBV-EC still predicts decreases in each of the flows considered (55, 37, and 64 cms, respectively for average, maximum and minimum flows), while WATFLOOD™ (17, 52, and 2.5 cms, respectively) and HMETS (47, 44, and 46

cms, respectively) both predict increases for each of the three characteristic flows. Each of the changes predicted by the models is realistic based on the way that the individual model calculates evaporation and other hydrological processes.

Patterns in the timing of the peak and yearly low flows displayed similar patterns as previous scenarios. Each of the hydrological models simulated that maximum flow would occur earlier in the year (four days for WATFLOOD^{TM}, and approximately three weeks each for the HBV-EC and HMETS models). Results also show that HMETS predicts yearly minimum flow nearly two months earlier on average and WATFLOOD^{TM} simulations show that the minimum flow would take place 18 days later on average. HBV-EC again showed a shift of the yearly low flow from the late winter to the fall period as a result of decreased summer flows due to higher evaporation levels. These timing changes are the result of increased flows during the winter and an earlier transition to snowmelt in the early spring. A full numerical summary of the timing of flow events may be found below (Table 29).

Table 29: Seasonal changes in flow, 2080s A2

	WATFLOOD^{TM}	HBV-EC	HMETS
DJF			
Avg % change	11.60	-23.48	22.61
Max % change	57.57	-4.41	62.35
Min % change	-9.72	-47.53	-18.63
Std. Dev. (%)	15.56	14.31	25.18
MAM			
Avg % change	12.98	4.12	46.47
Max % change	61.41	28.97	87.74
Min % change	-15.52	-30.19	-5.50
Std. Dev. (%)	22.44	13.95	25.64
JJA			
Avg % change	4.44	-29.66	11.44
Max % change	28.06	-6.38	46.38
Min % change	-18.93	-65.22	-26.34
Std. Dev. (%)	14.46	17.52	22.48
SON			
Avg % change	9.17	-47.47	14.68
Max % change	53.47	-23.47	54.69
Min % change	-30.02	-78.15	-27.61
Std. Dev. (%)	19.27	19.05	26.62

The above table (Table 29) confirms those results inferred in the previous section. On average, WATFLOOD^{TM} and HMETS each predict that flows will increase in each period of the year, while HBV-EC predicts an increase in spring freshet (MAM), with decreases for all other periods. This spring period (MAM) corresponds to the period with maximum increases for all models, while WATFLOOD^{TM} and HMETS both predict the smallest increases in the summer (JJA). This is in slight contrast to HBV-EC, which predicts the largest decrease in flow will occur during the fall (SON) period.

6.2 Summary and discussion of climate change results

The above sections outline the numerical values which were obtained from the climate change simulations completed as part of this research. Several interesting trends were noted in the results, and may be realized in the future. The first evident trend was that the results depended on the hydrological model that was used. This is apparent when examining the plot below (Figure 55). Results from the HBV-EC model tend to be lower than those obtained using either of the other models. This may be caused by many different factors, but in this case, the HBV-EC model is predicting a large increase in evaporation as a result of the changes in temperature (mostly increases) predicted by the GCMs. This difference compared to the other models can be attributed mainly to model structure and the evaporation calculation method which is used in HBV-EC. HBV-EC uses a calculation for evaporation based on a table of values input by a user that is more sensitive to temperature increases than either of the other hydrological models.
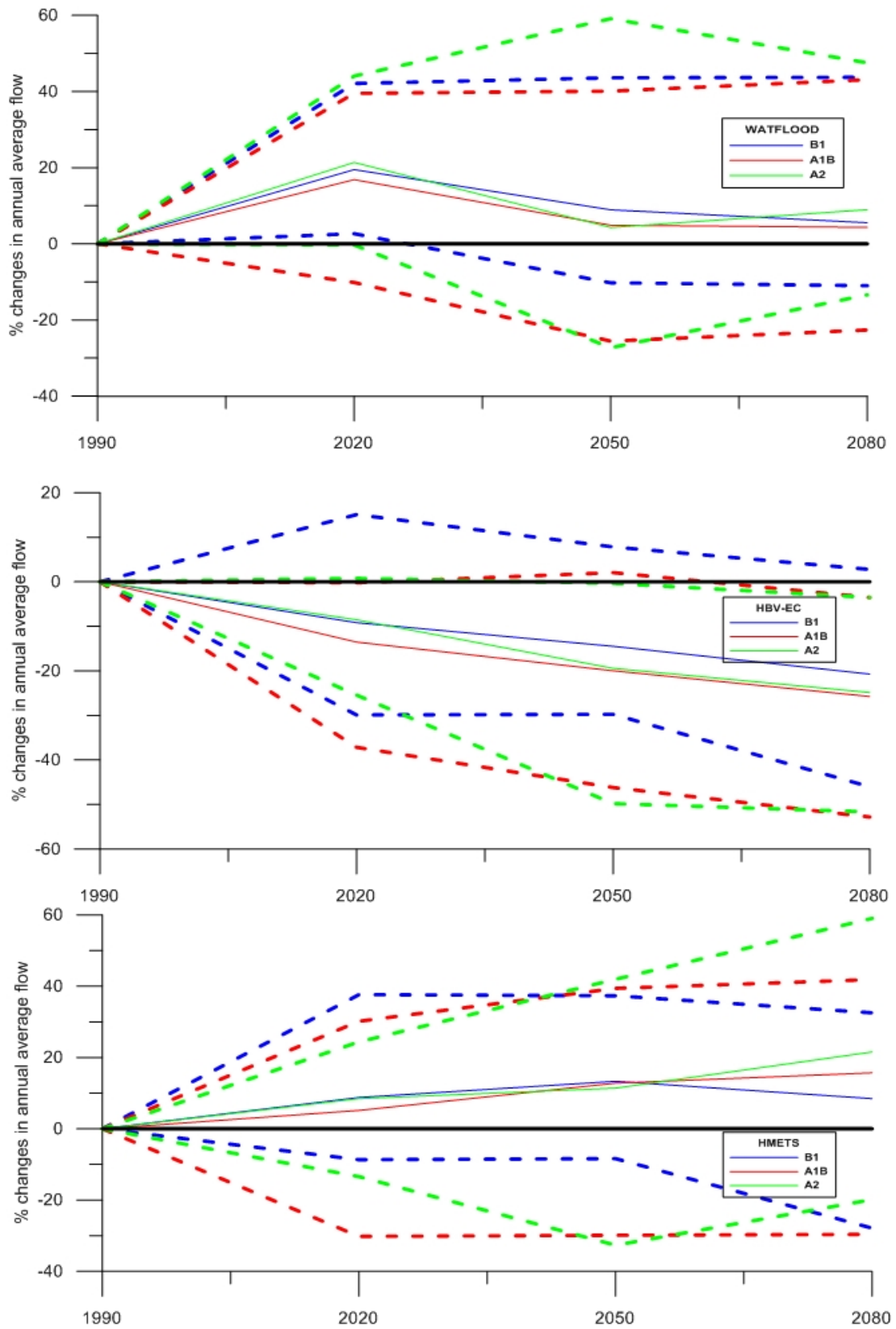
Figure 55: Average annual flow trends by climate model and hydrological model

Overall the results from each model show some similarities as well as some differences. As seen previously, HBV-EC predicts that the flows will decrease as time progresses toward the year 2080. WATFLOOD^{TM} predicts an initial increase followed by a slight decline towards 2080, and HMETS predicts that the average flow will continue to increase for each time period. Additionally, the trend is that the difference between the highest and lowest value for annual average flow increases as the future time horizons progress (evidenced by the "fanning out" in Figure 55). This suggests that the uncertainty present within the study has a much greater effect on the estimation of the flows in the 2080s than in earlier future time horizons, which is not an unexpected result.

In order to fully understand the range of impacts which may be experienced in the future, it is helpful to examine an envelope curve which displays the complete range of results. The following plots (Figure 56 through Figure 58) show the maximum, minimum, 95% confidence interval and average climate change annual average hydrographs and compare them to the baseline calibrated hydrograph for each of three hydrological models. The average from the CGCM3.1 results are also included in the figures in order to provide reference for the climate change impact figures introduced for each climate scenario and future time horizon earlier in the chapter (Figure 49 through Figure 54).
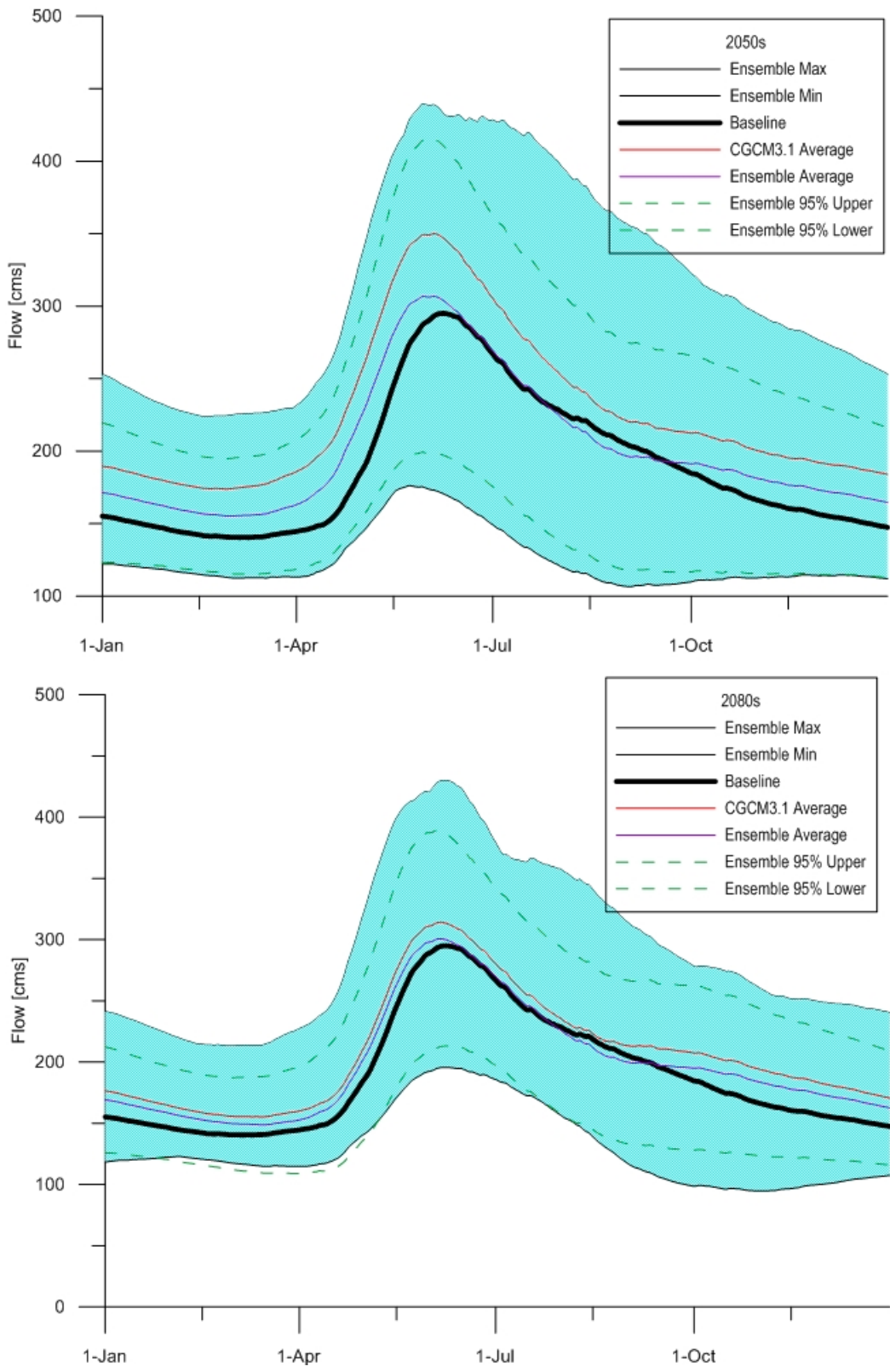
Figure 56: WATFLOOD future flow envelopes
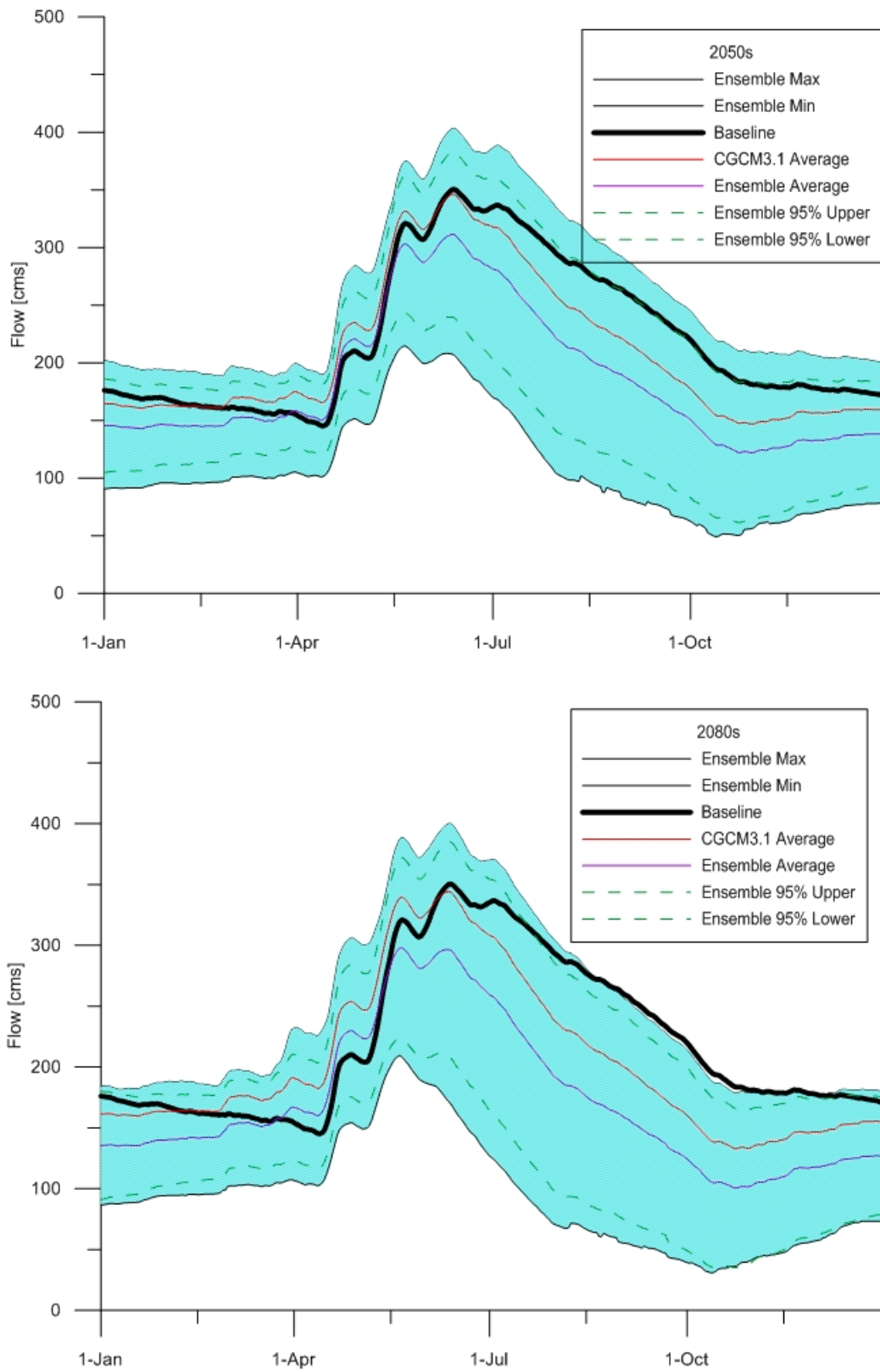
Figure 57: HBV-EC future flow envelopes
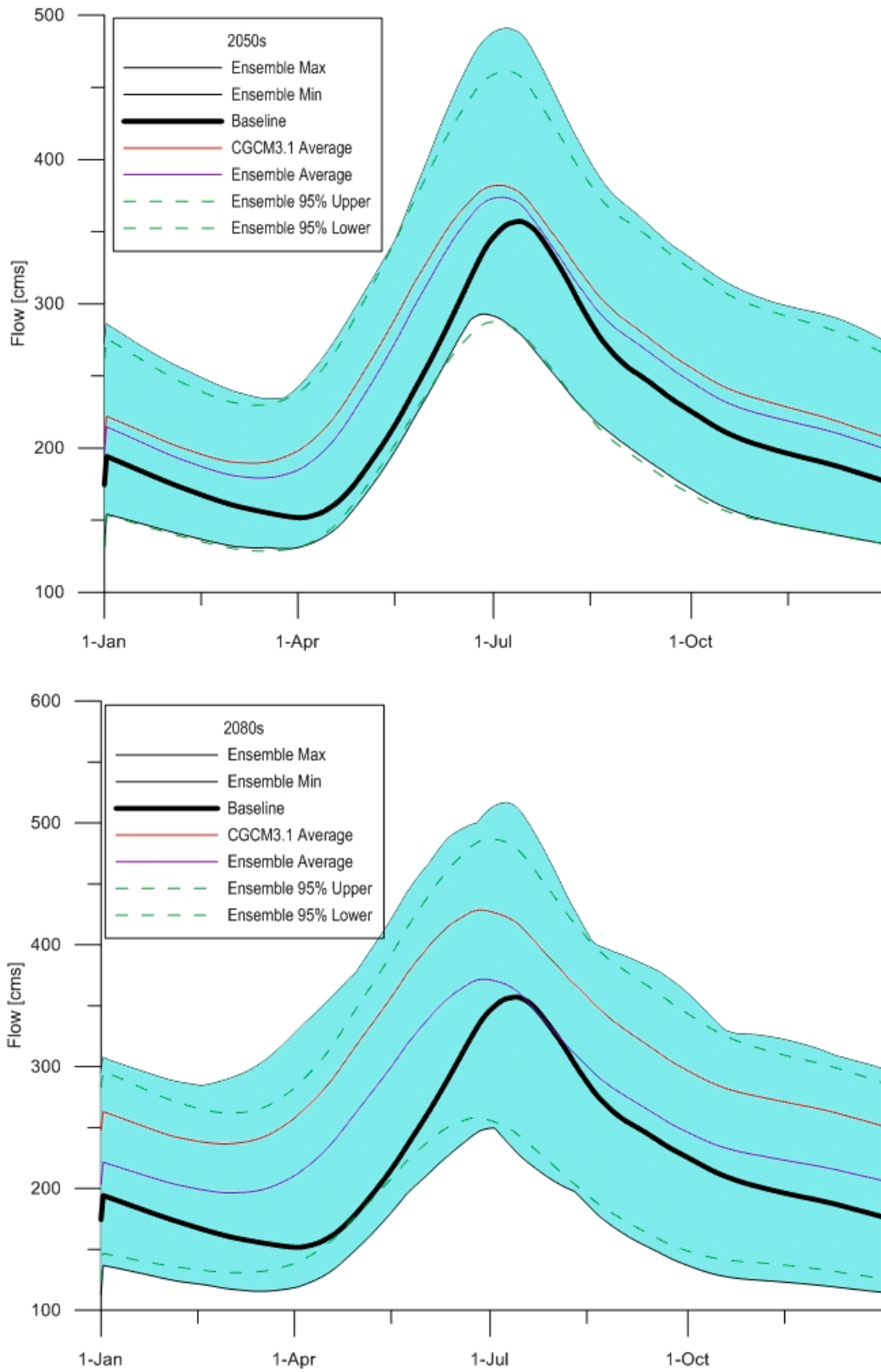
Figure 58: HMETS future flow envelopes

These envelope curves show the variation present in the results from the different GCMs. For each hydrological model, the CGCM3.1 flow results are higher than those for the overall ensemble, although still well within the 95% confidence interval. As is expected, the range in potential flow is largest during the open water season, and particularly during the spring melt event. The range is much smaller during the winter when flows are lower.

It is difficult to say which model is more suited to simulating hydrological change the Churchill River watershed, as each model was able to achieve a similar level of calibration according to the Nash-Sutcliffe and coefficient of determination performance metrics. If the assumption is made that the model which requires more data will give better results, then more weight should be given to the results from WATFLOOD™. However, because there is not an abundance of data available throughout the basin during the time period used for modelling, it can be argued that a model which uses the smallest amount of data (despite making a significant number of simplifying assumptions) may perhaps be more useful. In the later case, HMETS would have more weight in the overall scheme of the analysis. If a balance is sought between these data requirement extremes, then HBV-EC would be viewed as the optimal model in the study.

In fact, each of the models was included in the analysis due to the fact that they are each so different from each other, both in terms of their conceptual design, as well as the types of studies they have been previously utilised in (e.g. Toth, *et al.*, 2006; Andersson, Samuelsson, & Kjellstrom, 2011; Wetterhall, *et al.*, 2011). The fact that the simulated flows, resulting from similar level of calibration, differ so

163

much illustrates that there is a considerable amount of uncertainty related to the choice of hydrological model on such a large, and data sparse watershed.

It should be noted that the results which were least expected were from the HBV-EC model. Not only do the reductions in flow not agree with the results from the other hydrological models used in the study, they also are in contrast to the results obtained by other researchers in similar watersheds under similar climate change scenarios. Research in the climate change impact assessment area (Barnett, Adam, & Lettenmaier, 2005; Poulin, *et al.*, 2011) has pointed to an increase in the magnitude of the freshet event as well as a shift in the seasonality of the major flow events.

WATFLOOD^{TM} and HMETS each predict an increase in the spring freshet peak and all three of the models show a change in the timing of the spring maximum flow and the date that the annual minimum flow occurs on. Where the models disagree most is in their calculation of the flow volumes during the other, lower flow portions of the year that have very low precipitation and relatively high amounts of evaporation. Each of the models uses a slightly different method to calculate evaporation and several other processes and respond differently to small changes in precipitation and temperature. As a result, while the models give similar results when forced using observed data they do not give the same results under the climate change influenced meteorological data.

6.3 Potential effects on hydroelectric generation potential

After determining the range of impacts which climate change may have on the hydrological regime of the area in the future, the next step is to translate this impact to the potential change in hydroelectric generation potential. This is the direct economic impact that climate change will have on utilities such as Manitoba Hydro, and any future development plans for the river basin in the future. This impact is difficult to directly identify for the Churchill River because the major generating stations which would be affected by changes in streamflow from this basin do not sit directly on the Churchill River. As a result, any potential impact derived from these climatic changes is inherently dependent on several assumptions and encompasses a great deal of uncertainty. It is important to remember in this instance that there are several other river basins which contribute to these stations and they are also being affected by climate change. Effects on these other basins must also be studied and understood.

Each of the hydroelectric generating stations on the Burntwood and Nelson River systems, except for the Long Spruce GS, have some sort of reservoir or forebay system to allow them to retain excess water for a period of time and avoid spilling to maximize generation of electricity. This will be a benefit if future freshet flows do in fact increase, and may result in increases in the amount of electricity generated during late winter and early spring months. This capability to hold back some volume of water will also help the generating stations to save some of the water which arrives during the highest flow periods in the forebay for power production rather than spilling the water over and essentially wasting it.

There is some potential for climate change to affect the electricity requirements for the customers that Manitoba Hydro supplies as well. Increasing temperatures in the winter may reduce heating requirements and higher summer temperatures may increase cooling requirements during the summer. The ability to implement management strategies for the water resources of the area and understand the changes in the timing of major flow events may be the most important consideration in this region as the effects of climate change begin to be felt in this region in the future. Changes in future flows may require changes to the design of existing hydropower and facilities to allow for management of higher or lower volumes. Having less flow during the winter, which is typically the highest demand period of the year in Manitoba, may cause an imbalance in supply and demand in the future.

Chapter 7: Uncertainty Analysis and Discussion

In order to fully understand the impacts of climate change on the hydrology of a watershed, it is important to understand the uncertainty that is associated the streamflow simulation. Many of the elements which are required to formulate a potential future hydrograph have some measure of uncertainty inherent in their results.

There are several steps that must be completed in order to assess and understand the uncertainty related to any measurement or simulation, and the same is true of hydrological modelling and climate change impact assessments (Ellison, Rosslein, & Williams, 2000). The steps followed in this study include 1) identifying the major sources of uncertainty related to the estimation of future flows, 2) quantifying these uncertainties, and 3) comparing and combining the uncertainties to determine the overall uncertainty envelope for the simulation of climate change hydrological impacts. How these steps were carried out for the purposes of this study is explained in the sections which follow.

7.1 Identification of Sources of Uncertainty

There are numerous sources which contribute to the uncertainty related to estimating the impact of climate change within any hydrological basin. The sources which have been identified as the most prolific, based on previous studies, are the greenhouse gas emissions scenario and tendencies of future societies, global climate model structure, downscaling method, and the impact or

hydrological model used (Wilby R. L., 2005; Poulin, *et al.*, 2011). Several researchers have examined the contribution of each of these elements to the overall uncertainty of the hydrological modelling process (Akhtar, Ahmad, & Booij, 2009; Kay, *et al.*, 2009; Ludwig, *et al.*, 2009). The relative importance of each of these and how they were taken into account in this study will be further discussed below.

The greenhouse gas emission scenario provides a significant amount of uncertainty to the results of a study such as this one. The future tendencies of societies existing in the future world are clearly something we cannot possibly know, but can only speculate towards. There are several trends that must be considered and analyzed in order to determine the amount of greenhouse gas emission around the world, and the effects that these emissions will have on the climatic variables being predicted. These include, but are not limited to, the focus of future policies on regional versus global government cooperation, focus of scientific research on development of alternative cleaner energy sources, and the equalization of the world's economy between the richest and the poorest countries (IPCC, 2000). There are several perceivable patterns the future world could follow, and it is impossible to predict for certain which one will manifest itself in the future. It is for this reason that several different future scenarios have been analyzed in this study.

The second source of uncertainty that must be accounted for deals with the structure of the GCM (Kay, *et al.*, 2009; Knutti, *et al.*, 2010). Because each GCM does not model climate in the exact same way, their prediction of the future is

inevitably going to be different. This is partly due to using different methods to predict the different variables, and partly due to imperfect process understanding. In order to evaluate the uncertainty related to the structure of the individual GCMs, delta values from 23 different GCMs were used to simulate the future climate.

Another uncertainty is that associated with choice of downscaling method used to calculate the delta values from the GCM output. Downscaling may be accomplished by using an RCM, which is known as dynamical downscaling, or by some form of statistical downscaling. Statistical downscaling is a method of increasing the resolution of GCM data by deriving statistical relationships between observed variables on a small scale and their counterparts in the GCM on a large scale. This derivation is accomplished using regression analysis, weather typing, or neural network methods (Wilby, Dawson, & Barrow, 2002). Both downscaling methods has their own specific uncertainty associated with them and have been examined in detail in the reference works (Prudhomme & Davies, 2009; Chen, Brissette, & Leconte, 2011).

For this research, future climate data was taken directly from the GCM for the purposes of the climate change impact analysis. As a result there is no uncertainty related to a downscaling method. However, because only one set of delta values was used over the entire Churchill River basin (~250,000 km^2) for each of the GCM runs, there was no consideration of as the impact that basin-scale differences (such as topography, latitude, and land use, for example) may have on the future climate. As a result, one delta value was used for the entire

Churchill basin, and the basin's climate was assumed to change uniformly. Future studies into the impact of climate change on this basin should include projections using both of types of downscaling methods, and a comparison to this analysis from GCM data in order to increase the breadth of the results and determine if downscaling methods are warranted, in this case.

The final source of uncertainty listed in similar studies is the impact or hydrological model used to simulate streamflow in the catchment area (Wilby R. L., 2005). Hydrological models are essential for estimating the impact of climate change on runoff generated within a basin, but uncertainties result because of differing model structures, parameter estimation, an imperfect process understanding or representation within the model, uncertainty contained within forcing data used to drive the model, among others (Beven & Freer, 2001; Kirchener, 2006; Feyen, Kalas, & Vrugt, 2008; Renard, *et al.*, 2010).

In this study, the uncertainty related to hydrological model selection was evaluated in two ways. First, three different hydrological models (WATFLOOD[TM], HBV-EC, and HMETS) were set up, given the same forcing data, and calibrated to achieve a similar degree of statistical correlation to the observed hydrograph. Each of these models was simulated with the same set of climate change delta values. Additionally, to examine the uncertainty related to parameter estimation with the WATFLOOD[TM] hydrological model, several different parameter sets with comparable calibration statistics were used to drive the model using the same climate change delta values, for comparison. The difference between these model setups will help provide valuable information as to the parameter

170

sensitivity of the WATFLOOD^{TM} model in climate change impact assessment studies. WATFLOOD^{TM} was chosen for this portion of the analysis because it has the most complex parameter space and a method was available to generate multiple different comparable parameter sets.

Of course there are other sources of uncertainty within the project that have an effect on the results. One that needs to be considered as potentially contributing a significant amount of uncertainty to the results is the measurement of field data. Hydrometric (flow) measurements have an error range of ±5% in good conditions (i.e., well calibrated stage-discharge relationship, well maintained equipment, good river conditions for flow measurement, etc.) to as much as ±20% when the gauge is in a remote location and is not as well maintained on a regular schedule, the river bed is unstable, and the gauge prone to interference by natural hazards (Harmel, *et al.*, 2006). Additionally, there is uncertainty related to the distribution of point sources of data such as daily temperature and precipitation, as well as soil moisture and snow water equivalent for model initialization. The inverse distance weighting method was used to spatially distribute this point data in WATFLOOD^{TM} while no distribution was required for the other two models as a result of their distribution type. The inverse weighting method is a good approximation, but does introduce a measure of uncertainty and error to the hydrological modelling process as results may not be exact on a point to point basis. It should be noted that this method of data distribution does not consider local-scale heterogenities, such as topographical effects and also has difficulties with events such as convectional storms which occur very

sporadically on a spatial scale. To a lesser extent, there is also some uncertainty related to the measurement of the meteorological forcing data (i.e., actual temperature and precipitation), which is typically reported to be within ±5-15% (Dingman, 2002). This does not have a direct impact on the climate change portion of the study, but would have an effect on the model calibration portion.

7.2 Quantifying Uncertainty

After identifying the sources of uncertainty contributing to the results of the project, the next step is to put a numerical value to each of these. This process will facilitate a more in-depth understanding of the sources of uncertainty, as well as aid in calculation of the combined uncertainty.

In order to identify and quantify the uncertainty related to each component of the modelling system, each of the desired sources of uncertainty (emissions scenario, GCM structure, hydrological model structure, and hydrological model parameterization) was systematically isolated from the rest.

7.2.1   Uncertainty due to emissions scenario selection

The first source of uncertainty isolated was the selection of emissions scenarios. The IPCC has defined many different scenarios for the future emissions of greenhouse gases (IPCC, 2000). The selection of these scenarios in itself was a source of uncertainty due to the fact that none of them will likely match up exactly with what happens in the future. The three scenarios that were chosen identify a best case (B1), a worst case (A2) and a median scenario (A1B) creating an envelope which presumably contains a reasonably large range of possible future

GHG levels and future climates. The following tables (Table 30, Table 31, and Table 32) illustrate the differences in flow results which were found between each of these scenarios, averaged over each hydrological model for average, maximum and minimum flows during the 2050s future time horizon.

Table 30: Average flow results (% change) by emissions scenario for 2050s time horizon

| | Average Flow % change, 2050s | | | |
	B1	A1B	A2	Scenario Average
Average	+2.59	-0.76	-1.24	+0.19
Max	+29.59	+27.19	+33.58	+30.12
Min	-16.13	-33.88	-36.59	-28.86

Table 31: Maximum flow results (% change) by emissions scenario for 2050s time horizon

| | Max Flow % change, 2050s | | | |
	B1	A1B	A2	Scenario Average
Average	+3.97	+1.49	+0.63	+2.03
Max	+31.37	+28.80	+29.33	+29.83
Min	-17.54	-37.33	-39.45	-31.44

Table 32: Minimum flow results (% change) by emissions scenario for 2050s time horizon

| | Min Flow % change, 2050s | | | |
	B1	A1B	A2	Scenario Average
Average	1.29	-1.36	-1.99	-0.69
Max	+26.50	+24.27	26.97	+25.92
Min	-17.99	-33.33	-35.55	-28.96

A first examination of the results for the 2050s (Table 30) shows that each scenario returns similar results. However, small differences do exist between each of the possible future conditions. B1 has the highest average flow of any scenario (by 3.35 % of baseline flow or 7.07 cms), has the smallest decrease in annual minimum flow, and the highest increase to maximum flow. Conversely, A2 shows the most range between the highest and lowest values for each of the average and annual maximum and minimum flows. This is owing to the fact that

the A2 scenario has the largest increase to atmospheric carbon and that each of the GCMs responds differently to these elevated levels.

Overall, the selection of an emissions scenario does have an effect on the hydrological results obtained for the Churchill River basin. The difference between the highest and lowest scenario for average flow was 3.83% of the original (baseline) value (8.08 cms), while the range of the maximum flow changed by 3.36% of the original modelled flow (11.23 cms), and the minimum flow ranged by 3.28% (4.78 cms). Based on the above tables, the A2 scenario displays the largest range in predicted streamflow for each situation, while B1 has the smallest range. However, this is not as representative of the uncertainty related to emissions scenario selection as the average flow values.

A similar analysis was performed on the results for the 2080s future time horizon. The tabulated data is found below (Table 33, Table 34, and Table 35).

Table 33: Average flow results by emissions scenario for 2080s time horizon

	Average Flow % change, 2080s			
	B1	A1B	A2	Scenario Average
Avg. Q	-2.24	-1.91	+1.89	-0.75
Max. Q	+26.35	+27.16	+34.36	+29.29
Min. Q	-28.30	-35.02	-28.30	-30.54

Table 34: Maximum flow results by emissions scenario for 2080s time horizon

	Max Flow % change, 2080s			
	B1	A1B	A2	Scenario Average
Avg. Q	-0.42	-0.09	+4.80	+1.43
Max. Q	+32.66	+33.39	+42.79	+36.28
Min. Q	-28.16	-38.70	-30.38	-32.41

Table 35: Minimum flow results by emissions scenario for 2080s time horizon

	Min Flow % change, 2080s			
	B1	**A1B**	**A2**	**Scenario Average**
Avg. Q	-4.00	-3.91	-0.51	-2.81
Max. Q	+23.19	+23.73	+33.54	+26.82
Min. Q	-29.35	-33.57	-29.91	-30.94

The results of the uncertainty comparison from the 2080s time horizon (Table 33, Table 34, and Table 35) display a different pattern to those from the 2050s. The largest decrease in average flow occurs under the B1 scenario, while the largest increase is actually a result of the pessimistic A2 scenario. The A2 scenario again shows the largest range between the increase of the highest value and the decrease of the minimum value, with B1 displaying less extreme changes over this time period. This means that the increased emissions of the A2 scenario cause increased runoff as a result of higher precipitation increases than the B1 or A1B scenarios. Once again, the large range in results from the A2 scenario is the result of the highest amount of atmospheric carbon and the differing response of each GCM.

Again, it may be observed that the selection of emissions scenarios has an impact on the hydrological results in the Churchill River basin. During the 2080s, the range between the highest and lowest scenarios for average flow was 4.13% (8.71 cms), the difference between the highest and lowest maximum flow prediction was 5.22% (17.45 cms), and the range in minimum flow values was 3.49% (5.09 cms). In general, the B1 scenario actually predicts the lowest flows during this future time period, while the highest volumes are generated under the A2 emissions scenario.

It should be noted that results in this section are an aggregation of the results from all three hydrological models. This allows for the isolation of the uncertainty which is solely related to the selection of the emissions scenario. Uncertainty related to the hydrological model itself will be discussed in later sections.

7.2.2 Uncertainty due to GCM selection

While each of the GCMs used in this exercise were based on the same IPCC reports on future atmospheric condition, they were each set up in different ways, and as a result, gave different results. For each time period and scenario combination, the models provide different interpretations of what may happen climatologically (and eventually hydrologically after the climate variables are used for model forcing) within the basin. The following tables (Table 36, Table 37) illustrate the magnitude of the changes, and differences among GCMs.

Table 36: Comparison of flow (% change) results between GCMs, 2050s

Flow % change, 2050s			
	Average	Max	Min	Std. Dev.
B1				
Average Q	+2.59	+29.59	-16.13	21.23
Max Q	+6.20	+33.81	-17.07	22.91
Min Q	-0.23	+30.69	-24.88	22.48
A1B				
Average Q	-0.76	+27.19	-33.88	23.37
Max Q	+4.21	+31.24	-33.58	25.02
Min Q	-4.61	+29.72	-38.92	27.71
A2				
Average Q	-1.24	+33.58	-36.59	23.75
Max Q	+3.41	+30.05	-34.92	24.55
Min Q	-3.87	+30.31	-38.57	25.54

Upon examining the above results (Table 36), the variability resulting from the selection of a GCM is considerably larger than that from the selection of an emission scenario. The maximum fluctuation in the average flows within one emissions scenario was in excess of 70% of the baseline flow for the A2 storyline. Similar results were seen for each of the other scenarios, with A1B in excess of 60% and B1 over 45% difference between the highest and lowest average flows. Additionally, the fluctuations of the annual maximum and minimum flows were similar in magnitude to those seen for the average flows. During the 2050s future time period, the A2 scenario has the highest atmospheric carbon and is followed in order by A1B and B1. This indicates that the GCMs each treat these changes differently and the resulting hydrological variability is the result.

More information about the distribution of the changes in flow in the 2050s may be seen below (Figure 59). This series of histograms shows that the majority of the GCMs predict a set of future flows that are fairly similar to each other. Each of the sets of averages has outliers, which make it seem as though the datasets have more variability than the majority of the results show. For example, while the range of the B1 scenario is over 35% of the baseline average flow (Table 36), data from 12 GCMs (of 21 total GCMs) predicted that the flow would be between a 10% percent decrease and a 5% increase (Figure 59). Similar scenarios play out for each of the other emissions scenarios and characteristic flows. But, as was discussed earlier, each of the GCM outcomes has an equal likelihood of occurring in the future, and therefore cannot be discounted or discarded any

more than those results that are closer to the multi-GCM mean. These histograms illustrate well how there is a great deal of uncertainty related to the modelling of global future climates. The fact that so many of these widely accepted climate models can generate results with such large variability indicates that there are, similarly, many possibilities for the future hydrological regime. Results from this study therefore can only serve to outline an envelope which is likely to contain the actual future conditions.
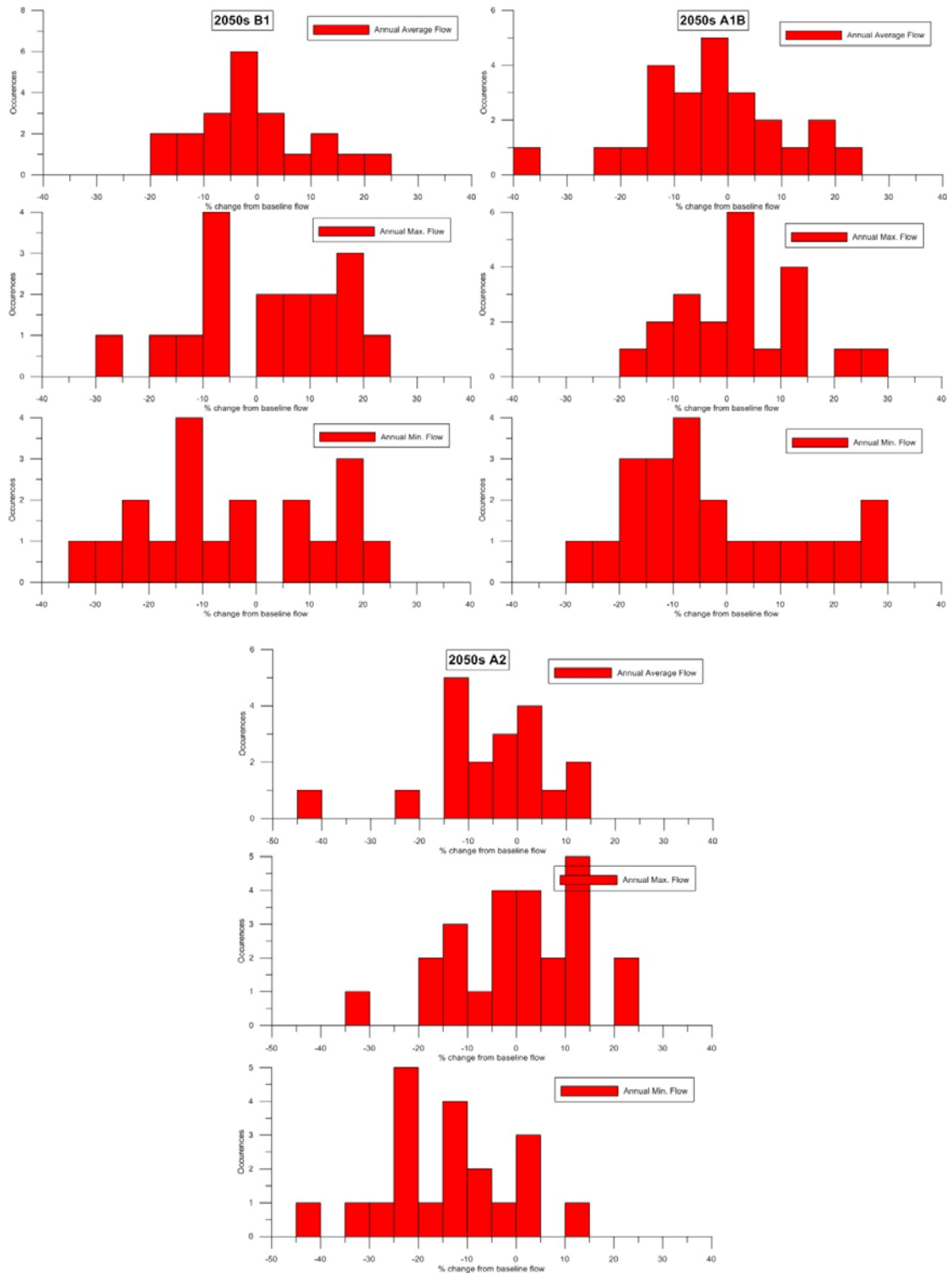
Figure 59: Results distribution by GCM for 2050s future time horizon

The variability by GCM for the 2080s future time horizon was also examined and Table 37 summarizes the statistics from the runs of each of the GCMs during this period. These results are very similar to those from the 2050s, with slight increases in the spread between the highest and lowest values of flow, which are attributed to the increased uncertainty in prediction further into the future.

Table 37: Comparison of flow (% change) change results between GCMs, 2080s

	Flow % change, 2080s			
	Average	Max	Min	Std. Dev.
B1				
Average Q	-2.24	+26.35	-28.30	19.02
Max Q	+2.35	+39.11	-24.45	17.84
Min Q	-5.92	+27.67	-34.01	24.84
A1B				
Average Q	-1.91	+27.16	-35.02	22.80
Max Q	+1.95	+38.36	-34.63	20.39
Min Q	-8.39	+29.92	-38.86	32.23
A2				
Average Q	+1.89	+34.36	-28.30	27.09
Max Q	+6.51	+41.63	-27.55	23.94
Min Q	-3.13	+38.75	-36.51	37.30

In each instance, the difference between the highest and lowest value was slightly larger those seen in the results from the 2050s time period. This is the expected result, however, the distribution of the data points (Figure 60) shows that the spread of the results is actually very similar to those seen in the 2050s (Figure 59), with the same tendency for outliers to exaggerate the extreme ends of the results. As with the results from the earlier section, none of the GCMs can be proven to be better or worse than any other GCM, so each result must be considered with equal weight.
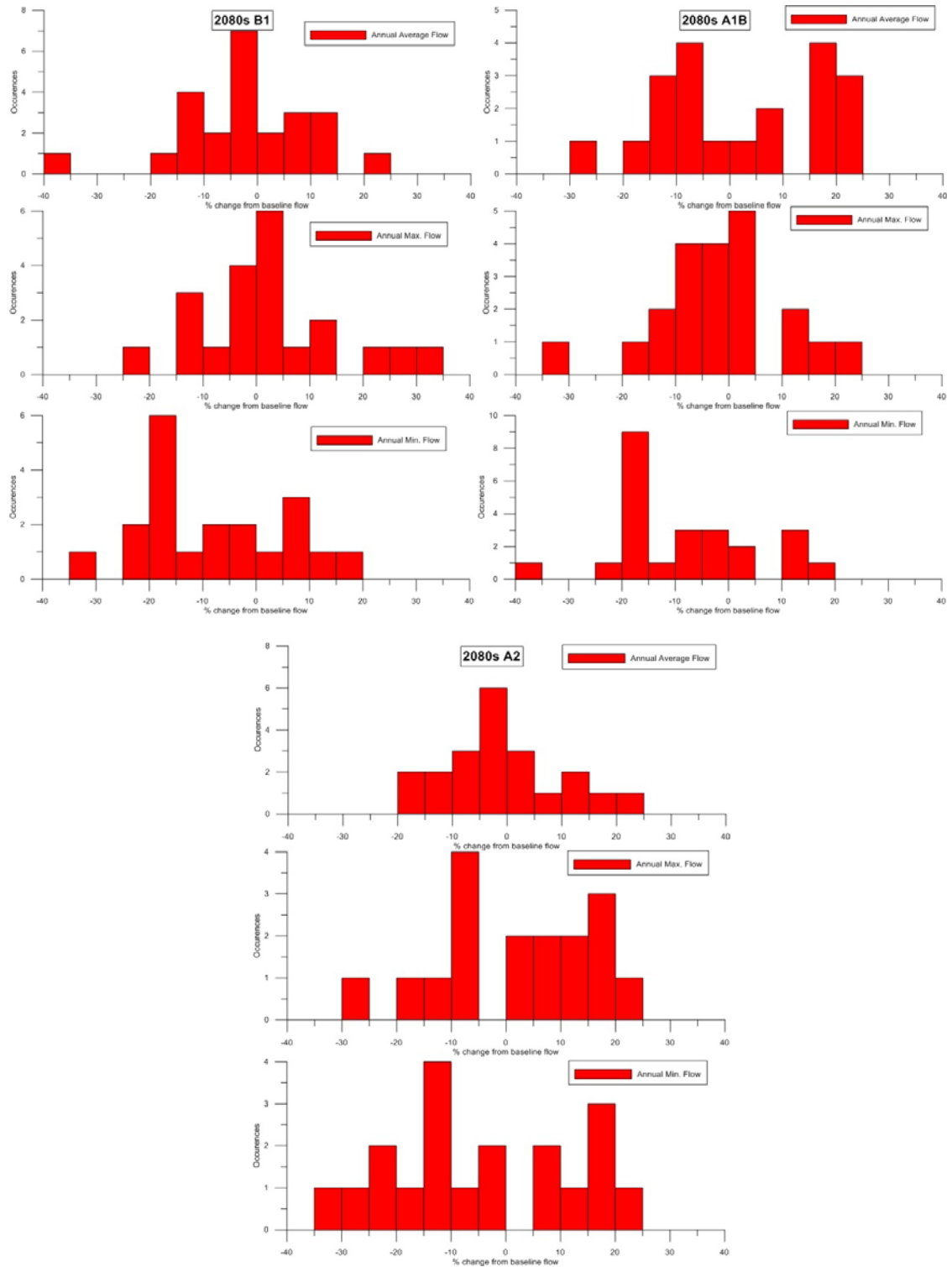
Figure 60: Results distribution by GCM for 2080s future time horizon

Using the same B1 emissions scenario average flow example that was discussed earlier, the range of climate change affected average flows was in excess of 50% of the average baseline flow value (Table 37). The histograms show that flows derived using data from 11 of the 21 GCMs fall between -10% to +5% change from the baseline flow.

In the case of uncertainty related to the selection of a GCM, results show that there is a considerable spread between the extreme ends of the distribution. However, there are outliers that tend to exaggerate this effect. Each of the GCMs were set up and calibrated externally to this project using their own distinct criteria. As a result, the temperature and precipitation fields for the Churchill River basin showed considerable variance from one model to the next for each of the emissions scenarios examined in this project.

7.2.3 Uncertainty due to hydrological model selection

In addition to the two sources of uncertainty already discussed, the selection of a hydrological model can also introduce uncertainty to the estimation of the impact of climate change. By calibrating each of the hydrological models in the study to represent the current conditions which exist in basin, the theory is that the models will be able to predict the flow trends with a certain stationarity of all conditions except for the climate. While the results displayed in chapter 6 show the range of results broken down by hydrological model, the following tables summarize the results from those sections (Table 38 and Table 39), with explanations and discussions to follow.

Table 38: Comparison of average, minimum and maximum flow results by hydrological model for 2050s time horizon

	Average Flow % Change, 2050s			
	WATFLOOD™	HBV-EC	HMETS	Model Average
B1				
Avg	+8.92	-14.47	+13.32	+2.59
Max	+43.61	+7.83	+37.33	+29.59
Min	-10.24	-29.76	-8.38	-16.13
A1B				
Avg	+4.88	-19.97	+12.80	-0.76
Max	+40.10	+2.06	+39.40	+27.19
Min	-25.55	-46.19	-29.90	-33.88
A2				
Avg	+4.29	-19.44	+11.42	-1.24
Max	+59.12	-0.34	+41.96	+33.58
Min	-27.29	-49.80	-32.67	-36.59

In general, for the 2050s time horizon the HBV-EC model predicts much lower flows than either of the HMETS and WATFLOOD™ simulations. The other two models seem to predict very similar results under the effects of climate change, which is consistent with the results displayed and discussed in Chapter 6. In the A2 scenario, the HBV-EC model does not yield a single predicted future hydrograph in which the average flow is higher than the average modelled baseline flow. This is in sharp contrast to the other models, which both predict that the average of the average flow in all simulations is an increase over the average flow modelled for the baseline period. This difference is a result of the different evaporation routines used in the different models and the tendency for HBV-EC to respond more than each of the other models to increased temperatures during the open water season as a result of its elevation banding and evaporation calculation method.

Table 39: Comparison of average, maximum, and minimum flow results by hydrological model for 2080s time horizon

	Average Flow % Change, 2080s			
	WATFLOOD^{TM}	HBV-EC	HMETS	Model Average
B1				
Avg	+5.53	-20.72	+8.47	-2.24
Max	+43.73	+2.77	+32.55	+26.35
Min	-10.99	-46.02	-27.90	-28.30
A1B				
Avg	+4.32	-25.74	+15.69	-1.91
Max	+43.11	-3.51	+41.87	+27.16
Min	-22.63	-52.80	-29.64	-35.02
A2				
Avg	+8.98	-24.86	+21.55	+1.89
Max	+47.54	-3.50	+59.05	+34.36
Min	-13.38	-51.65	-19.87	-28.30

The results from the 2080s show many similarities with the results from the 2050s. WATFLOOD^{TM} and HMETS both predict that, on average, the flows will increase, while the HBV-EC model results indicate that future flows will decrease, on average. The variances between the results from each model are higher in the 2080s than in the 2050s, but not by a large margin when compared to the variability between each of the hydrological models. This increased variability is attributed to the fact that the hydrological models each respond differently to climate change and the magnitude of climate change is larger in general in the 2080s than in the 2050s.

The fact that there is such difference in the results predicted by the three hydrological models used in this study underlines the fact that the selection of hydrological model is important in determining the impact of climate change within a basin. There are many hydrological models available to estimate the flow with varying degrees of complexity. Models should be selected based on

184

their individual characteristics and in accordance with project requirements. Where possible, the use of multiple models to provide a measure of certainty to the results is recommended.

7.2.3 Uncertainty due to hydrological model parameterization

After examining the uncertainty between the results of several hydrological models, it was determined that an investigation of the uncertainty related to the parameterization of a model was also in order. For this portion of the exercise, only the WATFLOOD^{TM} model was used because of its automatic calibration routine and large number of parameters which allow for a large number of reasonable, useable parameter sets. Each of these "reasonable" parameter sets were able to estimate the flow with a similar statistical outcome to the optimal parameter set used throughout the study.

There are many ways in which a parameter uncertainty may be conducted. Previous similar studies have used a Bayesian Monte-Carlo approach (Thyer, *et al.*, 2009), a Latin hypercube sampling (LHS) methodology (van Griensven, *et al.*, 2006) or the GLUE technique (Beven & Binley, 1992). Each of these methods involves sampling a range of parameters and evaluating model performance based on a certain criteria. Each of these methods is useful in their own way for both model calibration and parameter uncertainty estimation. The problem with these methods is that they are very time consuming considering the computation time of the WATFLOOD^{TM} Churchill River model and the large number of parameters to consider. The sheer number of simulations required made these methods unreasonable for this project.

185

The preferable parameter uncertainty estimation technique for implementation in this project was related to the DDS algorithm which was used to calibrate the model originally. The DDS-AU, or dynamically downscaled search, approximation of uncertainty method (Tolson & Shoemaker, 2008) is able to identify multiple acceptable parameter sets given a set of parameter bounds and an initial guess as to what that parameter might be. This methodology may be summed up as generating a number of different parameter sets and evaluating the model for each. The user defines a criteria which each of the parameter sets is compared to. The parameter set is identified as acceptable or behavioural if it meets this criterion and is discarded if it does not. The user specifies the number of acceptable parameter sets to generate. The program uses the same dynamically dimensioned search to determine which parameters should be adjusted and by how much.

It was not possible to utilise the DDS-AU algorithm as the algorithm was not made available for use in time for completion of this study. Instead, the most sensitive parameters in the model were determined using a manual calibration scheme. The DDS algorithm was used extensively to calibrate the seven most sensitive parameters in each of the six regions of the basin (for a total of 42 degrees of freedom in calibrating the model). The parameters chosen were ak (infiltration coefficient for bare ground), akfs (infiltration coefficient for snow covered ground), rec (interflow coefficient), r3 (overland flow roughness coefficient for bare ground), flz (lower zone flow coefficient), pwr (lower zone flow exponent), and r2n (Manning's n for channel flow). After the algorithm was

allowed to run for in excess of 1650 iterations, the results were sorted based on the value of the objective function returned. The 110 best performing sets of parameters were forced with the climate change values from one of the GCMs which had a sufficient number of model runs for each of the future scenarios (the CCCMA CGCM3.1 was used). The results from each of these parameterizations were compared and analyzed in order to determine the magnitude of uncertainty due to model parameterization in the climate change impact assessment. Figure 61 shows the annual average flow of the "best" parameter set against the 110th best parameter set, which was statistically the worst parameter set used in this exercise.
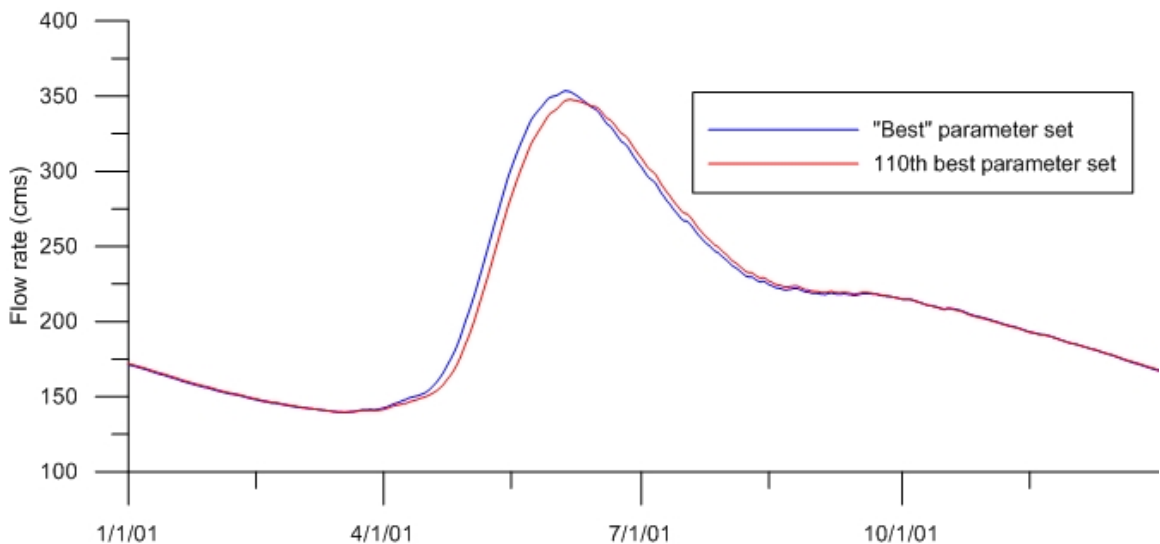
Figure 61: Comparison of the "best" and 110th best parameter sets annual average hydrograph

As the above plot of annual average flows from 1979-1995 shows, there is very little deviation between the best and worst parameter sets used. The two time series actually have a Nash-Sutcliffe efficiency coefficient between each other which exceeds 0.99. This indicates that the parameter sets used in this portion

of the exercise are each simulating the flow conditions in the basin with similar precision. Table 40 summarizes the analysis completed using all 110 parameter sets for the 2050s future time horizon. The complete set of parameters used for this portion of the project may be found in Appendix E.

Table 40: Simulated flow results (cms) from parameter uncertainty study for 2050s time horizon

	'Best'	Average	Max	Min	Std. Dev.	95% CI	
						Statistics from 110 parameterizations, 2050s (cms)	
B1							
Avg. Q	265.03	265.48	269.43	261.74	1.28	262.96	268.00
Max. Q	428.03	433.73	456.86	416.60	8.22	417.62	449.84
Min. Q	192.19	192.69	196.13	189.90	0.97	190.78	194.60
A1B							
Avg. Q	266.53	267.12	271.23	263.36	1.32	264.54	269.70
Max. Q	443.14	447.14	467.62	430.97	6.65	434.12	460.17
Min. Q	192.65	193.31	196.78	190.15	1.10	191.15	195.48
A2							
Avg. Q	228.70	229.19	233.65	225.63	1.23	226.79	231.59
Max. Q	377.01	381.59	401.98	365.29	6.71	368.43	394.74
Min. Q	162.85	163.28	166.40	160.91	0.81	161.70	164.86

Based on these results, it is evident that the parameterizations used in this study do not have as much effect on the variability of the results of climate change as some of the other sources of uncertainty considered in this study. The maximum flow seen in each of the simulations tends to show the most variation, while the average and minimum flows generally have less variation. This may be caused by the sensitivity of the snowmelt parameters, or may be the result of the sheer magnitude of the snowmelt-induced freshet flow. The average and minimum flows are governed by parameters that are less sensitive to small perturbations and as a result they do not change as significantly as the maximum yearly flow. The final column shows the 95% confidence interval for each of the flow

characteristics which were calculated in order to give an idea as to the general distribution of the results. The following table shows these very same results for the 2080s future time horizon (Table 41).

Table 41: Results from parameter uncertainty study for 2080s time horizon

	'Best'	Average	Max	Min	Std. Dev.	95% CI	
			Statistics from 110 parameterizations, 2080s (cms)				
B1							
Avg. Q	263.47	263.98	268.36	260.06	1.30	261.44	266.52
Max. Q	429.80	434.63	452.66	417.16	7.12	420.67	448.59
Min. Q	200.40	200.69	203.77	197.98	0.73	199.26	202.11
A1B							
Avg. Q	287.96	288.44	292.87	284.16	1.37	285.76	291.12
Max. Q	458.72	463.08	483.01	445.40	6.97	449.42	476.74
Min. Q	226.28	226.48	229.70	224.19	0.74	225.02	227.94
A2							
Avg. Q	260.15	260.65	264.85	256.93	1.28	258.14	263.16
Max. Q	436.79	441.38	463.00	422.02	7.78	426.12	456.63
Min. Q	184.97	185.48	188.76	182.57	0.93	183.65	187.31

Once again, the results from the 2080s mirror those of the 2050s very closely. The maximum variation is seen in the maximum annual flows, while the annual average and minimums tend to be less sensitive to changes in the parameters. In general it appears that the "best" parameter set which was used for the other portions of the projects slightly under predicts the future flows when compared to the average of the 110 parameter sets. However, in each case the results from this "best" parameter set fall well within the 95% confidence interval based on all of the simulations conducted for this study. This results from this portion of the study show that the parameter set used in the hydrological model does not have a large effect on the results. However, this may not be the case if the DDS-AU

algorithm was implemented fully and this effect must be examined in future studies.

The use of the DDS algorithm has several limitations in this case. The algorithm is always generally converging to a solution. The inability to start with different seed values of the optimization parameters means that the parameter sets used may be too similar to give a true indication of the uncertainty related to model parameterization. However, to remedy this would have required many more model simulations which would have resulted in massive delays on the order of months.

7.3 Comparison and combination of uncertainty

Based on this examination of the major sources of uncertainty in the estimation of the impact of climate change on the hydrology of the Churchill River basin, each of the sources contribute differently to the overall result. For instance, it is clear that the choice of GCM contributes more uncertainty than the choice of hydrological model, which in turn contributes more than the choice of emissions scenario, based on the ranges in the results from each of the respective uncertainty sources. This indicates that the largest source of uncertainty isolated here was actually derived from a modelling process which is completely external to this project.

The choice of hydrological model had more impact than the choice of parameterization, at least as shown by the range of parameterizations for the WATFLOOD^{TM} model. It is worth noting that the WATFLOOD^{TM} and HMETS

models provide results that closely mirror each other, while the HBV-EC model results show some similar trends but in general do not agree with the other two models. It is possible that this disparity in the results is due to the fact that the HBV-EC model was developed for modelling the hydrology of small mountainous catchments that have high levels of relief. It is thought that the Churchill basin is the largest application of this model to date, and the effects of climate change on a small mountainous basin are likely different than those in a large, flat, inland basin like the Churchill. As a result, this difference in results between hydrological models is not a complete surprise.

Each of the sources of uncertainty addressed in this thesis is necessary in order to estimate the impact of climate change. The effect of combining the uncertainties can be best seen in the plots and tables of the results from Section 6.2 (Figure 56, Figure 57, and Figure 58). These envelopes indicate that there is a great deal of information that is not known about climate change impacts on hydrological regimes, at least with certainty. Models are only representations of reality, and while the amount of uncertainty may seem to be too excessive, the reality is that some information is better than having no information about future flows.

7.4 Discussion on climate change results and uncertainty analysis

After examining all of the outputs generated by the models used in this project, there are several trends to note. First is that the impact of climate change is highly dependent on a number of factors that cannot yet, in present day, be

determined with certainty. The future emissions scenarios discussed in this study will not be realized if the global community does not make an active effort to reduce impacts on the environment. The results provided in this study serve to predict what could happen to hydrological regimes of northern regions under an assumed set of global circumstances.

The overall results of the modelling exercise indicate that there is a general increase in the amount of runoff which is produced within the basin into future time periods. This trend is especially clear if the results from the HBV-EC model are negated given it was only that one hydrological model that tended to predict lower flow rates under climate change. That said, one model differing in a suite of three could also be significant, which is why it has been included in the overall future streamflow predictive envelope. Each of the models also project that the timing of peak flow events will be advanced, occurring earlier in the spring (or even late winter); while the timing of the minimum flow events will also change, earlier in some cases and shifted to late summer from late winter in others. Understanding these changes timing will allow for better management of the water resources available to the utilities and other stakeholders.

The trends from the 2050s future time horizon (2040-2069) hydrographs are not significantly different than those generated for the 2080s future time horizon (2070-2099). The width of the uncertainty envelope is slightly increased in the later period due to the increased uncertainty of predicting 30 years further into the future (Figure 56, Figure 57, and Figure 58). The average changes in flow

that occur during the two time periods are similar, with slight variations depending on the emissions scenario and the hydrological model used.

Throughout the course of the uncertainty assessment, it became clear that the largest source of uncertainty was the choice of GCM. The range in average flows predicted by the climate models was as high as 70% of the baseline flow. Each of the climate models used were set up and calibrated differently, therefore their output for temperature and precipitation in the Churchill River basin differed. These outputs in turn caused a variety of different effects in the estimation of the hydrological impact resulting from climate change.

The second largest source of uncertainty was the choice of hydrological model. The range in average flows predicted by each of the hydrological models was up to 45% of the baseline. The models which were chosen are each very different in the way they simulate the hydrology of the drainage basin. Interestingly, the simplest model (HMETS) and the most sophisticated model (WATFLOOD^{TM}) produced similar results, while the HBV-EC model produced a set of results that were different from the other models. It should be recognized however that the sample size here is quite small, and by no means encompasses the entire realm of hydrological models (even though it encompasses the range in complexity of models). HBV-EC is a semi-distributed hydrological model which is conceptual in nature and has been successfully implemented in many small scale mountainous drainage basins. The Churchill River basin is believed to be the largest basin for which the model has ever been set up which introduces an additional measure of uncertainty in its own right, not to mention that it was developed for use in

mountainous regions and has not been extensively used in lower-relief terrain or in large scale basins such as the Churchill.

Other sources of uncertainty examined and found to have an effect on the results of the climate change impact study include the emissions scenario (as much as 4.38%) and parameterization of the WATFLOOD^{TM} hydrological model (approximately 9% of baseline flow). Parameterization was found to have less impact on the simulated flow results obtained, at least in the case of WATFLOOD^{TM}. This result will allow future climate change impact studies to concentrate efforts on the studying the most appropriate and significant contributing factors.

In order to understand the most likely impact to the Churchill River basin flow regime, the results in this report were averaged. This encompasses the different approaches and techniques used in each of the contributing sources of uncertainty, and the result is a change in the amount of flow in the entire basin. The envelope which contains the entire range of the results provides the best indication of the potential range of impacts of climate change. This wide envelope curve will allow resource managers to be ready for many possibilities in the future. It should be noted that the results reported here are unique to this study and the models (hydrological and climate) that were chosen. Results could potentially look different under another set of circumstances.

Chapter 8: Conclusions

The following sections serve to summarize the findings of the research completed for this project. The importance of these findings, along with their potential impact is also discussed. Finally, based on the knowledge gained during this study, some recommendations for future study are made.

8.1 Summary of Conclusions

Throughout the course of this study, several key conclusions have been drawn based on experience and knowledge gained. These conclusions come from each of the phases of the project and are as follows:

- Modelling large data sparse regions such as the Churchill River basin is difficult, but possible. Three hydrological models of varying complexity were successfully set up and calibrated to achieve similar statistical levels of calibration;

- The results of the climate change impact assessment show at least a small increase in the amount of flow expected, on average, for both the 2050s and 2080s future time horizons;

- The timing of major flow events is also expected to change. The majority of simulations saw an advance of the timing of the spring freshet peak to earlier in the year; and a shift in the timing of minimum flow events, with the result dependent on which hydrological model was used;

- After performing an uncertainty analysis, it was found that the largest source of uncertainty is the choice of which GCM is used (as much as 70% of average baseline flow). This was followed, in order, by the choice of hydrological model (up to 34% of average flow) and the choice of emissions scenario (as much as 5.2% of average flow); and

- The impact of hydrological model parameterization was examined using WATFLOOD^{TM} and was found to be minimal compared to the other sources of uncertainty (accounting for approximately 4% of average flow). The parameters examined caused more uncertainty in the maximum (peak) flow events than in the average and minimum flow events.

8.2 Significance of Findings

The conclusions drawn from this project are significant for several reasons. The first is that by setting up multiple hydrological models which are each calibrated to the hydrological regime of the Churchill River basin, it has been proven that models of varying complexity may be used to simulate the hydrology of large, data sparse drainage basins. However, the experience gained during this project suggests that a full understanding of the processes within these basins requires more data than is currently available. Additional meteorological and hydrological data, especially in the northern portions of the basin, would facilitate the process of hydrological modelling significantly. A more complete understanding of the current conditions will allow for a more informed estimation of the impacts of climate change within the basin.

The results of the climate change portion of the study suggest that there will be changes to the hydrological regime of the area within the next 100 years, perhaps even sooner. The changes in both the magnitude and timing of the flow events in the basin will require water resource managers who rely on the Churchill River to gain an understanding of the direct relationship between weather and hydrology, ideally using models to facilitate this understanding. If adaptation measures for current hydroelectric developments are researched and implemented, most changes predicted for the Churchill River's hydrological regime should be beneficial to utilities.

The uncertainty assessment portion of this study also brings forward some important information. By identifying the most significant contributor of uncertainty to the climate change impact assessment process, a greater understanding of the error sources in climate change impact assessments has been gained. Using this understanding of the sources of uncertainty, future studies using a similar methodology can better isolate and quantify the most influential factors. Additionally, these studies will be able to draw more informed conclusions based on a better understanding of the uncertainty of climate change, and presumably because they can ground truth some of the results being predicted today.

8.3 Potential Future Research Initiatives

In addition to the conclusions drawn in this study, this project has resulted in several opportunities for further research. These opportunities include:

- Examining the impact of land use changes on hydrology. This study only examines the impact of adjusting inputs (i.e., meteorological data) and assumes that all else in the models was stationary. This includes landcover and model parameterization. Examining the impact of changes, such as the increased occurrence of forest fires, or the increase in the amount of urban area as a result of population increases, on such large time scales will allow water resource managers to develop an even more complete understanding of the impact changes in the climate will have on hydrology.

- The inclusion of more high quality, continuous data will allow for a better analysis of the hydrology of the Churchill River basin. Because of the sparse resolution of meteorological data for model calibration, it was very difficult to set up and accurately parameterize the hydrological models. Products such as the Canadian Precipitation Analysis (CaPA) gridded precipitation data network can provide much higher resolution input data for model calibration, thereby reducing error and uncertainty in model parameterization and setup. An example of the results using the CaPA dataset compared to the hydrograph calculated using the observed meteorological data is shown below (Figure 62).
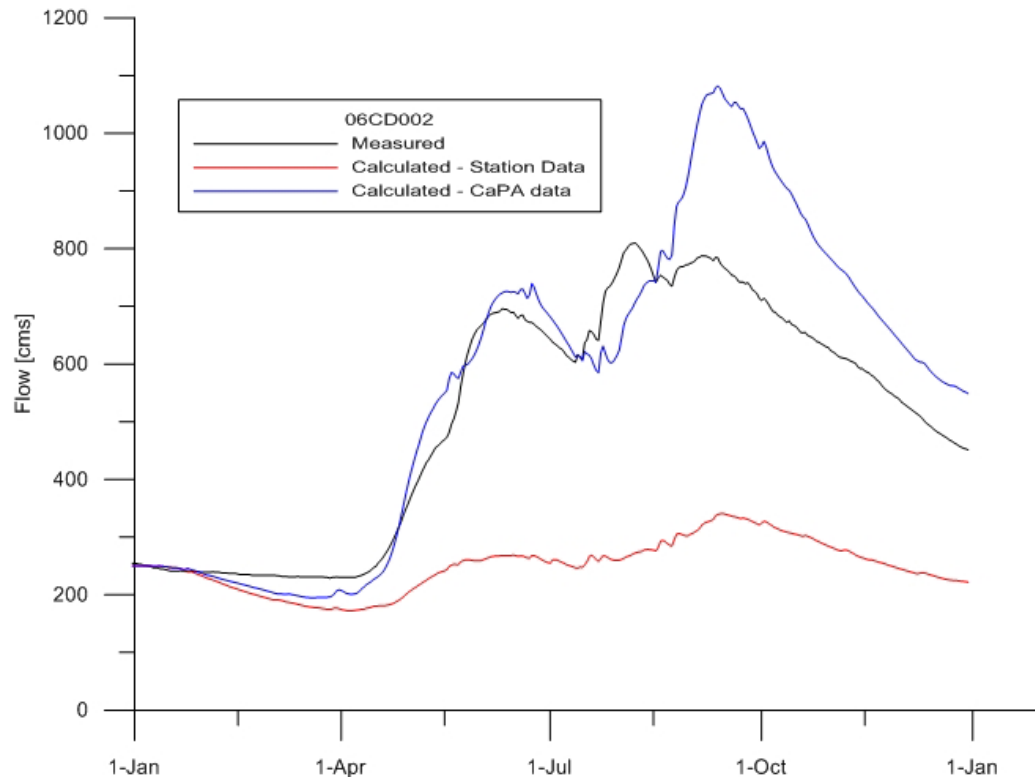
Figure 62: CaPA to CDCD flow comparison at gauge 06CD002 for 2005

The above hydrograph (Figure 62) shows that the model forced by the CaPA data is able to predict the flow in the Churchill River basin for the year 2005 much more accurately than the observed station data. Nash-Sutcliffe correlation values improved from -1.25 for the observed station data to 0.66 for the run using the CaPA dataset. This is just one example of the results obtained using this type of reanalysis data. Products such as this can be extremely useful in filling in the gaps that exist in traditional field station-based monitoring networks, both spatially and temporally. The resulting impact on the accuracy of simulated hydrographs can be significant, presuming the model is well calibrated and not calibrated to compensate for errors in input data.

- Setting up additional hydrological models to further confirm the results obtained by this study. The addition of more models, especially another semi-physically based, data intensive hydrological models could serve to provide more information on the uncertainty due to model choice, and the effect this has on the predicted hydrological envelope. Because all of the models used in this project did not respond in a similar manner, the addition of more models may potentially decrease the amount of uncertainty related to the choice of a hydrological model, and in turn the overall uncertainty related to the estimation of the impacts of climate change.

- Additionally, the use of smaller scale RCMs and statistical downscaling methods to estimate the impact of climate change could also assist in reducing uncertainty in the simulations.

- Finally, using a modified version of the delta method to adjust the variability of precipitation in the future is one way to address the problem of climate stationarity inherent in the delta method. Future studies of this type should consider implementing such a method.

Bibliography

Akhtar, M., Ahmad, N., & Booij, M. (2009). Use of regional climate model simulations as input for hydrological models in the Hindukush-Karakorum-Himalaya region. *Hydrology and Earth System Sciences, 13*, 1075-1089.

Andersson, L., Samuelsson, P., & Kjellstrom, E. (2011). Assessment of climate change impacto on water resources in the Pungwe river basin. *Tellus Series A - Dynamic Meteorology and Oceanography, 63*(1), 138-157.

Arora, V. (2001). Streamflow simulations for continental-scale river basins in a global atmospheric general circulation model. *Advances in Water Resources, 24*, 775-791.

Atlas of Canada. (1985). *Canada Drainage Basins.* Retrieved July 12, 2011, from Atlas of Canada: http://atlas.nrcan.gc.ca/site/english/maps/archives/5thedition/environment/water/mcr4055?maxwidth=1600&maxheight=1400&mode=navigator&upperleftx=0&upperlefty=0&lowerrightx=5136&lowerrighty=4528&mag=0.0625

Axworthy, L., Carr, J., J, D., Duguid, T., Hamblin, C., Hancharyk, M., . . . Spence, M. (2001). *Manitoba and Climate Change: Investing in our future. Report of the Manitoba Climate Change Taskforce.* Winnipeg: Manitoba Wildlands.

Bae, D.-H., Jung, I.-W., & Lettenmaier, D. P. (2011). Hydrologic uncertainties in climate change from IPCC AR4 GCM simulations for the Chungju Basin, Korea. *Journal of Hydrology, 401*(1-2), 90-105.

Barnett, T., Adam, J., & Lettenmaier, D. (2005, November 17). Potential impacts of a warming climate on water availability in snow-dominated regions. *Nature, 438*, 303-309.

Beriault, A. L., & Sauchyn, D. J. (2006). Tree-Ring Reconstructions of Streamflow in the Churchill River Basin, Northern Saskatchewan. *Canadian Water Resources Journal, 31*(4), 249-262.

Beven, K., & Binley, A. (1992). The future of distributed models: Model calibration and uncertainty prediction. *Hydrological Processes, 6*(3), 279-298.

Beven, K., & Freer, J. (2001). Equifinality, data assimilation, and uncertainty estimation in mechanistic modelling of clomplex environmental systems using the GLUE methodology. *Journal of Hydrology, 249*(1-4), 11-29.

Bloschl, G., & Montanari, A. (2010). Climate change impacts - throwing the dice? *Hydrological Processes, 24*(3), 374-381.

Bring, A., & Destouni, G. (2011). Relevance of hydro-climatic change projection and monitoring for assessment of water cycle changes in the Arctic. *A Journal of the Human Environment, 40*(4), 361-369.

Brissette, F. (2010). *Hydrology model Ecole de Technologie Superieure, User Manual.* Montreal, Quebec: Ecole de Technologie Superieure.

Canadian Hydraulics Centre. (2010). *Green Kenue Reference Manual.* Ottawa, Ontario: National Research Council.

Chen, J., Brissette, F. P., & Leconte, R. (2011). Uncertainty of downscaling method in quantifying the impact of climate change on hydrology. *Journal of Hydrology, 401*(3-4), 190-202.

Chen, J., Brissette, F. P., Poulin, A., & Leconte, R. (2011). Overall uncertainty study of the hydrological impacts of climate change for a Canadian watershed. *Water Resources Research, 47*, doi:10.1029/2011WR010602.

Chiew, F., Teng, J., Vaze, J., Post, D., Peraud, J., Kirono, D., & Viney, N. (2009). Estimating climate change impact on runoff across southeast Australia: Method, results, and implications of the modeling method. *Water Resources Research, 45*, doi:10.1029/2008WR007338.

Dingman, S. L. (2002). *Physical Hydrology.* Long Grove, Illinois: Waveland Press, Inc.

Dredge, L. *Photos 2001-116 and 2001-136.* Natural Resources Canada, courtesy the Geological Survey of Canada. Retrieved July 2, 2011

Ecological Stratification Working Group. (1995). *A National Ecological Framework for Canada.* Ottawa/Hull: Agriculture and Agri-Food Canada, Research Branch, Centre for Land and Biological Resources Research and Environment Canada, State of the Environment Directorate, Ecozone Analysis Branch.

Edwards, T. W., Birks, S. J., Luckman, B. H., & MacDonald, G. M. (2008). Climatic and hydrologic variability during the past millenium in the eastern Rocky Mountains and northern Great Plains of western Canada. *Quaternary Research, 70*(2), 188-197.

Ellison, S. L., Rosslein, M., & Williams, A. (2000). *Quantifying uncertainty in analytical measurement.* Eurachem/CITAC.

Feyen, L., Kalas, M., & Vrugt, J. A. (2008). Semi-distributed parameter optimization and uncertainty assessment for large-scale streamflow simulation using global optimization. *Hydrological Sciences, 53*(2), 293-308.

Flato, G., Boer, G., Lee, W., McFarlane, N., Ramsden, D., Reader, M., & Weaver, A. (2000). The Canadian Centre for Climate Modelling and Analysis global coupled model and its climate. *Climate Dynamics, 16*, 451-467.

GeoBase. (2000). *Canadian Digital Elevation Data.* Retrieved July 14, 2011, from Government of Canada, Natural Resources Canada, Earth Sciences Sector, Centre for Topographic Information: http://www.geobase.ca/geobase/en/browse.do?produit=cded&decoupage=250k&map=canada

Geobase. (2011, January 7). *Land Cover of Canada.* Retrieved July 14, 2011, from Government of Canada, Natural Resources Canada: http://www.geobase.ca/geobase/en/browse.do?produit=csc2000v&decoupage=250k&map=canada

Government of Canada, Natural Resources Canada. (1995). *Land Cover of Canada.* Retrieved July 14, 2011, from The Atlas of Canada: http://atlas.nrcan.gc.ca/site/english/maps/environment/land/landcover

Government of Canada, Natural Resources Canada, Earth Sciences Sector, Centre for Topographic Information. (2000). *Canadian Digital Elevation Data.* Retrieved July 14, 2011, from GeoBase: http://www.geobase.ca/geobase/en/browse.do?produit=cded&decoupage=250k&map=canada

Graham, L. P., Andreasson, J., & Carlsson, B. (2007). Assessing climate change impacts on hydrology from an ensemble of regional climate models, model scales and linking methods – a case study on the Lule River basin. *Climatic Change, 81*, 293-307.

Harmel, R., Cooper, R., Slade, R., Haney, R., & Arnold, J. (2006). Cumulative uncertainty in measured streamflow and water quality data for small watersheds. *American Society of Agricultural and Biological Engineers, 49*(3), 689-701.

Hryciuk, D. (2010). *Photos by David Cure-Hryciuk.* Retrieved May 17, 2011, from Panoramio:

http://v5.cache5.c.bigcache.googleapis.com/static.panoramio.com/photos/original/35812012.jpg?redirect_counter=1

Hryciuk, D. (2010). *Photos by David Cure-Hryciuk.* Retrieved May 17, 2011, from Panoramio:
http://v3.cache1.c.bigcache.googleapis.com/static.panoramio.com/photos/original/49876412.jpg?redirect_counter=1

Hutchinson, M. F., McKenney, D. W., Lawrence, K., Pedlar, J. H., Hokinson, R. F., Milewska, E., & Papadol, P. (2009). Development and Testing of Canada-Wide Interpolated Spatial Models of Daily Minimum–Maximum Temperature and Precipitation for 1961–2003. *American Meteorological Society, 48*(4), 725-741.

IPCC. (1990). *Climate Change: The IPCC Scientific Assessment.* Cambridge, UK and New York, NY, USA: Cambridge University Press.

IPCC. (1996). *IPCC Second Assessment: Climate Change 1995.* Cambridge, UK and New York, NY, USA: Cambridge University Press.

IPCC. (2000). *Special Report on Emissions Scenarios: Summary for Policy Makers.* Retrieved July 15, 2011, from http://www.ipcc.ch/pdf/special-reports/spm/sres-en.pdf

IPCC. (2001). *Climate Change 2001: The Scientific Basis.* Retrieved August 3, 2011, from http://www.grida.no/climate/ipcc_tar/wg1/index.htm

IPCC. (2001). *Third Assessment Report of the Intergovernmental Panel on Climate Change.* Cambridge, UK and New York, NY, USA: Cambridge University Press.

IPCC. (2007). *Fourth Assessment Report of the Intergovernmental Panel on Climate Change.* Cambridge UK and New York, NY, USA: Cambridge Unviersity Press.

Kavetski, D., Kuczera, G., & Franks, S. W. (2006). Calibration of conceptual hydrological models revisited: 1. Overcoming numerical artefacts. *Journal of Hydrology, 320*(1-2), 173-186.

Kay, A., Davies, H., Bell, V., & Jones, R. (2009). Comparison of uncertainty sources for climate change impacts: flood frequency in England. *Climatic Change, 92*(1-2), 41-63.

Kirchener, J. W. (2006). Getting the right answers for the the right reasons: Linking measurements, analyes, and models to advance the science of hydrology. *Water Resources Research, 42*, doi:10.1029/2005WR004362.

Kling, H., Fuchs, M., & Paulin, M. (2012). Runoff conditions in the upper Danube basin under an ensemble of climate change scenarios. *Journal of Hydrology, 424*, 264-277.

Knutti, R., Furrer, R., Tebaldi, C., Cermak, J., & Meehl, G. A. (2010). Challenges in combining projections from multiple climate models. *American Meteorological Society, 23*(10), 2739-2758.

Kouwen, N. (2011). WATFLOOD/WATROUTE Hydrological model routing & flow forecasting system. Waterloo, Ontario, Canada: University of Waterloo.

Le Treut, H., Somerville, R., Cubasch, U., Ding, Y., Mauritzen, C., Makssit, A., . . . Prather, M. (2007). Historical Overview of Climate Change. In S. Solomon, D. Qin, M. Manning, Z. Chen, M. Marquis, K. B. Averyt, . . . H. L. Miller (Eds.), *Climate Change 2007: The Physical Science Basis. Contribution of Working Group I to the Fourth Assessment Report of the Intergovernmental Panel on Climate Change.* Cambridge, United Kingdom and New York, NY, USA: Cambridge University Press.

Leconte, R. (2007). *Rapport d'étape – subvention de recherche et développement coopérative (RDC) - Impact of climate change in Canadian river basins and adaptation strategies for the hydropower industry.* Montreal, QC: École de technologie supérieure.

Lindstrom, G., Johansson, B., Persson, M., Gardelin, M., & Bergstrom, S. (1997). Development and test of the distributed HBV-96 hydrological model. *Journal of Hydrology, 201*(1-4), 272-288.

Ludwig, R., May, I., Turcotte, R., Vescovi, L., Braun, M., Cyr, J.-F., . . . Mauser, W. (2009). The role of hydrological model complexity and uncertainty in climate change impact assessment. *Advances in Geoscience, 21*, 63-71.

Manitoba Hydro. (2009). *Manitoba Hydro.* Retrieved January 19, 2012, from Manitoba Hydro's Churchill River Diversion: Final Licence Request und the Water Power Act to the Province of Manitoba: http://www.hydro.mb.ca/corporate/water_regimes/churchill_openhouse_09/introduction.pdf

Manitoba Hydro. (2011). *Churchill River Diversion*. Retrieved January 13, 2012, from Manitoba Hydro corporate site:

http://www.hydro.mb.ca/corporate/water_regimes/churchill_river_diversion.shtml

Manitoba Hydro. (2011). *Generating Stations*. Retrieved May 12, 2011, from Manitoba Hydro Corporate Site: http://hydro.mb.ca/corporate/facilities/generating_stations.shtml

Manitoba Hydro. (2011). *Projects*. Retrieved May 23, 2011, from Manitoba Hydro Corporate Site: http://hydro.mb.ca/projects/index.shtml?WT.mc_id=2600

Manitoba Hydro. (n.d.). *Churchill River Diversion*. Retrieved January 13, 2012, from Manitoba Hydro corporate site: http://www.hydro.mb.ca/corporate/water_regimes/churchill_river_diversion.shtml

Manitoba Wildlands. (2005). *Proposed and Existing Hydro Dams for Northern Manitoba.* Retrieved June 14, 2011, from Manitoba Wildlands: http://manitobawildlands.org/maps/mb_gen_stations.htm

Maurer, E. P., Brekke, L. D., & Pruitt, T. (2010). Contrasting Lumped and Distributed Hydrology Models for Estimating Climate Change Impacts on California Watersheds. *Journal of the American Water Resources Association, 46*(5), 1024-1035.

Miller, W. P., Butler, R. A., Piechota, T., Prairie, J., Grantz, K., & DeRosa, G. (2012). Water management decisions using multiple hydrologic models within the San Juan River basin under changing climate conditions. *Journal of Water Resources Planning and Management, 138*(5), 412-420.

Moradkhani, H., Hsu, K.-L., Gupta, H., & Sorooshian, S. (2005). Uncertainty assessment of hydrologic model states and parameters: Sequential data assimilation using the particle filter. *Water Resources Research, 41*, doi:10.1029/2004WR003604.

Mulvany, T. (1850). On the use of self-registering rain and flood gauges. *Inst. Civ. Eng. Proc.*, 1-8.

Nash, J. E., & Sutcliffe, J. V. (1970). River flow forecasting through conceptual models, Part I - A discussion of principles. *Journal of Hydrology, 10*, 282-290.

Poulin, A., Brissette, F., Leconte, R., Arsenault, R., & Malo, J.-S. (2011). Uncertainty of hydrological modelling in climate change impact studies in a

Canadian, snow-dominated river basin. *Journal of Hydrology, 409*, 626-636.

Prudhomme, C., & Davies, H. (2009). Assessing uncertainties in climate change impact analyses on the river flow regimes in the UK. Part 2: future climate. *Climatic Change, 93*(1), 197-222.

Renard, B., Kavetski, D., Kuczera, G., Thyer, M., & Franks, S. W. (2010). Understanding predictive uncertainty in hydrologic modeling: The challenge of identifying input and structural errors. *Water Resources Research, 46*, doi:10.1029/2009WR008328.

Rosenzweig, C., Casassa, G., Karoly, D. J., Imeson, A., Liu, C., Menzel, A., . . . Tryjanowski, P. (2007). Assessment of observed changes and responses in natural and managed systems. In M. L. Parry, O. F. Canziani, J. P. Palutikof, P. J. van der Linden, & C. E. Hanson (Eds.), *Climate Change 2007: Impacts, Adaptation, and Vulnerability. Contribution of Working Group II to the Fourth Assessment Report of the Intergovernmental Panel on Climate Change.* Cambridge, UK: Cambridge University Press.

Ruelland, D., Ardoin-Bardin, S., Collet, L., & Roucou, P. (2012). Simulating future trends in hydrological regime of a large Sudano-Sahelian catchment under climate change. *Journal of Hydrology, 424*, 207-216.

Slota, P. (2009). Quantifying the impacts of climate change on power generation in the Winnipeg River basin. B.Sc. thesis, University of Manitoba Department of Civil Engineering. Winnipeg, MB, Canada. (46 pgs).

Stadnyk-Falcone, T. (2008). Mesoscale Hydrological Model Validation and Verification using Stable Water Isotopes: The isoWATFLOOD Model. Ph.D. dissertation, University of Waterloo Department of Civil and Environmental Engineering. Waterloo, ON, Canada. (335 pgs.).

Thompson, D. B. (2007). *The Rational Method.* R.O. Anderson Engineering. Minden, NV, USA.

Thyer, M., Renard, B., Kavetski, D., Kuczera, G., Franks, S. W., & Srikanthan, S. (2009). Critical evaluation of parameter consistency and predictive uncertainty in hydrological modeling: A case study using Bayesian total error analysis. *Water Resources Research, 45*, doi:10.1029/2008WR006825.

Tolson, B. A., & Shoemaker, C. A. (2007). Dynamically dimensioned search algorithm for computationally efficient watershed model calibration. *Water Resources Research, 43*, doi:10.1029/2005WR004723.

Tolson, B. A., & Shoemaker, C. A. (2008). Efficient prediction uncertainty approximation in the calibration of environmental simulation models. *Water Resources Research, 44*, doi:10.1029/2007WR005869.

Toth, B., Pietroniro, A., Conly, F. M., & Kouwen, N. (2006). Modelling climate change impacts in the Peace and Athabasca catchment and delta: I - hydrological model application. *Hydrological Processes, 20*(19), 4197-4214.

van Griensven, A., Meixner, T., Grunwald, S., Bishop, T., Diluzio, M., & Srinivasan, R. (2006). A global sensitivity analysis tool for the parameters of multi-variable catchment models. *Journal of Hydrology, 324*(1-4), 10-23.

van Vuuren, D., Isaac, M., Kundzewicz, Z., Arnell, N., Barker, T., Criqui, P., . . . Screciu, S. (2011). The use of scenarios as the basis for combined assessment of climate change mitigation and adaptation. *Global Environmental Change, 21*(2), 575-591.

Vivoni, E., Mascaro, G., Mniszewski, S., Fasel, P., Springer, E., Ivanov, V., & Bras, R. (2011). Real-world hydrologic assessment of a fully-distributed hydrological model in a parallel computing environment. *Journal of Hydrology, 409*(1), 483-496.

Wang, J. J., Lu, X. X., & Kummu, M. (2009). Sediment load estimates and variations in the lower Mekong River. *River Research and Application, 27*(1), 33-46.

Warren, R., de la Nava Santos, S., Arnell, N. W., Bane, M., Barker, T., Barton, C., . . . Anderson, D. (2008). Development and illustrative outputs of the Community Integrated Assessment System (CIAS), a multi-institutional modular integrated assessment approach for modelling climate change. *Environmental Modelling Software, 23*(5), 592-610.

Wetterhall, F., Graham, L., Andreasson, J., Rosberg, J., & Yang, W. (2011). Using ensemble climate projections to assess probabilistic hydrological change in the Nordic region. *Natural Hazards and Earth System Sciences, 11*(8), 2295-2306.

Wilby, R. L. (2005). Uncertainty in water resource model parameters used for climate change impact assessment. *Hydrological Processes, 19*(16), 3201-3219.

Wilby, R., Charles, S., Zorita, E., Timbal, B., Whetton, P., & Mearns, L. (2004). *Guidelines for use of climate scenarios developed from statistical downscaling methods.* Intergovernmental Panel on Climate Change.

Wilby, R., Dawson, C., & Barrow, E. (2002). SDSM - a decision support tool for the assessment of regional climate change impacts. *Environment Modelling and Software, 17*, 147-159.

Woo, M. K., Long, T. Y., & Thome, R. (2009). Simulating monthly streamflow for the Upper Changjiang, China, under climatic change scenarios. *Hydrological Sciences, 54*, 596-605.

Xu, C.-y., Widen, E., & Halldin, S. (2005). Challenges, Modelling hydrological consequences of climate change - Progress and Challenges. *Advances in Atmospheric Sciences, 22*(6), 789-797.

Xu, H., Taylor, R. G., Kingston, D. G., Jiang, T., Thompson, J., & Todd, M. (2010). Hydrological modelling of the River Xiangxi using SWAT2005: A comparison of model parameterizations using station and gridded meteorological observations. *Quatern. Int., 226*, 54-59.

Appendix A: WATFLOOD™ model parameters

:FileType   WatfloodParameter   10.1   # parameter file version number
:CreationDate   ########
:GlobalParameters

:iopt	0	# debug level
:itype	0	# channel type - floodplain/no
:itrace	0	# Tracer choice
:a1	0	# ice cover weighting factor
:a2	1.5	# Manning`s correction for instream lake
:a3	0.05	# error penalty coefficient
:a4	0.03	# error penalty threshold
:a5	0.985	# API coefficien
:a6	450	# Minimum routing time step in seconds
:a7	0.5	# weighting - old vs. new sca value
:a8	0.135	# min temperature time offset
:a9	0.3	# max heat deficit /swe ratio
:a10	1	# exponent on uz discharce function
:a11	0.01	# bare ground equiv. veg height for ev
:a12	0.5	# min precip rate for smearing
:fmadjust	0	# snowmelt ripening rate
:fmalow	0	# min melt factor multiplier
:fmahigh	0	# max melt factor multiplier
:gladjust	0	# glacier melt factor multiplier
:rlapse	0	# precip lapse rate mm/m
:tlapse	0	# temperature lapse rate dC/m
:elvref	0	# reference elevation
:rainsnowtemp	0	# rain/snow temperature
:radiusinflce	300	# radius of influence km
:smoothdist	35	# smoothing diatance km
:flgevp2	2	# 1=pan;2=Hargreaves;3=Priestley-Taylor

:albe	0.11	# albedo????
:tempa2	0	#
:tempa3	375	#
:tton	500	#
:lat	56	latitude
:chnl(1)	1	# manning`s n multiplier
:chnl(2)	0.9	# manning`s n multiplier
:chnl(3)	0.8	# manning`s n multiplier
:chnl(4)	0.7	# manning`s n multiplier
:chnl(5)	0.6	# manning`s n multiplier

:EndGlobalParameters

#

:RoutingParameters							
:RiverClasses	6						
:RiverClassName	jean-marie	martin	birch	backstone	Pembina	Roseau	
:flz	0.000586	0.000975	0.002645	0.000524	0.000153	0.000743	# lower zone oefficient
:pwr	1.51991	1.89113	3.29303	3.00779	2.96221	2.44878	# lower zone exponent
:r1n	4.00E-03	0.3	0.4	4.00E-03	0.1	5.00E-02	# overbank Manning`s n
:r2n	0.0386	3.86202	1.01711	0.321281	0.1	0.251921	# channel Manning`s n
:mndr	1	1	1	1	1	1	# meander channel length multiplier
:aa2	1	1	1	500	1	1	# channel area intercept = min channel xsect area
:aa3	4.30E-02	4.00E-02	2.00E-02	4.30E-02	4.00E-02	2.00E-02	# channel area coefficient
:aa4	1	1	1	1	1	1	# channel area exponent
:theta	2.5	2	0.704	0.136	0.377	1	# wetland or bank porosity
:widep	10	20	20	30	20	20	# channel width to depth ratio
:kcond	0.37	0.654	0.4	0.5	0.654	0.654	# wetland/bank lateral conductivity
:pool	0	0	0	0	0	0	# average area of zero flow pools

:rlake	1	1.6	1.4	1.4	0.771	0.771			# in channel lake retardation coefficient
:EndRoutingParameters									
#									
:HydrologicalParameters									
:LandCoverClasses	8								
:ClassName	mix	conifer	crops	burn	wetland	wetland	water	impervious	# class name
:ds	10	1	5	1	0.1	0.1	0	1	# depression storage bare ground mm
:dsfs	10	1	0.5	1	0.1	0.1	0	1	# depression storage snow covered area mm
:rec	1.8027	0.065529	20.2514	10.5068	38.9923	31.1828	0.1	1.00E-11	# interflow coefficient
:ak	64.6858	0.208	5.87441	33.076	9.93463	1.20428	-0.1	1	# infiltration coefficient bare ground
:akfs	99.2252	56.4991	0.845613	97.9691	29.4897	24.5356	-0.1	1.00E-11	# infiltration coefficient snow covered ground
:retn	66.6	50	139	100	123	123	0.1	1.00E-11	# upper zone retention mm
:ak2	7.76E-02	1.46E-02	6.98E-02	0.148	6.52E-03	6.52E-03	1.00E-03	1.00E-11	# recharge coefficient bare ground
:ak2fs	5.12E-02	1.93E-02	2.33E-02	0.125	6.89E-02	6.89E-02	1.00E-03	1.00E-11	# recharge coefficient snow covered ground
:r3	52.7162	69.2544	87.3226	88.8591	0.962373	30.3427	4	19.7	# overland flow roughness coefficient bare ground
:r3fs	10	10	1	10	0.1	0.1	4	10	# overland flow roughness coefficient snow covered g
:r4	10	10	1	1	10	10	10	1	# overland flow roughness coefficient impervious are
:fpet	2.08	1	2.28	3	1.98	1.98	0.918	1	# interception evaporation * pet

:ftall	0.532	0.5	0.993	0.7	0.581	0.581	0	0.5	# reduction in PET for tall vegetation
:flint	1	1	1	1	1	1	1	1	# interception flag 1=on <
:fcap	0.15	0.15	0.15	0.15	0.15	0.15	0.15	0.15	# not used - replaced by re (retention)
:ffcap	0.1	0.1	0.1	0.1	0.1	0.1	0.1	0.1	# wilting point - mm of wa in uzs
:spore	0.3	0.3	0.3	0.3	0.3	0.3	0.3	0.3	# soil porosity
:fratio	1	1	1	1	1	1	1	1	# int. capacity multiplier

:EndHydrologicalParameters

#

:SnowParameters									
:fm	0.13	0.077	0.367	0.058	0.062	0.062	0.11	0.11	# melt factor mm/dC/hour
:base	-4.61	-2.054	0.966	-1.847	-1.821	-1.821	-99	-2	# base temperature dC
:fmn	0.1	0.1	0.1	0.1	0.1	0.1	0.1	0.1	# -ve melt factor
:uadj	0	0	0	0	0	0	0	0	# not used
:tipm	0.1	0.1	0.1	0.1	0.1	0.1	0.1	0.1	# coefficient for ati
:rho	0.333	0.333	0.6	0.333	0.333	0.333	0.333	0.333	# snow density
:whcl	0.035	0.035	0.035	0.035	0.035	0.035	0.035	0.035	# fraction of swe as water ripe snow
:alb	0.11	0.11	0.18	0.18	0.11	0.11	0.11	0.11	# albedo
:sublim_factor	0.288	0	0.442	0.5	0.114	0.114	0.01	0.01	# sublimation factor ratio
:idump	1	2	3	4	5	5	7	8	# receiving class for snow redistribution
:snocap	6000	6000	-600	-600	-600	-600	-600	-600	# max swe before redistrib
:nsdc	2	2	2	2	2	2	2	2	# no of points on scd curve allowed
:sdcsca	1	1	1	1	1	1	1	1	# snow covered area - rati
:sdcd	50	50	50	50	50	50	1000000	100	# swe for 100% snow covered area

:EndSnowParameters

\#

:InterceptionCapacityTable									
:IntCap_Jan	2.4	1	0.04	0.01	3	3	0.11	0.01	# interception capacity jan
:IntCap_Feb	2.4	1	0.04	0.01	3	3	0.11	0.01	# interception capacity feb
:IntCap_Mar	2.4	1	0.04	0.01	3	3	0.11	0.01	# interception capacity ma
:IntCap_Apr	2.4	1	0.04	0.01	3	3	0.11	0.01	# interception capacity apr
:IntCap_May	3	1	0.53	0.01	3	3	0.11	0.01	# interception capacity ma
:IntCap_Jun	4	1	1	0.01	3	3	0.11	0.01	# interception capacity jun
:IntCap_Jul	4	1	1.25	0.01	3	3	0.11	0.01	# interception capacity jul
:IntCap_Aug	4	1	1.5	0.01	3	3	0.11	0.01	# interception capacity aug
:IntCap_Sep	4	1	1	0.01	3	3	0.11	0.01	# interception capacity sep
:IntCap_Oct	2.4	1	0.28	0.01	3	3	0.11	0.01	# interception capacity oct
:IntCap_Nov	2.4	1	0.04	0.01	3	3	0.11	0.01	# interception capacity nov
:IntCap_Dec	2.4	1	0.04	0.01	3	3	0.11	0.01	# interception capacity dec

:EndInterceptionCapacityTable

\#

:MonthlyEvapotranspirationTable									
:Montly_ET_Jan	0	0	0	0	0	0	0	0	# monthly evapotranspirat jan mm
:Montly_ET_Feb	0	0	0	0	0	0	0	0	# monthly evapotranspirat feb mm
:Montly_ET_Mar	0	0	0	0	0	0	0	0	# monthly evapotranspirat mar mm
:Montly_ET_Apr	0	0	0	0	0	0	0	0	# monthly evapotranspirat apr mm
:Montly_ET_May	0	0	0	0	0	0	0	0	# monthly evapotranspirat may mm
:Montly_ET_Jun	0	0	0	0	0	0	0	0	# monthly evapotranspirat jun mm

:Montly_ET_Jul	0	0	0	0	0	0	0	0	# monthly evapotranspirat jul mm
:Montly_ET_Aug	0	0	0	0	0	0	0	0	# monthly evapotranspirat aug mm
:Montly_ET_Sep	0	0	0	0	0	0	0	0	# monthly evapotranspirat sep mm
:Montly_ET_Oct	0	0	0	0	0	0	0	0	# monthly evapotranspirat oct mm
:Montly_ET_Nov	0	0	0	0	0	0	0	0	# monthly evapotranspirat nov mm
:Montly_ET_Dec	0	0	0	0	0	0	0	0	# monthly evapotranspirat dec mm

:EndMonthlyEvapotranspirationTable

Appendix B: Summary of HBV-EC model parameters

The following parameters apply to the entire model:

Time Step	24 hours
Configuration	Parallel
Runoff FRAC	0.09
Runoff KF	0.009
Runoff Alpha	0.075
Runoff KS	0.005
Initial Fast Reservoir Discharge	0
Initial Slow Reservoir Discharge	296 cms

The following parameters are different for each of the Climate zones and values for each parameter fall within the given ranges:

Atmosphere RFCF	0.2-0.7
Atmosphere SFCF	1
Atmosphere PGRADL	0.0001-0.00016
Atmosphere PGRADH	0
Atmosphere EMID	4500-5000
Atmosphere TLAPSE	0.0065-0.007
Atmosphere TT	0
Atmosphere TTI	1.8-2
Atmosphere EPGRAD	0.0005-0.00065
Atmosphere ETF	0.5-0.56
Forest TFRAIN	0.8-0.9
Forest TFSNOW	0.8-0.9
Snow AM	0-0.5
Snow TM	0-2

Snow CMIN	2-2.2
Snow DC	1.7-2
Snow MRF	0.7-0.85
Snow CRFR	1.6-2
Snow WHC	0.05-.075
Snow LWR	2000-2500
Soil FC	185-200
Soil BETA	0.9-1
Soil LP	0.7
Glacier MRG	2
Glacier AG	0.05
Glacier DKG	0.05
Glacier KGMin	0.05
Glacier KGRC	0.7

The initial snow content for the basin is set by the user for each combination of elevation band, land cover type, slope, and aspect. Due to lack of data to do otherwise, the initial snow content was set to 250 mm of solid snow.

Appendix C: HMETS model parameters

```matlab
    Area=119000;      % basin area in sq.kms
    latitude=55.5;    % basin center point latitude [-90 (S) to +90
(N)]
    longitude=108;    % positive increasing toward the west from
Greenwich, example: Montreal is +73
    GMToffset=-7;     % time differential between local time and GMT.
For
                      % North-American estern time zone, enter -5 (-4 for
daylight savings time)
                      % NB: the algorithm does NOT take into account the
change from standard to
                      % daylight savings time.  Choose one or the other
using the GMToffset
                      % variable  GMToffset is only used when using a
hourly
                      % time step
    timestep='daily';   % choices are 'daily' and 'hourly'  NB: the
model works only at a
                      % one hour or one day time step
    discharge_data='exist';   %  'exist': the results will be compared
against observed data
                              %  'none' the results will NOT be
compared against
                              % observed data (for climate change
studies for example

    metfile='met_1979-2003';  % name of matlab file for weather data
(see below for details
    Qfile='q_1979-2003';  % name of discharge data file (only used if
dicsharge_data='exist'

%     metfile='CDDmet';  % name of matlab file for weather data (see
below for details
%     Qfile='CDDq';  % name of discharge data file (only used if
dicsharge_data='exist'

    % the following 2 lines are used only if precipitation data
regroups solid and liquid precip
    % and has to be separated in liquid and solid forms

    Tup = 1.5;    % precipitation is entirely liquid is average temp is
above Tup
    Tlow = -3;    % precipitation is entirely solid if average temp is
below Tlow

    rainCF = .7;  % correction factor for underestimation of rain gages
    snowCF = 1;  % correction factor for understimation of snow precip


%-------------------------------------------------------------------
----
%
```

```matlab
% model parameters with initial values
%
%---------------------------------------------------------------
----

    % hydrograph parameters (4 parameters)

    tp1=85;       % time to peak for surface runoff hydrograph
    tb1_minus_tp1=44;     % base time for surface runoff hydrograph
TB1>TP1 !!!
                % tp1 and tb1 are INTEGER and are either in days or in
                % hours depending on the time step

    shape_factor2 = 6;       % unsaturated zone hydrograph INTEGER

    % snow model parameters including melting, liquid retention by the
    % snowpack and refreezing process (10 parameters)

    ddf_min = 1.1;    % the degree-day-factor in mm/C/day ddf varies
during the season from ddf_min all the way
    ddf_plus = 5;    % to ddf_max (ddf_min + ddf_plus) as a function of
cumulative snowmelt.  This simulates the drop in surface albedo of the
snow
    Tbm = 0.35;     % base temperature for melting in C, -1 to 3
    Kcum = 0.045;   % in mm-1 , parameter for the calculation of degree-
day-factor  0.05 to 0.09

    fcmin = 0.05;   % minimum fraction water retention capacity of the
snowpack 0-0.1 (as a fraction of SWE)
    fcmin_plus = 0.17;   % maximum fraction water retention capacity
fcmax=fcmin+fcmin_plus of the snowpack 0.05-0.27 (as a fraction of SWE)
                    % the fraction water retention capacity goes from
fcmax
                    % all the way to fcmin as the snowpack ages
    Ccum = 0.018;   % in mm-1, parameter for the calculation of water
retention capacity

    Tbf = -1.7;     % base temperature for refreezing in C (-5 to 2),
based on average between min and mean air temperature
    Kf = 1.5;       % degree-day freezing factor in mm/C/day between 0
and 5
    exp_fe = 0.36; % exponent in freezing equation (0 - 1)

    % evapotranspiration (1 parameters)

    ET_efficiency = 0.6;

    % subsurface (3 parameters)

    runoff_frac = 0.11;
```

```matlab
rate1 = 0.005;
rate2 = 0.005;
max_level_reservoir1 = 75;    % mm
max_level_reservoir2 = 150;   % mm
```

Appendix D: Climate change simulation results

2050s B1
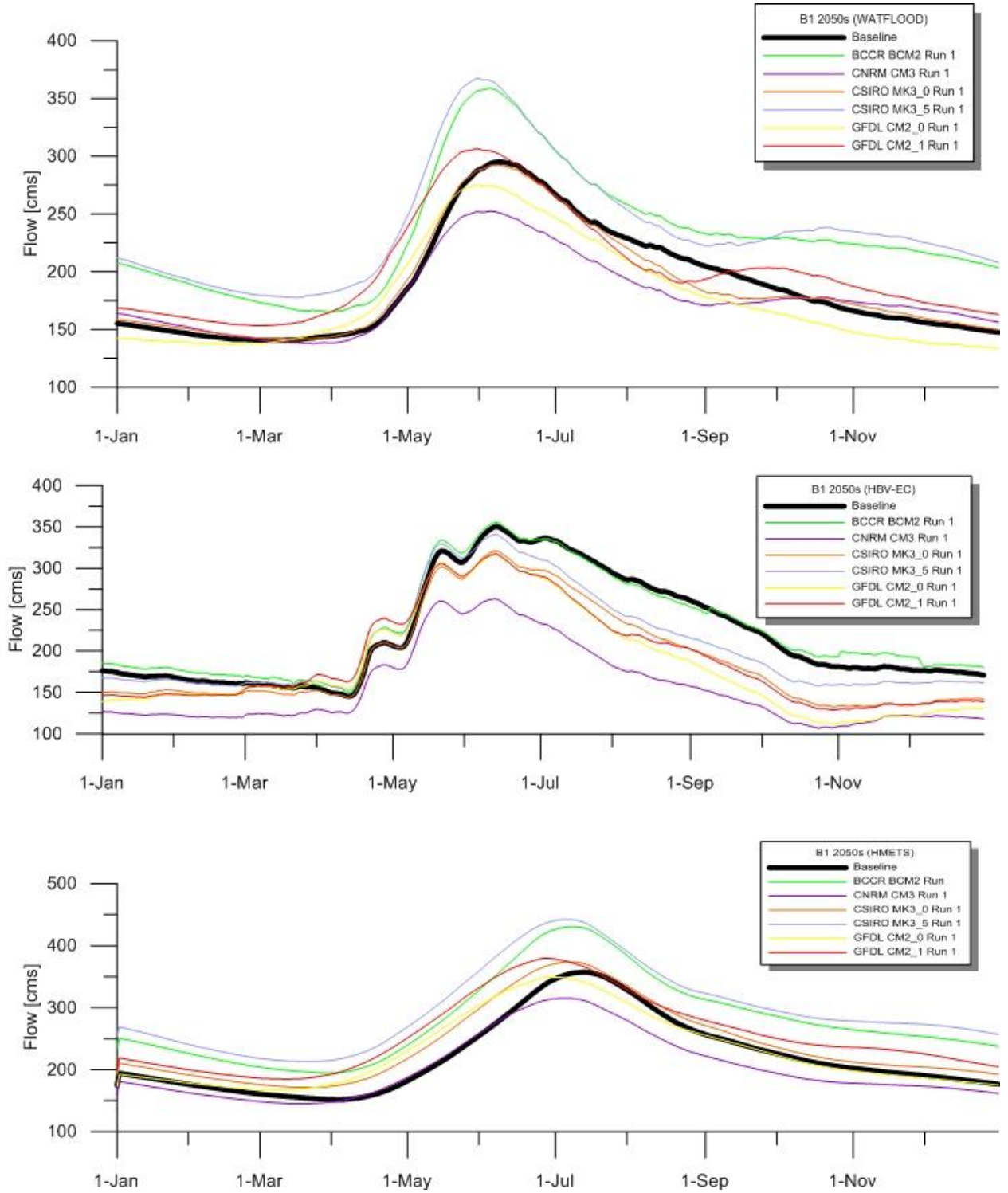
Figure 1: BCCR, CNRM, CSIRO, GFDL B1 2050s climate change hydrographs
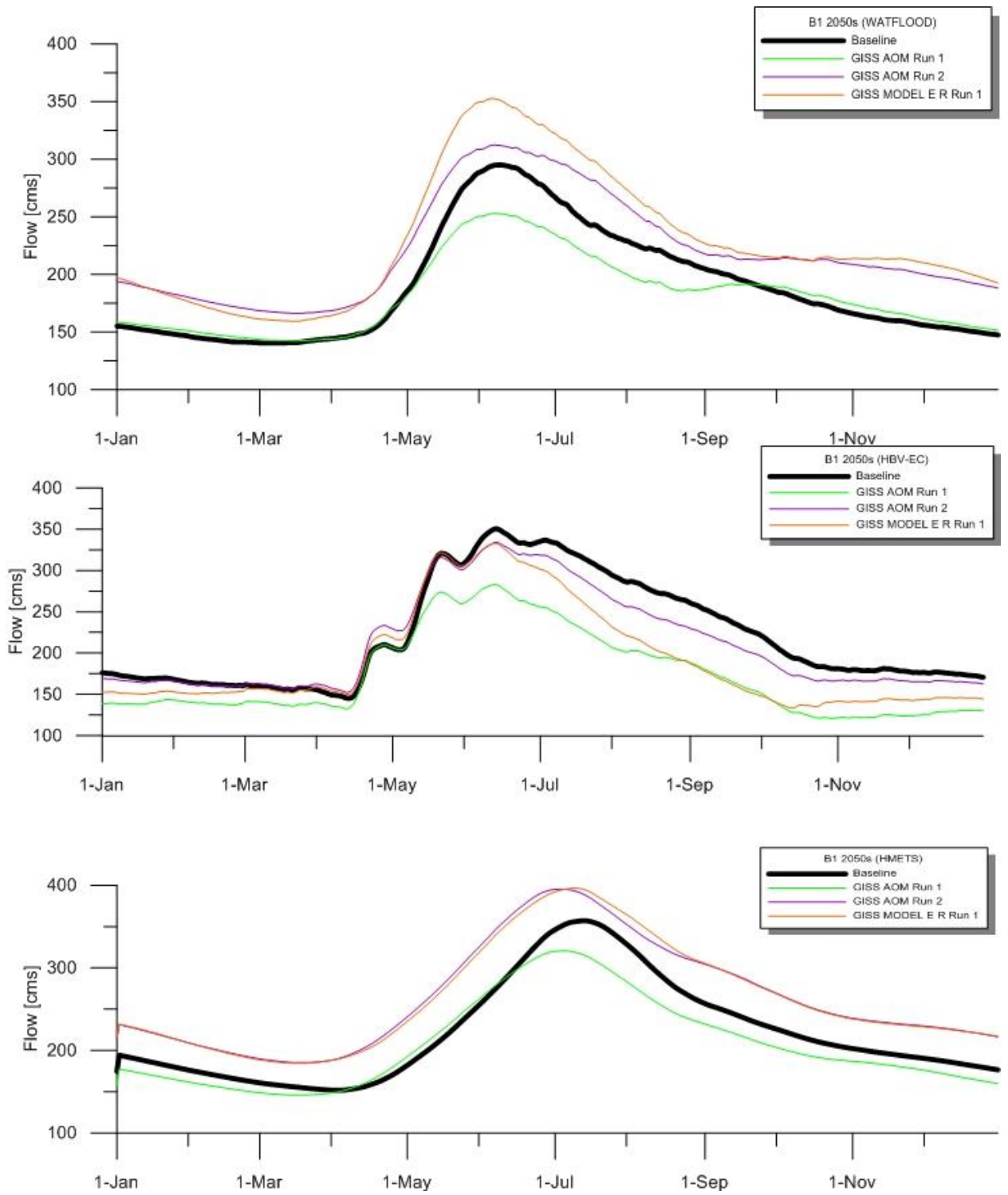
Figure 2: GISS B1 2050s climate change hydrographs
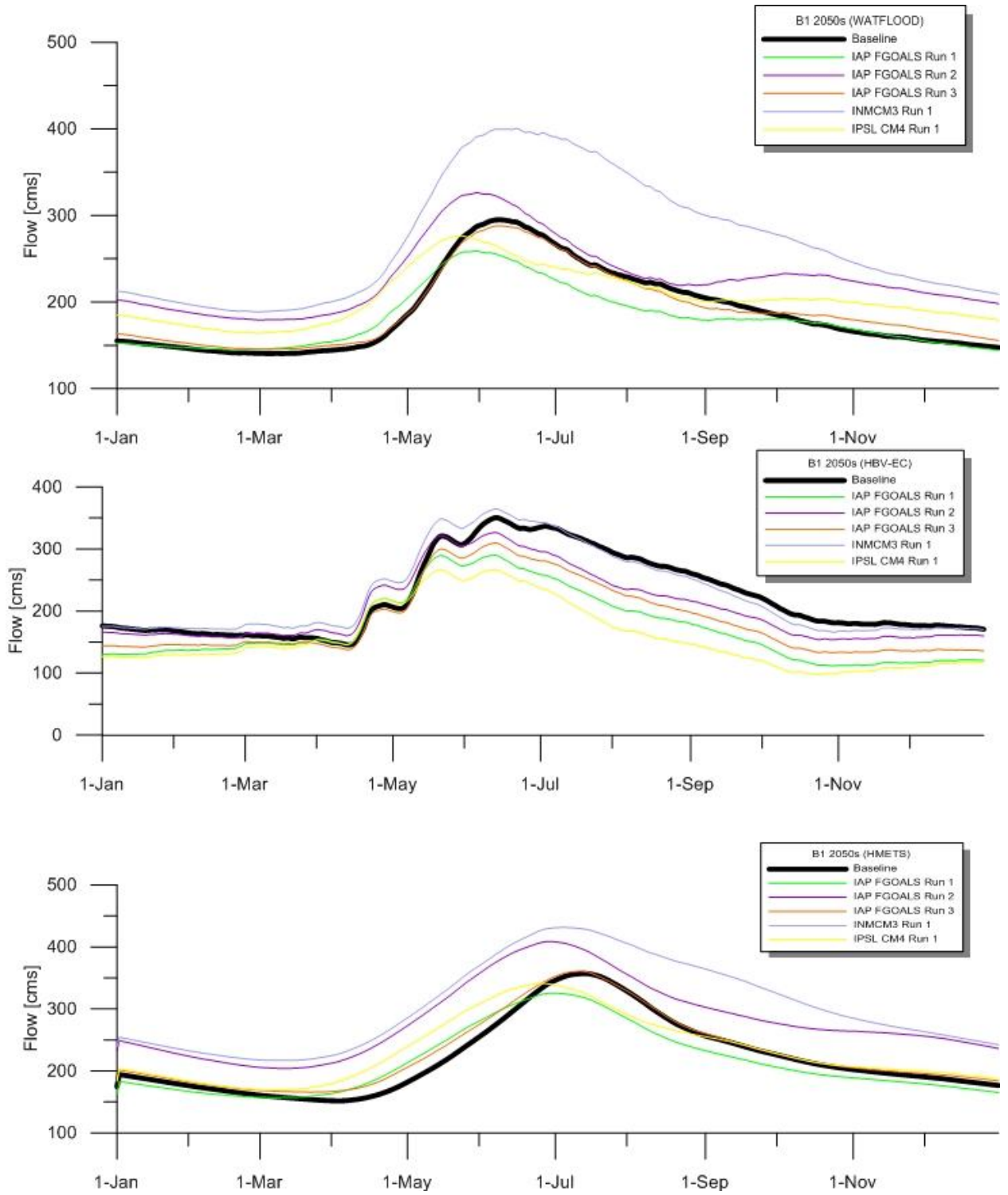
Figure 3: IAP, INMCM, IPSL B1 2050s climate change hydrographs
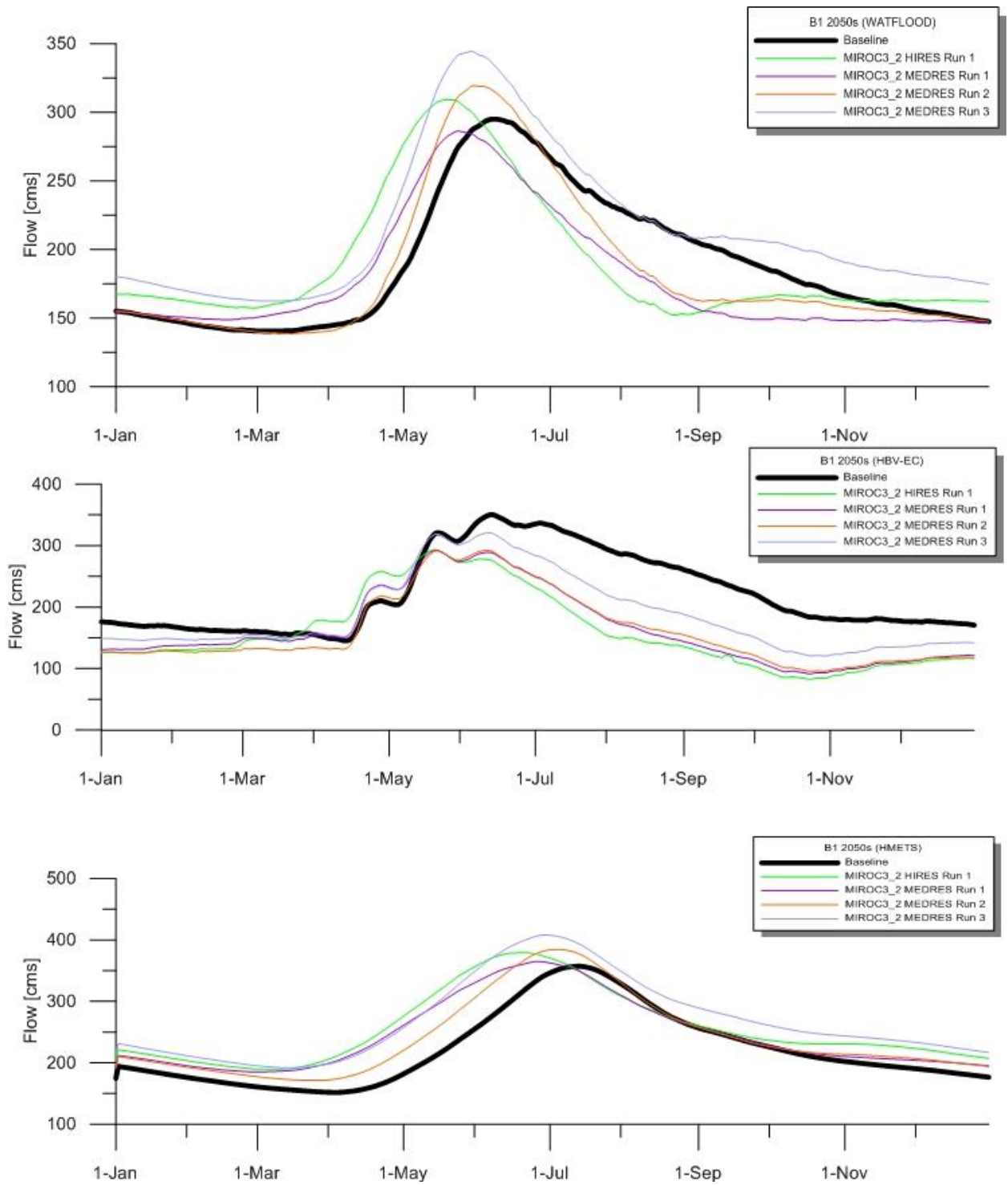
Figure 4: MIROC B1 2050s climate change hydrographs
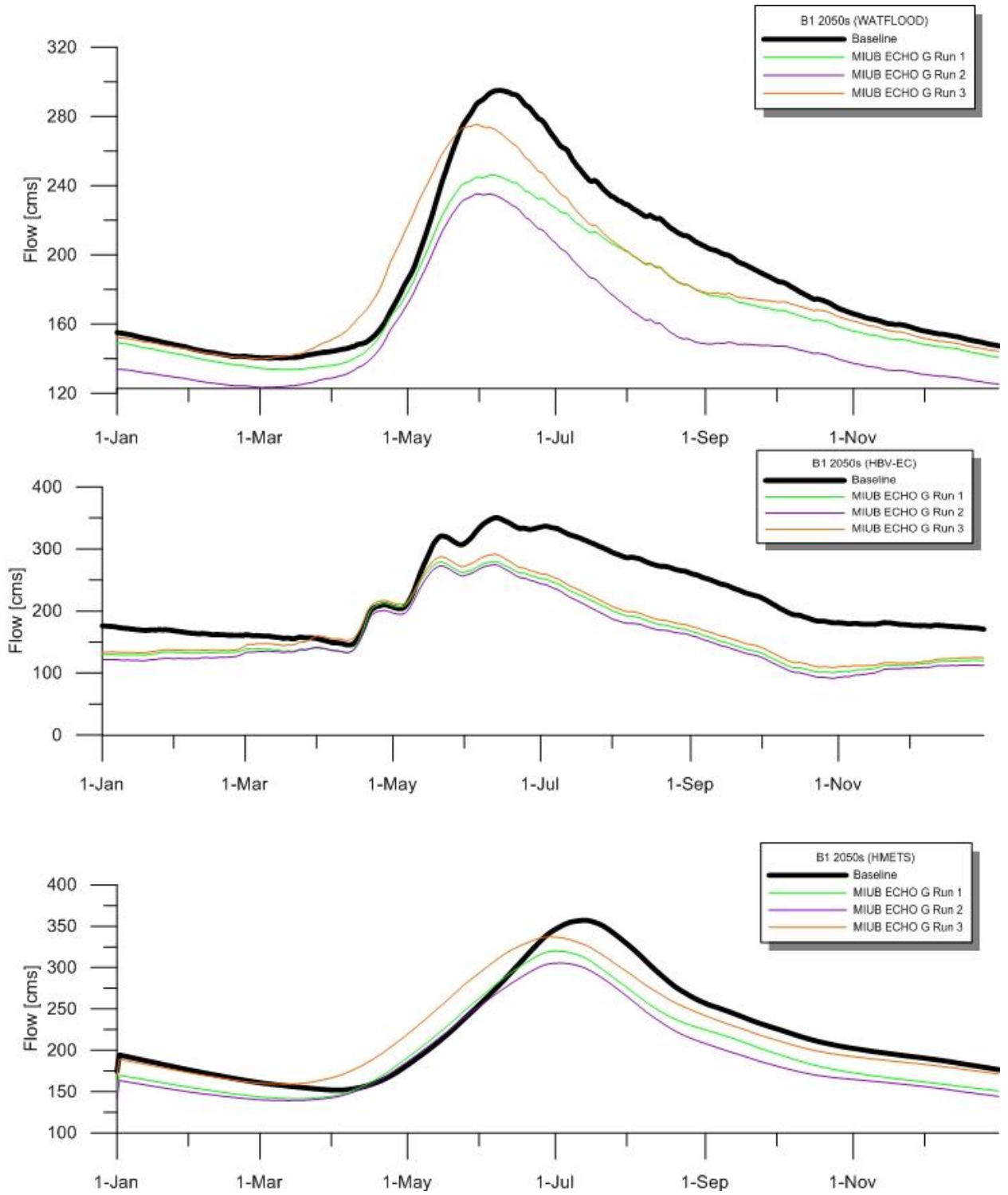
Figure 5: MIUB B1 2050s climate change hydrographs
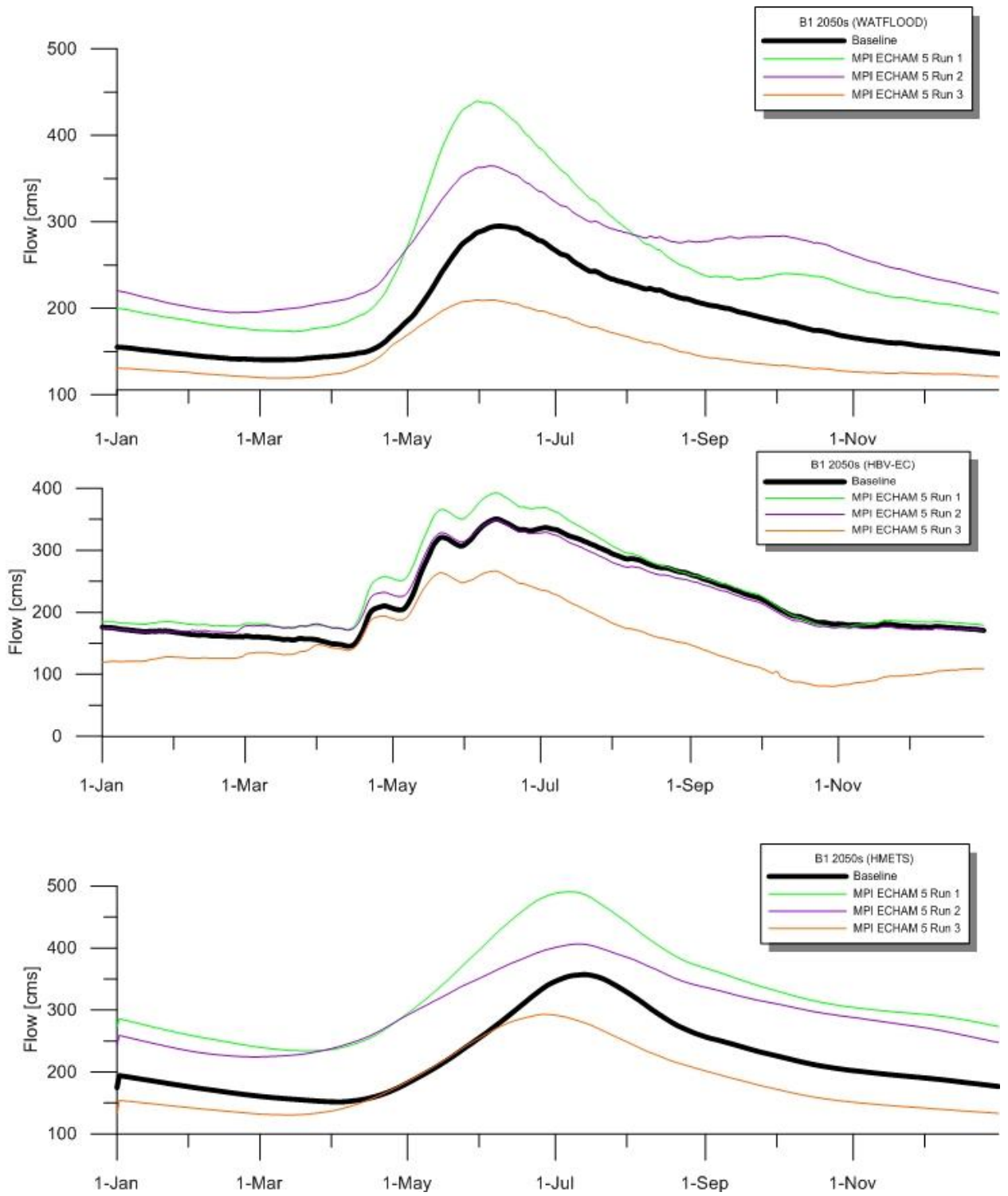
Figure 6: MPI B1 2050s climate change hydrographs
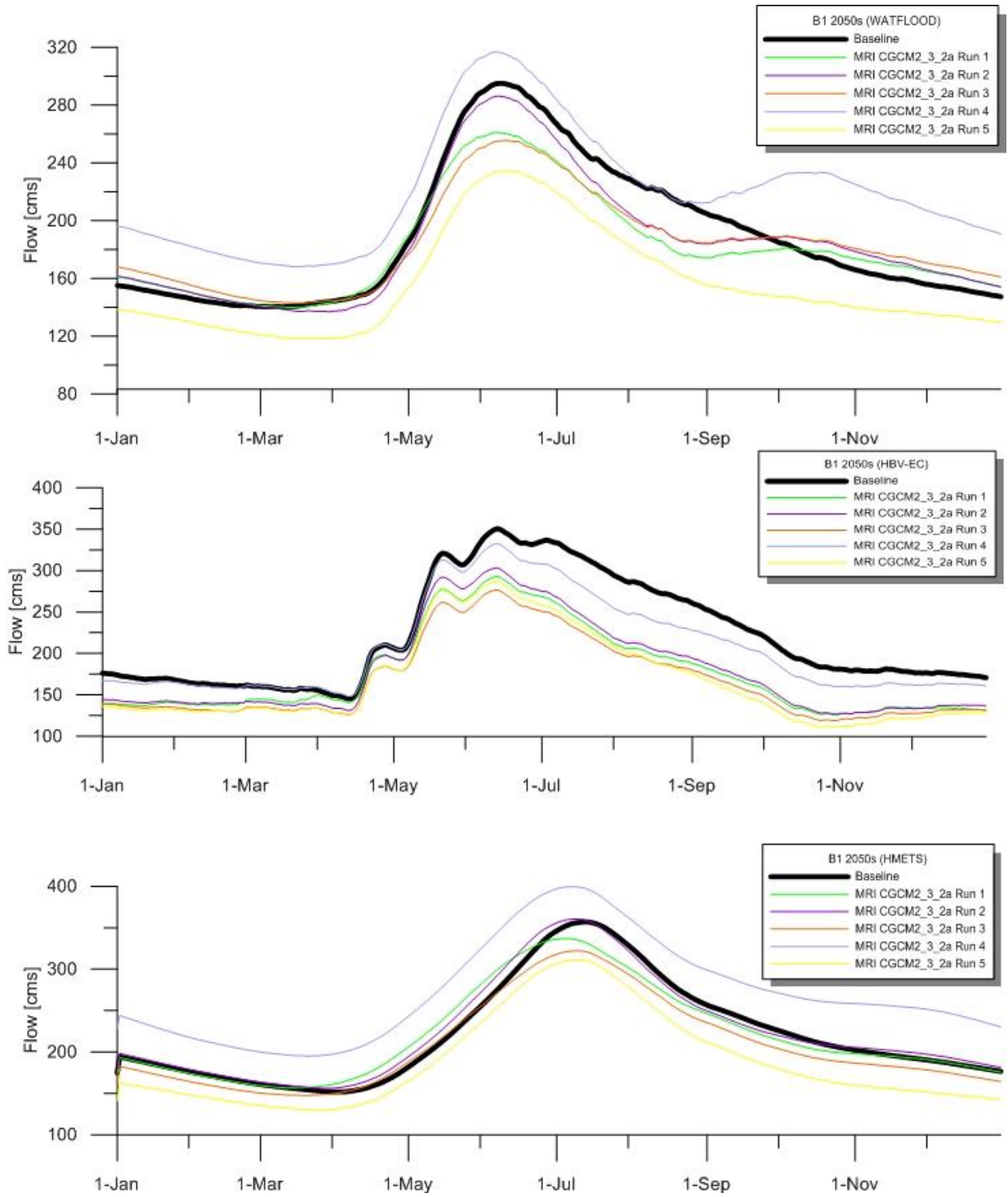
Figure 7: MRI B1 2050s climate change hydrographs
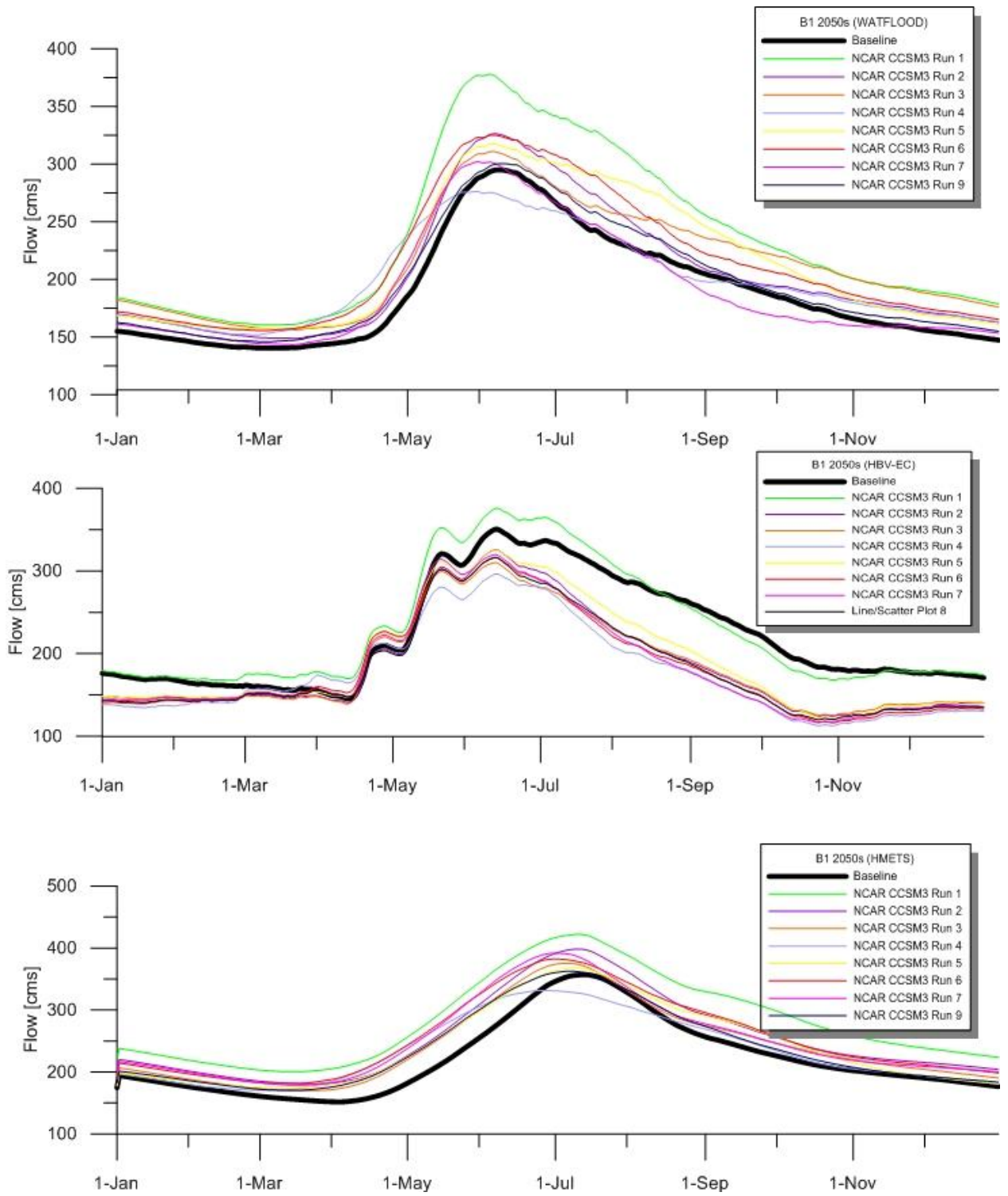
Figure 8: NCAR CCSM3 B1 2050s climate change hydrographs
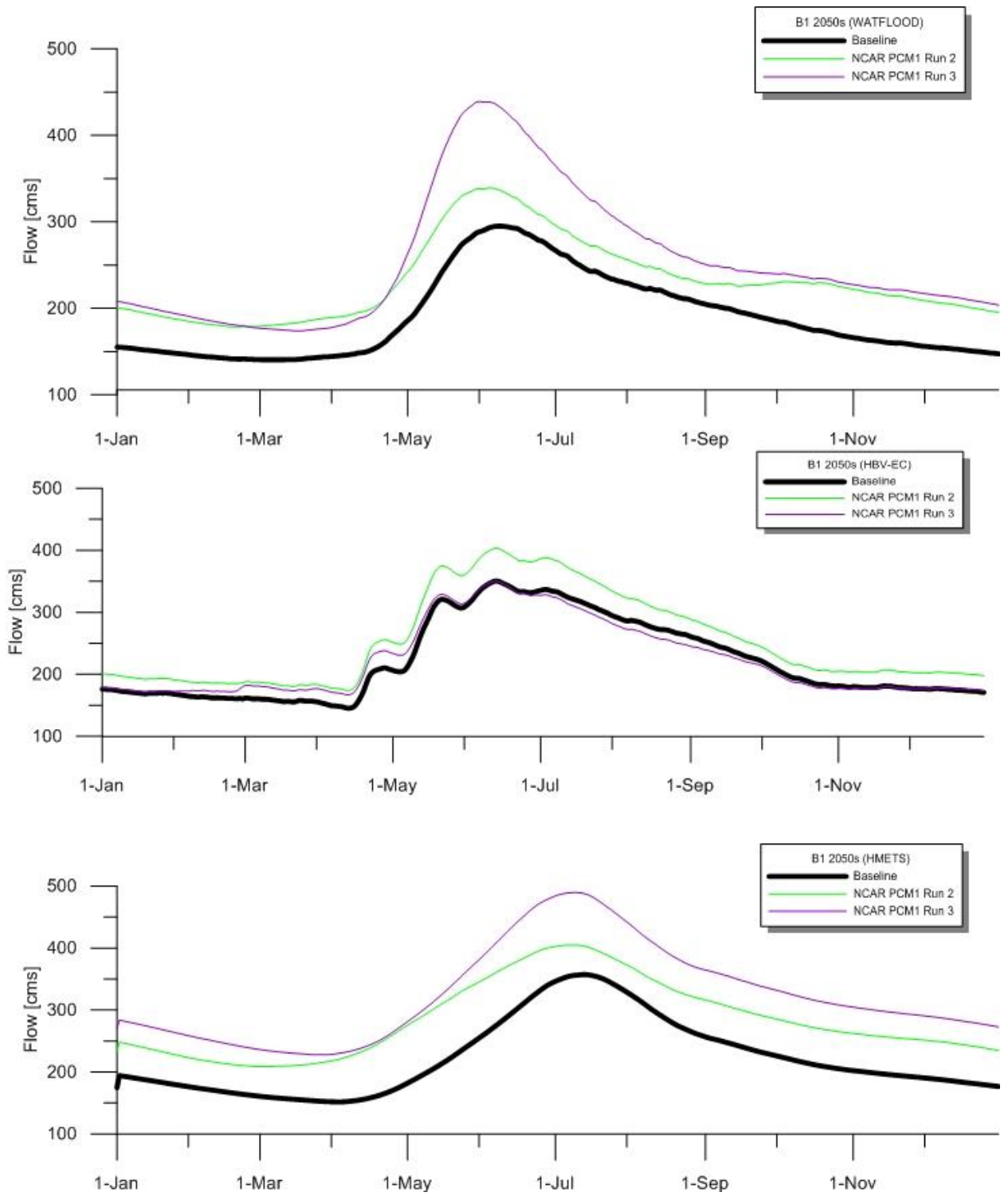
Figure 9: NCAR PCM1 B1 2050s climate change hydrographs
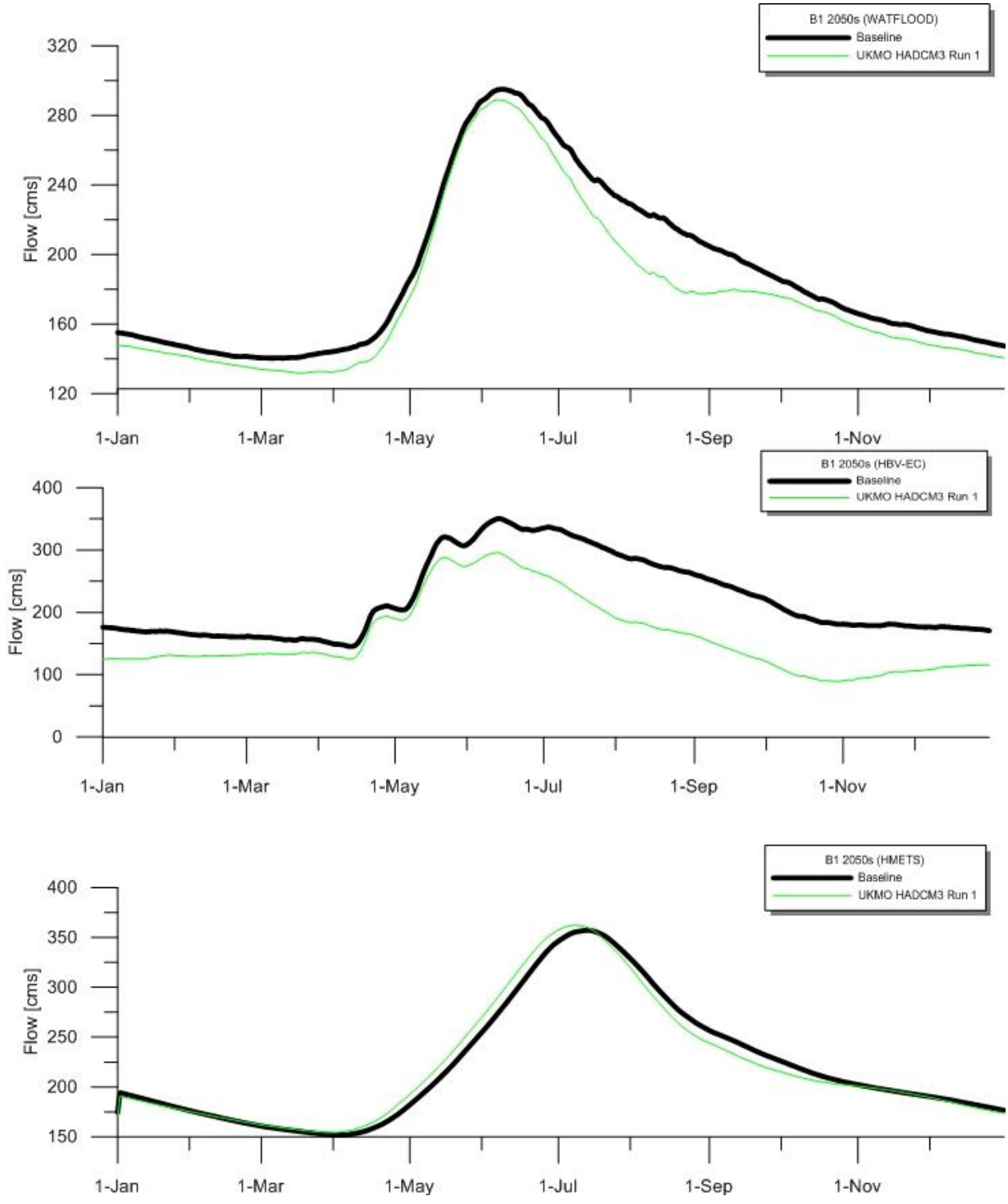
Figure 10: UKMO B1 2050s climate change hydrographs

2050s A1B
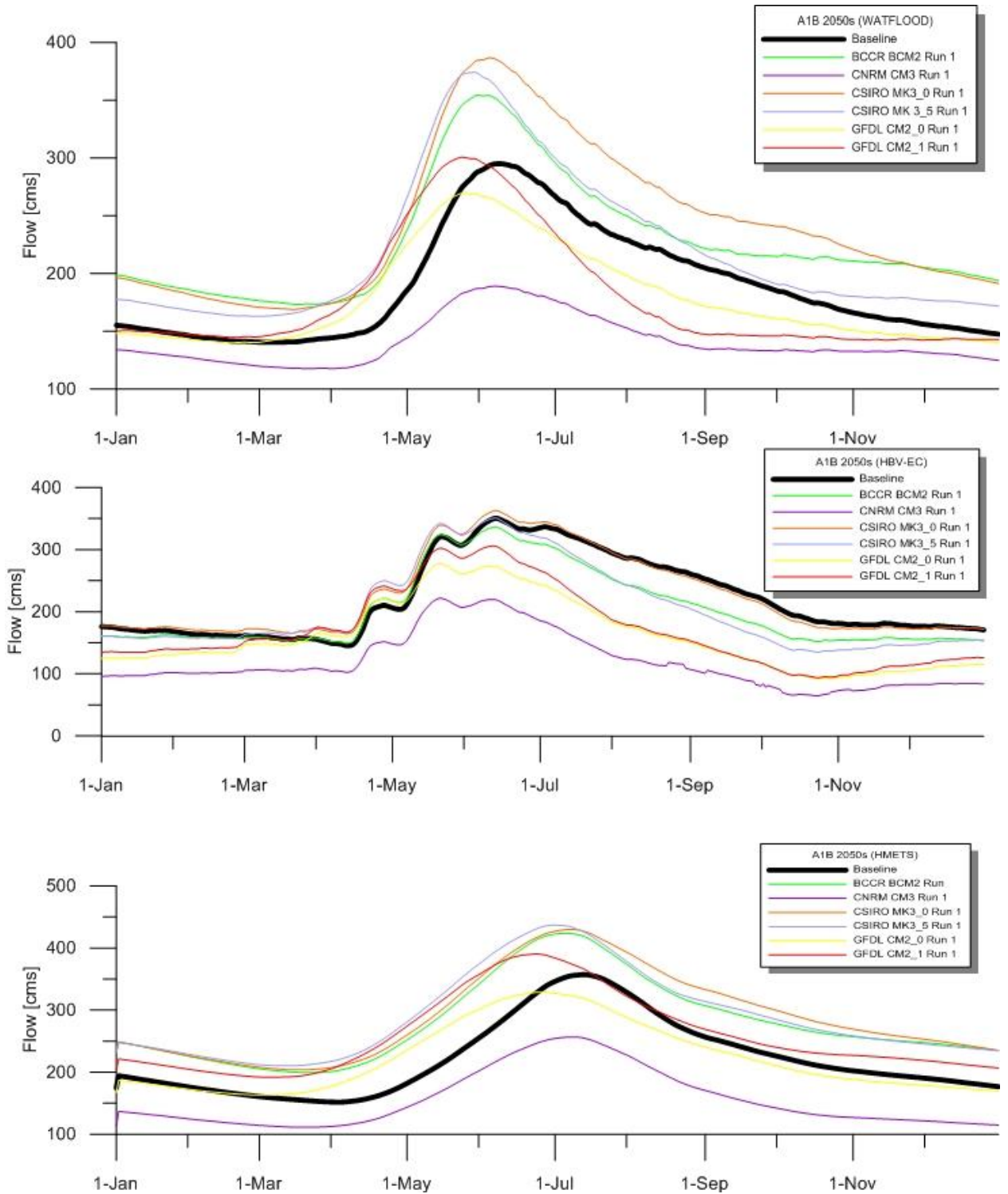
Figure 11: BCCR, CNRM, CSIRO, GFDL A1B 2050s climate change hydrographs
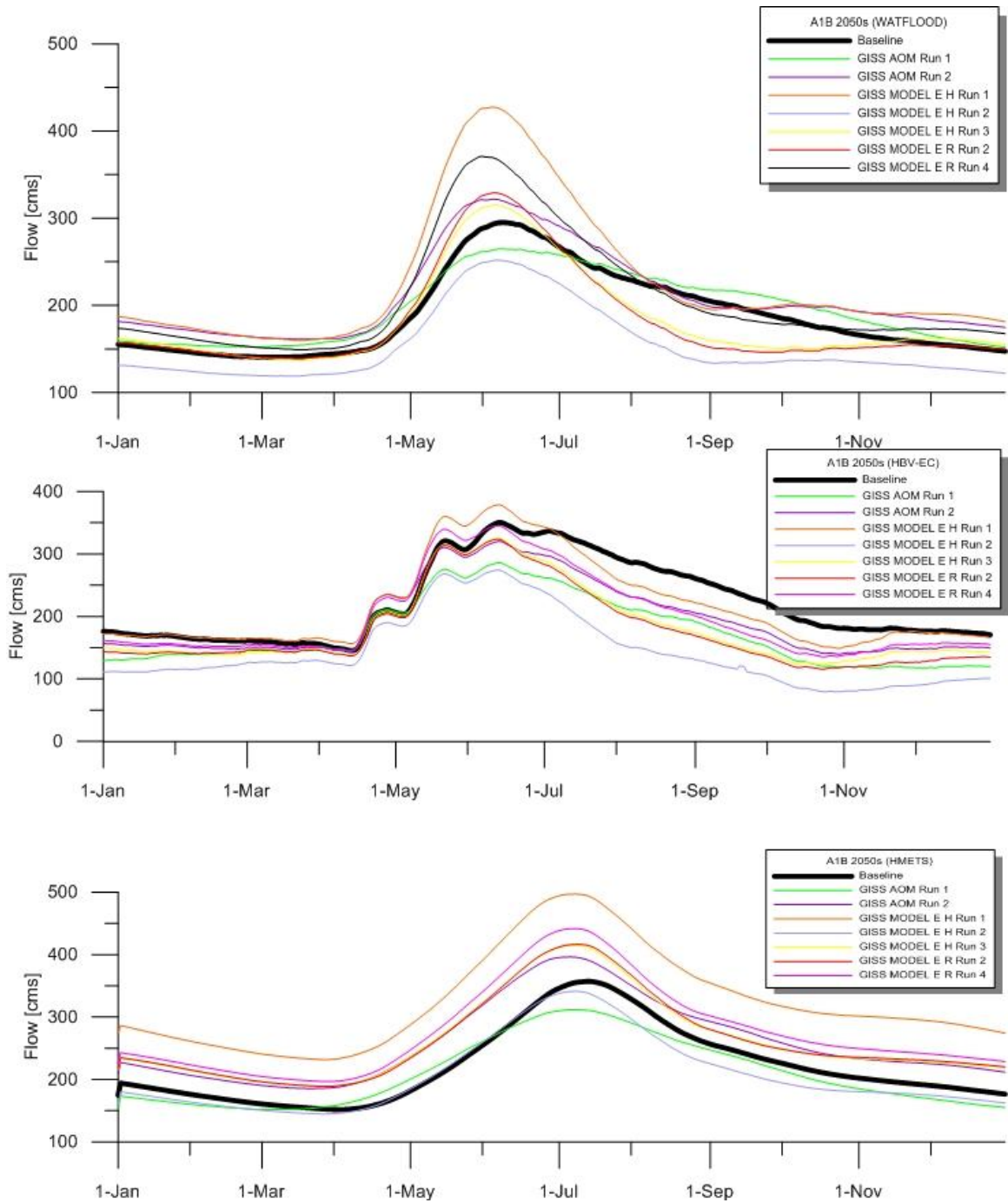
Figure 12: GISS A1B 2050s climate change hydrographs
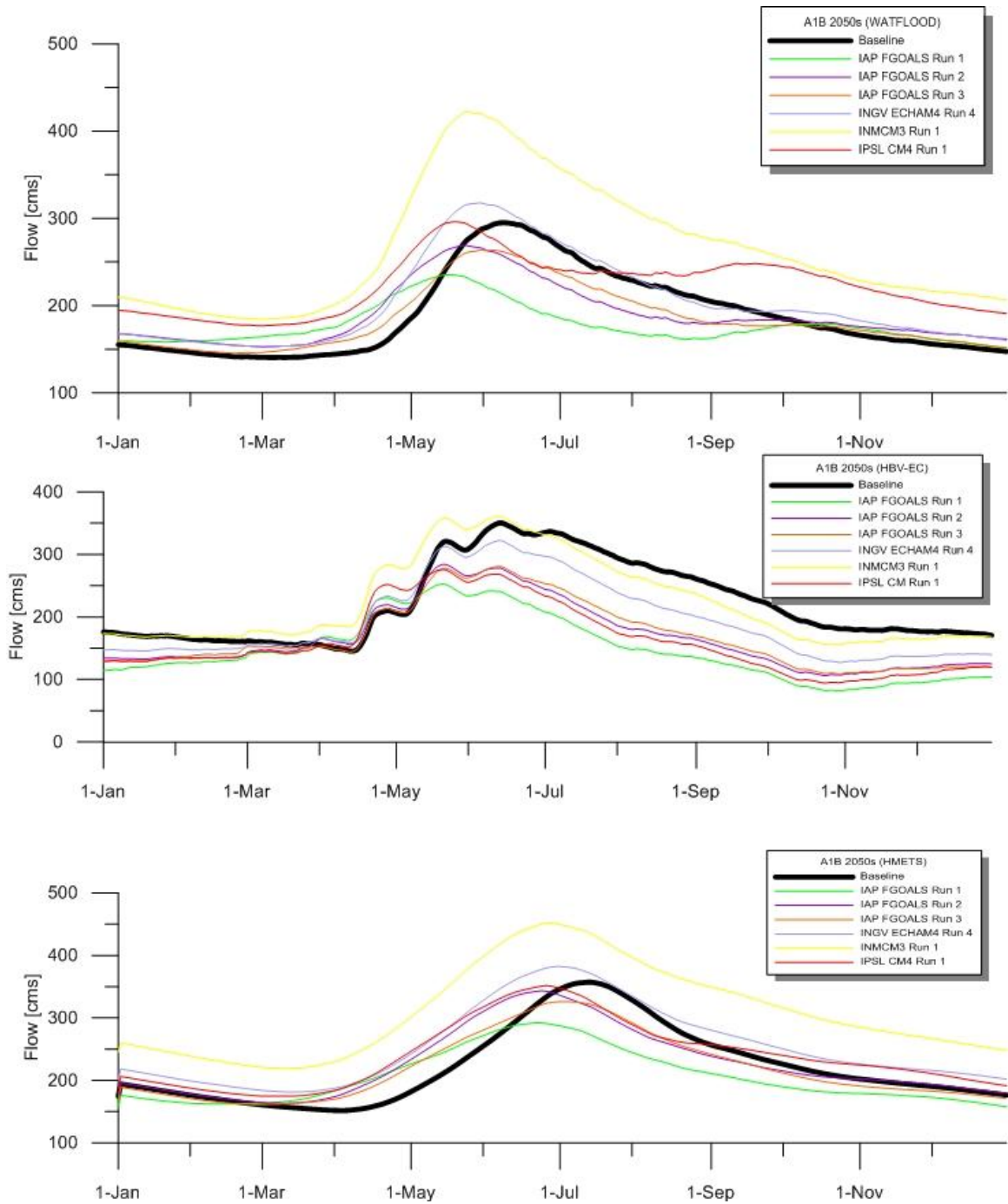
Figure 13: IAP, INGV, INMCM, IPSL A1B 2050s climate change hydrographs
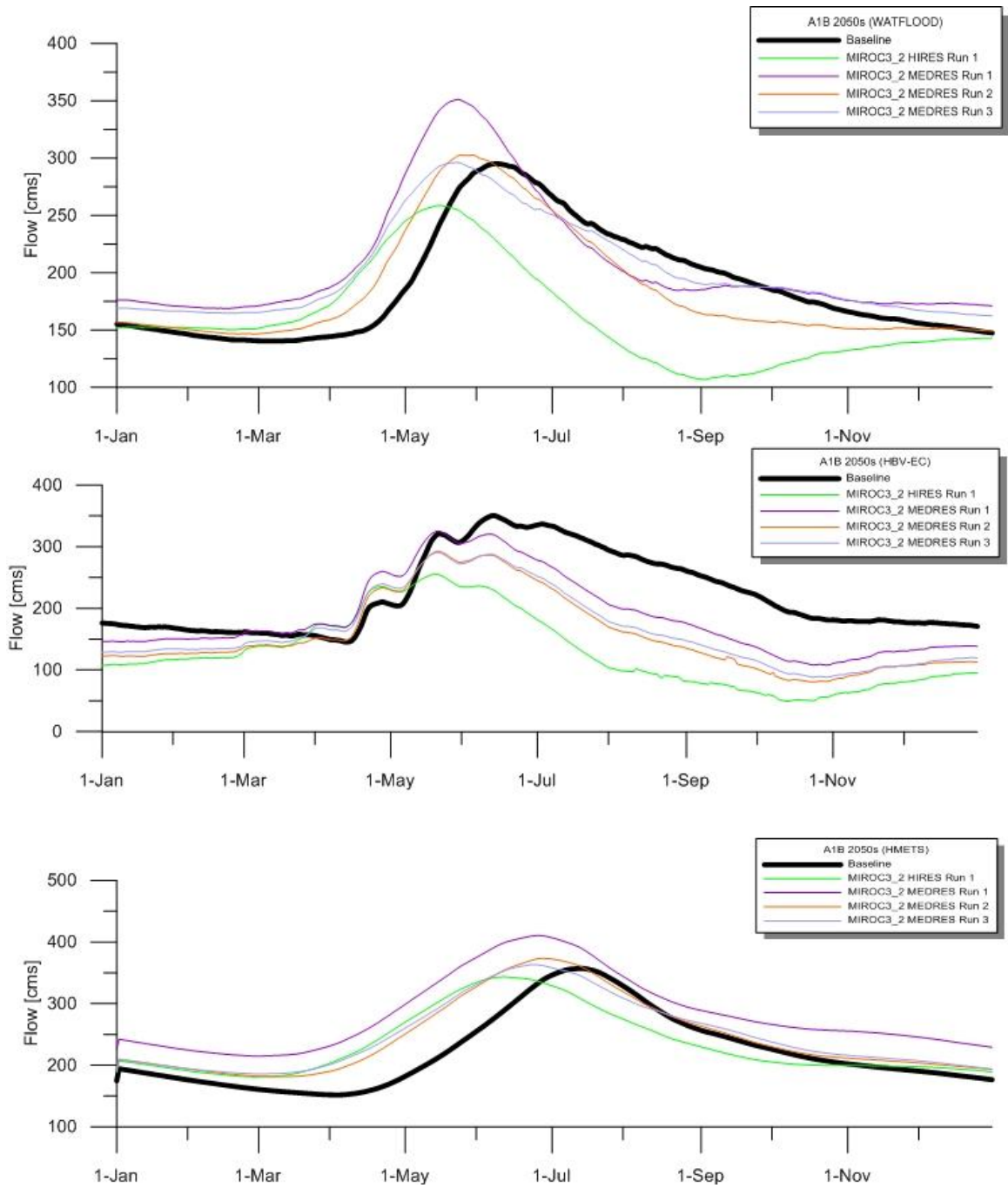
Figure 14: MIROC A1B 2050s climate change hydrographs
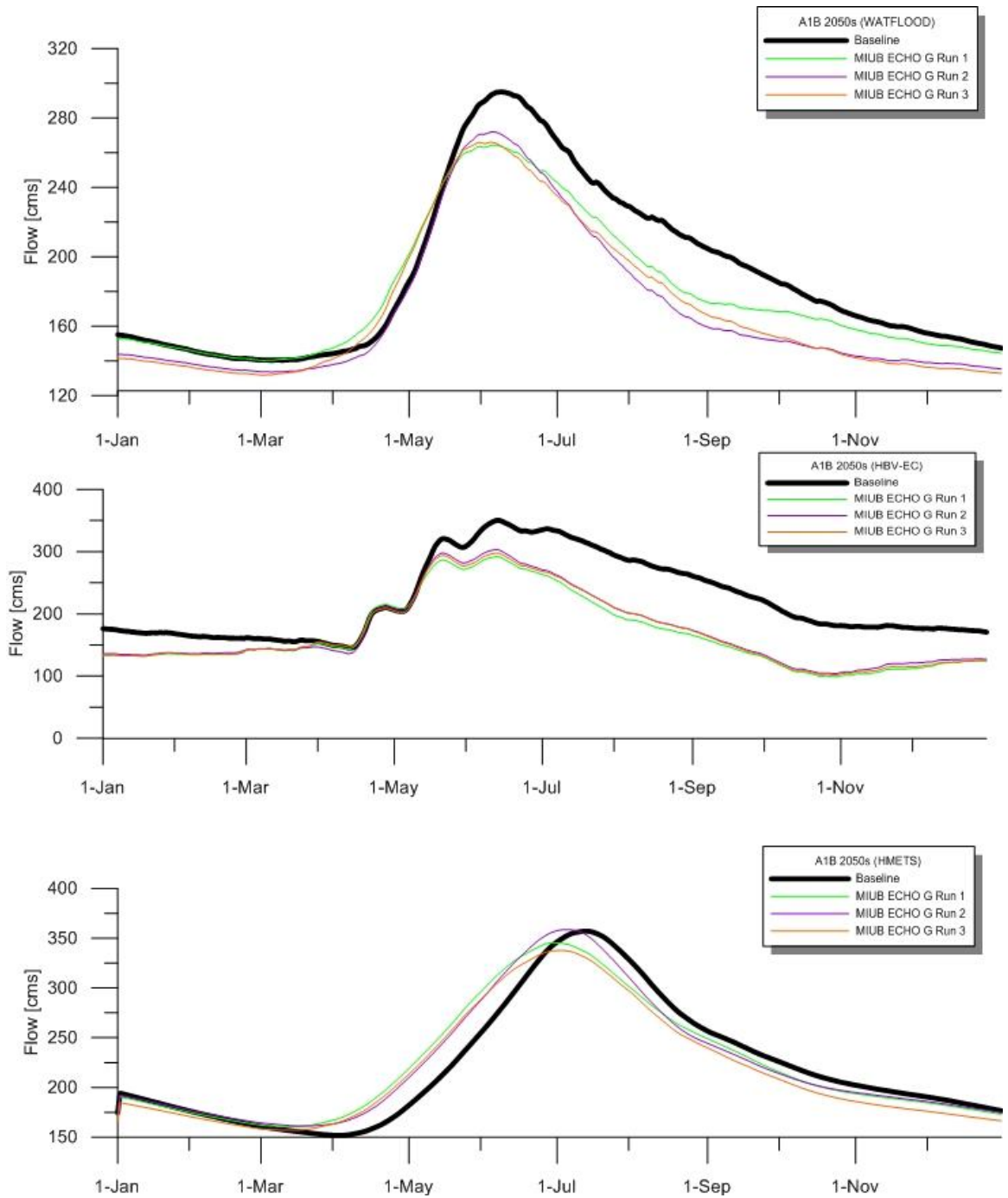
Figure 15: MIUB A1B 2050s climate change hydrographs
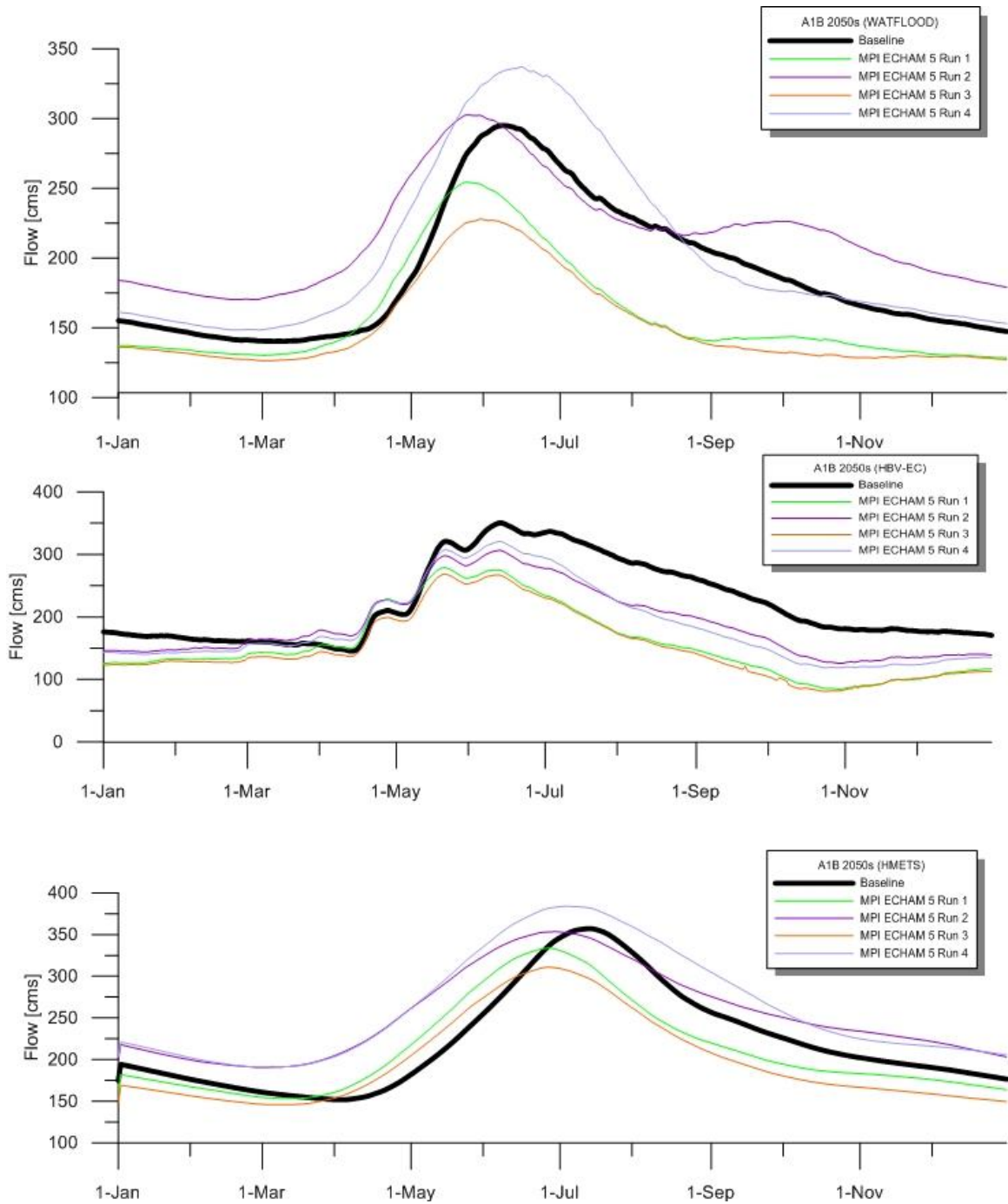
Figure 16: MRI A1B 2050s climate change hydrographs
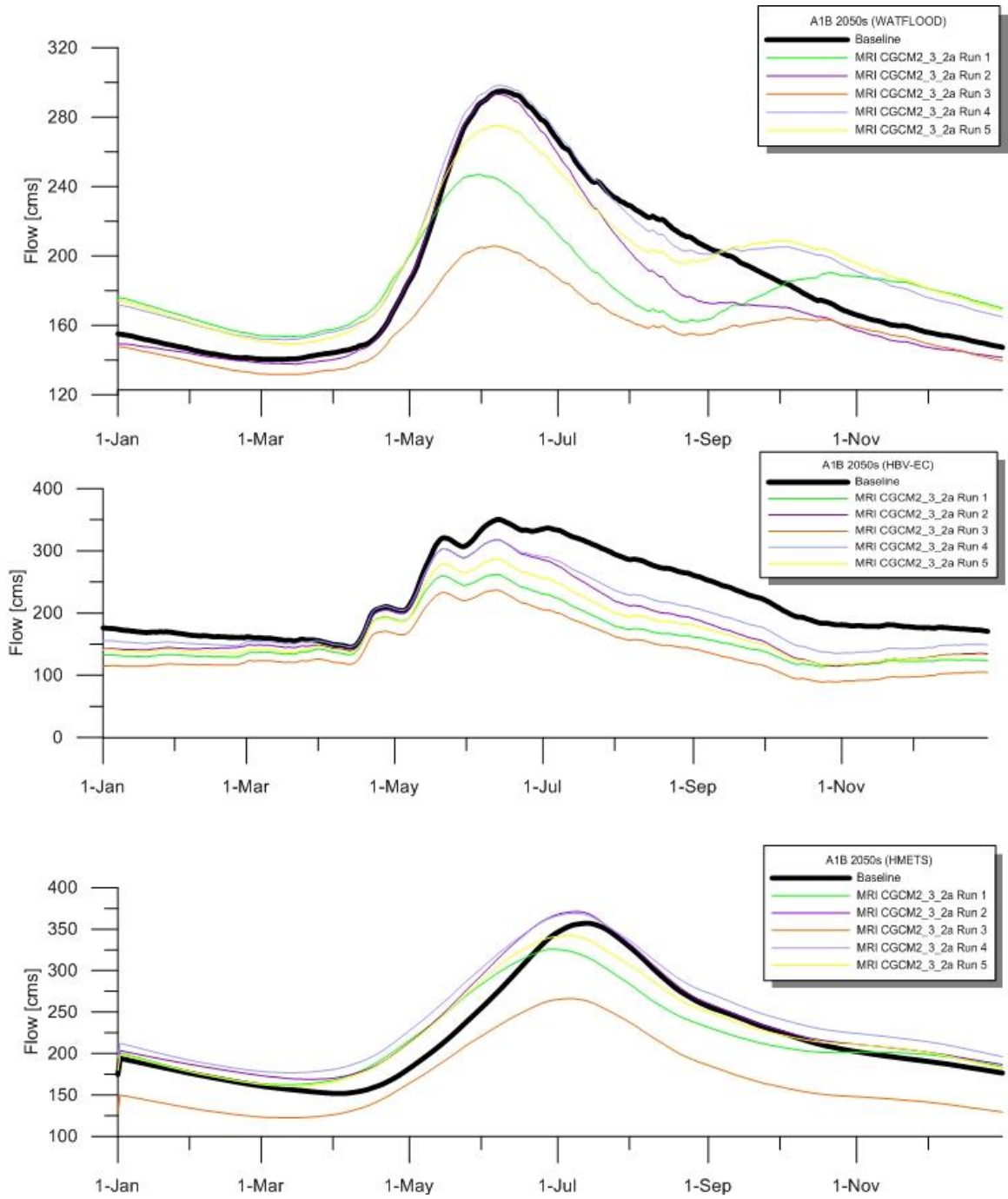
Figure 17: MRI A1B 2050s climate change hydrographs
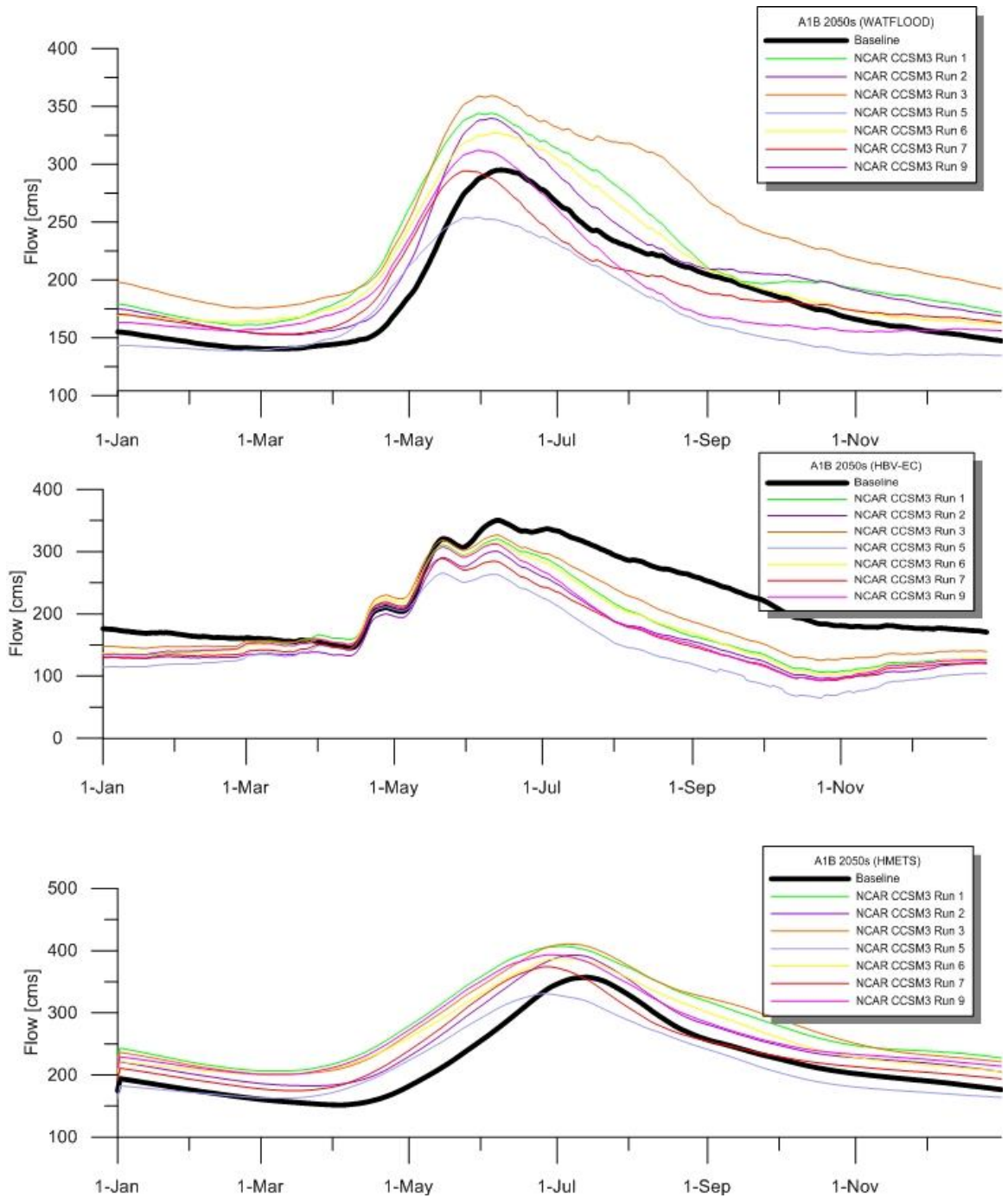
Figure 18: NCAR CCSM3 A1B 2050s climate change hydrographs
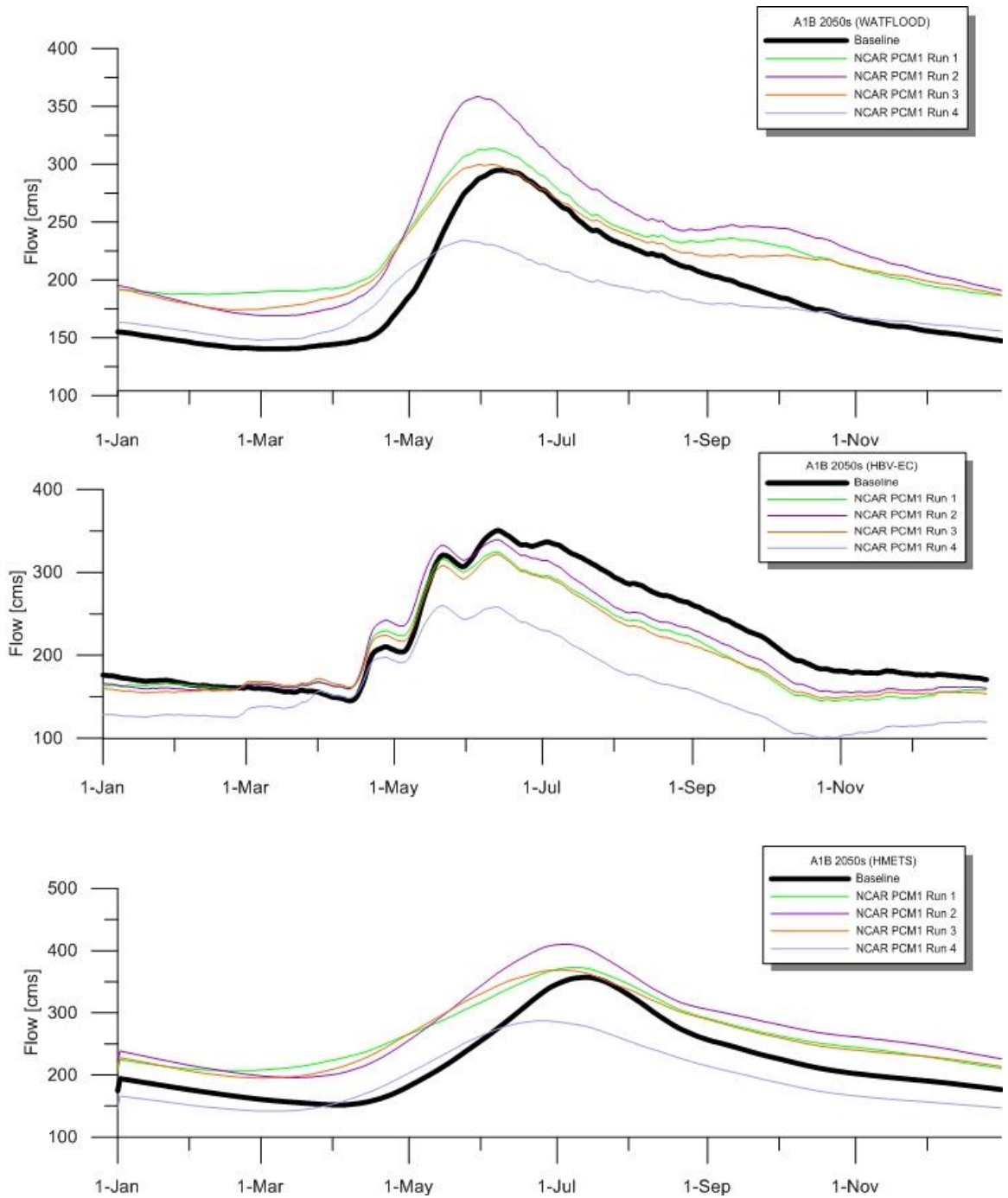
Figure 19: NCAR PCM1 A1B 2050s climate change hydrographs
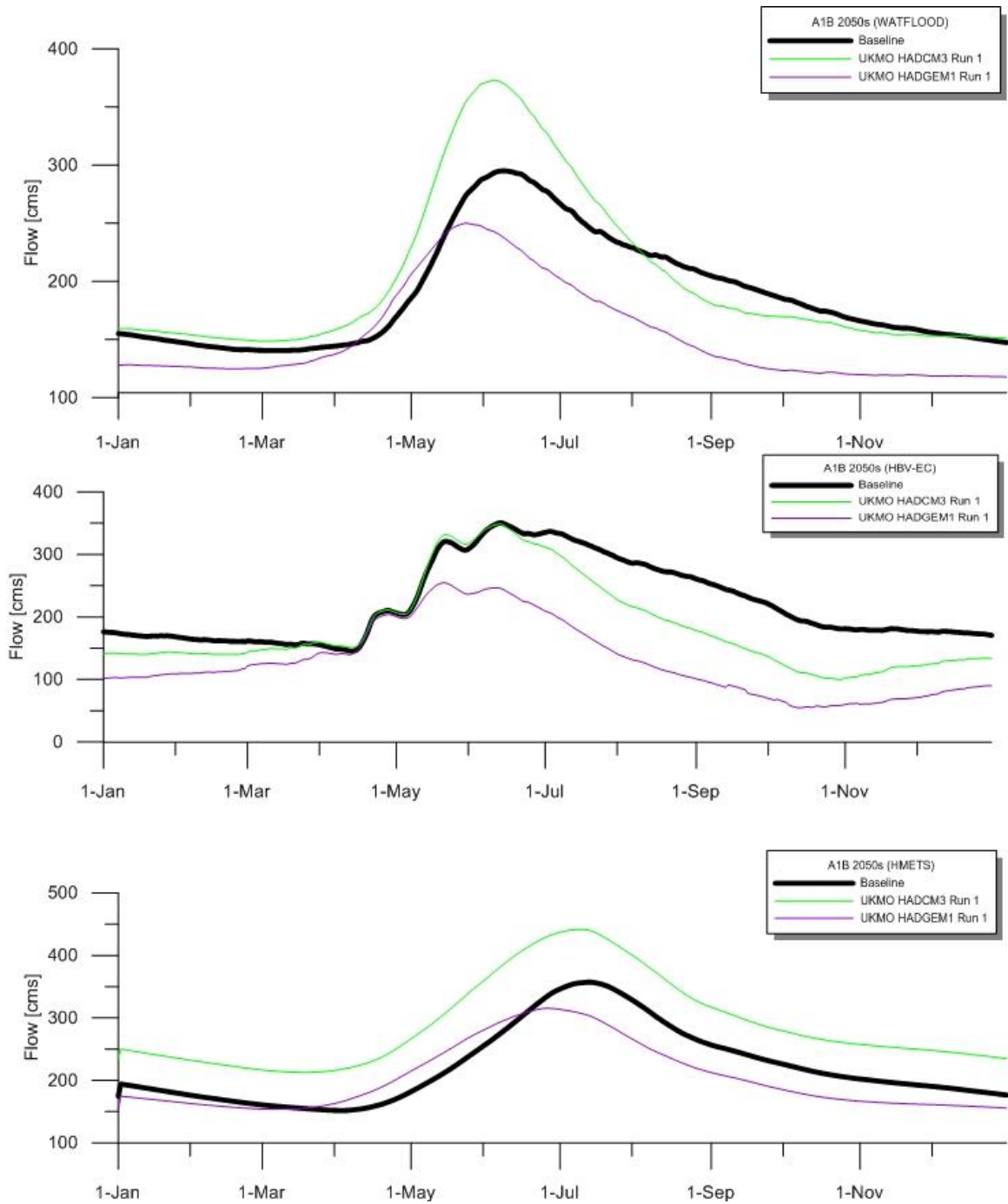
Figure 20: UKMO A1B 2050s climate change hydrographs

2050s A2
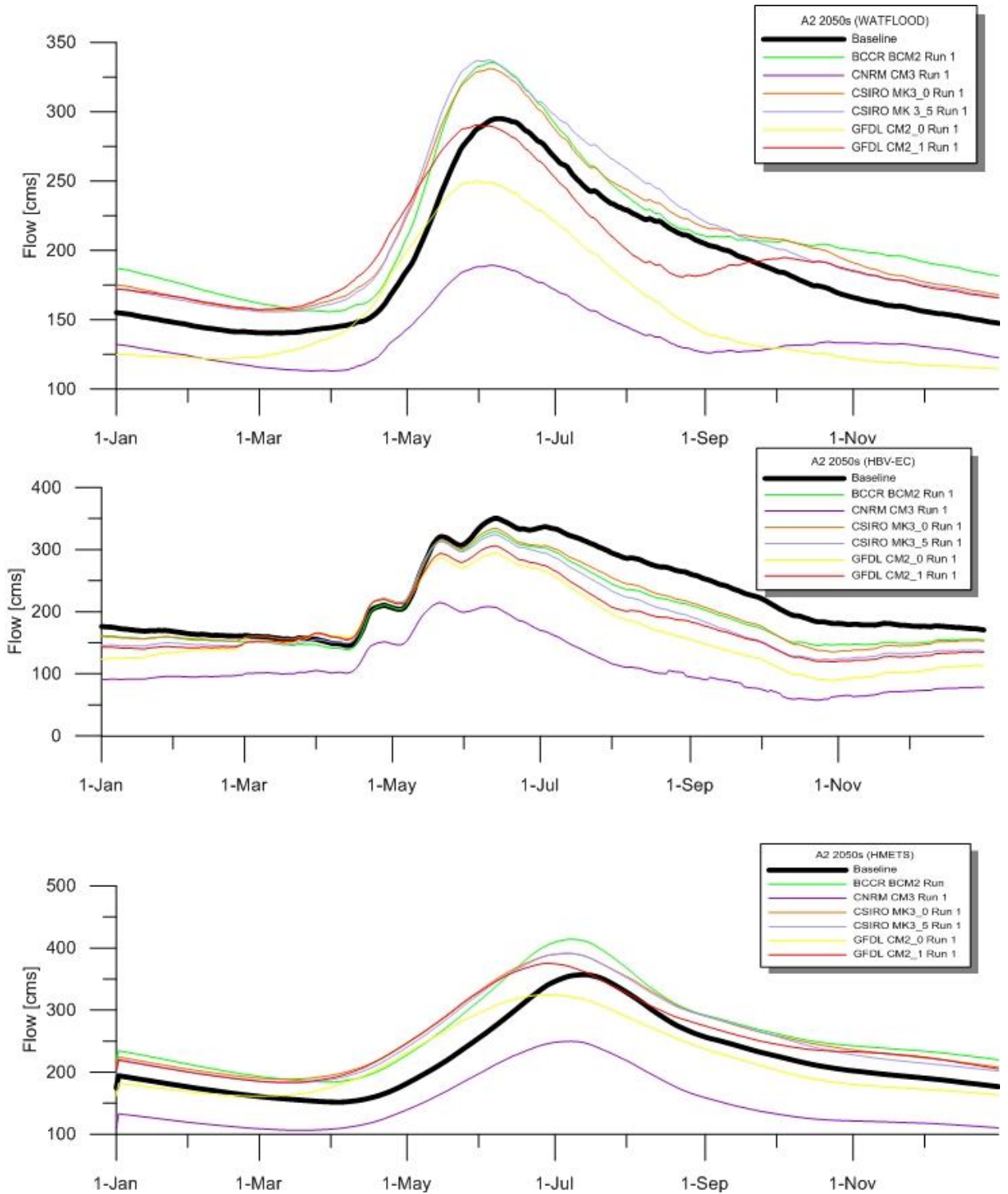
Figure 21: BCCR, CNRM, CSIRO, GFDL A2 2050s climate change hydrographs
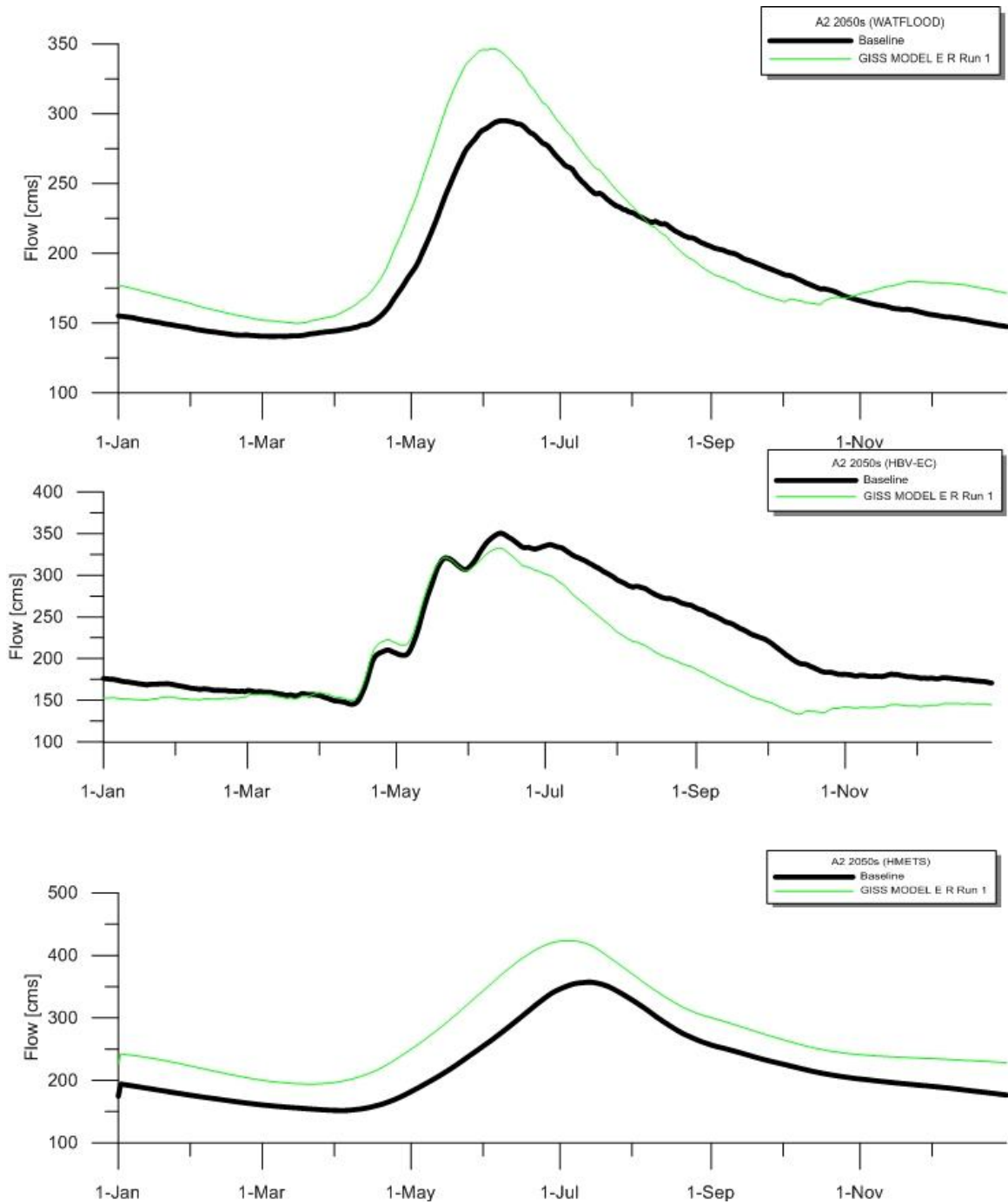
Figure 22: GISS A2 2050s climate change hydrographs
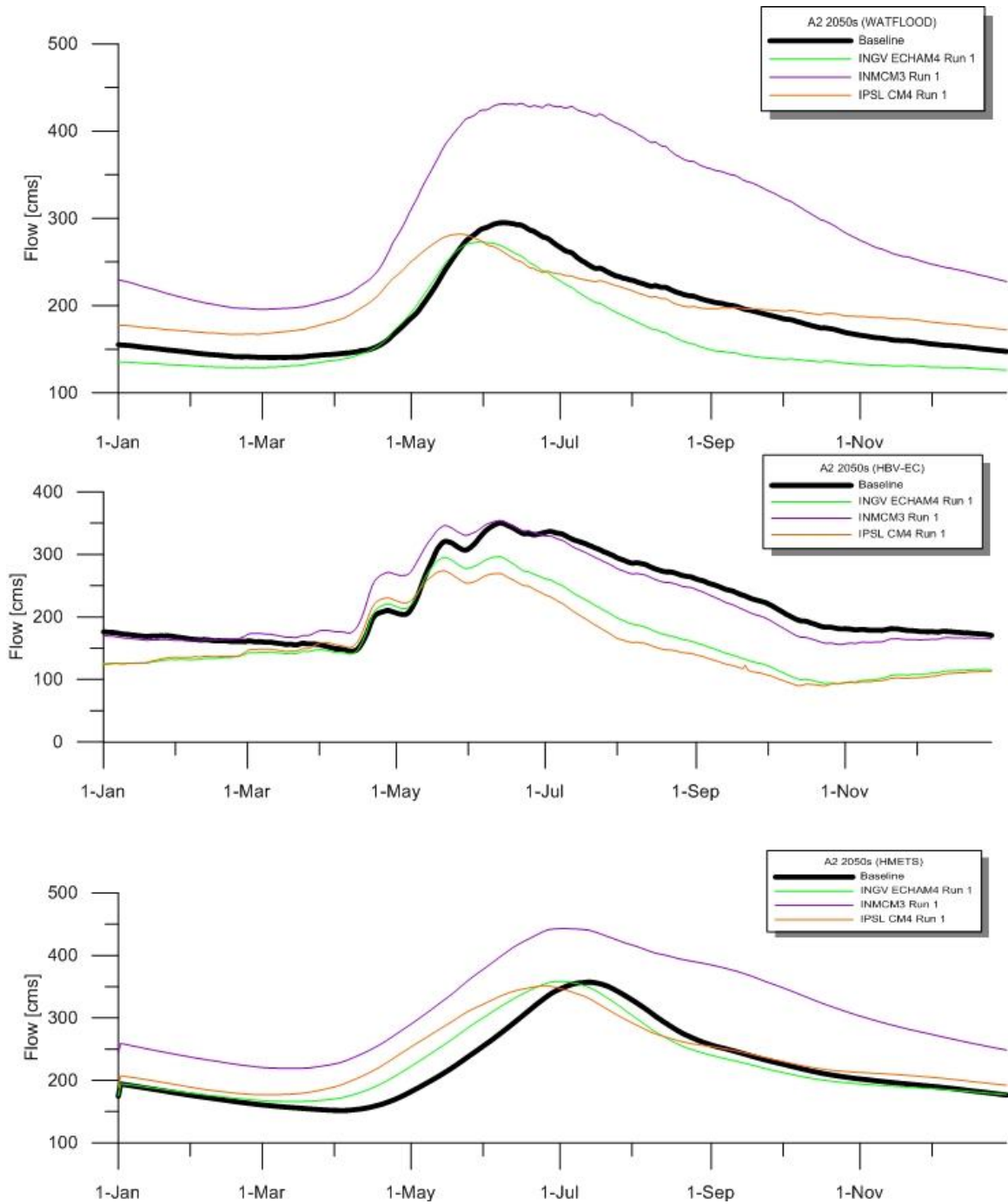
Figure 23: INGV, INMCM, IPSL A2 2050s climate change hydrographs
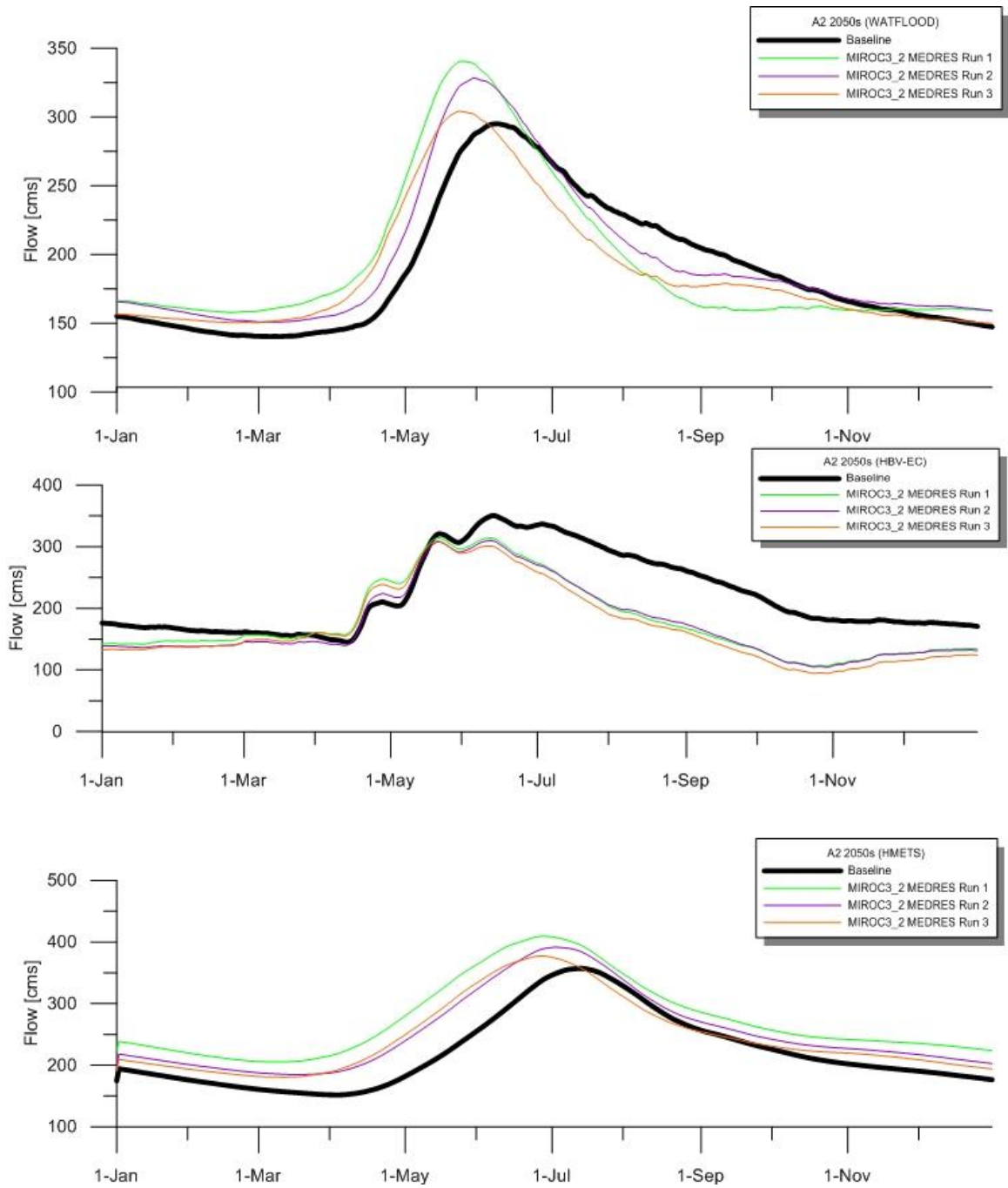
Figure 24: MIROC A2 2050s climate change hydrographs
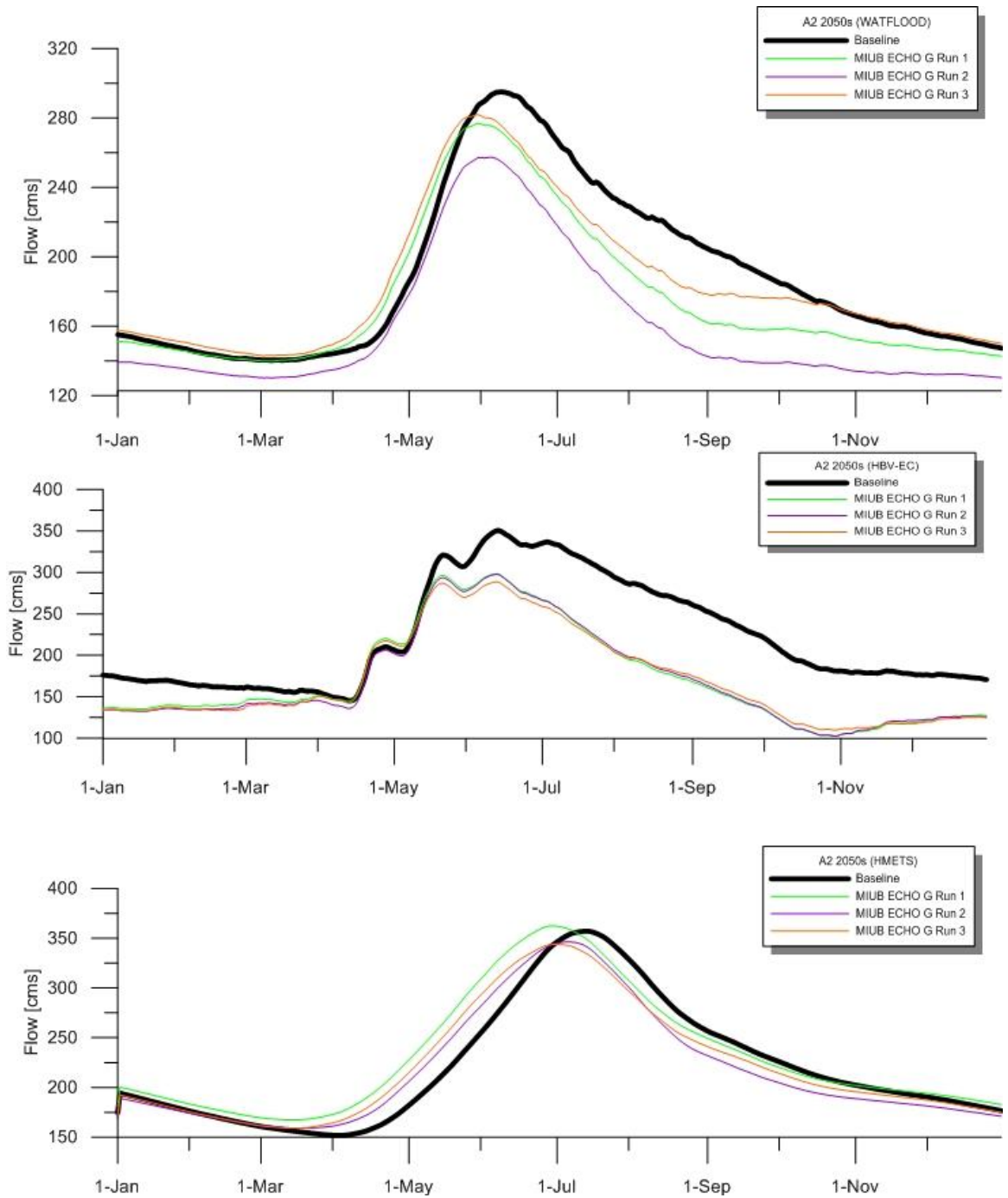
Figure 25: MIUB A2 2050s climate change hydrographs
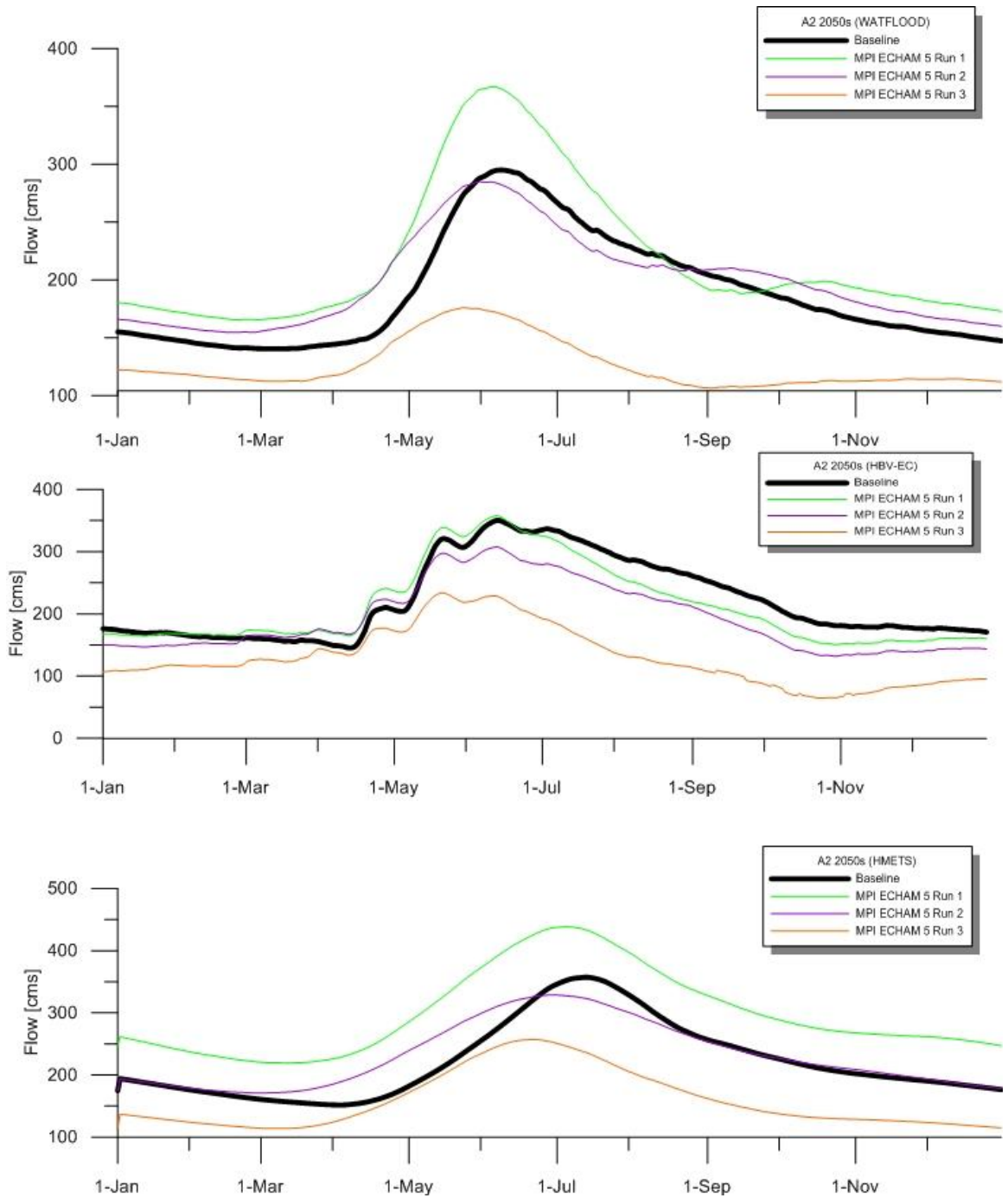
Figure 26: MPI A2 2050s climate change hydrographs
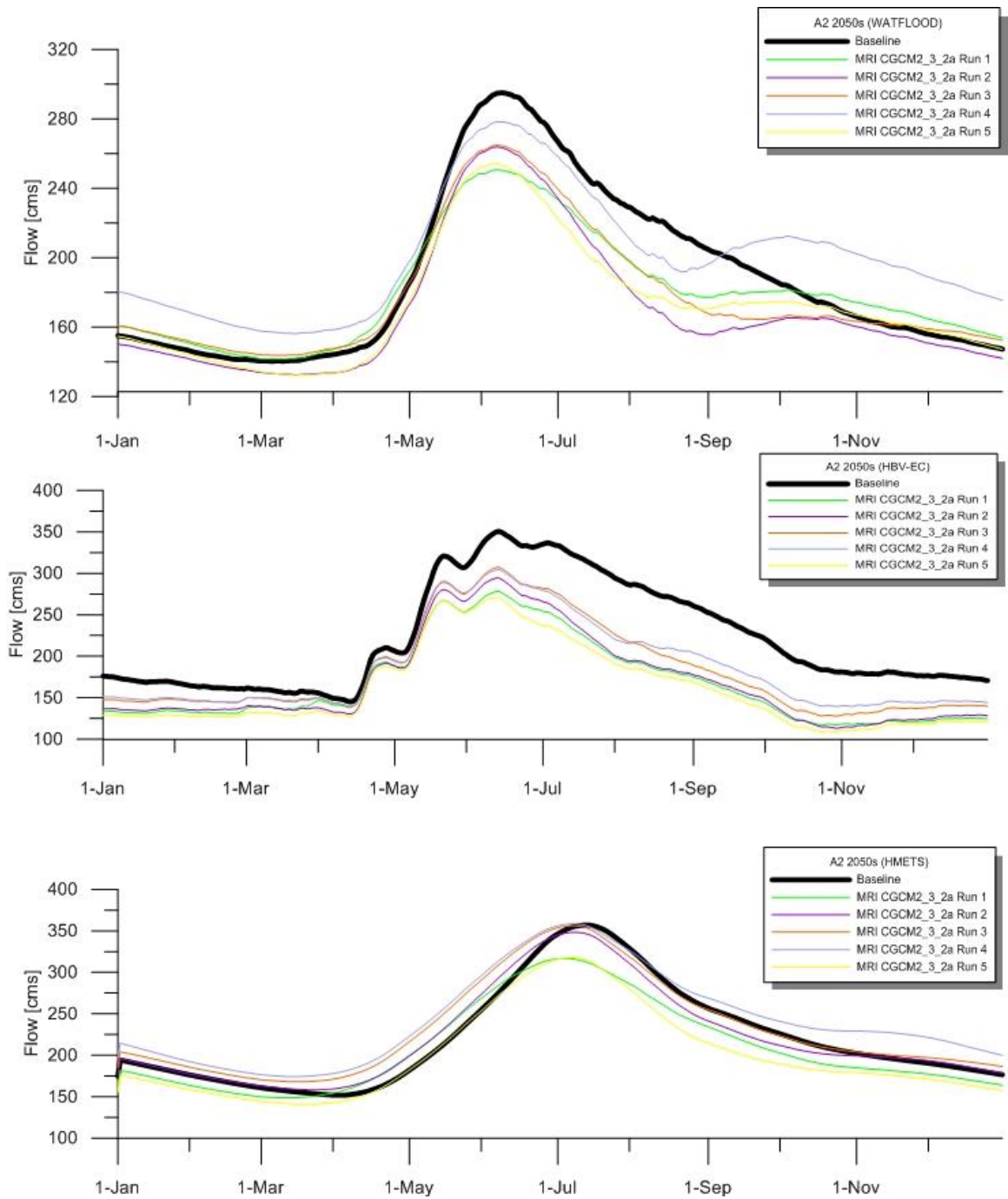
Figure 27: MRI A2 2050s climate change hydrographs
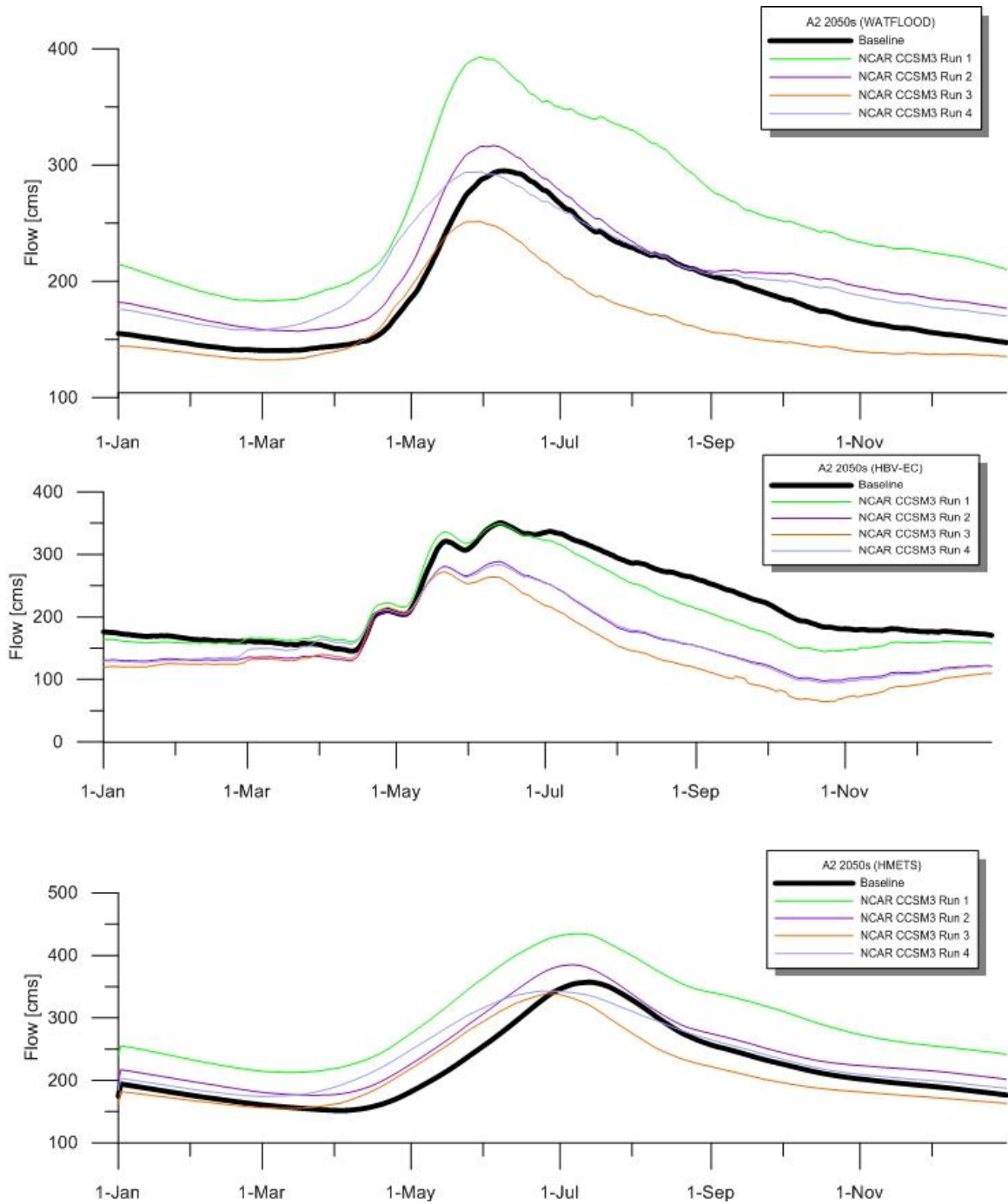
Figure 28: NCAR CCSM A2 2050s climate change hydrographs
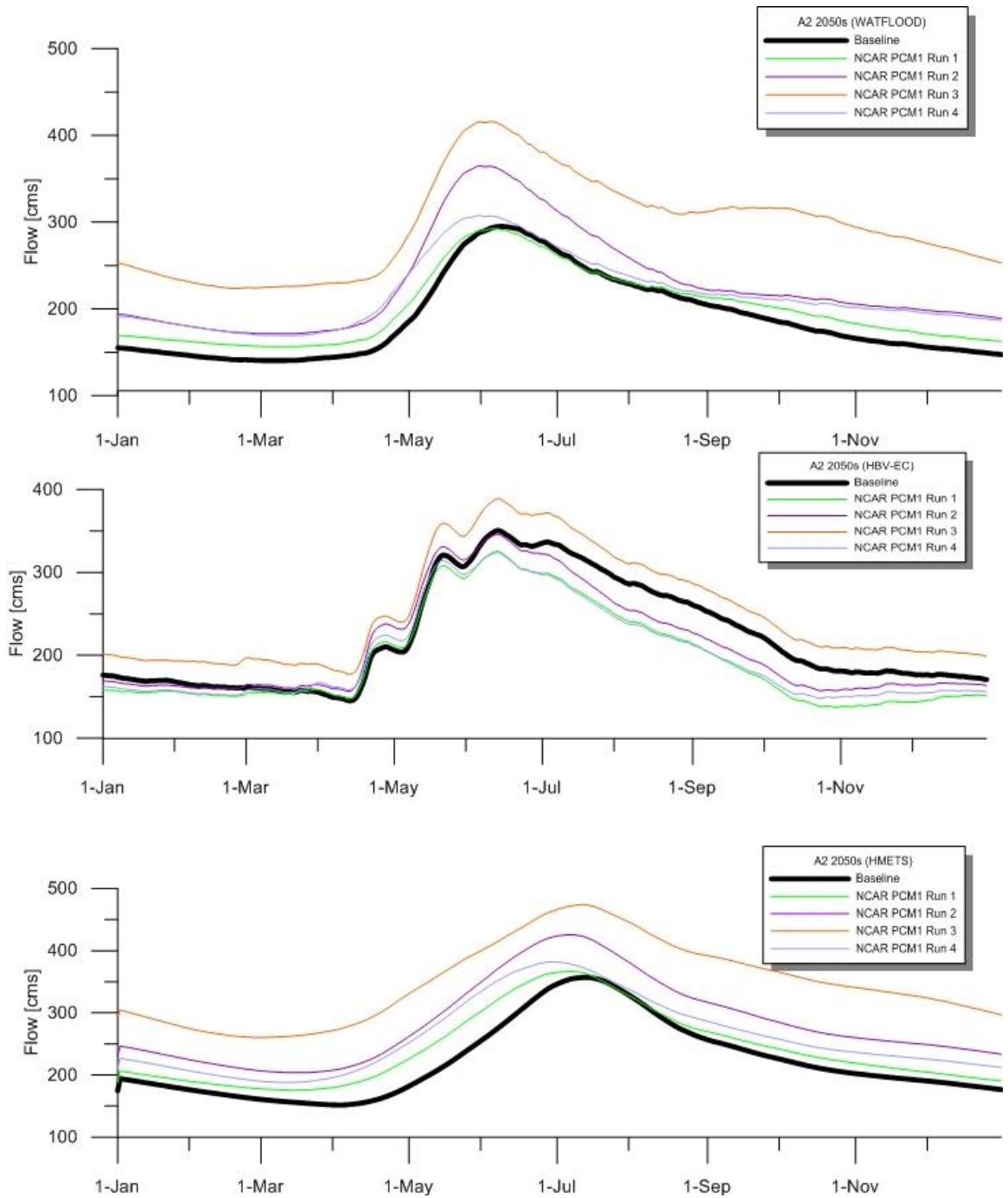
Figure 29: NCAR PCM A2 2050s climate change hydrographs
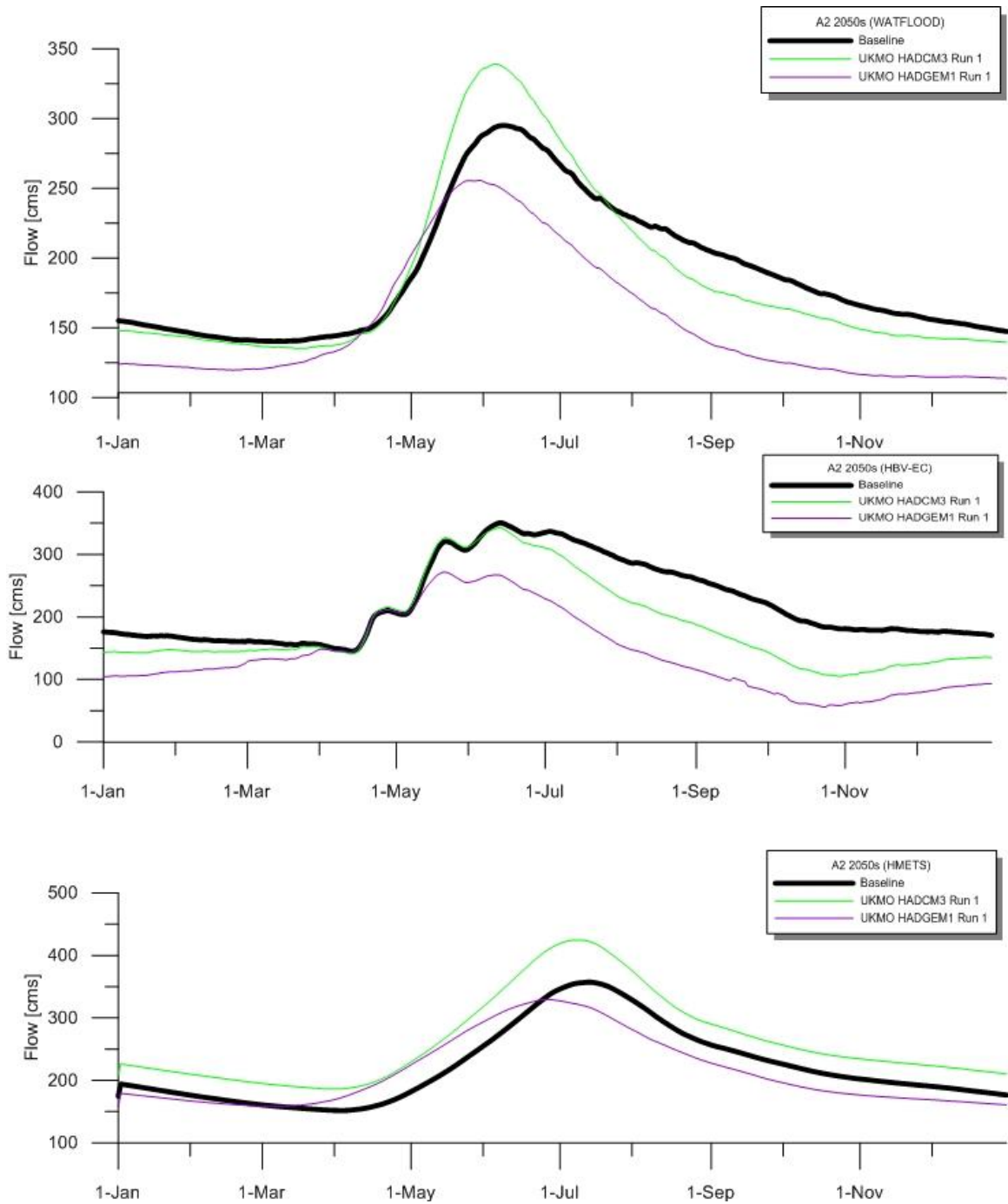
Figure 30: UKMO A2 2050s climate change hydrographs

2080s B1
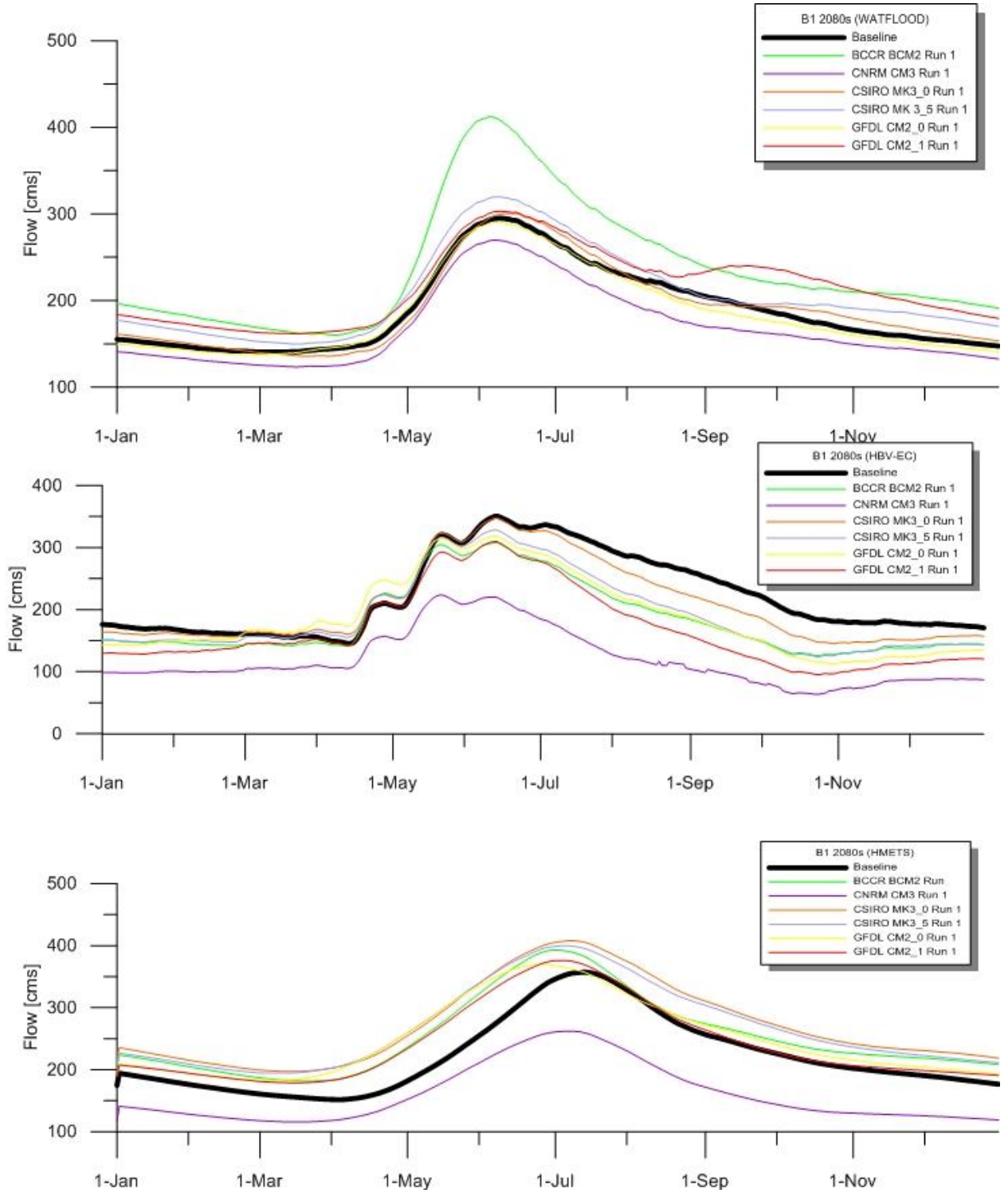
Figure 31: BCCR, CNRM, CSIRO, GFDL B1 2080s climate change hydrographs
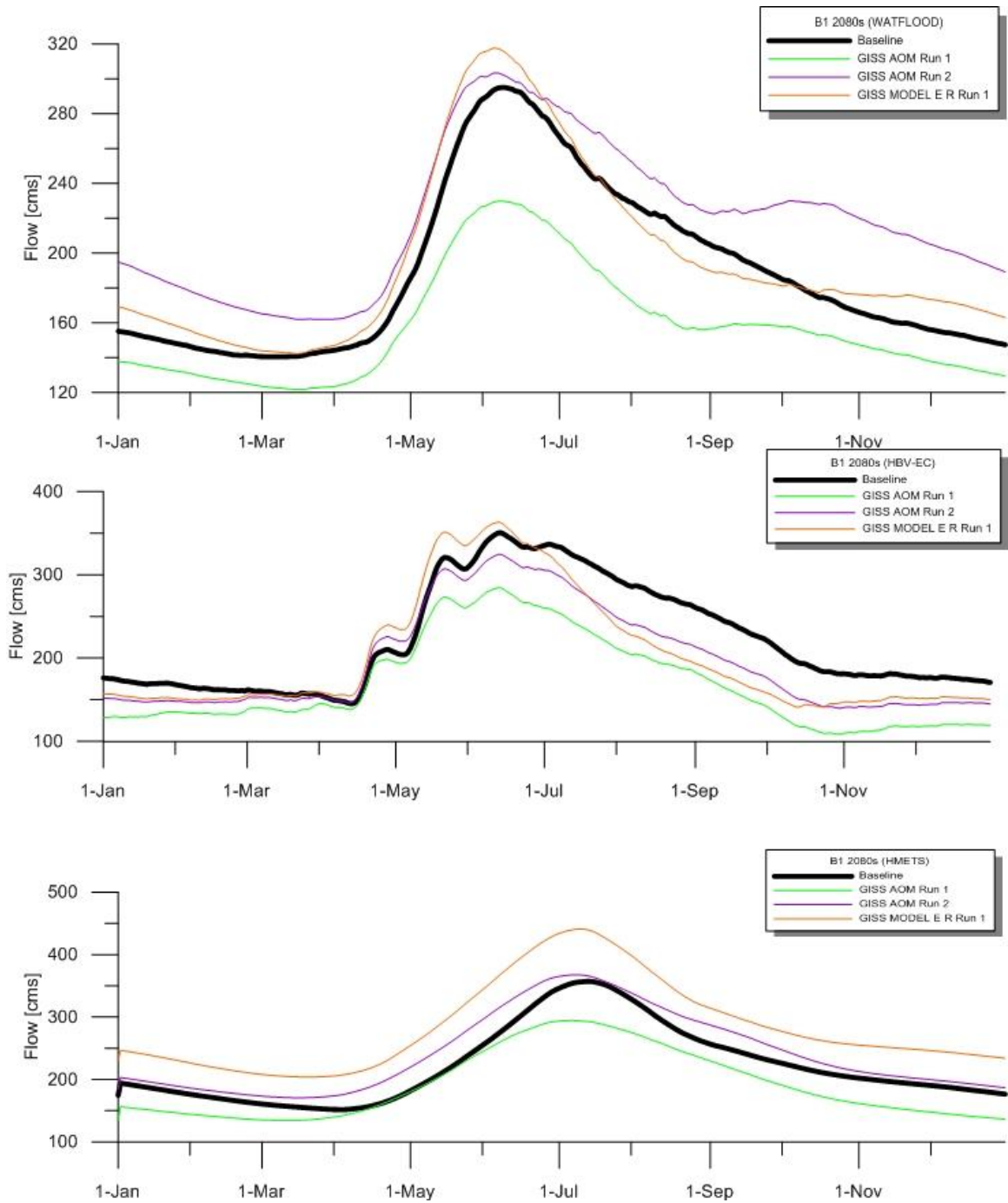
Figure 32: GISS B1 2080s climate change hydrographs
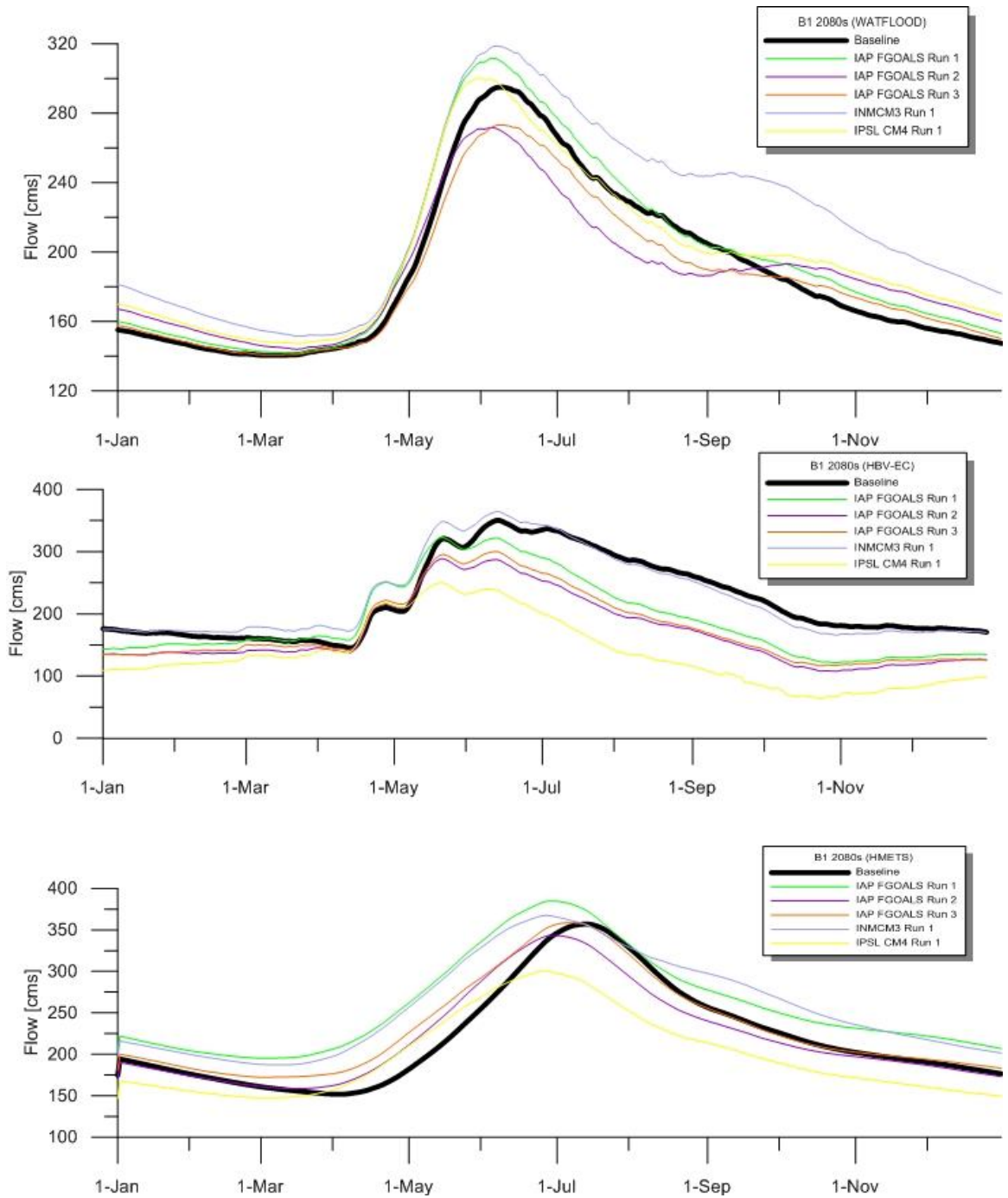
Figure 33: IAP, INMCM, IPSL B1 2080s climate change hydrographs
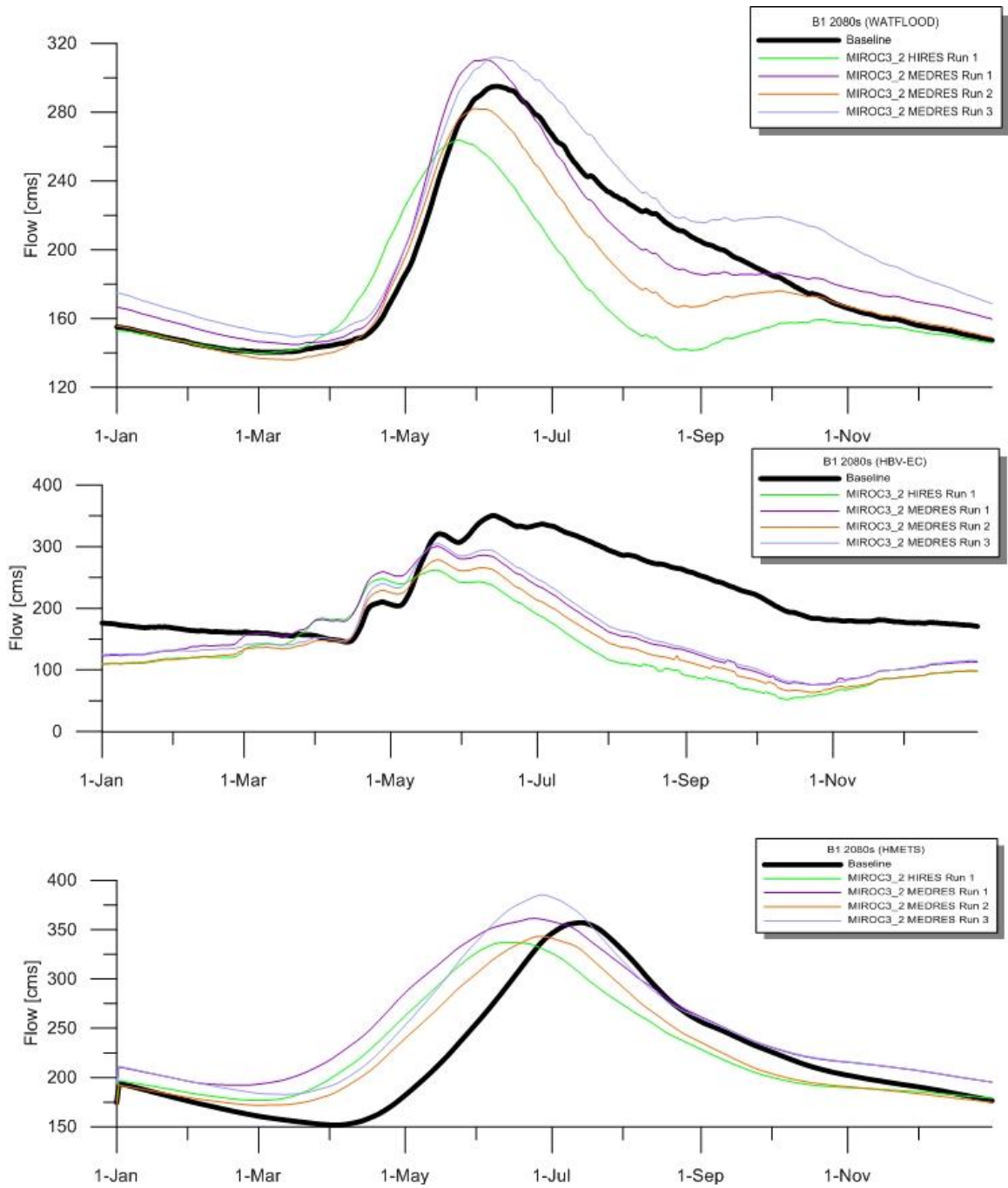
Figure 34: MIROC B1 2080s climate change hydrographs
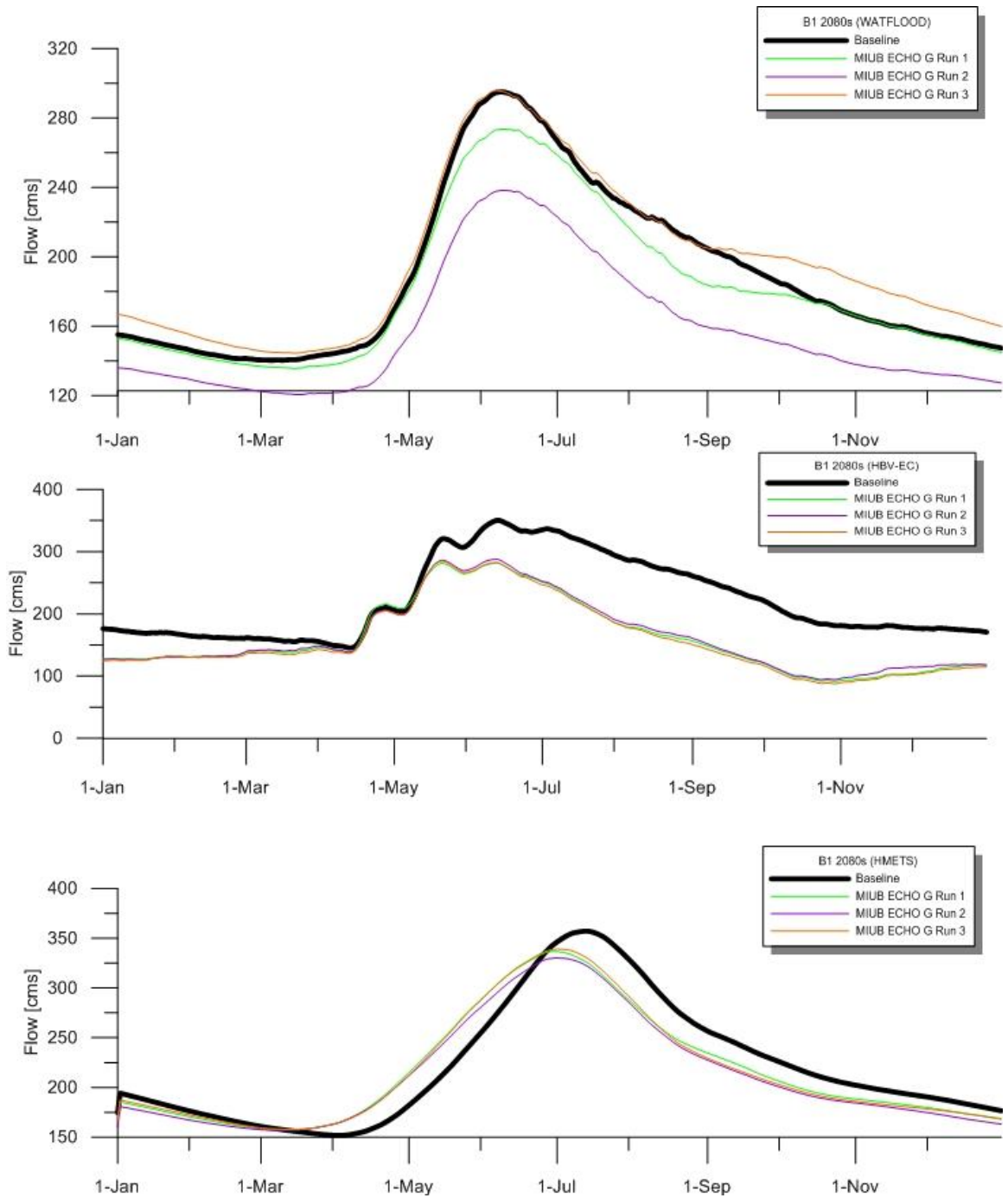
Figure 35: MIUB B1 2080s climate change hydrographs
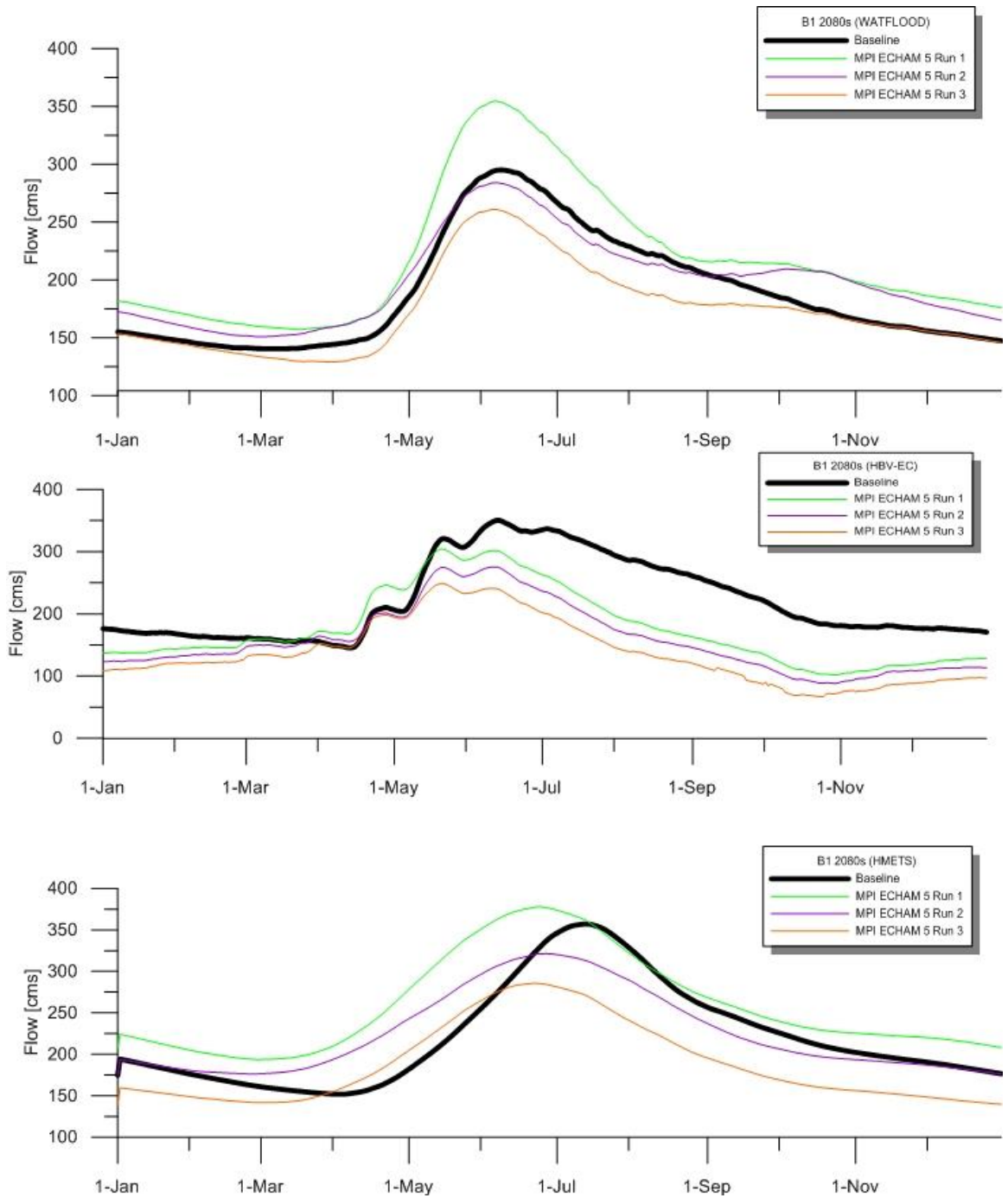
Figure 36: MPI B1 2080s climate change hydrographs
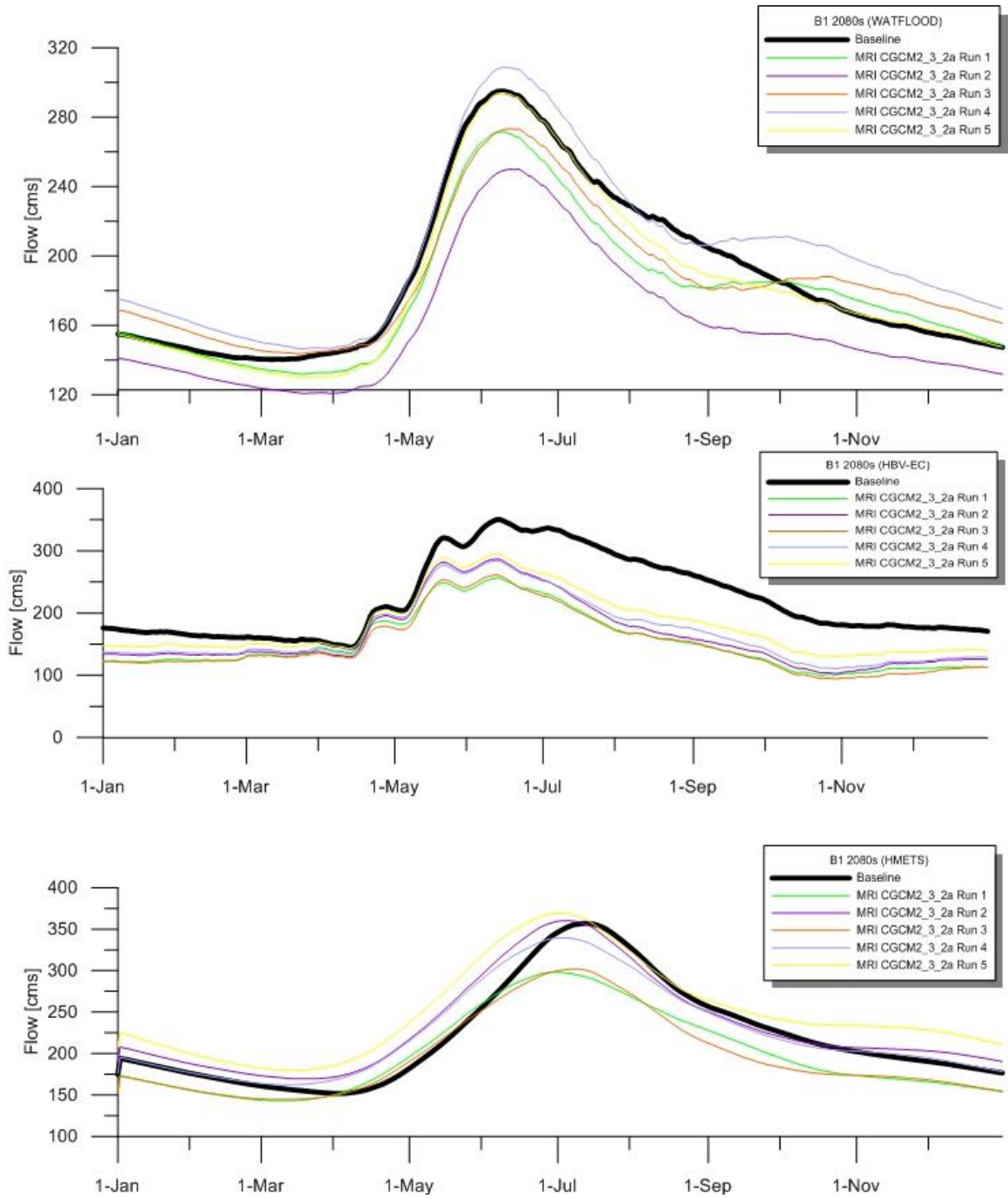
Figure 37: MRI B1 2080s climate change hydrographs
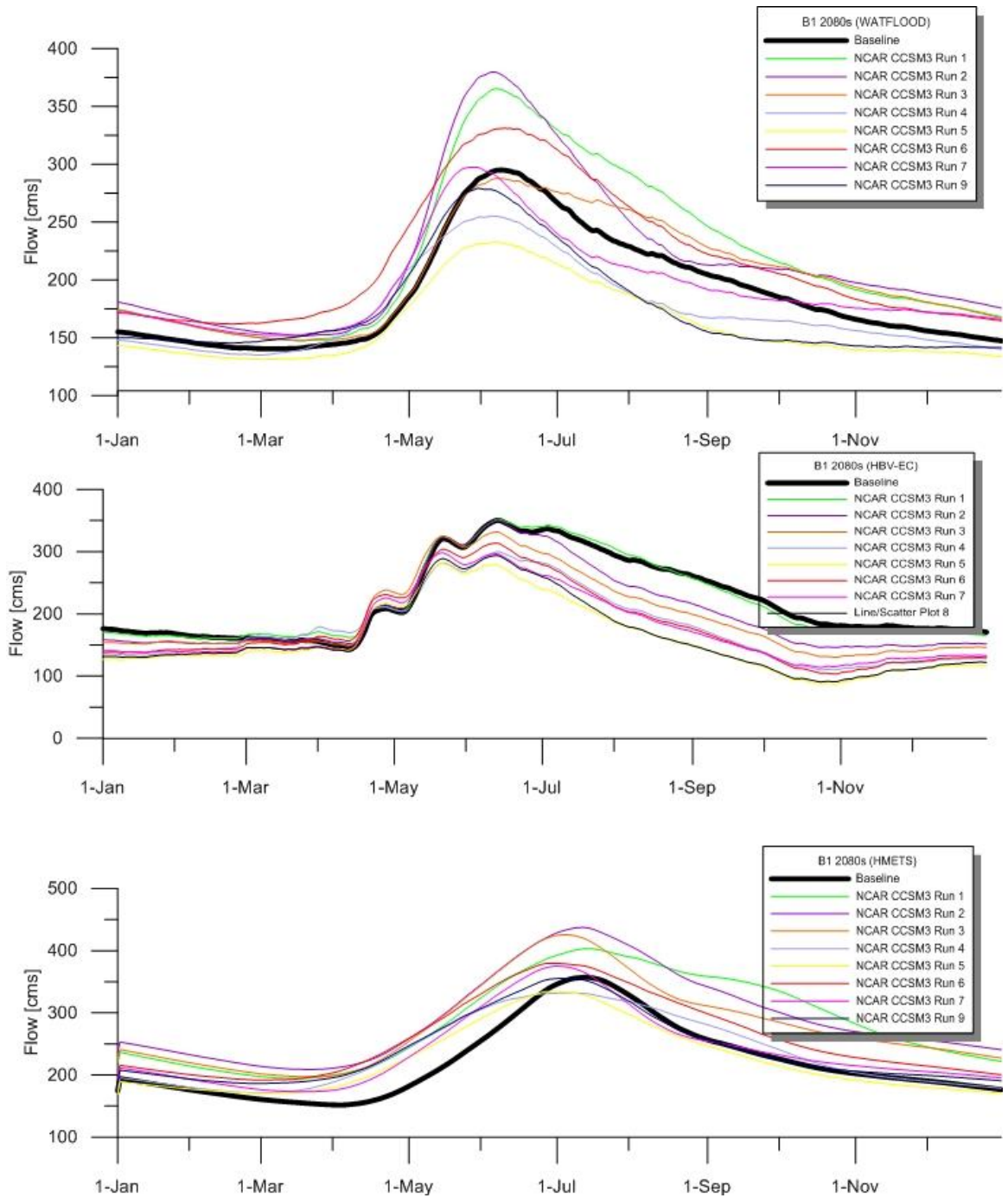
Figure 38: NCAR CCSM3 B1 2080s climate change hydrographs
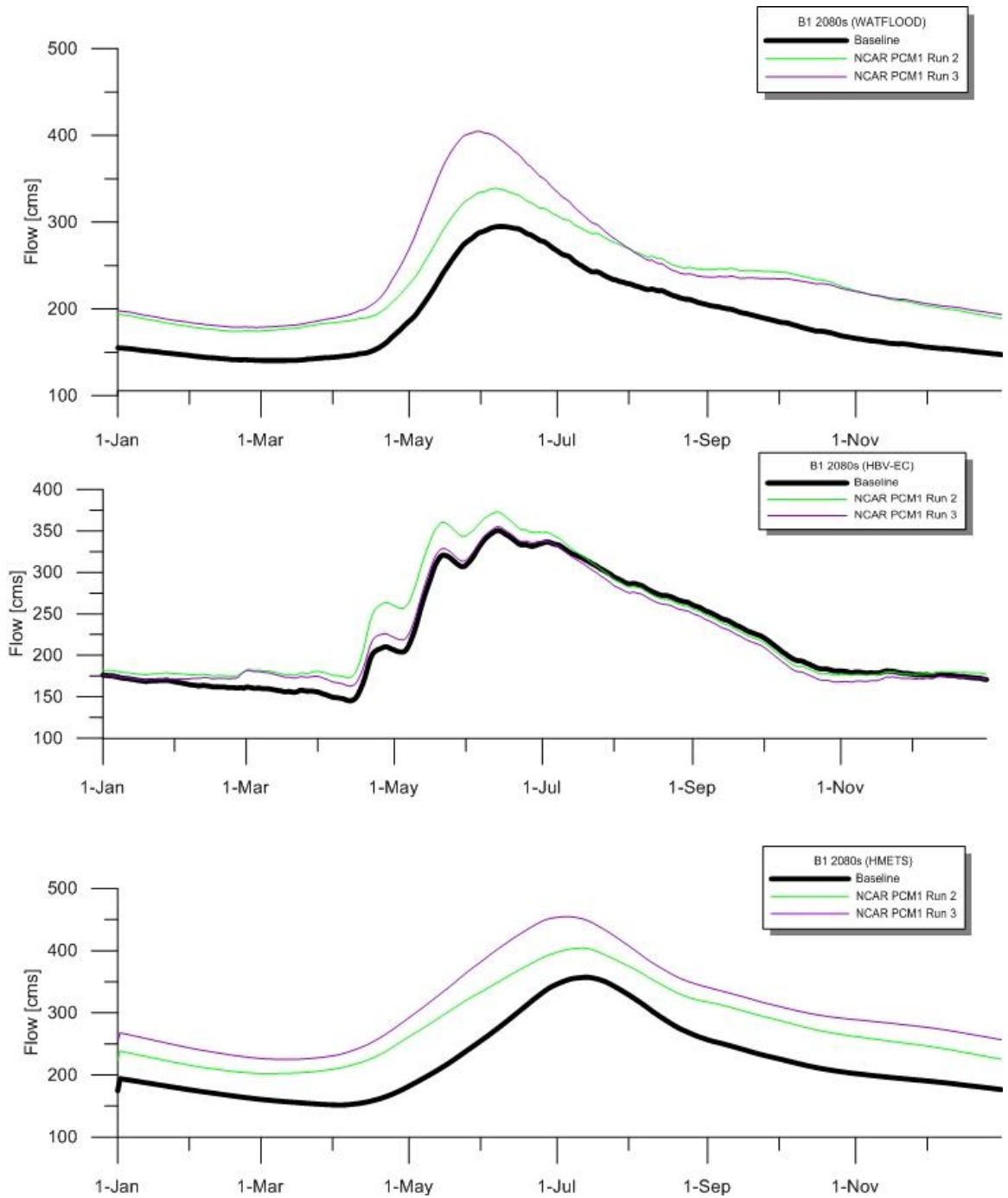
Figure 39: NCAR PCM1 B1 2080s climate change hydrographs
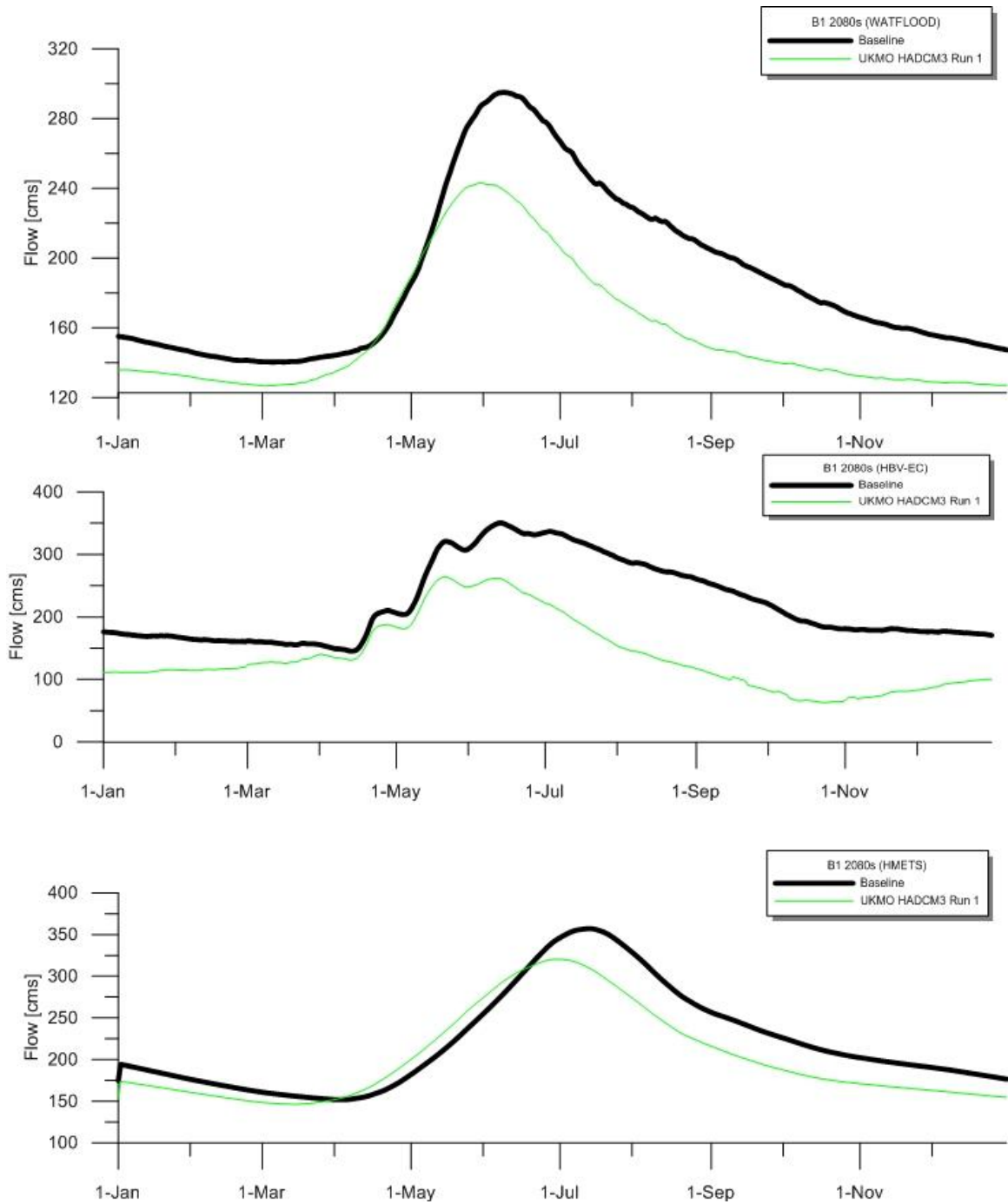
Figure 40: UKMO B1 2080s climate change hydrographs

2080s A1B
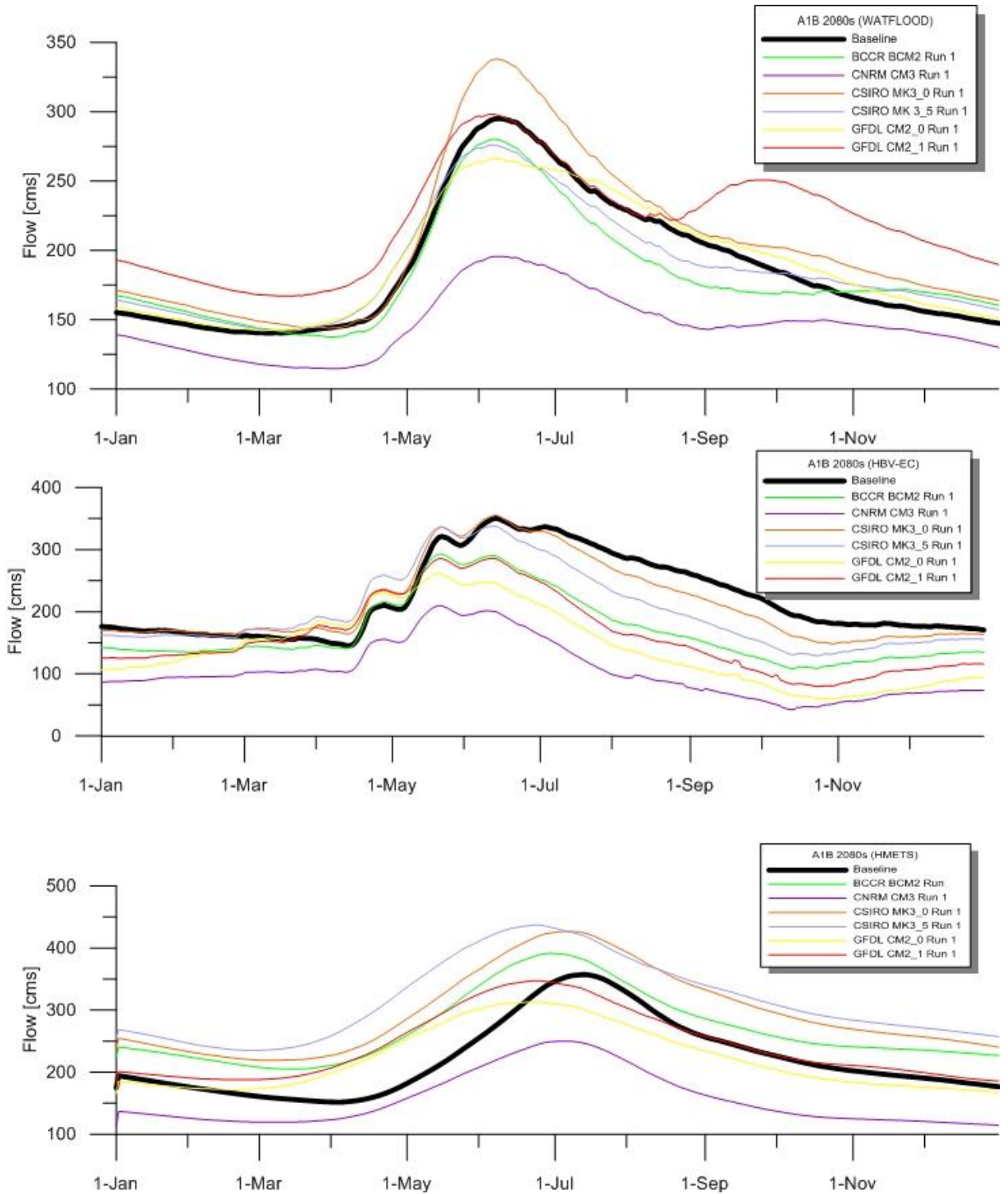
Figure 41: BCCR, CNRM, CSIRO, GFDL A1B 2080s climate change hydrographs
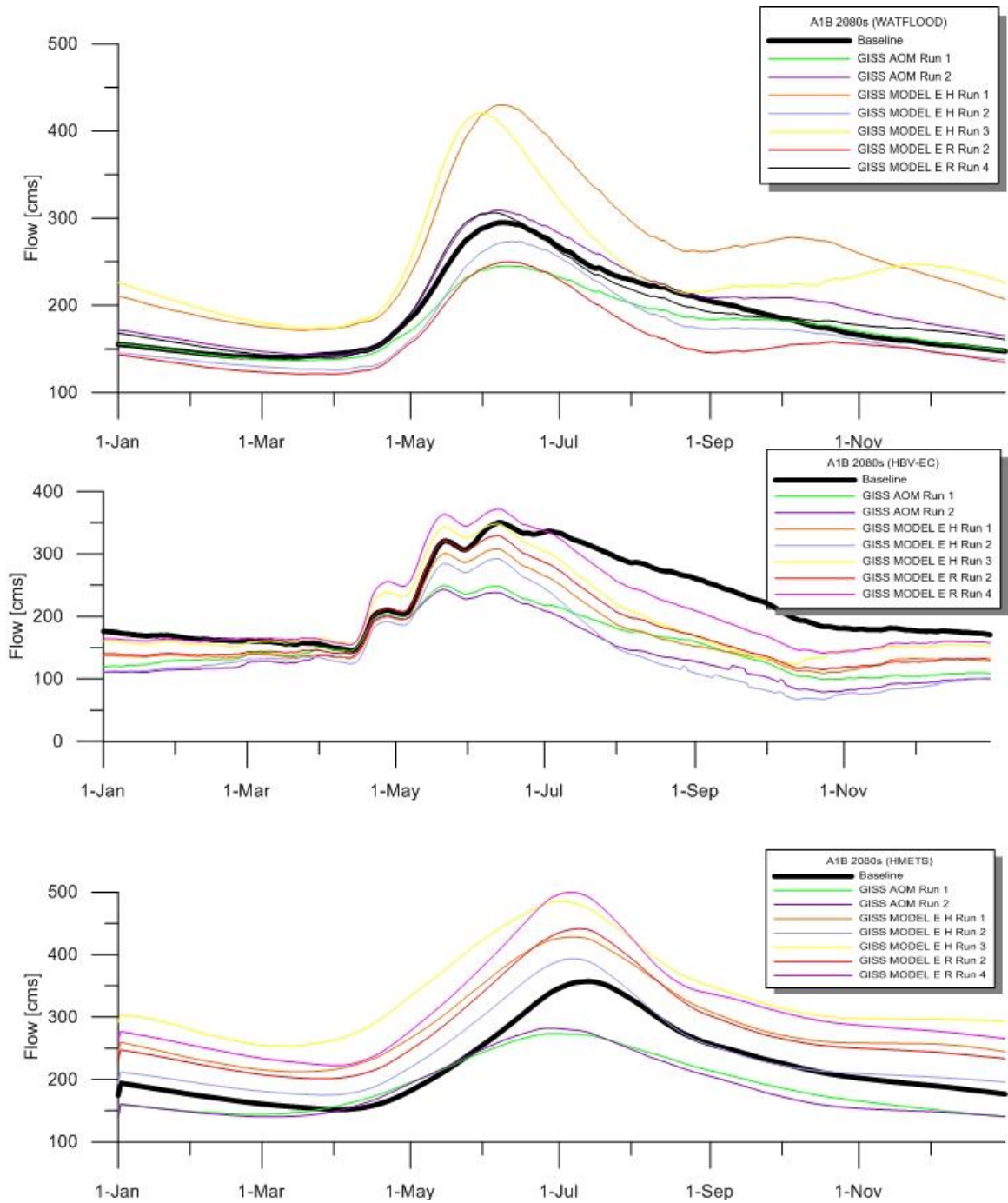
Figure 42: GISS A1B 2080s climate change hydrographs
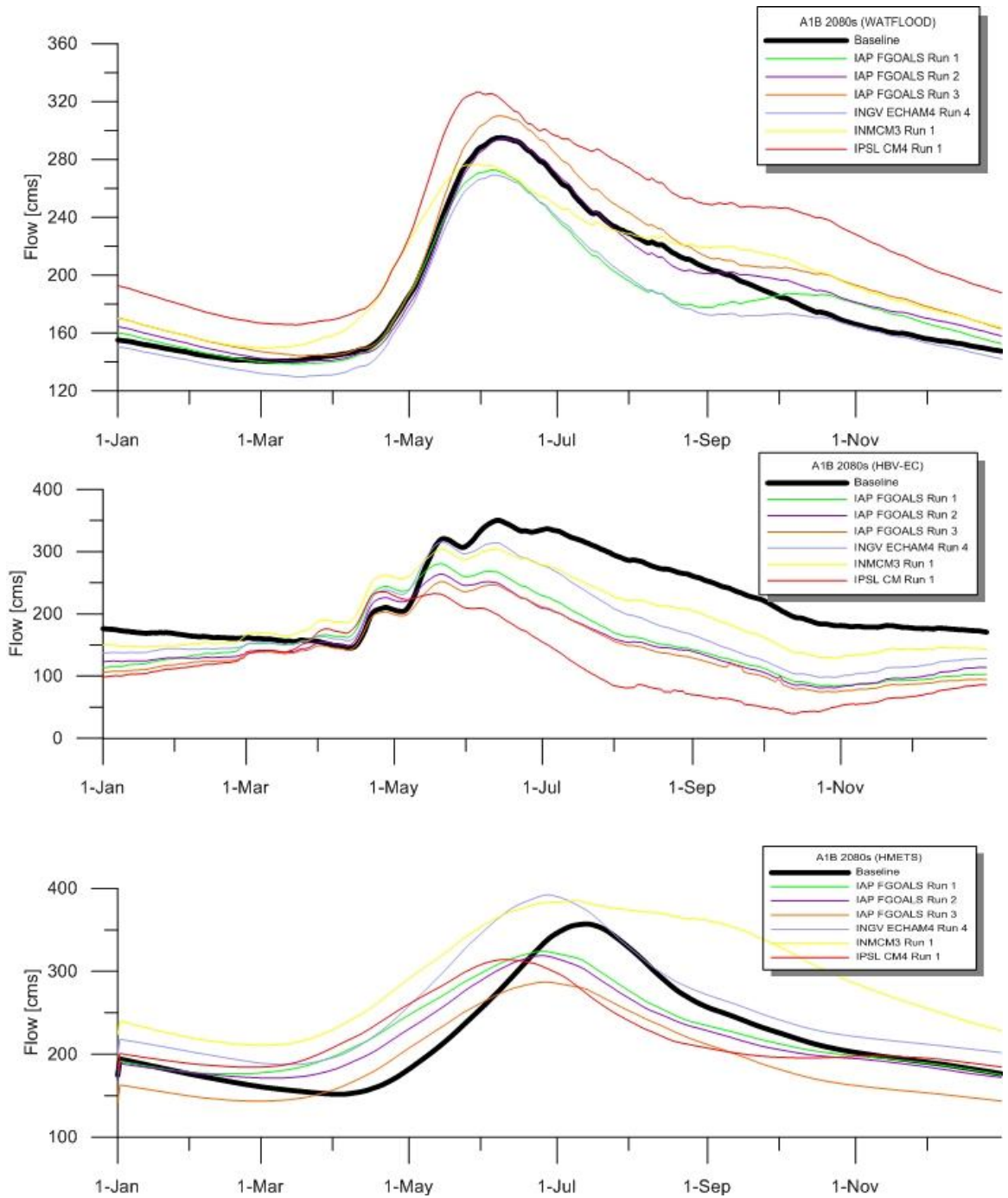
Figure 43: IAP, INGV, INMCM, IPSL A1B 2080s climate change hydrographs
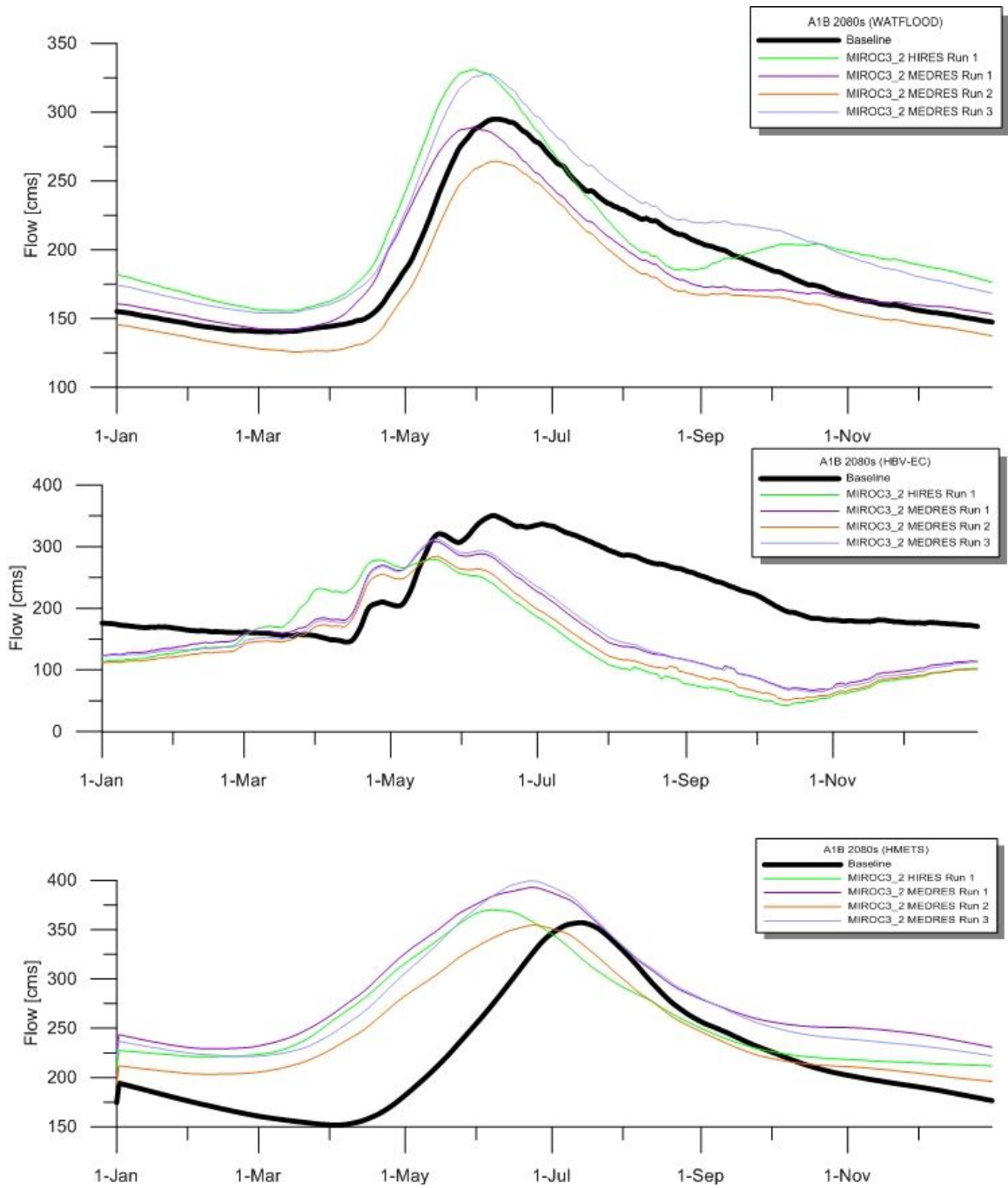
Figure 44: MIROC A1B 2080s climate change hydrographs
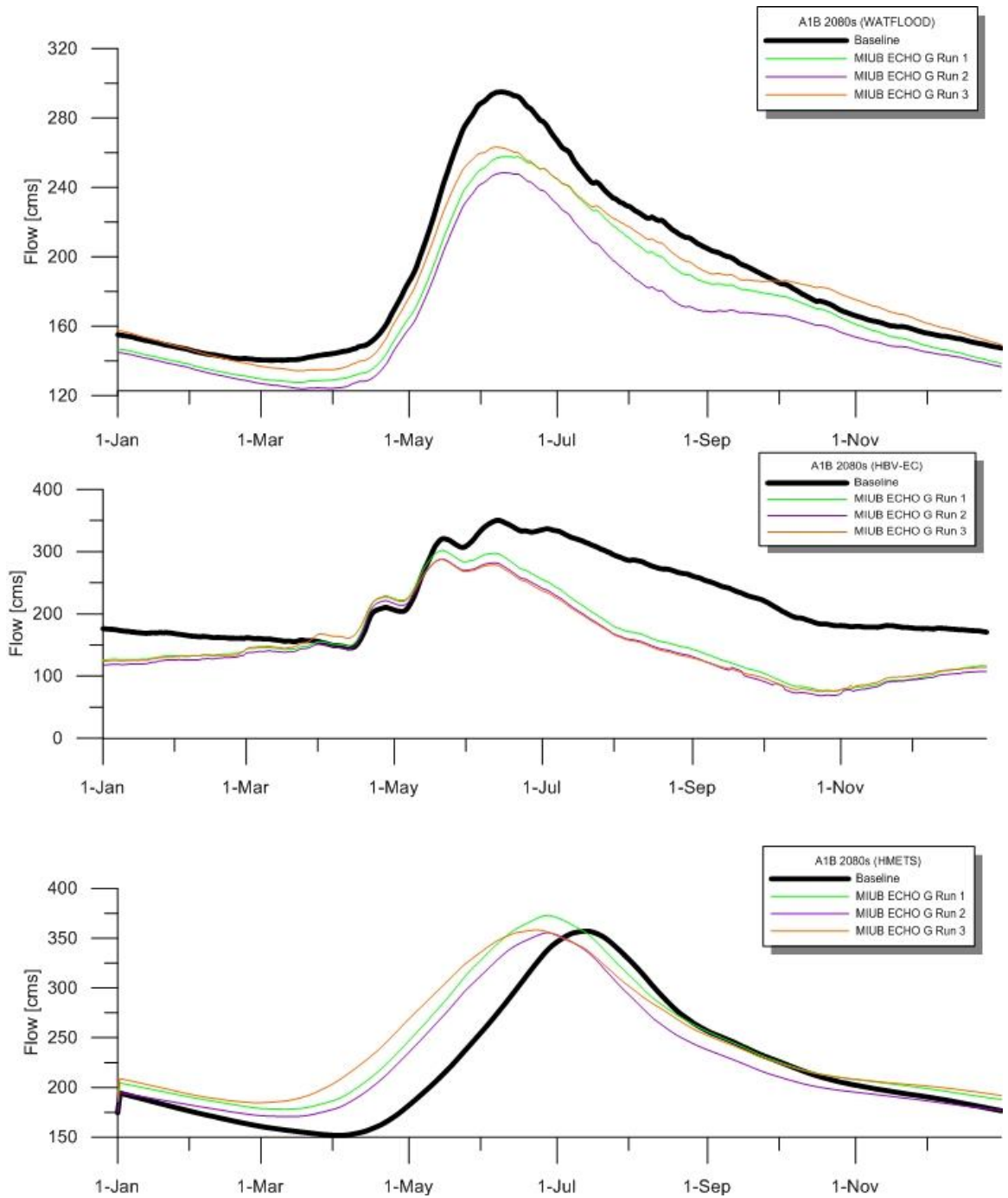
Figure 45: MIUB A1B 2080s climate change hydrographs
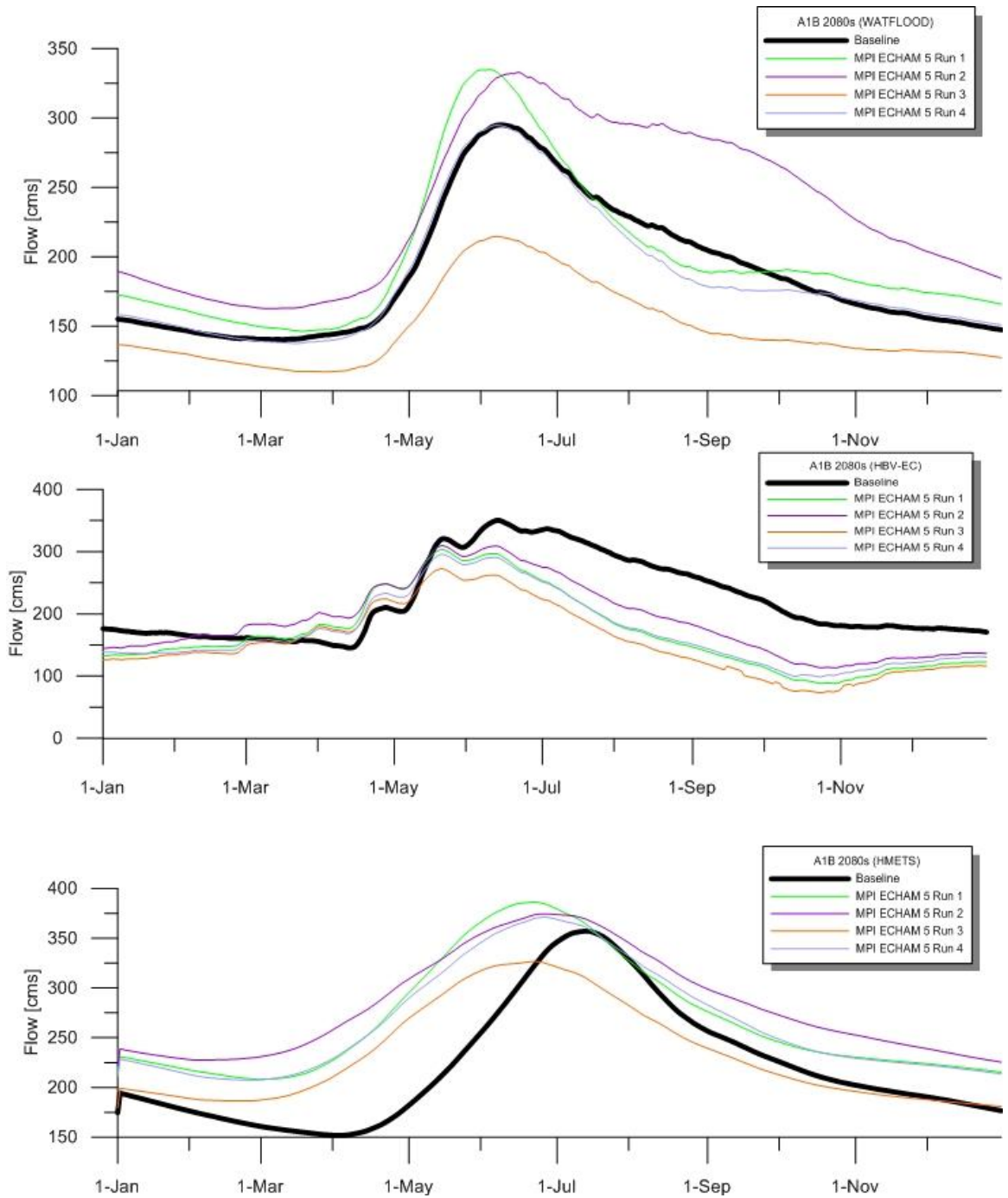
Figure 46: MPI A1B 2080s climate change hydrographs
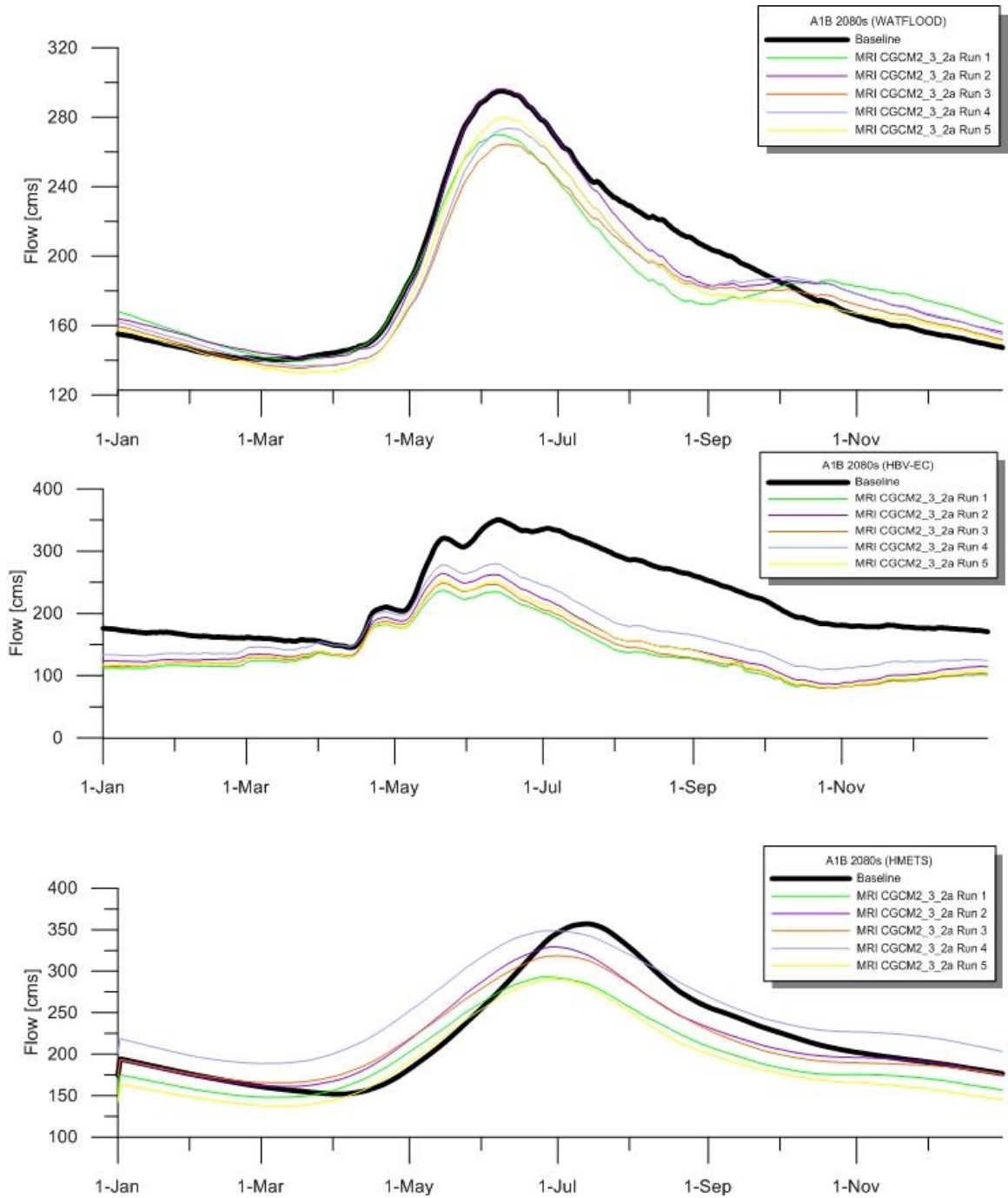
Figure 47: MRI A1B 2080s climate change hydrographs
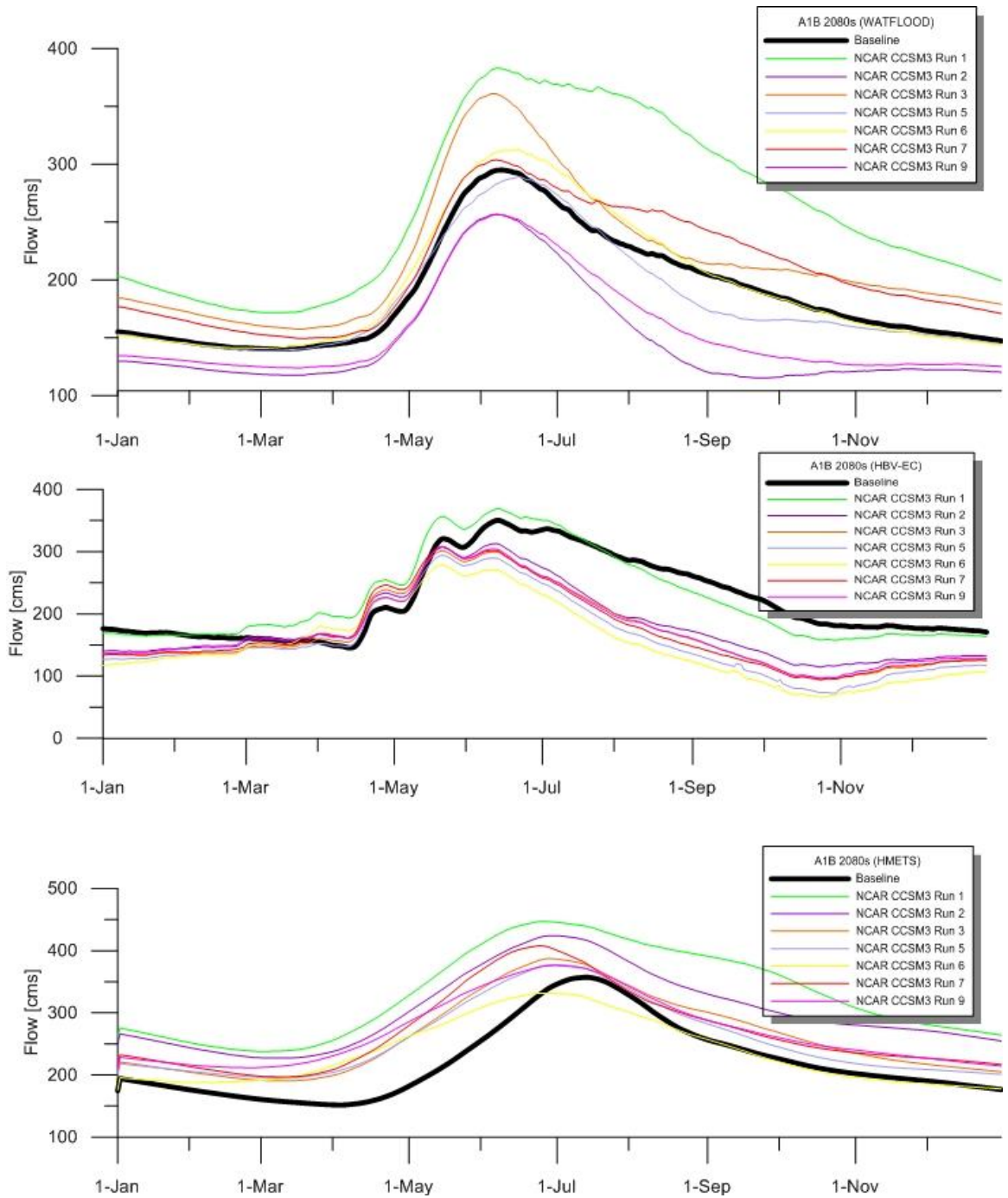
Figure 48: NCAR CCSM3 A1B 2080s climate change hydrographs
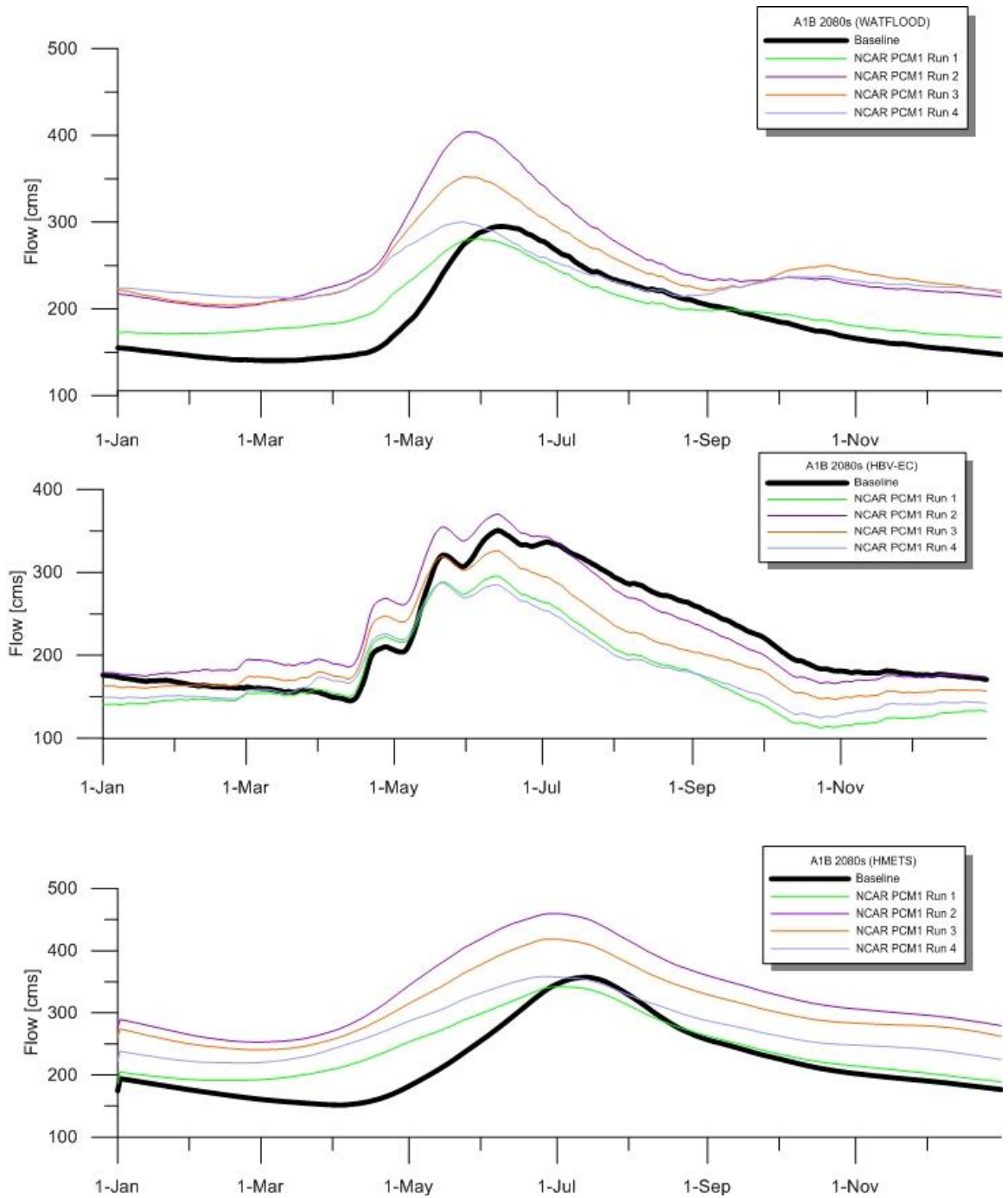
Figure 49: NCAR PCM1 A1B 2080s climate change hydrographs
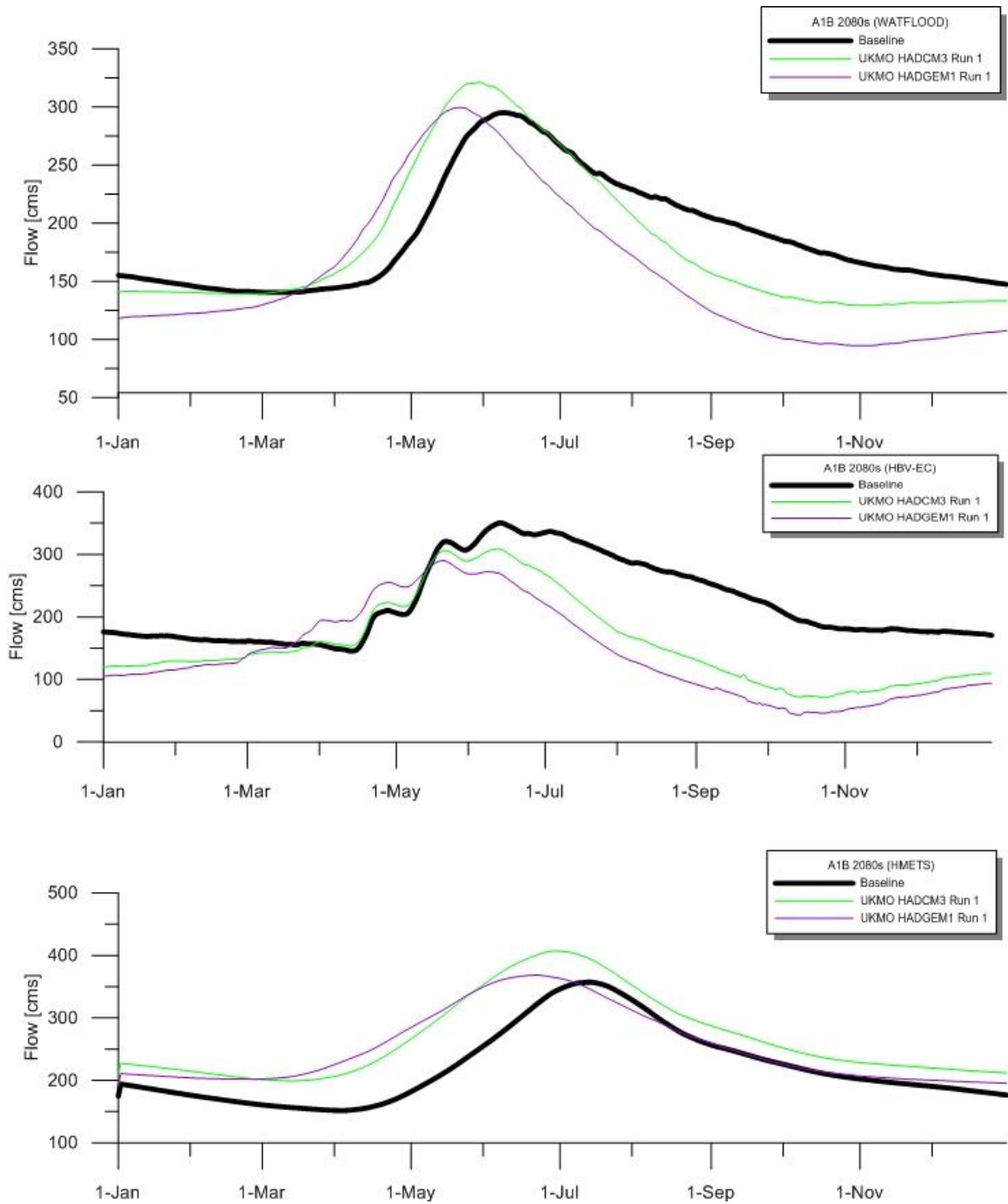
Figure 50: UKMO A1B 2080s climate change hydrographs

2080s A2
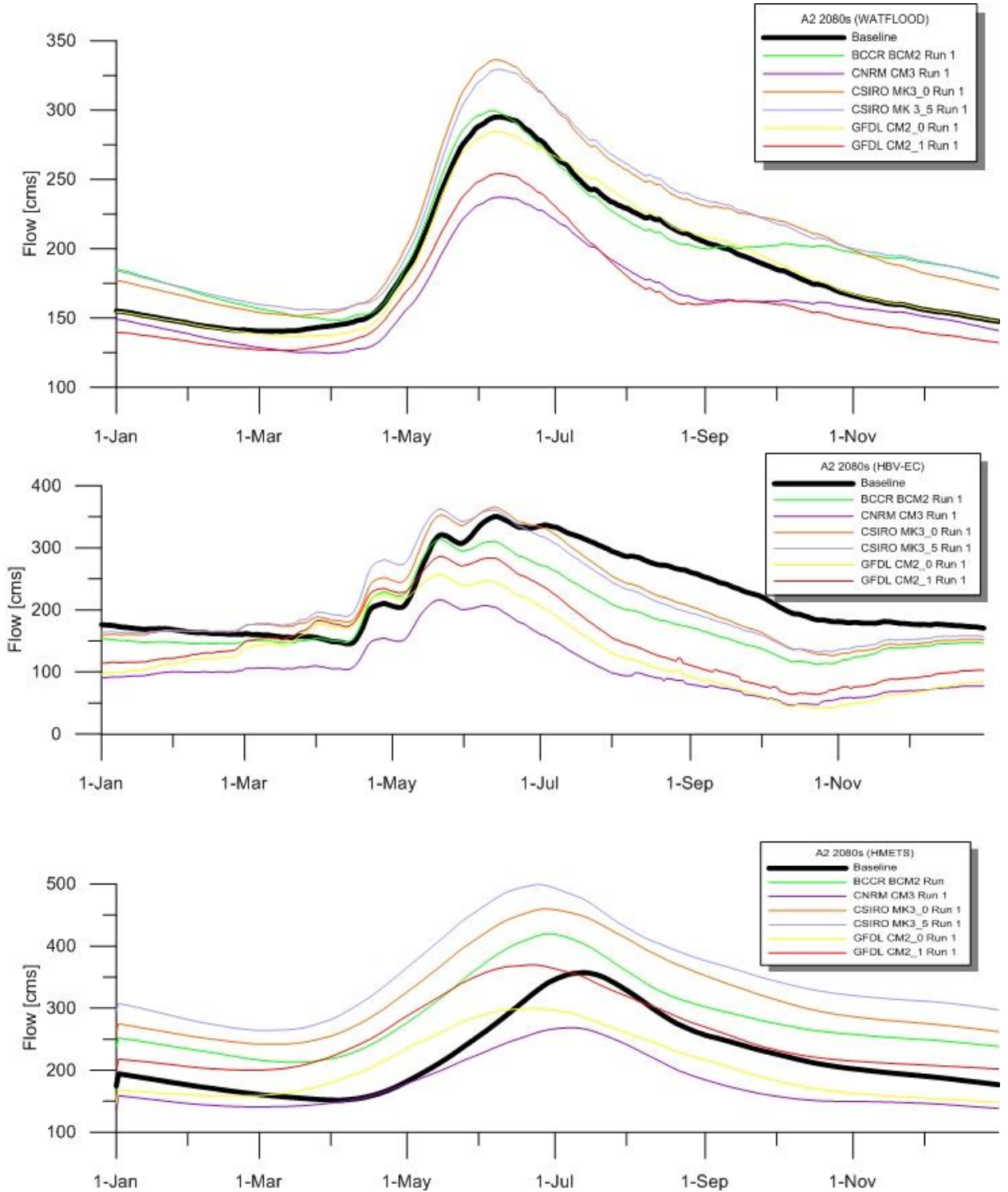
Figure 51: BCCR, CNRM, CSIRO, GFDL A2 2080s climate change hydrographs
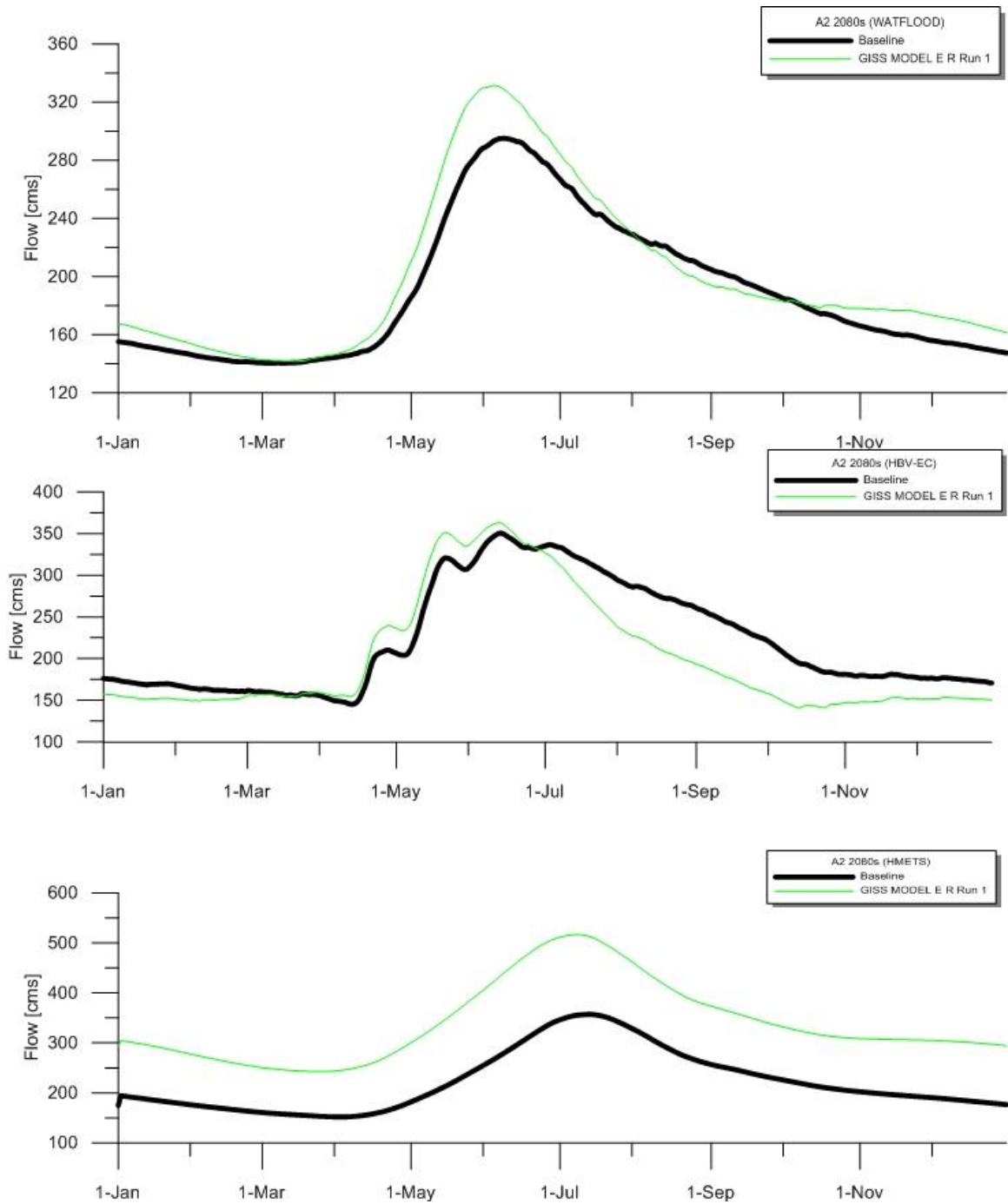
Figure 52: GISS A2 2080s climate change hydrographs
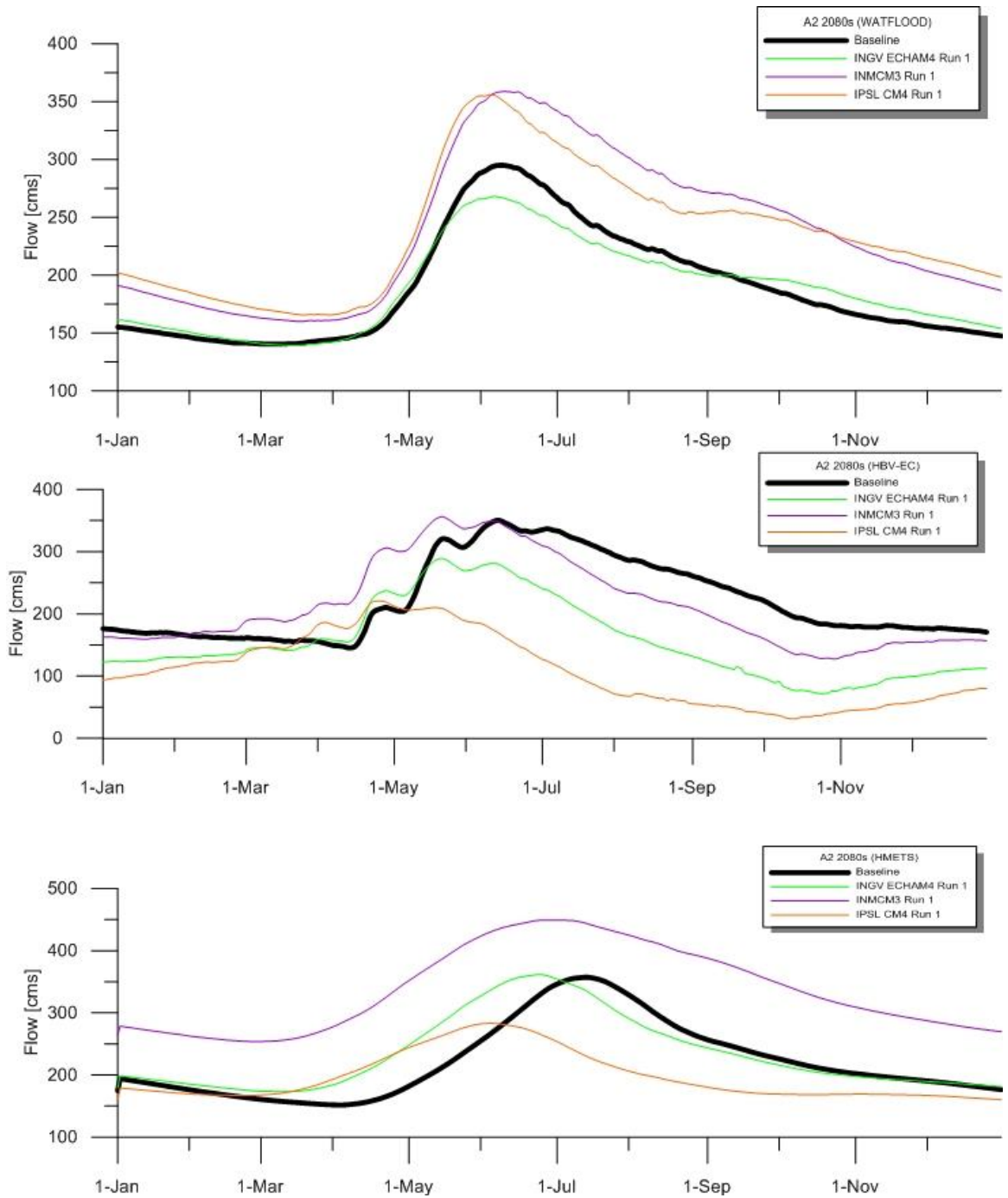
Figure 53: INGV, INMCM, IPSL A2 2080s climate change hydrographs
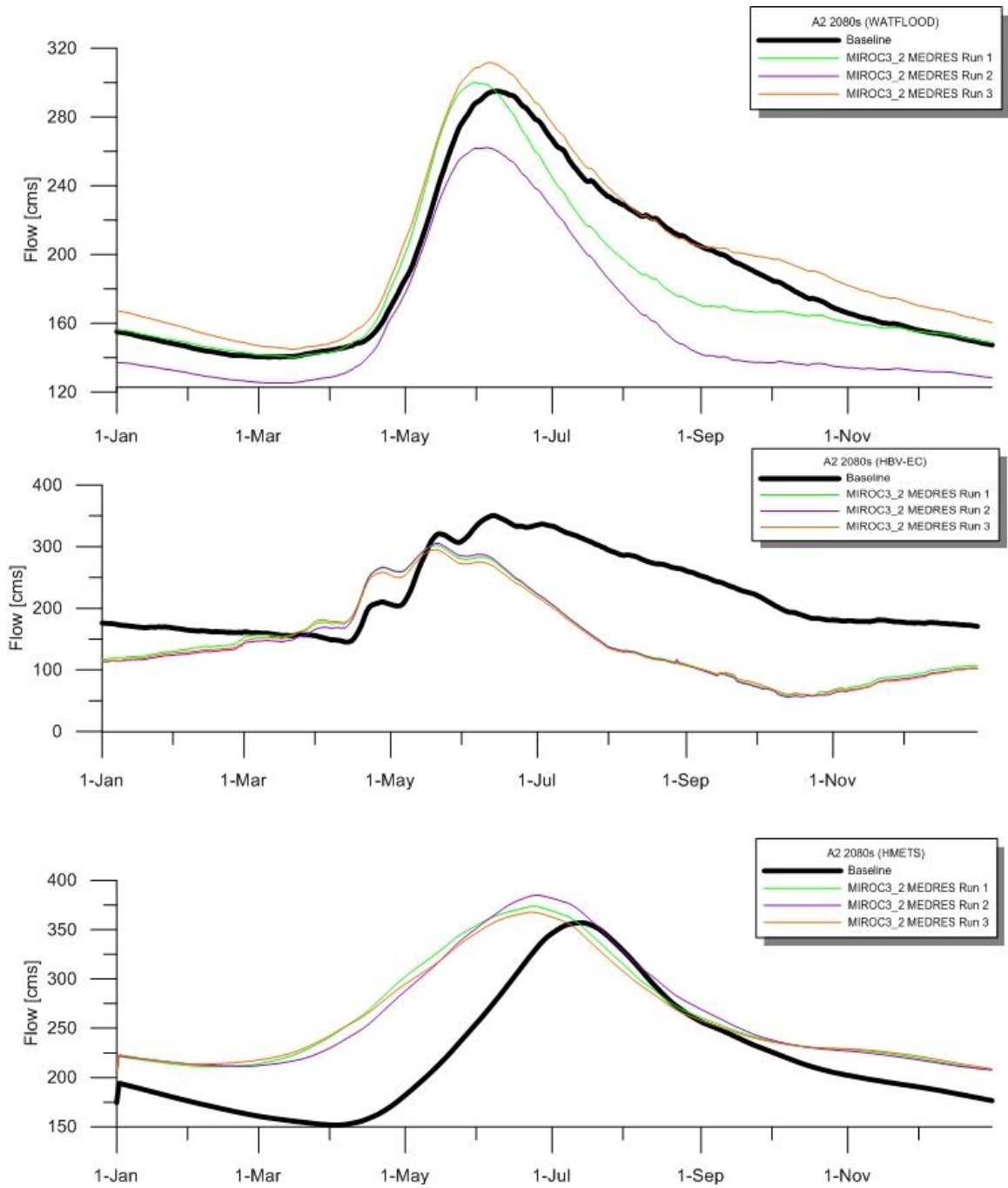
Figure 54: MIROC A2 2080s climate change hydrographs
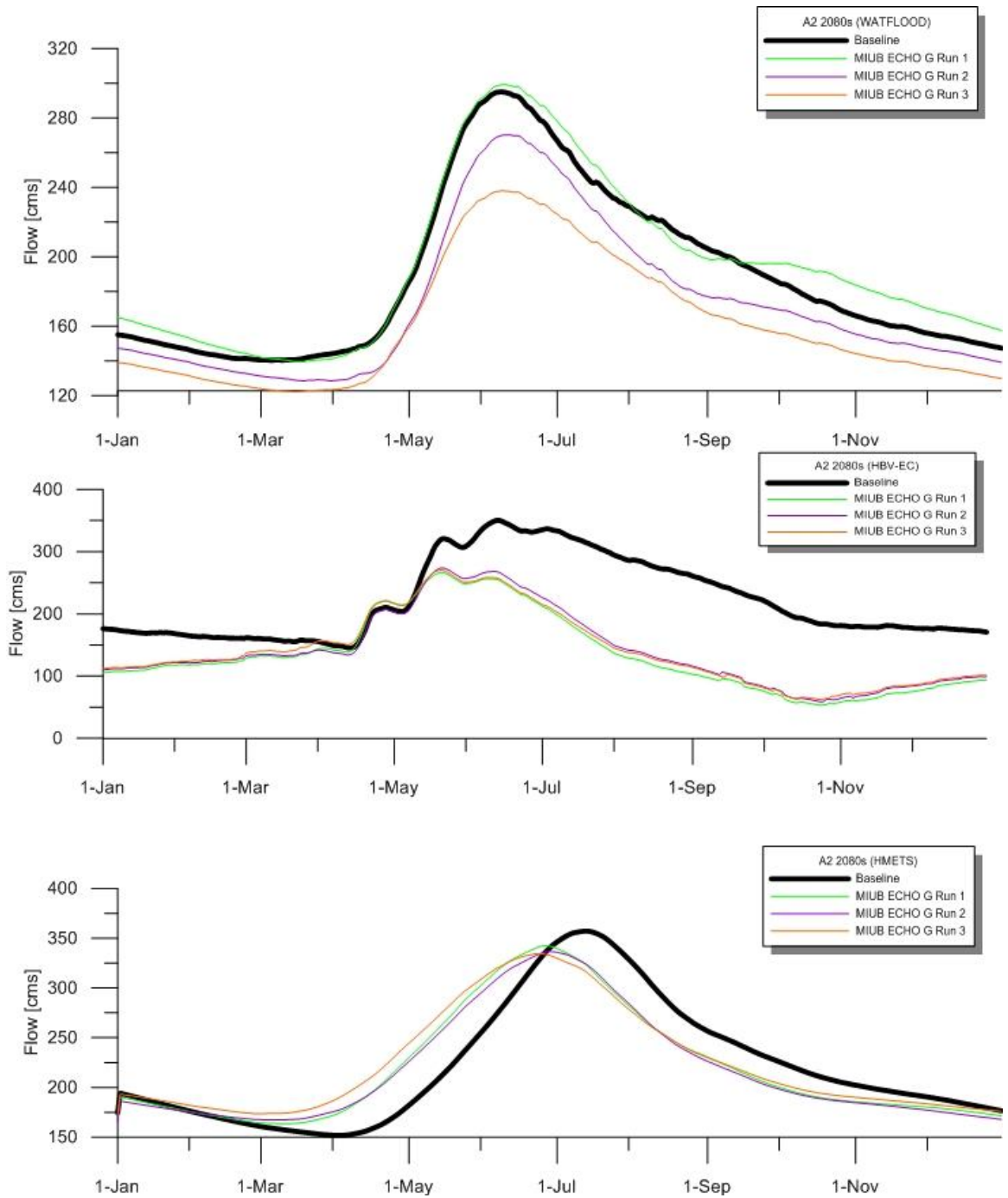
Figure 55: MIUB A2 2080s climate change hydrographs
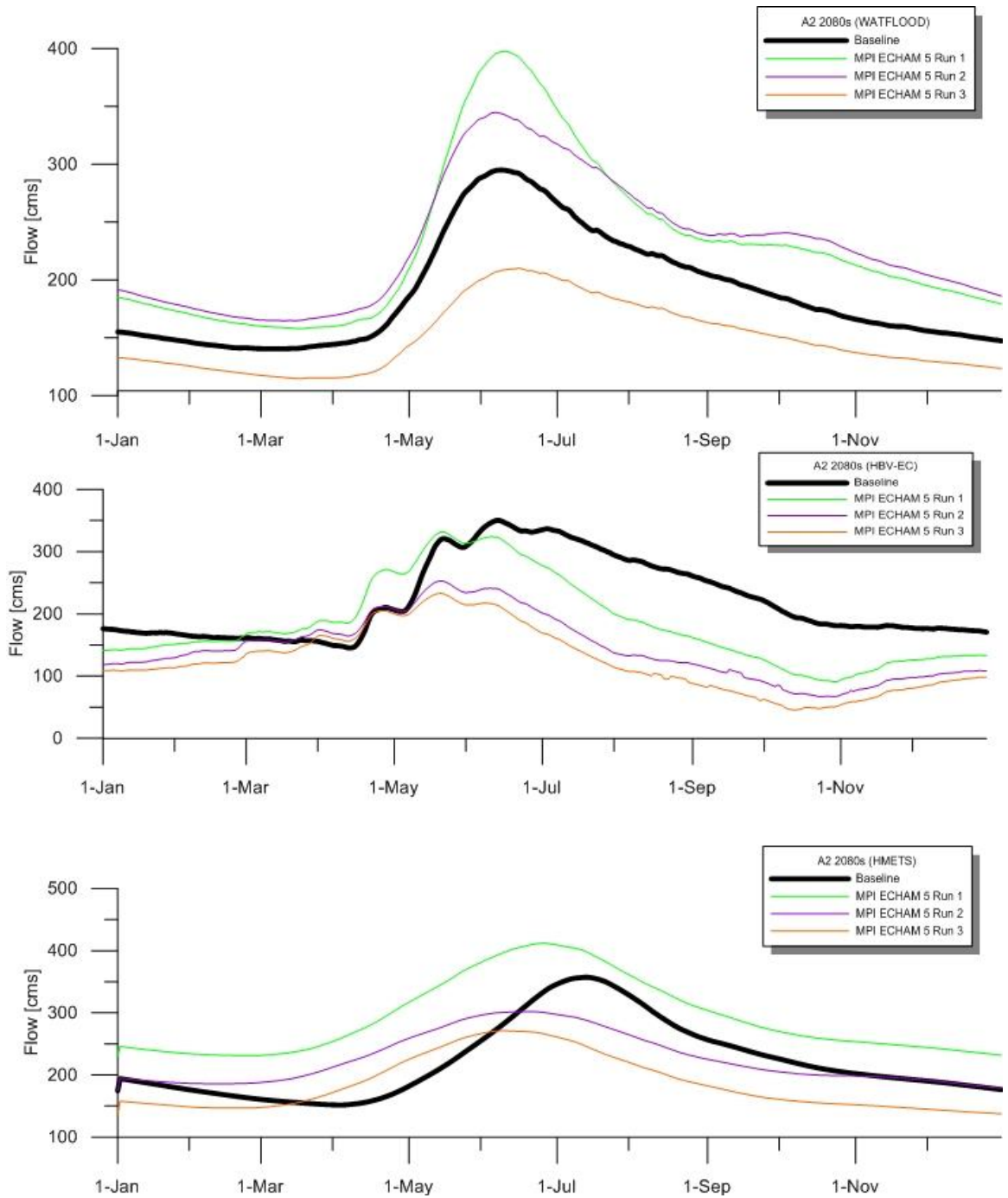
Figure 56: MPI A2 2080s climate change hydrographs
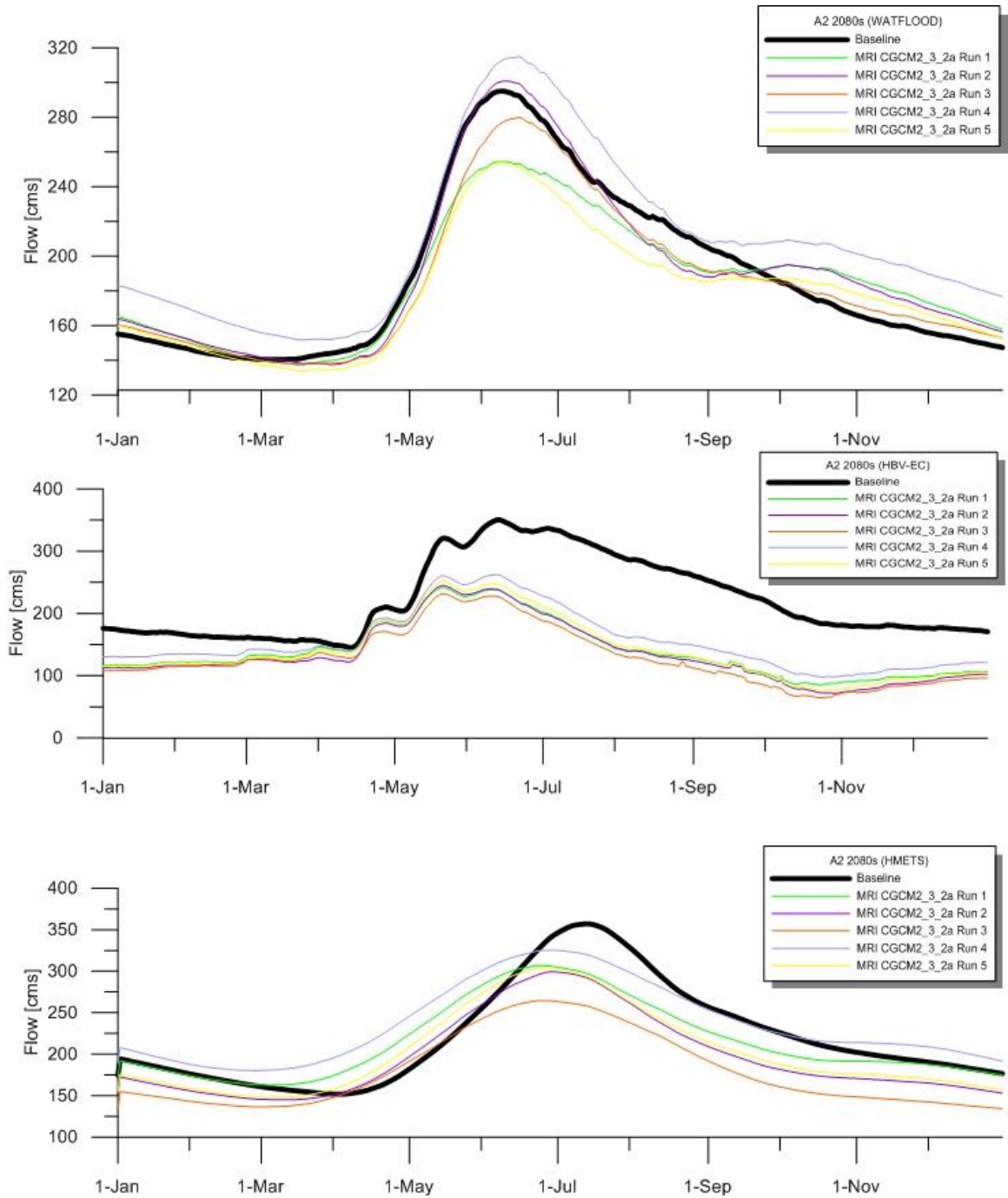
Figure 57: MRI A2 2080s climate change hydrographs
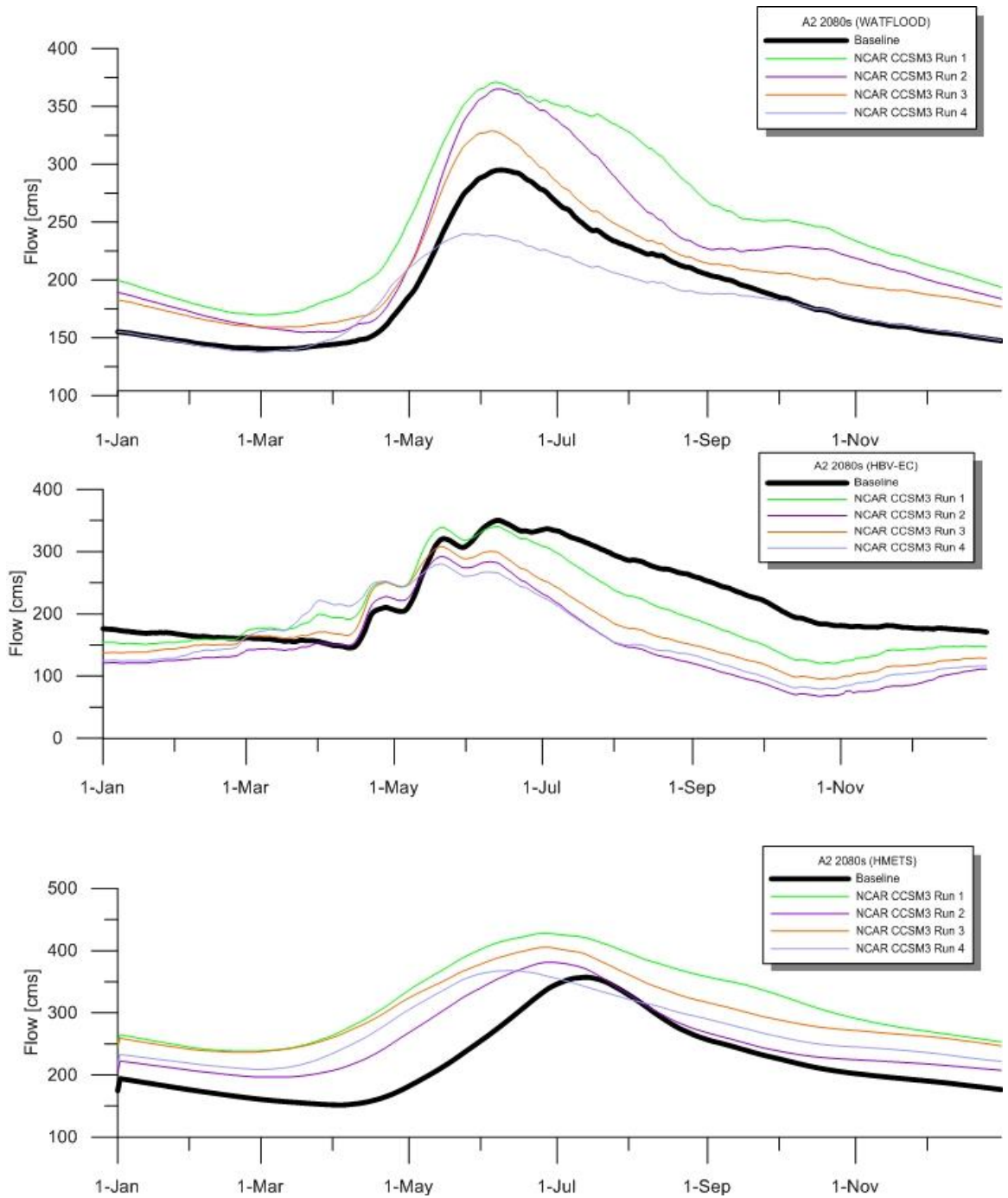
Figure 58: NCAR CCSM3 A2 2080s climate change hydrographs
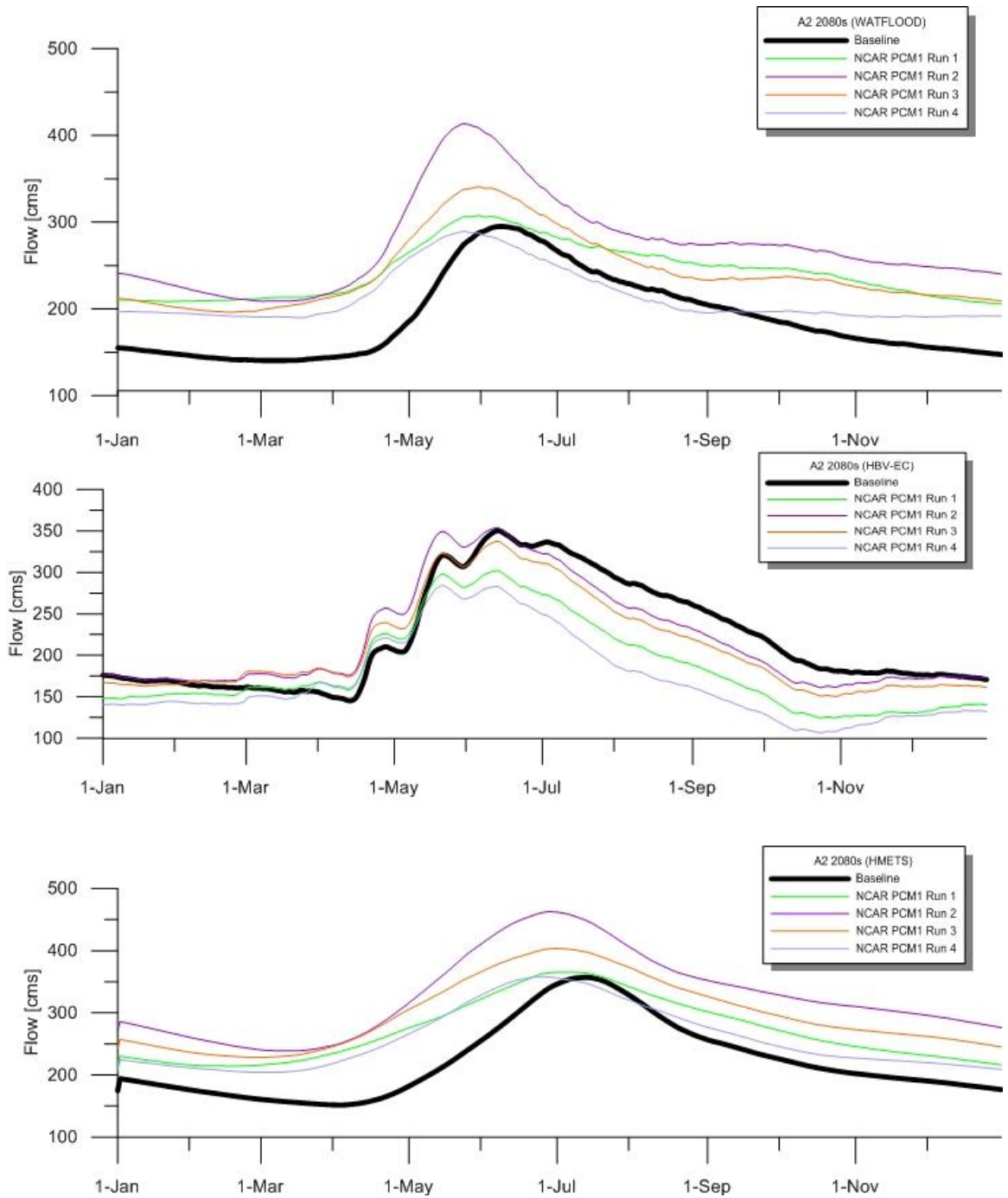
Figure 59: NCAR PCM1 A2 2080s climate change hydrographs
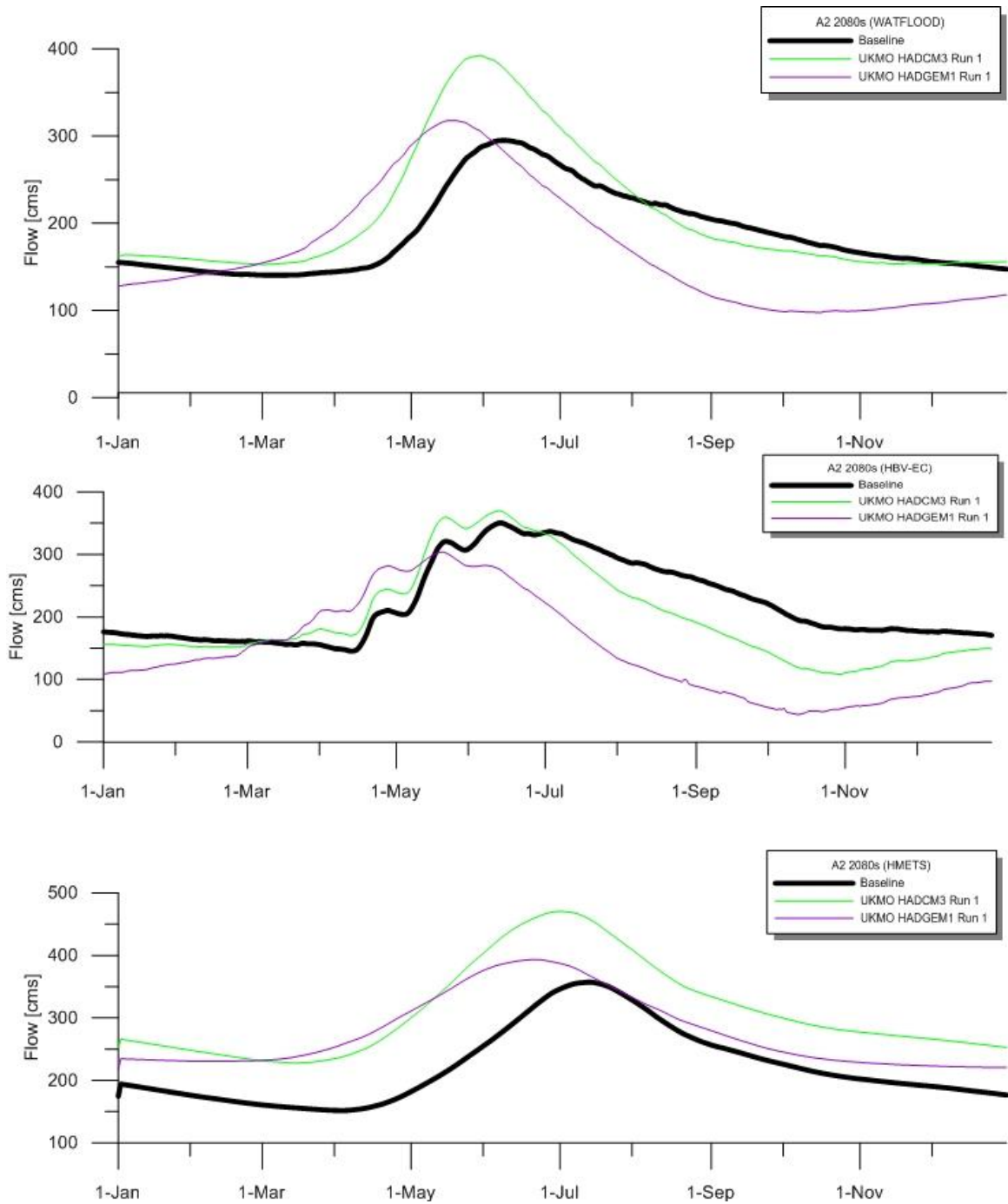
Figure 60: UKMO A2 2080s climate change hydrographs

Appendix E: WATFLOOD™ uncertainty assessment parameters

DDS optimization trial 1 outputs below:

#Fevals	Fbest	Ftest	| -> Decision variable values 1, 2, etc. producing Ftest -->					
Parameter Name			**Ak**					
Land Cover Classification			mix	conifer	crops	burn	wetland	wetland
1554	0.825625	0.825625	64.686	0.208	5.874	33.076	9.935	1.204
1654	0.825625	0.825625	64.686	0.208	5.874	33.076	9.935	24.931
1546	0.825664	0.825664	77.643	0.208	5.874	33.076	9.935	1.204
1566	0.825625	0.825843	96.329	0.208	5.874	33.076	9.935	1.204
1530	0.826028	0.826028	98.847	0.208	5.874	33.076	9.935	1.220
1542	0.826028	0.826028	98.847	0.208	5.874	33.076	9.935	1.204
1586	0.825625	0.826031	64.686	0.208	5.874	33.076	9.935	1.204
1602	0.825625	0.826313	64.686	0.208	5.874	33.076	9.935	1.204
1374	0.826449	0.826449	98.847	0.208	5.874	33.076	9.935	1.220
1417	0.826449	0.826449	98.847	0.208	5.874	33.076	9.935	1.220
1504	0.826449	0.826648	98.847	0.208	5.874	33.076	9.935	16.461
1466	0.826449	0.826649	98.847	0.208	5.874	33.076	9.935	1.220
1604	0.825625	0.826923	64.686	0.208	33.622	33.076	9.935	10.346
1514	0.826449	0.827051	85.515	0.208	5.874	33.076	9.935	1.220
1522	0.826449	0.827258	98.847	0.208	5.874	33.076	9.935	1.220
1359	0.827639	0.827639	98.847	0.208	5.874	33.076	9.935	19.822
1368	0.827639	0.827639	98.847	0.208	5.874	33.076	9.935	2.601
1341	0.827869	0.827869	98.847	0.208	5.874	33.076	9.935	19.822
1409	0.826449	0.827899	98.847	0.208	5.874	33.076	9.935	1.220
1349	0.827869	0.828420	98.847	0.208	5.874	33.076	9.935	19.822
1564	0.825625	0.829271	64.686	0.208	5.874	33.076	9.935	1.204
1473	0.826449	0.829279	98.847	0.208	5.874	33.076	9.935	1.220

1414	0.826449	0.829415	98.847	0.208	5.874	33.076	9.935	1.220
1495	0.826449	0.829557	98.847	0.208	5.874	18.670	9.935	1.220
1574	0.825625	0.829642	64.686	0.208	5.874	33.076	9.935	1.204
1393	0.826449	0.829701	98.847	0.208	5.874	33.076	9.935	1.220
1619	0.825625	0.829817	64.686	0.208	5.874	33.076	9.935	1.204
1518	0.826449	0.830013	98.847	0.208	5.874	33.076	9.935	1.220
1454	0.826449	0.830854	96.795	0.208	5.874	33.076	9.935	11.796
1443	0.826449	0.830859	98.847	0.208	5.874	33.076	9.935	1.220
1638	0.825625	0.831316	64.686	0.208	21.409	33.076	9.935	1.204
1558	0.825625	0.832090	64.686	0.208	12.471	33.076	9.935	1.204
1449	0.826449	0.832312	98.847	0.208	5.874	33.076	9.935	1.220
1581	0.825625	0.832398	64.686	0.208	5.874	33.076	9.935	1.204
1363	0.827639	0.832431	98.847	0.208	5.874	33.076	9.935	14.445
1478	0.826449	0.832773	97.541	0.208	8.720	33.076	9.935	1.220
1392	0.826449	0.832925	98.847	0.208	5.874	33.076	11.911	1.220
1532	0.826028	0.833015	98.847	0.208	5.874	33.076	9.935	1.220
1511	0.826449	0.833072	98.847	0.208	5.319	7.885	9.935	0.213
1556	0.825625	0.833121	64.686	0.208	5.874	63.230	9.935	8.756
1536	0.826028	0.833204	98.847	0.208	5.874	33.076	9.935	1.220
1576	0.825625	0.833421	64.686	0.208	5.874	14.994	9.935	1.204
1585	0.825625	0.833656	64.686	0.208	5.874	33.076	9.935	1.204
1502	0.826449	0.833671	98.847	0.208	18.787	33.076	9.935	1.220
1441	0.826449	0.833937	98.847	0.208	5.874	33.076	9.935	1.220
1340	0.834050	0.834050	98.847	0.208	5.874	33.076	9.935	19.822
1357	0.827869	0.834113	98.847	0.208	5.874	49.307	9.935	19.822
1588	0.825625	0.834285	64.686	0.208	5.874	33.076	9.935	1.204
1343	0.827869	0.834381	99.618	0.208	5.874	45.070	9.935	47.738

924	0.834398	0.834398	98.847	0.208	5.874	33.076	9.935	35.369
1215	0.834398	0.834398	98.847	0.208	5.874	33.076	9.935	35.369
570	0.834474	0.834474	98.847	0.208	5.874	33.076	9.935	35.369
1353	0.827869	0.834493	98.847	0.208	5.874	33.076	9.935	19.822
1548	0.825664	0.835048	77.643	0.208	5.874	33.076	9.935	1.204
1261	0.834398	0.835320	98.847	0.208	5.874	33.076	9.935	35.369
1601	0.825625	0.835411	64.686	0.208	5.874	33.076	9.935	1.204
1563	0.825625	0.835636	64.686	0.208	5.874	33.076	9.935	14.265
1547	0.825664	0.835860	77.643	0.208	5.874	33.076	9.935	1.204
684	0.834474	0.835897	98.847	0.208	5.874	33.076	9.935	35.369
1579	0.825625	0.836145	64.686	0.208	5.874	33.076	9.935	1.204
1517	0.826449	0.836204	98.847	0.208	5.874	33.076	9.935	6.469
1483	0.826449	0.836360	98.847	0.208	14.929	67.504	9.935	1.220
852	0.834474	0.836600	98.847	0.208	5.874	33.076	9.935	9.242
859	0.834474	0.836664	98.847	0.208	5.874	33.076	9.935	49.240
1345	0.827869	0.836880	74.835	0.208	5.874	36.478	9.935	19.822
1428	0.826449	0.837035	98.847	0.208	5.874	33.076	9.935	15.781
565	0.837045	0.837045	98.847	0.208	5.874	33.076	9.935	35.369
1596	0.825625	0.837052	64.686	0.208	5.874	33.076	9.935	1.204
1484	0.826449	0.837065	98.847	0.208	5.874	33.076	9.935	1.220
448	0.837408	0.837408	98.847	0.208	5.874	33.076	9.935	35.369
817	0.834474	0.837502	98.847	0.208	10.485	33.076	9.935	35.369
922	0.834474	0.837624	98.847	0.208	5.874	33.076	9.935	35.369
986	0.834398	0.837636	98.847	0.208	27.941	32.098	9.935	35.369
1072	0.834398	0.837908	98.847	0.208	5.874	33.076	9.935	35.369
994	0.834398	0.837917	98.847	0.208	5.874	33.076	9.935	35.369
1084	0.834398	0.837981	98.847	0.208	39.297	33.076	9.935	35.369

966	0.834398	0.838022	98.847	0.208	21.716	44.759	9.935	35.369
846	0.834474	0.838145	98.847	0.208	10.021	33.076	9.935	35.369
1438	0.826449	0.838276	98.847	0.208	5.874	33.076	9.935	1.220
1525	0.826449	0.838536	98.847	0.208	39.302	33.076	9.935	1.220
694	0.834474	0.838586	98.847	0.208	11.580	33.076	9.935	35.369
1134	0.834398	0.838646	98.847	0.208	5.874	33.076	9.935	35.369
1405	0.826449	0.838704	98.847	0.208	29.553	33.076	9.935	1.220
1412	0.826449	0.838711	98.847	0.208	5.874	33.076	9.935	3.027
920	0.834474	0.838719	98.847	0.208	5.874	33.076	9.935	35.369
753	0.834474	0.838724	81.155	0.208	5.874	46.679	9.935	44.560
1027	0.834398	0.838734	98.847	0.208	12.594	33.076	9.935	35.369
1462	0.826449	0.838783	98.847	0.208	5.874	33.076	9.935	1.220
1370	0.827639	0.838852	81.349	0.208	6.323	33.076	9.935	2.601
1294	0.834398	0.838996	98.847	0.208	5.874	33.076	9.935	35.369
838	0.834474	0.839102	98.847	0.208	5.874	33.076	9.935	35.369
1313	0.834398	0.839107	76.676	0.208	5.874	33.076	9.935	35.369
1490	0.826449	0.839479	98.847	0.208	5.874	33.076	9.935	1.220
1237	0.834398	0.839586	98.847	0.208	5.874	33.076	9.935	35.369
1291	0.834398	0.839605	98.847	0.208	5.874	55.028	9.935	35.369
590	0.834474	0.839676	98.847	0.208	5.874	33.076	9.935	35.369
1079	0.834398	0.839679	98.847	0.208	5.874	33.076	9.935	35.369
1367	0.827639	0.839722	98.847	0.208	5.874	33.076	9.935	19.822
1487	0.826449	0.839809	98.847	0.208	5.874	33.076	9.935	1.220
1268	0.834398	0.839823	98.847	0.208	5.874	29.289	9.935	35.369
1131	0.834398	0.839867	98.847	0.208	5.874	33.076	9.935	35.369
1320	0.834398	0.839871	79.524	0.208	5.874	33.076	9.935	68.567
979	0.834398	0.840271	98.847	0.208	13.238	5.866	9.935	35.369

1045	0.834398	0.840331	98.847	0.208	5.874	33.076	9.935	35.369
1557	0.825625	0.840332	64.686	0.208	5.874	33.076	9.935	1.204
1383	0.826449	0.840436	98.847	0.208	5.874	33.076	9.935	1.220
1544	0.826028	0.840527	98.847	0.208	5.874	33.076	9.935	6.768
1144	0.834398	0.840606	98.847	0.208	5.874	41.997	9.935	35.369
1446	0.826449	0.840628	98.847	0.208	5.874	33.076	9.935	1.220
1347	0.827869	0.840665	98.847	0.208	5.874	33.076	9.935	19.822

DDS optimization trial   1 outputs below:

#Fevals	Fbest	Ftest	| -> Decision variable values 1, 2, etc. producing Ftest -->					
Parameter Name			**Akfs**					
Land Cover Classification			mix	conifer	crops	burn	wetland	wetland
1554	0.825625	0.825625	99.225	56.499	0.846	97.969	29.490	24.536
1654	0.825625	0.825625	77.772	56.499	0.846	97.969	29.490	2.423
1546	0.825664	0.825664	99.225	56.499	0.846	97.969	29.490	24.536
1566	0.825625	0.825843	99.225	56.499	0.846	95.144	29.490	24.536
1530	0.826028	0.826028	99.225	56.499	0.846	97.969	29.490	58.645
1542	0.826028	0.826028	99.225	56.499	0.846	97.969	29.490	24.536
1586	0.825625	0.826031	99.225	56.499	0.846	97.969	29.490	24.536
1602	0.825625	0.826313	99.225	56.499	0.846	97.969	29.490	24.536
1374	0.826449	0.826449	92.284	36.042	0.846	97.969	14.874	83.313
1417	0.826449	0.826449	88.435	36.042	0.846	97.969	14.874	88.508
1504	0.826449	0.826648	88.435	36.042	0.846	97.969	14.874	88.508
1466	0.826449	0.826649	65.120	36.042	0.846	97.969	14.874	88.508

1604	0.825625	0.826923	99.174	56.499	0.846	84.038	29.490	24.536
1514	0.826449	0.827051	88.435	28.998	0.846	97.969	14.874	88.508
1522	0.826449	0.827258	88.435	36.042	0.846	97.969	14.874	88.508
1359	0.827639	0.827639	92.284	59.398	0.846	97.969	14.874	83.313
1368	0.827639	0.827639	92.284	36.042	0.846	97.969	14.874	83.313
1341	0.827869	0.827869	92.284	59.398	0.846	97.969	14.874	83.313
1409	0.826449	0.827899	92.284	36.042	0.846	97.969	14.874	83.313
1349	0.827869	0.828420	92.284	59.398	0.846	97.969	14.874	83.313
1564	0.825625	0.829271	99.225	56.499	0.846	97.969	29.490	24.536
1473	0.826449	0.829279	88.435	44.966	0.846	97.969	14.874	88.508
1414	0.826449	0.829415	92.284	36.042	0.846	97.969	14.874	83.313
1495	0.826449	0.829557	88.435	17.043	0.846	97.969	14.874	88.508
1574	0.825625	0.829642	99.225	56.499	0.846	97.969	29.490	24.536
1393	0.826449	0.829701	92.284	36.042	0.846	97.969	14.874	83.313
1619	0.825625	0.829817	99.225	56.499	0.846	97.969	30.945	24.536
1518	0.826449	0.830013	88.435	36.042	0.846	97.969	14.874	88.508
1454	0.826449	0.830854	88.435	36.042	0.846	97.969	7.831	70.618
1443	0.826449	0.830859	88.435	36.042	0.846	97.969	14.874	88.508
1638	0.825625	0.831316	99.225	56.499	0.846	97.969	29.490	24.536
1558	0.825625	0.832090	99.225	56.499	0.846	97.969	29.490	24.536
1449	0.826449	0.832312	88.435	36.042	0.846	97.969	14.874	88.508
1581	0.825625	0.832398	99.225	56.499	0.846	97.969	29.490	24.536
1363	0.827639	0.832431	92.284	59.398	0.846	97.969	4.000	83.313
1478	0.826449	0.832773	88.435	36.042	0.846	97.969	14.874	88.508
1392	0.826449	0.832925	92.284	36.042	0.846	97.969	14.874	83.313
1532	0.826028	0.833015	99.225	56.499	0.846	97.969	29.490	51.708
1511	0.826449	0.833072	96.236	36.042	0.846	86.474	14.874	89.889

1556	0.825625	0.833121	99.225	56.499	0.846	97.969	29.490	24.536
1536	0.826028	0.833204	99.225	80.363	0.846	97.969	29.490	58.645
1576	0.825625	0.833421	99.225	56.499	0.846	97.969	29.490	24.536
1585	0.825625	0.833656	99.225	56.499	6.955	85.468	29.490	24.536
1502	0.826449	0.833671	88.435	36.042	0.846	97.969	14.874	88.508
1441	0.826449	0.833937	93.192	36.042	0.846	97.969	14.874	88.508
1340	0.834050	0.834050	92.284	59.398	8.419	97.969	14.874	83.313
1357	0.827869	0.834113	92.284	64.693	0.846	97.969	14.874	83.313
1588	0.825625	0.834285	99.225	56.499	4.873	97.969	29.490	24.536
1343	0.827869	0.834381	92.284	59.398	0.846	97.969	14.874	83.313
924	0.834398	0.834398	92.284	31.724	8.419	97.969	14.874	83.313
1215	0.834398	0.834398	92.284	59.398	8.419	97.969	14.874	83.313
570	0.834474	0.834474	92.284	31.724	8.419	97.969	14.874	83.313
1353	0.827869	0.834493	92.284	69.464	0.846	83.880	14.874	83.313
1548	0.825664	0.835048	99.225	59.725	0.846	97.969	29.490	2.767
1261	0.834398	0.835320	92.284	59.398	8.419	97.969	14.874	83.313
1601	0.825625	0.835411	99.225	56.499	0.846	71.373	29.490	24.536
1563	0.825625	0.835636	99.225	56.499	0.846	97.969	29.490	24.536
1547	0.825664	0.835860	99.225	56.499	0.846	71.756	29.951	24.536
684	0.834474	0.835897	93.880	31.724	8.419	66.743	14.874	83.313
1579	0.825625	0.836145	99.225	58.157	0.846	97.969	23.505	24.536
1517	0.826449	0.836204	88.435	36.042	0.846	97.969	4.215	90.186
1483	0.826449	0.836360	88.435	36.042	0.846	97.969	14.874	88.508
852	0.834474	0.836600	77.953	31.724	8.419	86.511	14.874	83.313
859	0.834474	0.836664	92.284	31.724	8.419	97.969	14.874	88.823
1345	0.827869	0.836880	95.276	59.398	0.846	97.969	14.874	83.313
1428	0.826449	0.837035	88.435	69.851	0.846	97.969	14.874	88.508

565	0.837045	0.837045	92.284	31.724	8.419	73.954	14.874	83.313
1596	0.825625	0.837052	99.225	56.499	0.846	97.969	29.490	24.536
1484	0.826449	0.837065	88.435	19.040	0.846	97.969	14.874	88.508
448	0.837408	0.837408	98.229	24.800	5.966	81.540	14.874	57.213
817	0.834474	0.837502	92.284	48.673	8.419	83.269	14.874	83.313
922	0.834474	0.837624	90.273	31.724	8.419	97.969	14.874	83.313
986	0.834398	0.837636	92.284	31.724	8.419	97.969	14.874	83.313
1072	0.834398	0.837908	92.284	31.724	8.419	97.969	14.874	83.313
994	0.834398	0.837917	79.329	49.295	8.419	97.969	14.874	83.313
1084	0.834398	0.837981	60.514	31.724	8.419	94.525	14.874	83.313
966	0.834398	0.838022	92.284	31.724	8.419	97.969	14.874	84.597
846	0.834474	0.838145	92.284	31.724	8.304	97.969	14.874	83.313
1438	0.826449	0.838276	84.930	36.042	0.846	97.969	14.874	88.508
1525	0.826449	0.838536	88.435	36.042	0.846	97.969	14.874	88.508
694	0.834474	0.838586	92.284	31.724	8.419	97.969	14.874	82.603
1134	0.834398	0.838646	92.284	31.724	8.419	79.654	14.874	83.313
1405	0.826449	0.838704	92.284	36.042	0.846	97.969	14.874	90.471
1412	0.826449	0.838711	86.930	36.042	0.846	97.969	40.333	83.313
920	0.834474	0.838719	92.088	47.961	8.419	97.969	32.236	83.313
753	0.834474	0.838724	92.284	31.724	26.297	97.969	14.874	83.313
1027	0.834398	0.838734	73.715	31.724	8.419	92.662	14.874	83.313
1462	0.826449	0.838783	88.435	36.042	0.846	97.969	14.874	88.508
1370	0.827639	0.838852	92.284	36.042	0.846	97.969	14.874	83.313
1294	0.834398	0.838996	92.284	59.398	8.419	97.969	0.327	83.313
838	0.834474	0.839102	92.284	42.844	8.419	97.969	14.874	83.313
1313	0.834398	0.839107	92.284	65.975	8.419	97.969	15.371	83.313
1490	0.826449	0.839479	88.435	36.042	15.610	97.969	14.874	88.508

1237	0.834398	0.839586	94.141	59.398	8.486	97.969	14.874	83.313
1291	0.834398	0.839605	92.284	59.398	8.419	80.813	19.493	83.313
590	0.834474	0.839676	77.989	31.724	7.385	97.969	14.874	83.313
1079	0.834398	0.839679	92.284	31.724	8.419	97.969	14.874	78.734
1367	0.827639	0.839722	92.284	59.398	0.846	97.969	14.874	83.313
1487	0.826449	0.839809	88.435	36.042	0.846	97.969	14.874	88.508
1268	0.834398	0.839823	92.284	59.398	8.419	81.667	14.874	83.313
1131	0.834398	0.839867	92.284	31.724	8.419	97.969	14.874	83.313
1320	0.834398	0.839871	92.284	59.398	8.419	97.969	14.874	83.313
979	0.834398	0.840271	92.284	31.724	8.419	97.969	14.874	82.171
1045	0.834398	0.840331	61.412	14.900	1.604	91.825	16.198	83.313
1557	0.825625	0.840332	99.225	56.499	0.846	97.969	29.490	24.536
1383	0.826449	0.840436	92.284	36.042	0.846	97.969	14.874	83.313
1544	0.826028	0.840527	99.225	56.499	0.846	97.969	29.490	24.536
1144	0.834398	0.840606	92.284	31.724	5.833	92.943	14.874	83.313
1446	0.826449	0.840628	88.435	36.042	0.846	97.969	14.874	88.508
1347	0.827869	0.840665	92.284	72.509	31.881	97.969	43.381	75.922

DDS optimization trial   1 outputs below:

#Fevals	Fbest	Ftest		-> Decision variable values 1, 2, etc. producing Ftest -->				
Parameter Name			**rec**					
Land Cover Classification			**mix**	**conifer**	**crops**	**burn**	**wetland**	**wetland**
1554	0.825625	0.825625	1.803	0.066	20.251	10.507	38.992	31.183
1654	0.825625	0.825625	1.803	0.066	20.251	10.507	38.992	31.183
1546	0.825664	0.825664	1.803	0.066	20.251	10.507	38.992	31.183
1566	0.825625	0.825843	1.803	0.066	20.251	10.507	38.992	31.183

1530	0.826028	0.826028	1.803	0.066	20.251	10.507	38.992	31.183
1542	0.826028	0.826028	1.803	0.066	20.251	10.507	38.992	31.183
1586	0.825625	0.826031	1.803	0.066	20.251	10.507	48.389	31.183
1602	0.825625	0.826313	1.803	0.066	20.251	10.507	38.992	31.183
1374	0.826449	0.826449	1.803	0.066	20.251	10.507	38.992	31.183
1417	0.826449	0.826449	1.803	0.066	20.251	10.507	38.992	31.183
1504	0.826449	0.826648	1.803	0.066	20.251	10.507	38.992	42.934
1466	0.826449	0.826649	1.803	0.066	20.251	10.507	38.992	31.183
1604	0.825625	0.826923	1.110	0.066	20.251	10.507	38.992	31.183
1514	0.826449	0.827051	1.803	0.066	26.940	10.507	38.992	31.183
1522	0.826449	0.827258	1.803	0.066	20.251	10.507	54.319	20.328
1359	0.827639	0.827639	1.803	0.066	28.496	10.507	38.992	14.590
1368	0.827639	0.827639	1.803	0.066	28.496	10.507	38.992	27.929
1341	0.827869	0.827869	1.803	0.066	28.496	10.507	20.157	14.590
1409	0.826449	0.827899	1.803	0.066	20.251	10.507	38.992	31.183
1349	0.827869	0.828420	1.803	0.066	28.496	10.507	20.157	14.590
1564	0.825625	0.829271	0.937	0.066	20.251	10.507	38.992	31.183
1473	0.826449	0.829279	1.803	0.066	0.638	10.507	38.992	31.183
1414	0.826449	0.829415	1.803	0.066	20.251	10.507	38.992	31.183
1495	0.826449	0.829557	1.803	0.066	20.251	9.782	38.992	31.183
1574	0.825625	0.829642	1.803	0.066	20.251	10.507	38.992	31.183
1393	0.826449	0.829701	0.186	0.066	20.251	10.507	38.992	31.183
1619	0.825625	0.829817	1.803	0.066	20.251	10.507	38.992	31.183
1518	0.826449	0.830013	1.803	0.066	20.251	10.507	38.992	31.183
1454	0.826449	0.830854	1.803	0.066	20.251	10.507	38.992	31.183
1443	0.826449	0.830859	1.803	0.066	36.284	10.507	38.992	31.183
1638	0.825625	0.831316	1.803	0.066	20.251	10.507	38.992	13.627

1558	0.825625	0.832090	1.803	0.066	20.251	10.507	38.992	31.183
1449	0.826449	0.832312	1.803	0.066	20.251	10.507	38.992	31.183
1581	0.825625	0.832398	1.803	0.066	20.251	10.507	38.992	31.183
1363	0.827639	0.832431	1.803	0.066	28.496	10.507	38.992	14.590
1478	0.826449	0.832773	1.803	0.066	20.251	10.507	38.992	31.183
1392	0.826449	0.832925	1.803	0.066	20.251	10.507	38.992	31.183
1532	0.826028	0.833015	1.803	0.066	20.251	10.507	38.992	31.183
1511	0.826449	0.833072	1.803	0.066	20.251	10.507	52.360	15.458
1556	0.825625	0.833121	1.803	0.066	20.251	10.507	38.992	31.183
1536	0.826028	0.833204	1.803	0.066	45.726	10.507	38.992	31.183
1576	0.825625	0.833421	2.803	0.066	20.251	4.585	38.992	31.183
1585	0.825625	0.833656	0.155	0.066	20.251	10.507	38.992	31.183
1502	0.826449	0.833671	1.803	0.066	20.251	10.507	38.992	31.183
1441	0.826449	0.833937	1.803	0.066	20.251	10.507	38.992	31.183
1340	0.834050	0.834050	1.803	1.229	28.496	10.507	20.157	14.590
1357	0.827869	0.834113	2.489	0.066	64.671	10.507	20.157	14.590
1588	0.825625	0.834285	1.803	0.066	20.251	10.507	38.992	31.183
1343	0.827869	0.834381	4.615	0.066	16.522	18.182	20.157	14.590
924	0.834398	0.834398	1.803	1.229	28.496	10.507	20.157	14.590
1215	0.834398	0.834398	1.803	1.229	28.496	10.507	20.157	14.590
570	0.834474	0.834474	1.803	1.229	28.496	10.507	20.157	14.590
1353	0.827869	0.834493	1.803	0.066	33.769	10.507	20.157	4.837
1548	0.825664	0.835048	1.803	0.066	20.251	10.507	38.992	31.183
1261	0.834398	0.835320	1.803	1.229	28.496	10.507	20.157	14.590
1601	0.825625	0.835411	1.803	0.066	20.251	10.507	79.454	31.183
1563	0.825625	0.835636	1.803	0.066	27.059	10.507	38.992	12.601
1547	0.825664	0.835860	1.803	0.066	20.251	10.507	38.992	31.183

684	0.834474	0.835897	1.803	1.229	28.496	10.507	20.157	14.590
1579	0.825625	0.836145	1.803	0.066	20.251	10.507	38.992	31.183
1517	0.826449	0.836204	1.803	0.066	49.002	10.507	38.992	31.183
1483	0.826449	0.836360	1.803	0.066	20.251	10.507	38.992	31.183
852	0.834474	0.836600	1.803	1.229	28.496	10.507	20.157	14.590
859	0.834474	0.836664	1.803	0.955	28.496	10.507	20.157	11.825
1345	0.827869	0.836880	1.803	0.066	26.277	10.507	20.157	14.590
1428	0.826449	0.837035	1.803	0.066	20.251	10.507	38.992	31.183
565	0.837045	0.837045	1.803	1.229	59.490	10.507	20.157	14.590
1596	0.825625	0.837052	3.252	0.066	20.251	10.507	38.992	31.183
1484	0.826449	0.837065	1.803	0.066	29.562	10.507	38.992	31.183
448	0.837408	0.837408	1.014	1.229	59.490	0.060	20.157	14.590
817	0.834474	0.837502	1.803	1.229	28.496	10.507	20.157	14.590
922	0.834474	0.837624	1.803	1.229	28.496	10.507	20.157	14.590
986	0.834398	0.837636	0.493	1.229	4.300	10.507	47.009	14.590
1072	0.834398	0.837908	1.803	1.229	28.496	23.054	20.157	48.276
994	0.834398	0.837917	1.810	1.229	28.496	10.507	31.008	14.590
1084	0.834398	0.837981	1.803	1.229	28.496	12.533	20.157	14.590
966	0.834398	0.838022	1.070	1.229	28.496	10.507	20.157	14.590
846	0.834474	0.838145	1.803	1.229	28.496	10.507	20.157	14.590
1438	0.826449	0.838276	1.803	0.066	27.474	10.507	38.992	31.183
1525	0.826449	0.838536	4.715	0.066	20.251	10.507	38.992	31.183
694	0.834474	0.838586	1.803	1.229	28.496	10.507	20.157	14.590
1134	0.834398	0.838646	1.803	1.229	28.496	10.507	20.157	14.590
1405	0.826449	0.838704	1.803	0.831	20.251	10.507	38.992	31.183
1412	0.826449	0.838711	1.803	0.343	2.404	10.507	38.992	31.183
920	0.834474	0.838719	1.803	1.229	28.496	10.507	20.157	14.590

753	0.834474	0.838724	1.803	1.229	28.496	14.046	17.336	14.590
1027	0.834398	0.838734	0.375	0.602	28.496	8.053	20.157	14.590
1462	0.826449	0.838783	1.868	0.066	20.251	10.507	38.992	31.183
1370	0.827639	0.838852	1.803	0.066	28.496	10.507	38.992	27.929
1294	0.834398	0.838996	1.803	1.229	28.496	10.507	20.157	14.590
838	0.834474	0.839102	1.803	1.229	28.496	39.921	20.157	14.590
1313	0.834398	0.839107	1.803	1.229	28.496	10.507	20.157	14.590
1490	0.826449	0.839479	0.207	0.066	20.251	28.637	38.992	31.183
1237	0.834398	0.839586	1.803	1.229	28.496	10.507	20.157	14.590
1291	0.834398	0.839605	1.803	1.229	28.496	10.507	6.112	27.566
590	0.834474	0.839676	1.803	1.229	28.496	29.646	20.157	14.590
1079	0.834398	0.839679	1.803	1.229	28.496	10.507	20.157	14.590
1367	0.827639	0.839722	1.803	0.066	40.516	10.507	38.992	14.590
1487	0.826449	0.839809	7.328	0.066	20.251	10.507	38.992	31.183
1268	0.834398	0.839823	1.803	1.229	28.496	10.507	20.157	14.590
1131	0.834398	0.839867	1.803	1.229	28.496	10.507	20.767	14.590
1320	0.834398	0.839871	1.803	1.229	28.496	10.507	20.157	14.590
979	0.834398	0.840271	1.803	1.229	28.496	10.507	20.157	14.590
1045	0.834398	0.840331	1.803	1.229	28.496	27.323	20.157	14.590
1557	0.825625	0.840332	1.803	0.066	20.251	10.507	38.992	31.183
1383	0.826449	0.840436	1.803	0.066	20.251	10.507	2.677	31.183
1544	0.826028	0.840527	3.780	0.066	20.251	10.507	38.992	31.183
1144	0.834398	0.840606	1.803	1.229	28.496	10.507	20.157	14.590
1446	0.826449	0.840628	0.425	0.066	20.251	33.259	38.992	31.183
1347	0.827869	0.840665	1.803	0.578	28.496	10.507	20.157	14.590

DDS optimization trial   1 outputs below:

#Fevals	Fbest	Ftest	| -> Decision variable values 1, 2, etc. producing Ftest -->					
Parameter Name			r3					
Land Cover Classification			mix	conifer	crops	burn	wetland	wetland
1554	0.825625	0.825625	52.716	69.254	87.323	88.859	0.962	30.343
1654	0.825625	0.825625	52.716	69.254	87.323	88.859	0.962	30.343
1546	0.825664	0.825664	52.716	69.254	87.323	88.859	0.962	30.343
1566	0.825625	0.825843	52.148	69.254	87.323	84.524	0.962	30.343
1530	0.826028	0.826028	65.579	69.254	87.323	88.859	0.962	30.343
1542	0.826028	0.826028	52.716	69.254	87.323	88.859	0.962	30.343
1586	0.825625	0.826031	62.823	69.254	87.323	88.859	0.962	30.343
1602	0.825625	0.826313	52.716	69.254	87.323	88.859	0.962	10.902
1374	0.826449	0.826449	65.579	69.254	87.323	88.859	0.962	30.343
1417	0.826449	0.826449	65.579	69.254	87.323	88.859	0.962	30.343
1504	0.826449	0.826648	65.579	88.549	54.229	88.859	0.962	30.343
1466	0.826449	0.826649	65.579	69.254	87.631	77.139	0.962	30.343
1604	0.825625	0.826923	43.554	69.254	87.323	88.859	0.962	30.343
1514	0.826449	0.827051	38.550	69.254	87.323	88.859	0.962	30.343
1522	0.826449	0.827258	65.579	69.254	87.323	88.859	0.962	30.343
1359	0.827639	0.827639	65.579	69.254	76.519	88.859	0.962	30.343
1368	0.827639	0.827639	65.579	69.254	76.519	88.859	0.962	30.343
1341	0.827869	0.827869	65.579	69.254	76.519	88.859	0.962	30.343
1409	0.826449	0.827899	65.579	69.254	87.323	78.784	0.962	30.343
1349	0.827869	0.828420	65.579	69.254	94.340	88.859	0.962	30.343
1564	0.825625	0.829271	52.716	69.254	87.323	88.859	0.962	30.343
1473	0.826449	0.829279	65.579	96.185	87.323	88.859	0.962	30.343
1414	0.826449	0.829415	65.579	69.254	87.323	88.859	0.962	30.343

1495	0.826449	0.829557	65.579	69.254	87.323	88.859	0.962	30.343
1574	0.825625	0.829642	52.716	69.254	87.323	88.859	0.962	1.380
1393	0.826449	0.829701	65.579	69.254	87.740	90.886	0.962	30.343
1619	0.825625	0.829817	52.716	69.254	86.930	88.859	0.962	30.343
1518	0.826449	0.830013	65.579	69.254	87.323	88.859	0.962	30.343
1454	0.826449	0.830854	65.579	69.254	87.323	88.859	0.962	30.343
1443	0.826449	0.830859	65.579	69.254	87.323	88.859	0.962	30.343
1638	0.825625	0.831316	52.716	69.254	87.323	96.802	0.962	32.598
1558	0.825625	0.832090	52.716	69.254	87.323	88.859	0.962	30.343
1449	0.826449	0.832312	65.579	69.254	87.323	88.859	0.962	30.343
1581	0.825625	0.832398	52.716	69.254	87.323	88.859	0.962	30.343
1363	0.827639	0.832431	65.579	69.254	76.519	88.859	0.962	27.665
1478	0.826449	0.832773	65.579	69.254	87.323	88.859	0.962	30.343
1392	0.826449	0.832925	78.445	69.254	87.323	88.859	0.962	30.343
1532	0.826028	0.833015	46.733	69.254	87.323	88.859	0.962	30.343
1511	0.826449	0.833072	33.282	69.254	87.323	88.859	0.962	30.587
1556	0.825625	0.833121	52.716	69.254	87.323	88.859	0.962	30.343
1536	0.826028	0.833204	34.291	69.254	87.323	88.859	0.962	30.343
1576	0.825625	0.833421	52.716	69.254	87.323	88.859	0.962	12.685
1585	0.825625	0.833656	14.394	69.254	87.323	82.892	0.962	30.343
1502	0.826449	0.833671	65.579	69.254	87.323	88.859	0.962	30.343
1441	0.826449	0.833937	53.361	69.254	87.323	88.859	0.962	30.343
1340	0.834050	0.834050	65.579	70.840	76.519	88.859	0.962	30.343
1357	0.827869	0.834113	65.579	69.254	76.519	88.859	0.962	30.343
1588	0.825625	0.834285	52.716	69.254	87.323	88.859	0.962	30.343
1343	0.827869	0.834381	65.579	69.254	76.519	88.859	0.962	30.343
924	0.834398	0.834398	65.579	70.840	76.519	88.859	0.962	30.343

1215	0.834398	0.834398	65.579	70.840	76.519	88.859	0.962	30.343
570	0.834474	0.834474	65.579	70.840	76.519	88.859	0.962	52.463
1353	0.827869	0.834493	65.579	82.342	76.519	88.859	0.962	30.343
1548	0.825664	0.835048	52.716	69.254	87.323	75.709	0.962	38.644
1261	0.834398	0.835320	73.237	70.840	77.628	66.713	0.962	30.343
1601	0.825625	0.835411	52.716	69.254	87.323	88.859	0.962	30.343
1563	0.825625	0.835636	52.716	69.254	74.820	88.859	0.962	30.343
1547	0.825664	0.835860	52.716	93.833	93.613	88.859	0.962	30.343
684	0.834474	0.835897	41.385	70.840	76.519	64.322	0.962	78.092
1579	0.825625	0.836145	52.716	60.979	87.323	88.859	0.962	30.343
1517	0.826449	0.836204	65.579	69.254	87.323	88.859	0.962	30.343
1483	0.826449	0.836360	56.965	69.254	87.323	88.859	0.962	30.343
852	0.834474	0.836600	74.807	70.840	76.519	88.859	0.962	52.463
859	0.834474	0.836664	65.579	70.840	76.519	88.859	0.962	53.140
1345	0.827869	0.836880	65.579	69.254	78.043	86.515	0.962	30.343
1428	0.826449	0.837035	65.579	69.254	87.323	88.859	0.962	30.343
565	0.837045	0.837045	72.802	70.840	76.519	88.859	0.962	52.463
1596	0.825625	0.837052	55.967	69.254	87.323	88.859	0.962	23.685
1484	0.826449	0.837065	65.579	69.254	87.323	88.859	0.962	48.101
448	0.837408	0.837408	72.802	70.840	77.080	88.859	2.675	52.463
817	0.834474	0.837502	65.579	70.840	45.680	88.859	0.962	52.463
922	0.834474	0.837624	65.579	70.840	76.519	88.859	0.962	52.463
986	0.834398	0.837636	65.579	94.697	76.519	88.859	0.962	30.343
1072	0.834398	0.837908	65.579	72.783	76.519	88.859	0.962	30.343
994	0.834398	0.837917	65.579	70.840	76.519	88.859	0.962	30.343
1084	0.834398	0.837981	65.579	70.840	76.519	88.859	0.962	30.343
966	0.834398	0.838022	67.078	70.840	76.519	88.859	0.962	30.343

846	0.834474	0.838145	65.579	70.840	76.519	88.859	0.962	52.315
1438	0.826449	0.838276	65.579	69.254	87.323	88.859	0.326	30.343
1525	0.826449	0.838536	65.579	69.254	87.323	83.739	0.962	30.343
694	0.834474	0.838586	65.579	72.198	97.959	88.859	0.962	52.463
1134	0.834398	0.838646	65.579	70.840	76.519	88.859	0.962	30.343
1405	0.826449	0.838704	65.579	75.318	87.323	88.859	0.962	30.343
1412	0.826449	0.838711	65.579	69.254	87.323	92.322	0.962	30.343
920	0.834474	0.838719	65.579	70.840	76.519	88.859	0.962	55.207
753	0.834474	0.838724	65.579	70.840	68.848	73.217	0.962	52.463
1027	0.834398	0.838734	44.275	70.840	76.519	63.210	0.962	30.343
1462	0.826449	0.838783	65.579	69.254	87.323	88.859	0.962	30.343
1370	0.827639	0.838852	65.579	82.389	76.519	88.859	0.962	30.343
1294	0.834398	0.838996	65.579	70.840	76.519	88.859	0.962	32.108
838	0.834474	0.839102	78.505	70.840	76.519	75.280	0.962	52.463
1313	0.834398	0.839107	37.570	70.840	76.519	66.035	0.962	30.343
1490	0.826449	0.839479	65.579	69.254	75.557	88.859	0.962	30.343
1237	0.834398	0.839586	14.230	70.840	76.519	88.859	0.962	30.343
1291	0.834398	0.839605	65.579	70.840	76.519	95.595	0.962	30.343
590	0.834474	0.839676	65.579	70.840	76.519	88.859	0.962	52.463
1079	0.834398	0.839679	65.579	70.840	76.519	88.859	0.962	30.343
1367	0.827639	0.839722	65.579	84.635	76.519	88.859	0.962	30.343
1487	0.826449	0.839809	65.579	69.254	87.323	88.859	0.962	30.343
1268	0.834398	0.839823	65.579	70.840	76.519	88.859	0.962	30.343
1131	0.834398	0.839867	65.579	70.840	76.519	88.859	0.962	30.343
1320	0.834398	0.839871	65.579	70.840	76.519	89.401	0.962	32.264
979	0.834398	0.840271	52.884	70.840	76.519	88.859	0.962	30.343
1045	0.834398	0.840331	65.579	70.840	76.519	62.429	0.962	30.343

1557	0.825625	0.840332	52.716	69.254	87.323	87.432	0.962	30.343
1383	0.826449	0.840436	65.579	69.254	87.323	88.859	0.962	30.343
1544	0.826028	0.840527	52.716	69.254	86.635	88.859	0.170	30.343
1144	0.834398	0.840606	65.579	70.840	76.519	88.859	0.962	30.343
1446	0.826449	0.840628	65.579	69.254	87.323	88.859	0.962	30.343
1347	0.827869	0.840665	65.579	69.254	76.519	88.859	0.962	30.343

DDS optimization trial   1 outputs below:

#Fevals	Fbest	Ftest	| -> Decision variable values 1, 2, etc. producing Ftest -->					
Parameter Name			**flz**					
River Classification Name			jean-marie	martin	birch	backstone	Pembina	Roseau
1554	0.825625	0.825625	0.00059	0.00097	0.00265	0.00052	0.00015	0.00074
1654	0.825625	0.825625	0.00059	0.00097	0.00252	0.00052	0.00015	0.00074
1546	0.825664	0.825664	0.00059	0.00097	0.00265	0.00052	0.00015	0.00074
1566	0.825625	0.825843	0.00059	0.00097	0.00265	0.00052	0.00012	0.00074
1530	0.826028	0.826028	0.00059	0.00097	0.00265	0.00052	0.00015	0.00074
1542	0.826028	0.826028	0.00059	0.00097	0.00265	0.00052	0.00015	0.00074
1586	0.825625	0.826031	0.00059	0.00097	0.00265	0.00052	0.00015	0.00074
1602	0.825625	0.826313	0.00059	0.00097	0.00265	0.00052	0.00015	0.00074
1374	0.826449	0.826449	0.00059	0.00097	0.00265	0.00052	0.00015	0.00074
1417	0.826449	0.826449	0.00059	0.00097	0.00265	0.00052	0.00015	0.00074
1504	0.826449	0.826648	0.00059	0.00097	0.00265	0.00052	0.00013	0.00074
1466	0.826449	0.826649	0.00059	0.00086	0.00265	0.00052	0.00015	0.00074
1604	0.825625	0.826923	0.00080	0.00097	0.00446	0.00052	0.00015	0.00074
1514	0.826449	0.827051	0.00059	0.00093	0.00265	0.00052	0.00015	0.00074
1522	0.826449	0.827258	0.00059	0.00097	0.00265	0.00052	0.00015	0.00074

1359	0.827639	0.827639	0.00059	0.00097	0.00216	0.00052	0.00015	0.00072
1368	0.827639	0.827639	0.00059	0.00097	0.00216	0.00052	0.00015	0.00072
1341	0.827869	0.827869	0.00059	0.00097	0.00216	0.00052	0.00015	0.00072
1409	0.826449	0.827899	0.00059	0.00051	0.00265	0.00052	0.00015	0.00074
1349	0.827869	0.828420	0.00059	0.00097	0.00114	0.00052	0.00015	0.00072
1564	0.825625	0.829271	0.00059	0.00097	0.00265	0.00052	0.00015	0.00074
1473	0.826449	0.829279	0.00059	0.00097	0.00265	0.00052	0.00015	0.00074
1414	0.826449	0.829415	0.00059	0.00084	0.00265	0.00052	0.00015	0.00074
1495	0.826449	0.829557	0.00075	0.00097	0.00265	0.00052	0.00015	0.00074
1574	0.825625	0.829642	0.00059	0.00097	0.00243	0.00052	0.00015	0.00086
1393	0.826449	0.829701	0.00059	0.00097	0.00265	0.00052	0.00015	0.00074
1619	0.825625	0.829817	0.00059	0.00097	0.00102	0.00052	0.00015	0.00065
1518	0.826449	0.830013	0.00059	0.00097	0.00265	0.00052	0.00015	0.00074
1454	0.826449	0.830854	0.00060	0.00097	0.00265	0.00052	0.00015	0.00074
1443	0.826449	0.830859	0.00059	0.00097	0.00265	0.00052	0.00015	0.00074
1638	0.825625	0.831316	0.00059	0.00097	0.00265	0.00052	0.00015	0.00095
1558	0.825625	0.832090	0.00059	0.00097	0.00265	0.00052	0.00015	0.00074
1449	0.826449	0.832312	0.00059	0.00097	0.00265	0.00052	0.00022	0.00074
1581	0.825625	0.832398	0.00082	0.00097	0.00265	0.00052	0.00015	0.00074
1363	0.827639	0.832431	0.00059	0.00097	0.00238	0.00052	0.00015	0.00072
1478	0.826449	0.832773	0.00059	0.00097	0.00265	0.00052	0.00015	0.00074
1392	0.826449	0.832925	0.00059	0.00097	0.00265	0.00052	0.00015	0.00074
1532	0.826028	0.833015	0.00059	0.00097	0.00265	0.00053	0.00015	0.00074
1511	0.826449	0.833072	0.00067	0.00097	0.00265	0.00052	0.00015	0.00074
1556	0.825625	0.833121	0.00059	0.00097	0.00265	0.00052	0.00015	0.00074
1536	0.826028	0.833204	0.00059	0.00097	0.00265	0.00052	0.00015	0.00074
1576	0.825625	0.833421	0.00059	0.00097	0.00265	0.00052	0.00015	0.00074

1585	0.825625	0.833656	0.00059	0.00097	0.00265	0.00052	0.00015	0.00074
1502	0.826449	0.833671	0.00059	0.00097	0.00265	0.00052	0.00004	0.00050
1441	0.826449	0.833937	0.00059	0.00097	0.00265	0.00052	0.00015	0.00074
1340	0.834050	0.834050	0.00059	0.00097	0.00216	0.00052	0.00015	0.00072
1357	0.827869	0.834113	0.00059	0.00097	0.00229	0.00052	0.00015	0.00075
1588	0.825625	0.834285	0.00059	0.00097	0.00213	0.00052	0.00013	0.00074
1343	0.827869	0.834381	0.00059	0.00082	0.00216	0.00052	0.00015	0.00072
924	0.834398	0.834398	0.00059	0.00097	0.00216	0.00052	0.00015	0.00072
1215	0.834398	0.834398	0.00059	0.00097	0.00216	0.00052	0.00015	0.00072
570	0.834474	0.834474	0.00059	0.00097	0.00216	0.00052	0.00015	0.00072
1353	0.827869	0.834493	0.00059	0.00097	0.00216	0.00052	0.00015	0.00063
1548	0.825664	0.835048	0.00059	0.00097	0.00265	0.00052	0.00015	0.00074
1261	0.834398	0.835320	0.00059	0.00097	0.00216	0.00052	0.00021	0.00072
1601	0.825625	0.835411	0.00059	0.00078	0.00265	0.00052	0.00015	0.00074
1563	0.825625	0.835636	0.00059	0.00097	0.00265	0.00052	0.00032	0.00074
1547	0.825664	0.835860	0.00059	0.00097	0.00289	0.00052	0.00015	0.00074
684	0.834474	0.835897	0.00059	0.00097	0.00294	0.00052	0.00015	0.00072
1579	0.825625	0.836145	0.00059	0.00097	0.00265	0.00052	0.00015	0.00074
1517	0.826449	0.836204	0.00065	0.00097	0.00265	0.00052	0.00015	0.00074
1483	0.826449	0.836360	0.00059	0.00092	0.00265	0.00052	0.00015	0.00074
852	0.834474	0.836600	0.00039	0.00097	0.00216	0.00052	0.00026	0.00072
859	0.834474	0.836664	0.00059	0.00097	0.00136	0.00052	0.00015	0.00072
1345	0.827869	0.836880	0.00096	0.00097	0.00216	0.00052	0.00015	0.00072
1428	0.826449	0.837035	0.00059	0.00097	0.00265	0.00052	0.00015	0.00074
565	0.837045	0.837045	0.00041	0.00097	0.00149	0.00076	0.00015	0.00072
1596	0.825625	0.837052	0.00059	0.00097	0.00265	0.00052	0.00015	0.00074
1484	0.826449	0.837065	0.00059	0.00097	0.00265	0.00052	0.00015	0.00090

448	0.837408	0.837408	0.00041	0.00097	0.00149	0.00076	0.00015	0.00072
817	0.834474	0.837502	0.00059	0.00097	0.00216	0.00052	0.00065	0.00072
922	0.834474	0.837624	0.00059	0.00097	0.00216	0.00052	0.00015	0.00057
986	0.834398	0.837636	0.00059	0.00079	0.00216	0.00052	0.00026	0.00090
1072	0.834398	0.837908	0.00059	0.00097	0.00216	0.00052	0.00015	0.00072
994	0.834398	0.837917	0.00059	0.00097	0.00432	0.00052	0.00015	0.00072
1084	0.834398	0.837981	0.00063	0.00098	0.00216	0.00052	0.00015	0.00072
966	0.834398	0.838022	0.00059	0.00097	0.00216	0.00052	0.00015	0.00072
846	0.834474	0.838145	0.00059	0.00097	0.00131	0.00052	0.00015	0.00069
1438	0.826449	0.838276	0.00059	0.00097	0.00265	0.00052	0.00015	0.00095
1525	0.826449	0.838536	0.00059	0.00097	0.00265	0.00052	0.00034	0.00074
694	0.834474	0.838586	0.00059	0.00097	0.00216	0.00052	0.00015	0.00043
1134	0.834398	0.838646	0.00059	0.00075	0.00216	0.00052	0.00015	0.00072
1405	0.826449	0.838704	0.00059	0.00097	0.00265	0.00057	0.00037	0.00074
1412	0.826449	0.838711	0.00059	0.00097	0.00265	0.00052	0.00015	0.00074
920	0.834474	0.838719	0.00042	0.00097	0.00216	0.00052	0.00015	0.00072
753	0.834474	0.838724	0.00059	0.00097	0.00360	0.00044	0.00000	0.00072
1027	0.834398	0.838734	0.00059	0.00087	0.00216	0.00052	0.00015	0.00072
1462	0.826449	0.838783	0.00059	0.00097	0.00265	0.00052	0.00015	0.00074
1370	0.827639	0.838852	0.00059	0.00097	0.00216	0.00052	0.00015	0.00089
1294	0.834398	0.838996	0.00059	0.00097	0.00216	0.00052	0.00015	0.00072
838	0.834474	0.839102	0.00058	0.00068	0.00216	0.00052	0.00015	0.00072
1313	0.834398	0.839107	0.00059	0.00097	0.00216	0.00052	0.00015	0.00072
1490	0.826449	0.839479	0.00059	0.00097	0.00265	0.00052	0.00015	0.00074
1237	0.834398	0.839586	0.00059	0.00097	0.00353	0.00052	0.00017	0.00084
1291	0.834398	0.839605	0.00059	0.00097	0.00216	0.00052	0.00015	0.00077
590	0.834474	0.839676	0.00059	0.00097	0.00137	0.00052	0.00015	0.00072

1079	0.834398	0.839679	0.00059	0.00097	0.00216	0.00052	0.00015	0.00036
1367	0.827639	0.839722	0.00059	0.00097	0.00216	0.00052	0.00015	0.00072
1487	0.826449	0.839809	0.00059	0.00097	0.00265	0.00052	0.00015	0.00074
1268	0.834398	0.839823	0.00059	0.00097	0.00216	0.00052	0.00011	0.00072
1131	0.834398	0.839867	0.00059	0.00088	0.00216	0.00052	0.00026	0.00072
1320	0.834398	0.839871	0.00043	0.00097	0.00309	0.00052	0.00015	0.00072
979	0.834398	0.840271	0.00059	0.00097	0.00261	0.00052	0.00015	0.00072
1045	0.834398	0.840331	0.00059	0.00097	0.00216	0.00083	0.00015	0.00072
1557	0.825625	0.840332	0.00059	0.00097	0.00265	0.00047	0.00015	0.00074
1383	0.826449	0.840436	0.00059	0.00097	0.00265	0.00052	0.00015	0.00037
1544	0.826028	0.840527	0.00059	0.00097	0.00265	0.00052	0.00015	0.00074
1144	0.834398	0.840606	0.00059	0.00097	0.00216	0.00052	0.00007	0.00072
1446	0.826449	0.840628	0.00070	0.00097	0.00265	0.00052	0.00015	0.00074
1347	0.827869	0.840665	0.00059	0.00097	0.00216	0.00052	0.00015	0.00069

DDS optimization trial   1 outputs below:

#Fevals	Fbest	Ftest		-> Decision variable values 1, 2, etc. producing Ftest -->					
Parameter Name			**pwr**					
River Classification Name			**jean-marie**	**martin**	**birch**	**backstone**	**Pembina**	**Roseau**
1554	0.825625	0.825625	1.520	1.891	3.293	3.008	2.962	2.449
1654	0.825625	0.825625	1.520	1.891	3.293	3.008	2.962	2.449
1546	0.825664	0.825664	1.520	1.891	3.293	3.008	2.962	2.369
1566	0.825625	0.825843	1.520	1.891	3.293	3.008	2.962	2.449
1530	0.826028	0.826028	1.520	1.891	3.074	3.008	2.962	2.369

1542	0.826028	0.826028	1.520	1.891	3.074	3.008	2.962	2.369
1586	0.825625	0.826031	1.520	1.891	3.293	3.008	2.962	2.449
1602	0.825625	0.826313	1.520	1.643	3.293	3.008	2.962	2.449
1374	0.826449	0.826449	1.520	1.891	3.074	3.008	1.935	2.369
1417	0.826449	0.826449	1.520	1.891	3.074	3.008	1.935	2.369
1504	0.826449	0.826648	1.520	1.891	3.074	3.008	1.935	2.369
1466	0.826449	0.826649	1.520	1.891	3.074	3.008	1.935	2.369
1604	0.825625	0.826923	1.520	2.019	3.293	3.008	2.962	2.449
1514	0.826449	0.827051	1.520	1.891	3.074	3.008	1.935	2.369
1522	0.826449	0.827258	1.520	1.891	3.074	3.008	1.935	2.369
1359	0.827639	0.827639	1.520	1.891	3.074	3.008	1.935	2.369
1368	0.827639	0.827639	1.520	1.891	3.074	3.008	1.935	2.369
1341	0.827869	0.827869	1.480	1.891	3.074	3.008	1.935	2.546
1409	0.826449	0.827899	1.520	1.891	3.074	3.008	1.935	2.369
1349	0.827869	0.828420	1.480	1.891	3.074	3.008	1.935	2.546
1564	0.825625	0.829271	1.520	1.891	3.293	3.008	2.962	2.449
1473	0.826449	0.829279	1.520	1.891	3.074	3.008	1.935	2.369
1414	0.826449	0.829415	1.520	1.891	3.074	3.008	1.935	2.369
1495	0.826449	0.829557	1.520	2.247	3.074	3.008	1.935	2.369
1574	0.825625	0.829642	1.520	1.891	3.293	3.008	2.962	2.364
1393	0.826449	0.829701	1.520	1.413	3.074	3.008	1.935	2.369
1619	0.825625	0.829817	1.520	1.891	3.293	3.008	2.962	2.449
1518	0.826449	0.830013	1.520	1.891	3.074	3.008	1.935	2.369
1454	0.826449	0.830854	1.520	1.891	3.074	3.008	1.935	2.369
1443	0.826449	0.830859	1.520	1.891	3.074	3.008	1.935	2.132
1638	0.825625	0.831316	1.520	1.891	3.293	3.008	2.962	2.449
1558	0.825625	0.832090	1.520	1.891	3.293	3.008	2.962	2.449

1449	0.826449	0.832312	1.948	1.891	3.074	3.008	2.011	2.369
1581	0.825625	0.832398	1.520	1.891	3.293	3.008	2.962	2.904
1363	0.827639	0.832431	1.520	1.891	3.275	3.008	2.771	2.369
1478	0.826449	0.832773	1.520	1.891	3.074	3.008	1.935	2.369
1392	0.826449	0.832925	1.520	1.891	3.074	3.008	1.935	2.369
1532	0.826028	0.833015	1.508	1.891	3.074	3.008	2.962	2.369
1511	0.826449	0.833072	1.520	1.891	3.074	3.008	1.935	2.369
1556	0.825625	0.833121	1.520	1.891	3.293	3.355	2.962	2.449
1536	0.826028	0.833204	1.520	1.891	3.074	3.008	2.962	2.369
1576	0.825625	0.833421	1.520	1.891	3.293	3.008	2.962	2.449
1585	0.825625	0.833656	1.520	1.891	2.916	3.008	2.962	2.449
1502	0.826449	0.833671	1.520	1.891	3.074	3.008	1.935	2.369
1441	0.826449	0.833937	1.858	1.891	3.074	3.008	2.468	2.369
1340	0.834050	0.834050	1.480	2.286	3.074	3.008	1.935	2.546
1357	0.827869	0.834113	1.480	1.891	3.074	3.008	1.935	2.546
1588	0.825625	0.834285	1.520	1.891	3.293	3.008	2.884	2.449
1343	0.827869	0.834381	1.480	1.891	3.074	3.008	1.935	2.546
924	0.834398	0.834398	1.480	2.286	3.074	3.008	1.935	2.546
1215	0.834398	0.834398	1.480	2.286	3.074	3.008	1.935	2.546
570	0.834474	0.834474	1.480	2.286	3.074	3.008	1.935	2.663
1353	0.827869	0.834493	1.478	1.891	3.074	3.008	1.935	2.546
1548	0.825664	0.835048	1.598	1.891	3.293	3.008	2.962	2.113
1261	0.834398	0.835320	1.480	2.286	3.074	3.008	1.935	2.546
1601	0.825625	0.835411	1.414	1.891	3.293	3.008	2.962	2.449
1563	0.825625	0.835636	1.520	1.859	3.293	3.008	2.867	2.809
1547	0.825664	0.835860	1.520	1.891	3.293	3.008	2.962	2.369
684	0.834474	0.835897	1.480	1.506	3.296	3.008	1.935	2.663

1579	0.825625	0.836145	1.520	1.891	3.293	3.008	2.962	2.449
1517	0.826449	0.836204	1.520	1.910	3.074	3.008	1.935	2.369
1483	0.826449	0.836360	1.520	1.891	3.074	3.008	1.935	2.369
852	0.834474	0.836600	1.480	2.286	3.074	3.008	1.935	2.916
859	0.834474	0.836664	1.480	2.286	3.074	3.008	1.935	2.409
1345	0.827869	0.836880	1.875	1.891	3.074	3.008	1.935	3.296
1428	0.826449	0.837035	1.520	1.891	3.074	3.008	1.611	2.369
565	0.837045	0.837045	1.480	2.286	3.329	3.345	1.935	2.663
1596	0.825625	0.837052	1.520	1.891	3.293	3.008	2.962	2.449
1484	0.826449	0.837065	1.520	1.891	3.074	2.768	1.935	2.369
448	0.837408	0.837408	1.480	2.286	3.329	3.345	1.935	2.945
817	0.834474	0.837502	1.480	2.286	3.074	3.008	1.935	2.663
922	0.834474	0.837624	1.480	2.286	3.074	3.008	1.708	2.663
986	0.834398	0.837636	1.480	2.286	3.074	3.008	1.691	2.546
1072	0.834398	0.837908	1.480	2.286	3.074	3.008	1.935	2.546
994	0.834398	0.837917	1.480	2.286	3.074	3.008	1.935	2.546
1084	0.834398	0.837981	1.480	2.286	3.074	3.008	1.935	2.546
966	0.834398	0.838022	1.480	2.286	3.074	3.008	1.935	2.546
846	0.834474	0.838145	1.480	2.286	3.074	3.008	1.728	2.663
1438	0.826449	0.838276	1.520	1.891	3.074	3.008	1.935	2.369
1525	0.826449	0.838536	1.500	1.891	3.155	3.008	1.935	2.369
694	0.834474	0.838586	1.480	2.286	3.074	2.288	1.935	2.663
1134	0.834398	0.838646	1.480	2.286	3.074	3.008	1.935	2.546
1405	0.826449	0.838704	1.520	1.891	3.074	3.008	1.614	2.369
1412	0.826449	0.838711	1.520	1.891	2.834	3.008	1.935	2.369
920	0.834474	0.838719	1.480	2.286	3.074	2.958	1.935	2.663
753	0.834474	0.838724	1.584	2.286	3.074	3.489	1.935	2.663

1027	0.834398	0.838734	1.480	2.286	3.074	3.008	1.935	2.546
1462	0.826449	0.838783	1.795	2.087	3.074	3.008	1.935	2.369
1370	0.827639	0.838852	1.520	1.891	3.007	3.008	1.457	2.369
1294	0.834398	0.838996	1.480	2.286	3.074	3.047	1.642	2.546
838	0.834474	0.839102	1.480	2.286	3.074	3.032	1.935	2.663
1313	0.834398	0.839107	1.480	2.286	3.178	3.008	2.335	2.304
1490	0.826449	0.839479	1.520	1.891	3.074	3.008	1.935	2.369
1237	0.834398	0.839586	1.480	2.286	3.446	3.008	1.935	3.373
1291	0.834398	0.839605	1.480	2.286	2.751	3.008	1.935	2.546
590	0.834474	0.839676	1.480	2.286	3.074	3.008	1.678	3.389
1079	0.834398	0.839679	1.480	2.286	3.074	3.008	1.935	2.546
1367	0.827639	0.839722	1.520	1.891	3.074	3.008	1.935	2.369
1487	0.826449	0.839809	1.520	1.891	3.074	3.008	1.935	2.369
1268	0.834398	0.839823	1.480	2.286	3.074	3.008	1.935	2.546
1131	0.834398	0.839867	1.480	2.286	3.041	3.008	1.935	2.546
1320	0.834398	0.839871	1.480	2.286	2.578	3.008	1.935	2.546
979	0.834398	0.840271	1.480	2.629	3.074	3.008	1.935	2.427
1045	0.834398	0.840331	1.480	2.286	3.074	3.008	1.935	2.546
1557	0.825625	0.840332	1.520	1.891	3.438	3.008	2.962	2.449
1383	0.826449	0.840436	1.520	1.891	3.074	3.347	2.365	2.369
1544	0.826028	0.840527	1.520	1.891	3.338	3.008	2.962	2.369
1144	0.834398	0.840606	1.480	2.286	3.074	3.008	1.935	2.546
1446	0.826449	0.840628	1.520	1.891	3.074	3.008	1.935	2.369
1347	0.827869	0.840665	1.480	1.891	3.074	3.008	1.775	3.107

DDS optimization trial   1 outputs below:

#Fevals	Fbest	Ftest	| -> Decision variable values 1, 2, etc. producing Ftest -->					
Parameter Name			r2n					
River Classification Name			jean-marie	martin	birch	backstone	Pembina	Roseau
1554	0.825625	0.825625	0.039	3.862	1.017	0.321	0.100	0.252
1654	0.825625	0.825625	0.039	3.862	1.017	0.321	0.100	0.252
1546	0.825664	0.825664	0.039	3.862	1.017	0.321	0.100	0.252
1566	0.825625	0.825843	0.039	3.862	1.017	0.321	0.100	0.252
1530	0.826028	0.826028	0.039	3.862	1.409	0.321	0.100	0.252
1542	0.826028	0.826028	0.039	3.862	1.409	0.321	0.100	0.252
1586	0.825625	0.826031	0.039	3.862	0.532	0.321	0.100	0.252
1602	0.825625	0.826313	0.039	3.862	1.017	0.321	0.100	0.252
1374	0.826449	0.826449	0.039	3.862	1.409	0.321	0.100	0.252
1417	0.826449	0.826449	0.039	3.862	1.409	0.321	0.100	0.252
1504	0.826449	0.826648	0.039	3.862	1.409	0.321	0.100	0.252
1466	0.826449	0.826649	0.039	3.862	1.409	0.321	0.100	0.252
1604	0.825625	0.826923	0.039	3.862	1.017	0.321	0.100	0.252
1514	0.826449	0.827051	0.039	3.862	1.409	0.321	0.047	0.252
1522	0.826449	0.827258	0.039	3.862	2.459	0.321	0.100	0.252
1359	0.827639	0.827639	0.039	3.862	1.409	0.321	0.100	0.252
1368	0.827639	0.827639	0.039	3.862	1.409	0.321	0.100	0.252
1341	0.827869	0.827869	0.039	3.877	1.409	0.321	0.100	0.252
1409	0.826449	0.827899	0.039	3.862	1.409	0.321	0.100	0.252
1349	0.827869	0.828420	0.039	3.877	1.409	0.321	0.100	0.252
1564	0.825625	0.829271	0.039	3.862	1.017	0.321	0.100	0.252
1473	0.826449	0.829279	0.039	3.862	1.770	0.321	0.100	0.252
1414	0.826449	0.829415	0.039	3.862	1.409	0.321	0.100	0.275
1495	0.826449	0.829557	0.039	3.862	1.409	0.321	0.100	0.252

1574	0.825625	0.829642	0.039	3.862	1.017	0.321	0.100	0.252
1393	0.826449	0.829701	0.039	3.862	1.409	0.321	0.100	0.252
1619	0.825625	0.829817	0.039	3.862	1.017	0.321	0.100	0.252
1518	0.826449	0.830013	0.039	3.862	1.409	0.321	0.100	0.272
1454	0.826449	0.830854	0.039	3.862	1.409	0.321	0.100	0.252
1443	0.826449	0.830859	0.039	3.862	1.409	0.321	0.100	0.252
1638	0.825625	0.831316	0.039	3.862	1.017	0.321	0.100	0.252
1558	0.825625	0.832090	0.039	3.862	1.017	0.321	0.100	0.252
1449	0.826449	0.832312	0.039	3.862	1.409	0.321	0.100	0.252
1581	0.825625	0.832398	0.039	3.862	1.017	0.321	0.100	0.181
1363	0.827639	0.832431	0.039	3.862	1.608	0.321	0.100	0.252
1478	0.826449	0.832773	0.039	3.862	1.409	0.321	0.100	0.252
1392	0.826449	0.832925	0.039	3.862	1.246	0.321	0.100	0.252
1532	0.826028	0.833015	0.039	3.862	1.409	0.321	0.100	0.252
1511	0.826449	0.833072	0.039	3.862	1.409	0.321	0.100	0.252
1556	0.825625	0.833121	0.039	3.862	1.017	0.321	0.100	0.252
1536	0.826028	0.833204	0.039	3.862	1.409	0.321	0.100	0.252
1576	0.825625	0.833421	0.039	3.862	1.017	0.321	0.100	0.252
1585	0.825625	0.833656	0.039	3.862	1.017	0.321	0.100	0.252
1502	0.826449	0.833671	0.039	3.862	1.409	0.321	0.100	0.252
1441	0.826449	0.833937	0.039	3.862	1.409	0.321	0.100	0.252
1340	0.834050	0.834050	0.039	3.877	1.409	0.321	0.100	0.252
1357	0.827869	0.834113	0.039	3.877	1.409	0.321	0.100	0.252
1588	0.825625	0.834285	0.039	3.862	1.017	0.321	0.100	0.252
1343	0.827869	0.834381	0.039	3.877	1.409	0.767	0.100	0.252
924	0.834398	0.834398	0.039	3.877	1.945	0.321	0.100	0.252
1215	0.834398	0.834398	0.039	3.877	1.945	0.321	0.100	0.252

570	0.834474	0.834474	0.039	3.877	1.945	0.321	0.100	0.252
1353	0.827869	0.834493	0.039	3.877	1.409	0.321	0.100	0.252
1548	0.825664	0.835048	0.039	3.862	1.017	0.321	0.100	0.252
1261	0.834398	0.835320	0.039	3.877	1.945	0.321	0.100	0.252
1601	0.825625	0.835411	0.039	3.862	1.017	0.321	0.068	0.252
1563	0.825625	0.835636	0.039	3.862	1.017	0.321	0.100	0.252
1547	0.825664	0.835860	0.039	3.862	1.017	0.321	0.100	0.252
684	0.834474	0.835897	0.039	3.877	1.945	0.321	0.100	0.252
1579	0.825625	0.836145	0.039	3.862	1.017	0.321	0.100	0.252
1517	0.826449	0.836204	0.039	3.862	1.409	0.321	0.100	0.252
1483	0.826449	0.836360	0.039	3.862	1.409	0.321	0.100	0.252
852	0.834474	0.836600	0.039	3.877	1.945	0.321	0.100	0.252
859	0.834474	0.836664	0.039	3.877	1.945	0.321	0.100	0.252
1345	0.827869	0.836880	0.039	3.877	1.409	0.321	0.100	0.252
1428	0.826449	0.837035	0.039	3.862	1.409	0.321	0.100	0.252
565	0.837045	0.837045	0.039	3.877	1.945	0.321	0.100	0.252
1596	0.825625	0.837052	0.039	3.773	1.017	0.321	0.100	0.252
1484	0.826449	0.837065	0.039	3.862	1.409	0.321	0.100	0.252
448	0.837408	0.837408	0.039	3.877	1.945	0.321	0.100	0.252
817	0.834474	0.837502	0.039	3.877	1.945	0.321	0.116	0.252
922	0.834474	0.837624	0.039	3.877	1.945	0.321	0.100	0.252
986	0.834398	0.837636	0.039	3.877	1.945	0.321	0.100	0.252
1072	0.834398	0.837908	0.039	3.877	1.945	0.321	0.100	0.252
994	0.834398	0.837917	0.039	3.877	1.945	0.321	0.100	0.252
1084	0.834398	0.837981	0.039	3.877	1.945	0.321	0.100	0.252
966	0.834398	0.838022	0.039	3.877	1.945	0.321	0.100	0.252
846	0.834474	0.838145	0.039	3.877	1.415	0.321	0.100	0.252

1438	0.826449	0.838276	0.039	3.862	1.409	0.321	0.100	0.252
1525	0.826449	0.838536	0.039	3.862	1.409	0.321	0.100	0.252
694	0.834474	0.838586	0.039	3.877	0.869	0.321	0.100	0.252
1134	0.834398	0.838646	0.039	3.877	1.945	0.546	0.100	0.252
1405	0.826449	0.838704	0.039	3.862	1.409	0.335	0.100	0.252
1412	0.826449	0.838711	0.039	3.862	1.409	0.321	0.100	0.252
920	0.834474	0.838719	0.039	3.877	1.945	0.321	0.100	0.252
753	0.834474	0.838724	0.039	3.877	1.945	0.321	0.100	0.158
1027	0.834398	0.838734	0.039	3.877	1.945	0.321	0.100	0.252
1462	0.826449	0.838783	0.039	3.679	1.409	0.321	0.100	0.252
1370	0.827639	0.838852	0.039	3.862	1.409	0.321	0.100	0.252
1294	0.834398	0.838996	0.039	3.877	1.860	0.321	0.100	0.117
838	0.834474	0.839102	0.039	3.877	1.945	0.321	0.100	0.252
1313	0.834398	0.839107	0.039	3.877	1.340	0.321	0.100	0.252
1490	0.826449	0.839479	0.039	3.862	1.409	0.321	0.100	0.252
1237	0.834398	0.839586	0.039	3.877	1.312	0.321	0.100	0.252
1291	0.834398	0.839605	0.039	3.877	1.945	0.321	0.100	0.252
590	0.834474	0.839676	0.039	3.877	1.945	0.321	0.100	0.252
1079	0.834398	0.839679	0.039	3.877	1.945	0.321	0.100	0.252
1367	0.827639	0.839722	0.039	3.862	1.409	0.321	0.100	0.252
1487	0.826449	0.839809	0.039	3.862	1.409	0.321	0.100	0.252
1268	0.834398	0.839823	0.039	3.877	1.945	0.321	0.100	0.252
1131	0.834398	0.839867	0.039	3.877	1.945	0.321	0.100	0.252
1320	0.834398	0.839871	0.039	3.877	1.945	0.321	0.100	0.252
979	0.834398	0.840271	0.039	3.877	1.945	0.321	0.100	0.252
1045	0.834398	0.840331	0.039	3.877	0.566	0.321	0.100	0.252
1557	0.825625	0.840332	0.039	3.862	1.017	0.321	0.100	0.252

1383	0.826449	0.840436	0.039	3.862	1.409	0.321	0.100	0.252
1544	0.826028	0.840527	0.039	3.862	1.409	0.321	0.100	0.252
1144	0.834398	0.840606	0.039	3.877	1.945	0.321	0.100	0.252
1446	0.826449	0.840628	0.039	3.862	1.409	0.463	0.100	0.252
1347	0.827869	0.840665	0.039	3.877	1.409	0.321	0.100	0.252